Analysis of anther dehydration; a process required for anther dehiscence and pollen release

RUTH DENNIS BSc PGCE MSc

Thesis submitted to the University of Nottingham for the degree of Doctor of Philosophy

September 2017

ACKNOWLEDGEMENTS

First and foremost, I need to thank Zoe- I couldn't have asked for a better supervisor and mentor and you were always being there to provide advice and guidance when I needed it. You have also been extremely supportive to me on a personal level, throughout the various curveballs that life's thrown at me during the last four years and I appreciate that so much. I can't say thanks enough either for arranging my PIP at Shanghai Jiao Tong University, it was a fantastic experience that I got so much out of. Your initiative regarding the stomata work turned into an extremely rewarding and interesting collaboration with the University of Sheffield and I need to thank Julie, Lee and Jess for making me feel so welcome and for all of their help.

I have been fortunate to have been a part of a great lab group and I would like to thank everyone who has been in A47 (past and present), for all the chats, laughter, and of course cake over the years! In particular I need thank Alison and Jose, the group is really lucky to have fantastic post-docs who always make time to help.

Lee, it's been absolutely amazing to have my best friend living not only in the same country, but in the same city for the first time in years. Your advice regarding the write up has been invaluable and it is true best friend who spends six hours proof-reading your thesis on a Saturday night, I am really touched and so grateful for all of your help.

Tom, you've joined me on this journey at the very end but I don't know how I would have got through the write up without your constant support and encouragement. Knowing that you were always there on the other end of the phone and that you believed in me, meant everything. Thanks also for getting me into reading the Harry Potter books for the first time, because Hogwarts turned out to be the perfect escape (and I did finish them first in the end!).

Lastly, but definitely not least, I need to thank my family. Carla, Jon, Alex and Anya thank you so much for willingly cat sitting throughout

the write up and giving me the freedom to work wherever I wanted. Mum and Dad thank you for everything. You've shown me how important it is to be positive through challenging times and I think your attitudes are inspirational. I would like to dedicate this to you both.

ABSTRACT

In flowering plants, the opening of the anther to release pollen is carefully timed to maximise reproductive potential. Manipulation of this process is an important tool for plant breeding and the production of hybrid crops. Dehydration of the anther epidermis, combined with the presence of secondary thickening within the endothecium layer, is required to create biomechanical changes that enable anther dehiscence. Both passive and active processes contribute to the targeted removal of water from the anther walls, however the genetic factors controlling water movement are not known. Furthermore, the presence of stomata on anthers may enhance water loss via evaporation.

In plants, active movement of water can be achieved by regulation of water channels and by changes to the osmotic potential of organs; this was explored in the context of changes in the anther driving anther dehiscence and pollen release. qRT-PCR analysis was used to identify aquaporin and sucrose transporter genes that are upregulated during anther dehiscence in *Arabidopsis thaliana*. For genes of interest, the phenotypes of available mutants were characterised. Combinations of single, double and triple mutants showed changes in fertility and variations in floral organ lengths. Analysis of GUS reporter lines showed that the promoter activity of different aquaporins is confined to specific parts of the flower. The results suggest that certain aquaporins isoforms enhance hydraulic conductivity in different parts of the flower, which could contribute to water transport required for petal and filament extension.

The importance of evaporation during anther dehydration was also investigated. The phenotypes of *Arabidopsis* mutant lines with varying stomatal densities were characterised, and changes in fertility were investigated under different environmental conditions. High relative humidity delayed anther dehiscence and affected pollen viability, resulting in reduced fertility. Plants that have no anther stomata were most severely affected. These results suggest that

water loss via evaporation is important for anther opening in *Arabidopsis*, and that the presence of stomata on anthers facilitates this process.

ABBREVIATIONS

ABA: Abscisic acid

BCP: Bicellular Pollen

bp: base pair

cDNA: Complementary Deoxyribonucleic acid

CO_2: carbon dioxide

DAPI: 4',6-diamidino-2-phenylindole

d: day(s)

DNA: Deoxyribonucleic acid

dNTP: Deoxynucleotide Triphosphate

EtOH: Ethanol

FDA: Fluorescein diacetate

GA: Gibberellin

GFP: Green Fluorescent Protein

GUS: β-glucuronidase

h: hour(s)

HCl: Hydrochloric acid

Het: Heterozygous

Hm: Homozygous

JA: Jasmonic acid

Kb: kilobase pair

l: Litre

LB: Luria Broth

M: molar

mM: millimolar

m: metre

min: minute(s)

ml: millilitre

mRNA: Messenger Ribonucleic acid

MS: Murashige and Skoog Basal Medium

NIP: Nodulin26-like Intrinsic Protein

ng: nanogram

nm: nanometre

OE: Overexpression

PBS: Phosphate Buffered Saline

PCR: Polymerase Chain Reaction

PIP: Plasma Membrane Intrinsic Protein

PMI: Pollen Mitosis I

PMII: Pollen Mitosis II

qRT-PCR: Quantitative Reverse-Transcriptase Polymerase Chain Reaction

RNAi: RNA interference

RT: Room Temperature

s: second(s)

SIP: Small Basic Intrinsic Protein

T-DNA: Transfer DNA

TIP: Tonoplast Intrinsic Protein

μg: microgram

μl: microlitre

UTR: Untranslated Region

v: volume

w: weight

wt: Wild type

wk: week

WUE: water use efficiency

LIST OF FIGURES

LIST OF TABLES

CONTENTS PAGE

CHAPTER 1 INTRODUCTION

1.1 An overview of pollen and anther development in *Arabidopsis thaliana*

1.1.1 Early Anther Development

The flowers of the model plant *Arabidopsis thaliana* (family *Brassicaceae*) are synonymous with that of a 'perfect flower', where the male reproductive organs, the stamens, are located within the third whorl of the flower (Causier et al., 2010). Each of the four whorls (sepals, petals, stamens and carpels) is defined by the single or overlapping expression of three classes of homeotic genes: A, B and C. In *Arabidopsis*, six stamen primordia are initiated by the joint expression of B and C class genes, in conjunction with a fourth-class E, whose gene product is required for the formation of a multimeric complex which binds DNA within the promoter region of target genes (Theissen and Saedler, 2001).

Each stamen comprises of a filament and an anther (figure 1.1A). The filament is a stem which supplies water and nutrients to the two-lobed anther, within which the pollen develops (Scott et al., 2004). Pollen and anther development occur simultaneously, and the latter has been divided into 14 developmental stages based on cytological and morphological studies in *Arabidopsis* (Sanders et al., 1999). Broadly speaking, there are two phases of anther development and anther stages 1-8 describe in detail the events of the first phase. Phase one establishes the anther's morphology and includes cell and tissue differentiation, specification of the pollen mother cells and meiosis (Goldberg et al., 1993; Sanders et al., 1999). During the second developmental phase (anther stages 9-14) pollen grains differentiate and mature, the anther enlarges and the filament extends to optimise positioning of the anther for pollen release. A switch from cell specification and differentiation to cell degeneration marks the progression from phase one to two (Goldberg et al., 1993; Sanders et al., 1999).

The 14 stages of anther development occur concurrently with *Arabidopsis* flower stages 5-16, with initiation of the stamen primordia happening at the fifth stage of flower development when the petal primordia also appear (Smyth et al., 1990). Three layers of tissue producing cells within the floral meristem, L1-3, divide and differentiate to consequently produce the epidermis, subepidermis and vascular and connective tissue. Within the L2 layer, archesporial cells at the corners of the anther primordia are responsible for the formation of the four anther locules which hold the microsporangia (Goldberg et al., 1993; Sanders et al., 1999). Archesporial derived primary parietal cells (PPC) and primary sporogenous cells (PSC) generate somatic and reproductive cells respectively. The PPC divide periclinally (parallel to the outer epidermis) which increases the number of cell layers so that by the end of anther stage five each of the four microsporangia contain meiocytes surrounded by separate somatic layers: the tapetum, middle layer, endothecium and epidermis (figure 1.1B) (Ma, 2005; Scott et al., 2004).

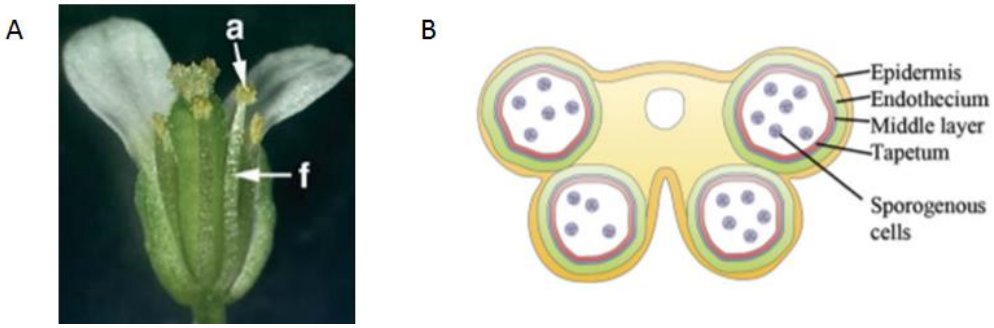

Figure 1.1: The *Arabidopsis* flower and diagram of an anther. Figure adapted from (Ma, 2005; Wilson et al., 2011).

A: *Arabidopsis* flower dissected to reveal the stamens, with the filament (f) and anther (a) labelled.
B: Cross-section of an *Arabidopsis* anther showing the two lobes and the four locules which hold the microsporangia. Each microsporangium contains reproductive sporogenous cells surrounded by somatic cell layers: the tapetum (red), middle layer (blue), endothecium (green) and outer epidermis (yellow).

Plant cell signalling is central to developmental processes and a number of membrane-bound Leucine-Rich Repeat Receptor-Like Kinases (LRR-RLKs) have been identified as coordinators of early

anther development. A feedback loop between LRR-RLKs *BARELY ANY MERISTEM 1* and *2 (BAM1/ 2)* and transcriptional regulator *SPOROCYTELESS/NOZZLE (SPL/NZZ)* controls the specification of sporogenous cells and their location, which is restricted to the centre of each locule (Feng and Dickinson, 2010; Hord et al., 2006; Yang et al., 1999; Zhao, 2009). The number of meiocytes and the formation of the tapetum are subsequently determined by a signalling pathway containing LRR-RLKs *EXTRA SPOROGENOUS CELLS/EXCESS MICROSPOROCYTES1 (EXS/EMS1)*, and *SOMATIC EMBRYOGENESIS 1* and *2 (SERK1/2)* (Albrecht et al., 2005; Canales et al., 2002; Colcombet et al., 2005; Zhao et al., 2002). The ligand of EXS/EMS1 is a small secreted cysteine-rich peptide encoded by *TAPETAL DETERMINANT1* (*TPD1*) (Huang et al., 2016; Jia et al., 2008; Yang et al., 2003, 2005). Mutants *tpd1, exs/ems1* and *serk1serk2* all share a characteristic phenotype of extra meiocytes, an absent tapetum and aborted meiosis (Albrecht et al., 2005; Canales et al., 2002; Colcombet et al., 2005; Yang et al., 2003, 2005; Zhao et al., 2002). Recently, Huang et al. revealed *TPD1* as part of a molecular mechanism by which somatic cells influence reproductive cell fates and vice versa (Huang et al., 2016). They suggest a model in which *TPD1* is secreted from the precursors of microsporocytes and binds *EMS1* at the plasma membrane of secondary parietal cells (derived from PPC), promoting their periclinal division and leading to formation of the middle layer and tapetal cell precursors. Once differentiated, functional tapetal cells repress the proliferation of microsporocytes. In the *tpd1* or *ems1* mutant, signalling is blocked, leading to an absence of the tapetum and an excess of microsporocytes (Huang et al., 2016).

Other regulators required for normal anther development are redundant LRR-RLKS *ERECTA (ER), ERECTA-LIKE1 (ERL1)*, *ERL2* and Mitogen Activated Protein Kinases (MAPK) *MPK3* and *MPK6,* which are also involved in the signal transduction pathway that controls stomatal patterning (see figure 5.1) (Bush and Krysan, 2007; Hord et al., 2008; Shpak et al., 2003, 2004). Loss of function of *ER/ERL*

and *MPK3/MPK6* result in similar phenotypes, including abnormal differentiation of anther cells and a reduced number of anther lobes, therefore it is likely that they act within the same pathway (Hord et al., 2008). *ER/ERL* and *MPK3/6* are thought to act distinctly from *EXS/EMS1, SERK1/2* and *TPD1*, and it has recently been shown that phosphorylation of *SPL* by *MPK3/6* is required for SPL/NZZ function (Hord et al., 2008; Zhao et al., 2017). *ROXY 1* and *2,* which encode redundantly acting glutaredoxins (oxidoreductase enzymes), provide another example of post-transcriptional regulation of early anther development (Xing and Zachgo, 2008). *ROXY 1* and *2* function downstream of *SPL/NZZ* and double mutants have a distinct phenotype; sporogenous cell formation is affected in the adaxial anther lobes, and differentiation of PMC and the tapetum are affected in the abaxial lobes (Xing and Zachgo, 2008). Basic leucine zipper transcription factors *TGA9/10* are presumed to be activation targets of ROXY *1/2,* as mutants *tga9/10* also exhibit differential developmental defects in the adaxial and abaxial lobes (Murmu et al., 2010).

1.1.2 Pollen development and the role of the tapetum

Cell types within the anther develop at different rates, however by the fifth stage of anther development all are present including the pollen mother cells (PMC) which are derived from the PSC (Sanders et al., 1999). While the middle layer, endothecium and epidermis offer structure and support to the anther and play a critical role in the release of the pollen (dehiscence), it is the tapetal layer that surrounds the microsporocytes which is essential for the development of viable pollen (Goldberg et al., 1993). Throughout pollen development the tapetum acts as a nurse tissue which secretes nutrients required for pollen development and the components required for pollen wall synthesis (Goldberg et al., 1993). PMC begin meiosis at anther stage six and produce a tetrad of haploid

microspores separated by callose walls (Sanders et al., 1999). Even at this early stage the presence of the tapetum is critical; in the *exs/ems1* mutant tetrads do not form and the microsporocytes degenerate (Zhao et al., 2002).

The pollen wall is essential to the survival of the male sperm cells as this complex structure provides protection from unfavourable conditions such as desiccation, high temperatures and attack from microbes. It also acts as a genetic barrier which enables plants to identify self from non-self and therefore avoid undesirable fertilization (Ariizumi and Toriyama, 2011). The pollen wall comprises of two layers, the intine and the outer exine. The intine is composed of pectins and celluloses derived from the microspore itself and the exine is predominantly made from sporopollenin, an incredibly resistant natural polymer which is synthesized from precursors secreted by the tapetum (Jiang et al., 2013). Synthesis of the pollen wall begins at the tetrad stage, before enzymes released from the tapetum cause the callose walls to break down and free the microspores (figure 1.2A). Following the release of microspores, the tapetum starts to degenerate by programmed cell death (PCD) and secretes sporopollenin precursors (Jiang et al., 2013). The microspores undergo the first of two mitotic divisions at anther stage eleven (Sanders et al., 1999). Firstly, a large vacuole develops which forces the nucleus to the side of the cell, and then a large vegetative cell and a small generative cell are produced by mitosis (Ma, 2005). *Arabidopsis thaliana* has trinucleate pollen, which means the generative cell undertakes a second mitotic division before pollen maturation is complete. In plants which have binucleate pollen this occurs after the pollen germinates (Ma, 2005).

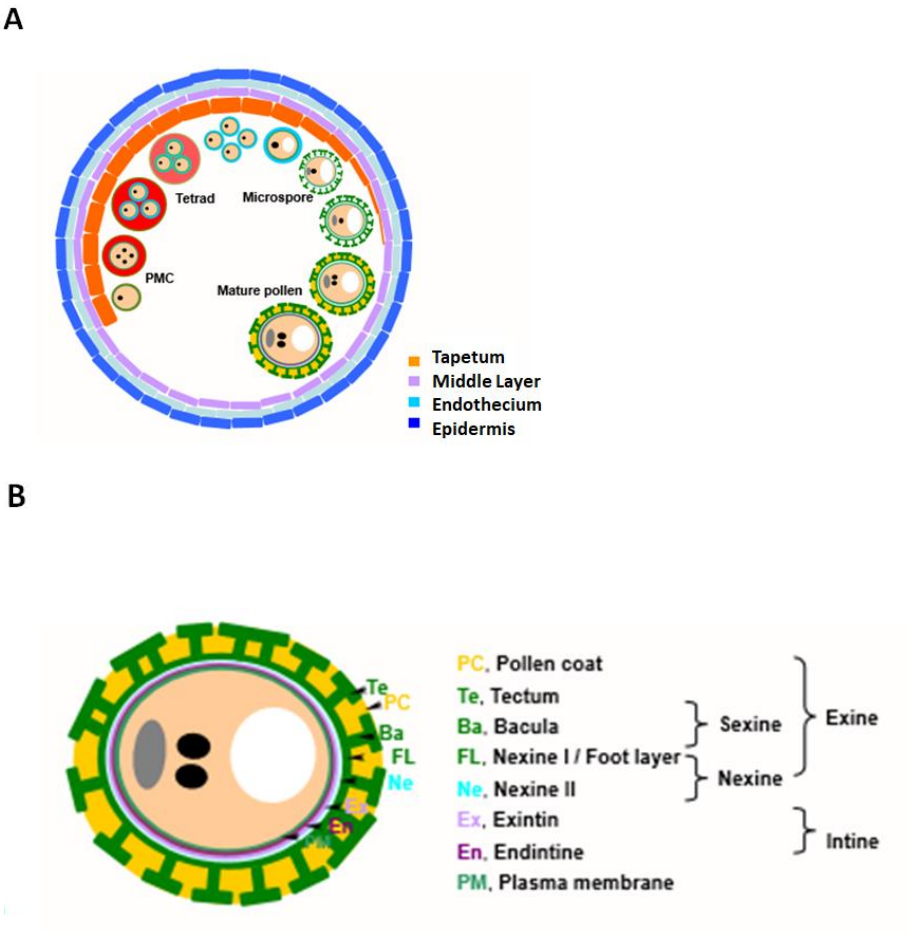

Figure 1.2: Development and structure of the pollen wall in *Arabidopsis thaliana*. Figure adapted from (Jiang et al., 2013).

A: Schematic of pollen wall development in *Arabidopsis thaliana*. Pollen wall development begins at the tetrad stage when the microspores produce a fibrillar polysaccharide matrix called the primexine. This acts as a sporopollenin receptor on which the mature exine is built after the release of microspores. The intine (which consists of pectins and celluloses produced by the microspores) is complete by the binucleate stage.
B: Diagram of pollen wall structure. The exine may be subdivided into a bilayered nexine and the outer sexine. The sexine consists of rod-like bacula and tectum, which are uniquely sculpted and covered in pollen coat material. The intine is also bilayered and consists of the exintine and endintine.

A complex transcriptional network controls tapetum function and pollen development (figure 1.3). One of the key regulators is *DYSFUNCTIONAL TAPETUM1 (DYT1)*, which is a basic helix-loop-helix (bHLH) transcription factor which is highly expressed in the tapetum during anther stages five and six. Studies have shown that *DYT1* acts downstream of *SPL/NZZ,* and *EXS/EMS1* is also a positive regulator of *DYT1* (Feng et al., 2012; Zhang et al., 2006). The tapetum of the

dyt1 mutant does not function normally: the tapetal cells become vacuolated, the meiocytes are surrounded by abnormally thin callose walls and, although meiosis does occur, functional microspores are not produced. As a transcription factor, *DYT1* was postulated to control expression of other genes. This was confirmed by transcriptome analysis, which showed that *DYT1* regulates pathways required for pollen coat formation, lipid metabolism, flavonoid and lignin biosynthesis and modification of cell walls (Feng et al., 2012; Zhang et al., 2006).

Two of the downstream targets of *DYT1* are *ABORTED MICROSPORES (AMS)* (Sorensen et al., 2003; Xu et al., 2010, 2014) and *MALE STERILITY 1 (MS1)* (Ito and Shinozaki, 2002; Vizcay-Barrena and Wilson, 2006; Wilson et al., 2001; Yang et al., 2007a). *AMS* is another bHLH transcription factor that is expressed in the tapetum from early meiosis right through to pollen mitosis II. In the *ams* mutant the tapetum is vacuolated and the microspores fail to develop a pollen wall and subsequently collapse. Like *DYT1, AMS* has recently been shown to be a diverse regulator which controls many of the metabolic processes required for pollen wall formation (Sorensen et al., 2003; Xu et al., 2010, 2014). *DYT1* regulates *AMS* and other downstream genes via *DEFECTIVE IN TAPETAL DEVELOPMENT AND FUNCTION 1 (TDF1),* a transcription factor which is essential for tapetal development (Gu et al., 2014).

MS1 is a nuclear located transcription factor with a PHD finger motif that is expressed in the tapetum during the tetrad stage (Ito and Shinozaki, 2002; Vizcay-Barrena and Wilson, 2006; Wilson et al., 2001; Yang et al., 2007a). Although *MS1* only has a short window of expression, it is crucial for normal pollen development. In the *ms1* mutant pollen develops an abnormal exine and the tapetum degrades necrotically rather than by regulated PCD (Ito and Shinozaki, 2002; Vizcay-Barrena and Wilson, 2006; Wilson et al., 2001; Yang et al., 2007a). As well as regulating late genes required for biosynthesis of pollen wall components, *MS1* co-ordinates the expression of a number of cysteine proteases which may be initiators of tapetal PCD

(Yang et al., 2007a). Yang et al. propose that MS1 does not regulate pollen wall biosynthesis genes directly, but acts via interaction with one or more transcription factors, including MYB99 (Ito et al., 2007a; Yang et al., 2007a). *MYB99* may be partially redundant in function to *MYB80*, which is another transcription factor involved in regulating pollen formation (Alves-Ferreira et al., 2007).

AMS regulates MS1 via MYB80 (Feng et al., 2012; Zhu et al., 2011), however, Ferguson et al. describe a biphasic expression pattern for the AMS protein with separate regulatory targets, which suggests that AMS has distinct functions during early and late pollen development (figure 1.3) (Ferguson et al., 2017). An initial peak in AMS protein expression occurs from pollen meiosis to the tetrad stage. At this stage AMS expression overlaps with DYT1, and it may be that the proteins interact to activate early targets or competitively form a complex with bHLH transcription factors. Activation of late targets (occurring during a second peak in AMS protein expression at pollen mitosis I) is predicted to occur via feed forward loops. Ferguson et al. hypothesise that the second peak in AMS protein expression is either caused by the protein becoming stabilised, or by a reduction in protein degradation (Ferguson et al., 2017). MS1 is predicted to indirectly and negatively regulate *AMS* expression through repression of upstream *TDF1* and by promoting degradation of the AMS protein (Ferguson et al., 2017).

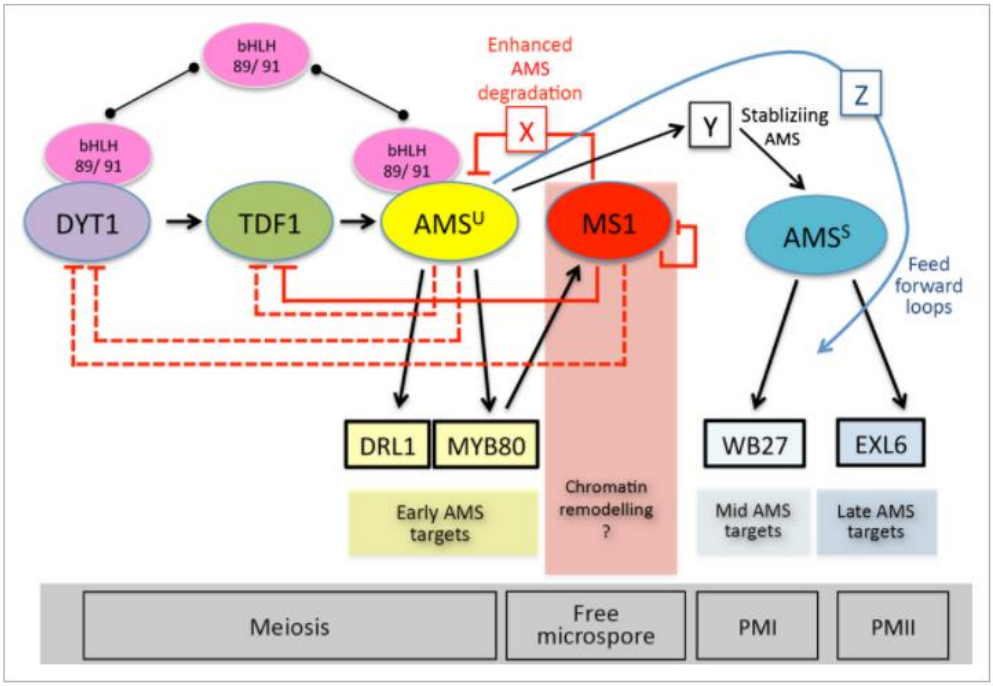

Figure 1.3: Model for the regulation of key transcription factors controlling tapetum function and pollen development. Figure adapted from (Ferguson et al., 2017).

The AMS protein has a biphasic expression pattern in tapetum; an early peak occurs between pollen meiosis and the tetrad stage (anther stages 6-7) and a later peak follows during pollen mitosis I (anther stage 10). At each peak, the AMS protein has distinct regulatory targets. AMS may regulate late targets via feed-forward loops. A competitive interaction between AMS and bHLH89/bHLH91 transcription factors and DYT1 is predicted by modelling. The two peaks in AMS protein levels are potentially created by MS1 indirectly promoting AMS degradation and by repression of upstream regulators. AMS^U, unstable protein; AMS^S, stable protein; X, Y and Z, unknown factors; arrows, direct regulation; lines ending with a bar, repression; lines with a line ending with circle, protein interactions. Dashed lines indicate a minor regulatory role (as predicted by modelling).

1.2 The process of anther dehiscence and its regulation

1.2.1. The process of anther dehiscence in *Arabidopsis thaliana*

In self-fertilizing plants like *Arabidopsis thaliana* the timing of anther opening is critical; not only must the female pistil be receptive but both the stigma and the filament of the stamen need to be optimally positioned at the time of pollen release (Steiner-Lange et al., 2003).

The process of dehiscence begins with the differentiation of two specialized cell types, the septum and the stomium, which are located in the notch-like area between the two locules in each anther lobe. The two notch regions, where the stomium will subsequently develop, are initiated at anther stage four. The septum can first be distinguished at anther stage nine and is comprised of a few cells immediately beneath the epidermis between the two locules (Sanders et al., 1999, 2005). At the start of dehiscence, the septum degenerates creating a bilocular anther. Pollen is subsequently released through the stomium, a differentiated region of the epidermis which is one cell thick (figure 1.4). Prior to dehiscence, the endothecium expands and cells acquire secondary thickening in the cell walls. It is this, combined with changes to the water status of the anther, that creates the forces required to rupture the stomium and release the pollen (Wilson et al., 2011).

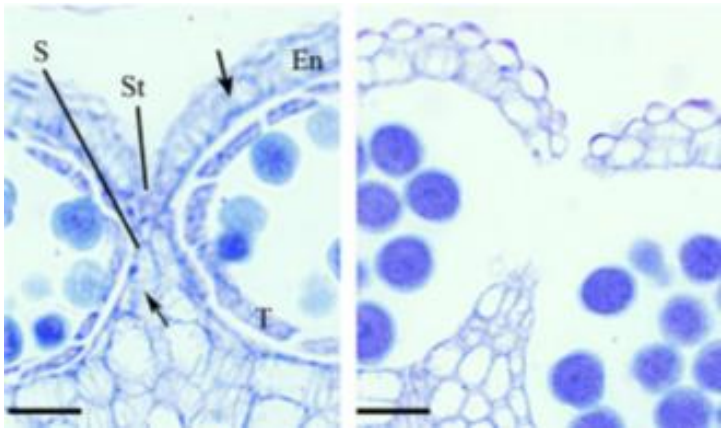

Figure 1.4: *Arabidopsis thaliana* anther showing septum (S) and stomium (St) regions before and after rupture. Figure adapted from (Wilson et al., 2011)**.**

Arrows indicate bands of secondary thickening in the endothecium (En). Bar=50μm.

Degeneration of the septum and stomium during anther dehiscence occurs via carefully timed PCD. Breakdown of the septum happens at anther stages eleven to twelve and is thought to involve enzymes related to cell wall loosening and degradation (Sanders et al., 1999; Wilson et al., 2011). Differentiation of the stomium begins at anther stage eleven and is followed by its degeneration and rupture at anther

stage 13 (Sanders et al., 1999). Evidence suggests that a functional stomium with a normal programme of cell death is essential for dehiscence. Plants expressing the cytotoxic barnase gene and the anti-cytotoxic barstar gene under different promoters were used to show that specific ablation of the stomium prevented dehiscence (Beals and Goldberg, 1997). In the *non-dehiscence 1* mutant, a random program of cell death causes complete degeneration of endothecium and results in indehiscent anthers (Sanders et al., 1999).

The deposition of bands of cellulose and lignin within the internal walls of the endothecial cells at anther stage 11, is central to the role of the endothecium in dehiscence (Sanders et al., 1999; Wilson et al., 2011). Firstly, an inward force on the stomium is caused by the uneven swelling of the endothecial cells at a time when it is already weakened. The bands of thickening within the inner cell walls mean that only the outside of the cells is able to expand, and this generates an inward pressure which disrupts the stomium. Later the endothecial cells lose water and again the lignified walls act differentially; by shrinking at a slower rate they cause an outward pressure which retracts the anther wall and breaks open the stomium to release the pollen (Keijzer, 1987; Wilson et al., 2011).

MYB26/MS35 encodes a MYB transcription factor which specifically regulates secondary cell wall thickening in the endothecium (Dawson et al., 1999; Steiner-Lange et al., 2003; Yang et al., 2007b). The mutant produces viable pollen which is not released. In the *myb26/ms35* mutant the endothecial secondary cell wall thickenings are not present and although the stomium is ruptured the anther walls do not retract, emphasizing the importance of lignification to create the final force required for anther opening (Dawson et al., 1999; Steiner-Lange et al., 2003; Yang et al., 2007b). Yang et al. found overexpression of *MYB26/MS35* causes ectopic lignification, suggesting that it regulates genes of the lignin biosynthetic pathway, however no notable changes in pathway gene expression were observed (Yang et al., 2007b). Two genes that were upregulated by

MYB26/MS35 overexpression were *NAC SECONDARY WALL THICKENING PROMOTING FACTOR1* and *2*, which had previously been shown to act redundantly in regulating the secondary thickening of the endothecium (Mitsuda et al., 2005; Yang et al., 2007b). Recent work by Yang et al. shows that although *MYB26/MS35* directly regulates *NST1/2*, overexpression expression of *NST1/2* in the *myb26/ms35* mutant does not rescue dehiscence and actually only results in limited ectopic secondary thickening in the epidermis, indicating a requirement for *MYB26* for normal thickening (Yang et al., 2017). Although *MYB26/MS35* is widely expressed in floral tissues, the protein is specifically localised to the endothecium, suggesting that it is subject to post-transcriptional or post-translational regulation. It appears that MYB26/MS35 enables an increase in the NST1/2 transcripts, and subsequent induction of secondary thickening genes, by controlling an additional factor. This unknown factor either enables the activation/stabilization of the NST1/2 proteins or removes an inhibitor involved in their breakdown.

Other genes that appear to be regulated by *MYB26/MS35* are *IRREGULAR XYLEM 1(IRX1), IRX3, IRX8* and *IRX12*, all of which are involved in thickening of secondary cell walls (Yang et al., 2007b). An *Arabidopsis* F-box protein SAF1 (Secondary Wall Thickening-Associated F-box 1) has been identified as a negative regulator of endothecium secondary wall thickening and overexpression of *SAF1* led to down regulation of a number of *IRX* genes (Kim et al., 2012). Yang et al. suggest that SAF1 may regulate secondary thickening by causing the breakdown of MYB26/MS35 or NST1/2 (Yang et al., 2017). Another gene putatively required for secondary wall thickening is *RECEPTOR-LIKE PROTEIN KINASE 2 (RPK2),* which encodes a plasma membrane bound LRR-RLK (Mizuno et al., 2007). *rpk2* mutants displayed insufficient secondary thickening in the endothecium and were indehiscent. Mizuno et al. propose that either RPK2 is required for endothecial thickening or else other developmental defects, including an undifferentiated middle layer and

an enlarged vacuolated tapetum, inhibit the normal development of the endothecium (Mizuno et al., 2007).

1.2.2 Variation in anther dehiscence between different species

Overall the process of anther dehiscence is quite conserved, however differences in the structural formation of the anther and the mechanism of anther opening do exist (Wilson et al., 2011). Structural differences amongst the *Solanaceae* have been well studied. Dehiscing anthers are most commonly longitudinal but in *Solanum* they are often poricidal or poricido-longitudinal depending upon the opening shape of the stomium (Carrizo García et al., 2008). Poricidal anthers open through a pore at the apex, whereas longitudinal anthers open along a slit on the lateral side, and poricido-longitudinal anthers open via a pore connected to a longitudinal slit (Carrizo García et al., 2008). Similarly in the *Poaceae*, anther opening occurs either at the apex, or through a longitudinal slit, or at the apex and the base of the slit (Keijzer et al., 1996). Differences in the speed, timing and extent of pollen release influences how pollination occurs, for example in poricidal anthers the pollen remains enclosed until vibrations from a pollinator release it (Bonner and Dickinson, 1989; Carrizo García et al., 2008). Another characteristic typical of the *Solanum s*pecies is the differentiation of subepidermal cells into a circular cell cluster which accumulates calcium oxalate crystals. The circular cell cluster is located in the notch region of the anther and has been described in detail in tobacco (Sanders et al., 2005). It has been shown in *Petunia* that these crystals adhere to the pollen after the circular cell cluster degenerates and later dissolve into aqueous drops located on the surface of the stigma. It seems that the subsequent increase in calcium concentration on the stigma enables pollen germination to occur (Iwano et al., 2004).

The most disputed point in the mechanism of anther opening is the rupture of the septum, which has been attributed to both mechanical

rupture and enzymatic lysis (Matsui et al., 2000). In *Hordeum distichum* (two-rowed barley), forced opening of the florets revealed a link between pollen grain swelling and the rupture of the septum and stomium (Matsui et al., 2000). The septum only ruptured in florets at the middle of the inflorescence (panicle) where the pollen grains were mature and able to swell. In these anthers, the stomium subsequently split at the apex as a result of: combined pressure from locule wall bending and pollen swelling. Pollen swelling occurs rapidly and therefore cannot be attributed to the breakdown of starch within the pollen. It is hypothesised that an influx of K^+ ions into the pollen causes water to follow by osmosis (Matsui et al., 2000). This mechanism for anther opening has also been observed in *Oryza sativa* (rice), which suggests that it may be characteristic of the *Poaceae* (Matsui et al., 1999a). The rice mutant *anther indehiscence 1* (*aid1*) has some sterile spikelets which are indehiscent. In the sterile spikelets, the septum and stomium remain intact, which is thought to be due to a lack of pollen pressure caused by small pollen grains that do not accumulate starch properly (Zhu et al., 2004). In other species rupture of the septum has been largely attributed to enzymatic lysis. Keijzer showed that force generated from the dehydration of the endothecium was not required to open the septum (Keijzer, 1987). In tomato, the presence of ricinosomes was detected in the cells of the septum, endothecium, middle layer, connective tissue and epidermal cells in proximity to the stomium (Senatore et al., 2009). Ricinosomes are PCD specific organelles derived from the rough-endoplasmic reticulum. They contain enzymes which are released as the vacuole collapses during PCD. The presence of these particular organelles in tomato confirms that, in this species at least, enzymatic lysis of the septum is central to its degradation (Senatore et al., 2009).

In *Zea mays* (maize), lysis of the cell walls of both septum and stomium cells is a prerequisite for anther opening (Keijzer et al., 1996). The breakdown of the radial walls of epidermal cells making up the stomium begins after the septum and was sufficient to open

the stomium completely over a longitudinal slit. This was subsequently followed by outward locule wall bending caused by the presence of secondary thickening in the endothecium cells and desiccation resulting mainly from low relative humidity and evaporation (Keijzer et al., 1996). Experiments in rice confirm that the outward bending of the locule wall requires desiccation (as this does not occur in one hundred percent relative humidity) but the rupture of septum and stomium do not (Matsui et al., 1999b). These subtle differences in the dehiscence process between different species illustrate how regulation of septum and stomium rupture, and the outward bending of the locule wall, vary. The former are typically more programmed events, while the latter is susceptible to influence by the environment (García et al., 2006).

1.2.3 Hormonal regulation of dehiscence in *Arabidopsis thaliana*

The plant hormone jasmonic acid (JA), and its derivatives-jasmonates, regulate a number of developmental processes as well as co-coordinating responses to biotic and abiotic stresses (Wasternack and Hause, 2013). JA is synthesized from precursor linolenic acid, and biosynthetic mutants are affected in key steps of the biosynthesis pathway. These include: fatty acid desaturase triple mutant *fad3-2 fad7-2 fad8*, *DEFECTIVE IN ANTHER DEHISCENCE1 (dad1), DELAYED DEHISCENCE1* and *2* (*dde1/2)* and *opr3* (Ishiguro et al., 2001; von Malek et al., 2002; McConn and Browse, 1996; Park et al., 2002; Sanders et al., 2000; Stintzi and Browse, 2000). Mutants of the biosynthetic pathway share phenotypic features of delayed dehiscence, a reduction in pollen viability and the elongation of filaments. This, combined with the fact that mutant phenotypes can be rescued by the application of JA, supports a role for JA in regulating pollen release (Scott et al., 2004). *DAD1*, encoding an enzyme catalysing an early stage of JA biosynthesis, has been identified as a

direct regulatory target of homeotic C class gene *AGAMOUS* (Ito et al., 2007b). The finding that *AGAMOUS* mediates late stamen development through *DAD1* offers an insight into how homeotic genes manage to co-ordinate the development of whole organs (Ito et al., 2007b). The role of JA in dehiscence is further supported by the male sterile *coi1* signalling mutant which also has shorter filaments, abnormally vacuolated pollen and is non-dehiscent. *COI1* encodes an F-box protein which, in the presence of JA flags negative repressors of the JA response for degradation via ubiquitination. In the mutant, negative repressors cannot be removed even in the presence of JA, so therefore plants are unresponsive to endogenously applied JA (Feys et al., 1994; Wasternack and Hause, 2013; Xie et al., 1998).

While there is no doubt that jasmonates are required for normal dehiscence, the exact role of JA remains to be elucidated. Morphological examination of the *dad1* mutant revealed that all aspects of the dehiscence program were normal up to immediately before stomium rupture (Ishiguro et al., 2001). At the time of flower opening, dehydration of the endothecium and subsequently breakage of the stomium, had not yet occurred (Ishiguro et al., 2001). Based on these observations Ishiguro et al. advocated a model for how JA regulates water transport in the anthers (figure 1.5), suggesting that JA regulates the expression of genes related to water movement (Ishiguro et al., 2001). A wider role for JA has also been proposed, postulating JA regulates anther PCD (Zhao and Ma, 2000).

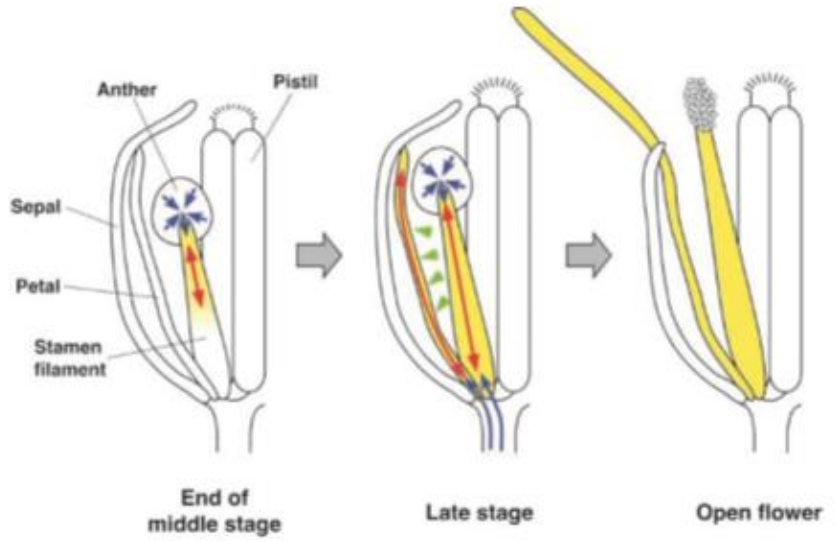

Figure 1.5: Model for JA regulated water transport within the anther. Figure adapted from (Ishiguro et al., 2001).

The petals and filaments actively take up water (blue arrows) and elongate (red arrows) in response to JA initially produced in the upper part of the filament. Water moves from the anther locules to the filament. By the late stage JA is being produced throughout the filament, causing water to be taken up from the pedicels and the anther walls, giving rise to filament elongation and dehiscence. Transmission of JA is shown with green arrows.

Transcriptional profiling experiments have shown that jasmonates act via a complex signalling network to instigate JA responses. Two transcription factors that were highly expressed in the stamens in response to JA were *MYB21* and *MYB24* (Mandaokar and Browse, 2009; Mandaokar et al., 2006). The *myb21* mutant has filaments which fail to elongate and delayed dehiscence while the *myb21myb24* double mutant fails to dehisce altogether. Application of exogenous jasmonate didn't rescue the mutant phenotypes, which suggests that these MYB proteins could act as components of a jasmonate response like COI1 (Mandaokar et al., 2006). More recently it was shown that a third MYB transcription factor, MYB108, works in conjunction with MYB24 and downstream of MYB21 to mediate JA induced responses for male fertility (Mandaokar and Browse, 2009). There are also various upstream mechanisms that control late stamen development by regulating JA biosynthesis. Gibberellic acid (GA) also modulates floral development, partially (although not totally) through MYB transcription factors including MYB21 and MYB24, and this seems to

be through upstream regulation of the JA pathway (Cheng et al., 2009). Recently two new regulators of anther dehiscence have been identified in *Arabidopsis*. The first, *DEFECTIVE IN ANTHER DEHISCENCE1 (DAD1)-Activating Factor (DAF1),* is a ring type E3 ligase that upregulates the expression of *DAD1,* presumably through the targeting of unknown repressor proteins for ubiquitination (Peng et al., 2013). The second, *ANTHER INDEHISCENCE FACTOR (AIF),* is a NAC-like gene and a negative repressor that reduces expression of genes in the JA biosynthetic pathway (Shih et al., 2014). *AIF* is expressed in the anthers, pollen and upper filaments during anther stages 7-11. Expression of *AIF* significantly decreases from flower stage 12, enabling JA biosynthesis in the stamen and dehiscence. Ectopic expression of *AIF* caused complete indehiscence (Shih et al., 2014).

There is evidence that auxin also plays a part in late stamen development through the regulation of JA. Expression of auxin biosynthesis genes *YUC2* and *YUC6* has been shown to be required for normal pollen and anther development (Cecchetti et al., 2008; Cheng et al., 2006). *YUC2* and *YUC6* are expressed in the anther from stage 8, with expression decreasing to nothing between stages ten to twelve (Cecchetti et al., 2008). Auxin response factors (ARFs) activate auxin responsive genes, although in the absence of auxin they are inhibited by negative repressors (Aux/IAA proteins) (Kepinski and Leyser, 2002). In the *arf6arf8* double mutant, JA levels are low and anthers fail to dehisce, however the phenotype can be rescued by the application of JA (Nagpal et al., 2005; Tabata et al., 2010). It has been suggested that *ARF6* and *ARF8* repress class I *KNOX* genes, which are repressors that inhibit JA biosynthesis via the suppression of *DAD1* (Tabata et al., 2010).

Genes encoding auxin receptors are essential for an auxin response, as these receptors interact with auxin and enable the removal of Aux/IAA proteins from ARFs (Kepinski and Leyser, 2002). Conversely, in the quadruple auxin receptor mutant *tir1afb1afb2afb3*, dehiscence occurs early and levels of JA biosynthetic genes *DAD1* and *OPR3* are

increased, suggesting that auxin negatively regulates JA biosynthesis (Cecchetti et al., 2008, 2013). Cecchetti et al. also found that *MYB26* was negatively regulated by auxin and they propose that as auxin levels decrease at anther stages 11-12, levels of both *MYB26* and *JA* increase and independently enable dehiscence to occur (figure 1.6) (Cecchetti et al., 2013). Further support for the role of auxin as a negative repressor of JA biosynthesis in late stamen development, comes from the mp^{abn} allele. *MONOPTEROS (MP)* is an ARF, and the gain-of-function mp^{abn} allele lacks the domain required to interact with Aux/IAA repressors and is therefore constitutively switched on (Garrett et al., 2012). As mp^{abn} has a non-dehiscent phenotype which can be rescued by the application of JA, this suggests that *MP* activates expression of a negative repressor which represses JA biosynthetic genes. A possible explanation for the opposing roles identified for *MP* and *ARF6/8* in auxin-dependent regulation of JA, is that the level of JA activation depends on the relative balance of the activities of these factors (Garrett et al., 2012).

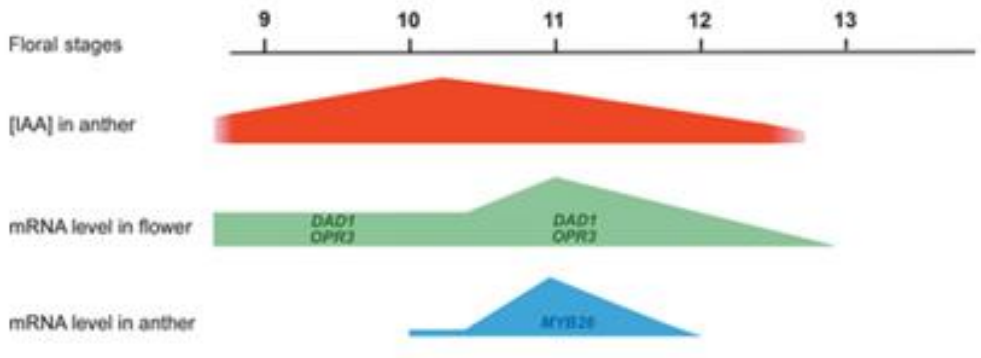

Figure 1.6: Model for hormonal control of anther dehiscence. Figure adapted from (Cecchetti et al., 2013).

Auxin concentration (red), *DAD1/OPR3* mRNA levels (green) and *MYB26* mRNA level (blue), are shown at flower stages 9-13.

1.3 Factors affecting water flux during pollen and anther development

The development of the male gametophyte can be divided into distinct phases which require specific hydration levels (Firon et al., 2012). During pollen development, pollen grains gain water and increase in volume during intine and exine wall formation, then lose water reaching a minimum content when they are fully mature (Firon et al., 2012). Pollen desiccation induces a metabolically dormant state that enables survival of environmental stresses experienced during dispersal (Taylor and Hepler, 1997). After degeneration of the tapetum the locular fluid surrounding the pollen grains is reabsorbed in preparation for pollen release (Pacini, 2000). Following dispersal, and providing it lands on a compatible stigma under suitable conditions, rehydration of the pollen grain triggers a transition to a period of active growth whereupon the pollen germinates and produces a pollen tube which delivers the sperm cells to the embryo sac of the ovary (Firon et al., 2012; Selinski and Scheibe, 2014). The molecular mechanisms that enable these changes in pollen water content include: water transport via aquaporins, (universal protein membrane channels, see section 3.1), and osmoregulation via the accumulation of various carbohydrates and proline (Firon et al., 2012).

Changes to the water status of the anther are critical to the biomechanical process of anther opening and result from active processes, evaporation, or both (Nelson et al., 2012). It is generally accepted that low relative humidity accelerates anther opening, while high relative humidity reduces passive transpiration from the anther, resulting in delayed or inhibited dehiscence (Firon et al., 2012). In *Ricinus communis* L. (castor bean), a relative humidity of 98% completely prevented anther opening, while in *Gasteria verrucosa,* the presence of open stomata on the anthers was shown to affect the speed of anther opening (see section 5.1) (Bianchini and Pacini, 1996; Keijzer, 1987). The method of dehydration varies between

species however, and in *Solanum Lycosperium* (tomato) and *Petunia hybrida* there is evidence of an active process taking place (section 4.1) (Bonner and Dickinson, 1989; Ge *et al*., 2000, 2001). In *Arabidopsis*, water movement as a result of ion accumulation is important for anther opening. The double mutant *nhx1 nhx2,* which lacks two vacuole located Na^+/K^+(NHX) antiporters, had reduced filament extension and predominantly indehiscent anthers. It seems that K^+ accumulation contributes to an osmotic driving force required for filament cell expansion and anther dehiscence (Bassil et al., 2011).

Aquaporins are required for normal anther dehiscence in tobacco (Bots et al., 2005a). Based on their findings, Bots et al. proposed a model for the role of aquaporins in the dehydration process. They suggested that the presence of PIP2 aquaporins in the connective tissue and anther walls, combined with the breakdown of the tapetum, enables hydraulic continuity throughout the anther. This, when combined with an osmotic gradient, draws water into the vascular bundle (Bots et al., 2005a). Stadler et al. hypothesise that, in *Arabidopsis*, accumulation of sucrose in the connective tissue prior to dehiscence, creates an osmotic gradient that causes dehydration of the endothecium (section 4.1) (Stadler et al., 1999). Another developmental process that requires the redistribution of carbohydrates for osmoregulation, is flower opening. Flower opening enables pollinators to access male and bisexual flowers, and leads to pollination and fertilization in female and bisexual flowers (Doorn et al., 2003). This usually rapid process is caused by an uneven growth of the petals; the adaxial side grows more rapidly than the abaxial side due to differential osmoregulation induced by sucrose import or mobilization of storage carbohydrates (Beauzamy et al., 2014; Doorn et al., 2003).

1.4 Project Aims and Applications

Dehydration of the anther is essential for dehiscence (section 1.2.1) however the genetic control of this process has not been extensively studied. Knowledge of pollen and anther development is not only extremely important for understanding the process of plant sexual reproduction but also for plant breeding. Control over pollen release can be used to restrict the spread of genetically modified (GM) pollen and protect the environment (Wilson and Zhang, 2009). The production of higher yielding hybrid crops requires male sterile lines to prevent inbreeding and promote outcrossing. As a result of heterosis (hybrid vigour) plants are phenotypically superior with proven yield increases (Wilson and Zhang, 2009).

The aim of this project was to investigate the genetic factors controlling water movement within *Arabidopsis thaliana* stamens and to analyse the role of stomata on anthers, so as to elucidate the dehydration process required for anther dehiscence and pollen release in *Arabidopsis*.

The expression patterns and potential function of ***Arabidopsis* aquaporin genes** in anthers, were investigated by qRT-PCR analysis and using GUS reporter and single T-DNA insertional lines (chapter 3).

The expression patterns, and potential function of ***Arabidopsis* sucrose transporter genes** in anthers, were investigated by qRT-PCR analysis and using GUS reporter and single T-DNA insertional lines (chapter 4).

The occurrence and patterning of **stomata on anthers** was analysed, and the significance of their presence for facilitating water loss via evaporation was investigated (chapter 5).

CHAPTER 2 MATERIALS AND METHODS

2.1 Plant Material and Growth Conditions

2.1.1 Plant Material for Chapter 3

Seed for *Arabidopsis* single T-DNA insertion lines was obtained from The Nottingham *Arabidopsis* Stock Centre (NASC). Seed for the *pip1;2pip2;1*, *pip1;2pip2;1pip2;6* double and triple mutants and *PromPIP1;2*-GFP-GUS*, PromPIP2;1*-GFP-GUS, reporter lines was kindly supplied by Christophe Maurel (CNRS - Centre national de la recherche scientifique). The PIP1;5pro::PGWB3 and PIP2;7pro::PGWB3 GUS reporter lines were generated in the Wilson Lab, University of Nottingham. Seed for *myb26* single mutant came from the Wilson Lab. Basic information for each of the lines is summarised in table 2.1. Plants were grown under the growth conditions described in section 2.1.4.

Table 2.1: Summary of *Arabidopsis* aquaporin lines, Hm, homozygous.

Gene(s)	AGI Code (s)	Line	Reference
myb26	AT3G13890	Single mutant (Segregating)	(Dawson et al., 1999)
pip2;5	AT3G54820	Single T-DNA insertion mutant SALK_072405	(Alonso et al., 2003)
pip2;6	AT2G39010	Single T-DNA insertion mutant SALK_118213	(Alonso et al., 2003)
pip2;7	AT4G35100	Single T-DNA insertion mutant SALK_068839	(Alonso et al., 2003)
pip2;8	AT2G16850	Single T-DNA insertion mutant SALK_099098	(Alonso et al., 2003)
dad1	AT2G44810	Single T-DNA insertion mutant SALK_138439	(Alonso et al., 2003)
pip1;2pip2;1	AT2G45960 AT3G53420	Double mutant (Hm)	(Prado et al., 2013)
pip1;2pip2;1pip2;6	AT2G45960 AT3G53420 AT2G39010	Triple mutant (Hm)	(Prado et al., 2013)
PIP1;2	AT2G45960	*PromPIP1;2*-GFP-GUS	(Postaire et al., 2010)
PIP2;1	AT3G53420	*PromPIP2;1*-GFP-GUS	(Péret et al., 2012)
PIP1;5	AT4G23400	*PIP1;5*pro::PGWB3 (GUS reporter line)	Section 3.2.2
PIP2;7	AT4G35100	*PIP2;7*pro::PGWB3 (GUS reporter line)	Section 3.2.2

Single T-DNA insertion lines were genotyped by two separate PCR reactions (section 2.2.3.2) using gene specific primers and a primer specific to the T-DNA left border (LB1b.3F). Primers used for genotyping the T-DNA insertions lines are given in table A1.

2.1.2 Plant Material for Chapter 4

Seed for *Arabidopsis* single T-DNA insertion lines was obtained from The Nottingham *Arabidopsis* Stock Centre (NASC). The SUC1pro::PGWB3 GUS reporter line was generated in the Wilson Lab, University of Nottingham. Basic information for each of the lines is summarised in table 2.2. Plants were grown under the growth conditions described in section 2.1.4.

Table 2.2: Summary of *Arabidopsis* sucrose transporter lines.

Gene	AGI Code	Line	Reference
suc1	AT1G71880	Single T-DNA insertion mutant SALK_072405	(Alonso et al., 2003)
suc2	AT1G22710	Single T-DNA insertion mutant SALK_072405	(Alonso et al., 2003)
suc5	AT1G71890	Single T-DNA insertion mutant SALK_118213	(Alonso et al., 2003)
dad1	AT2G44810	Single T-DNA insertion mutant SALK_138439	(Alonso et al., 2003)
SUC1	AT1G71880	SUC1pro::PGWB3 (GUS reporter line)	Section 4.2.2

Single T-DNA insertion lines were genotyped by two separate PCR reactions (section 2.2.3.2) using gene specific primers and a primer specific to the T-DNA left border (LB1b.3F or LB3F). Primers used for genotyping the T-DNA insertions lines are given in table A2.

2.1.3 Plant Material for Chapter 5

2.1.3.1 *Arabidopsis thaliana* lines

Seed for eight *Arabidopsis* lines with changes in stomatal development was supplied by Professor Julie Gray (University of Sheffield). Basic information for each of the lines is summarised in

table 2.3. Plants were grown under the growth conditions described in section 2.1.4.

Table 2.3: Summary of *Arabidopsis* lines with altered stomatal development. Hm, homozygous.

Gene (s)	AGI code(s)	Line	Reference
sdd1	AT1G04110	Single mutant (Hm)	(Hunt and Gray, 2009)
tmm	AT1G80080	Single mutant (Hm)	(Hunt and Gray, 2009)
basl tmm	AT1G80080 AT5G60880	Double mutant (Hm)	(Hunt and Gray, 2010)
STOMAGEN	AT4G12970	Overexpression (Hm)	(Hunt et al., 2010)
EPF2	AT1G34245	Overexpression (segregating)	(Hunt and Gray, 2009)
EPFL7	AT1G71866	Overexpression (Hm)	Dutton et al. (submitted)
focl1_1	AT2G16630	Single mutant (Hm)	(Hunt et al., 2017)
focl1_2	AT2G16630	Single mutant (Hm)	(Hunt et al., 2017)

The *EPF2* overexpressing line was segregating for the vector, therefore plants were genotyped to identify those overexpressing *EPF2* (figure 2.1). Transformed plants were identified by a single PCR reaction (section 2.2.3.2) which used primers EPF2F and EPF2R (primer specific annealing temperature=59°C), to amplify a 691bp fragment of the vector. The *EPF2* transgene was inserted between the att sites of the ctapi vector (see appendix), the forward primer was located within *EPF2* region and the reserve primer in the ctapi region.

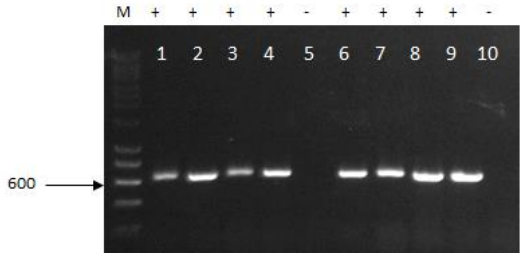

Figure 2.1: Genotyping example for *EPF2 OE* line.

Lanes 1-10 show DNA amplified from ten plants using primer pair EPF2F (TCAGTCGCCGAATCATGTAG)/EPF2R (CTTCAGGCTCTGGATGAAGG). +/- indicates the presence/absence of the vector fragment. The size of the amplicon is 691bp. M, hyperladder™ 1kb

2.1.3.2 *Triticum aestivum* (wheat) lines

The wheat variety Fielder is a hexaploid bread wheat. Over-expression constructs for a wheat orthologue of *EPF1/EPF2* (named *TaEPFL1*) were made at the University of Sheffield. The *TAEPFL1* gene (TGACv1_scaffold_641036_U: 17,763-18,194) was isolated from genomic DNA and plants were transformed by NIAB (National Institute of Agricultural Botany) using the vector pSc4Act-R1R2-SCV, which is under the control of the rice actin promoter. Plants were grown in a growth chamber under a 12-hour photoperiod in controlled conditions: 22/16C day/night temperature, 60% relative humidity and 400umol photons/m^2/s light intensity.

2.1.4 General Growth Conditions

Arabidopsis thaliana seeds were sown in 9cm diameter pots or 12 cell Plant Plug Trays (Dejex) in Levington M3 compost (Everris). Pots were encased in plastic sleeves, and trays were covered with transparent plastic propagator lids, to retain humidity for germination. The plastic sleeves, and/or air vents on the propagator lids were opened 2-3 d after germination. Propagator lids were removed by the four-rosette leaves stage, to prevent etiolation of seedlings. Plants were grown in a growth room under a 16 h photoperiod in controlled conditions; day/night temperatures of 21/18ºC (+/- 2ºC), and a light intensity of 111umol s^{-1} m^{-2}, provided by warm, white fluorescent lights.

2.1.5 Staging of *Arabidopsis thaliana* flower buds

Flower buds of *Arabidopsis thaliana* were collected in four stages based on size and position. Within each bud stage there are several phases of pollen development (table 2.4) which correspond to

previously described flower and anther stages (Sanders et al., 1999; Smyth et al., 1990).

Table 2.4: Description of *Arabidopsis thaliana* bud stages, including pollen development and corresponding flower and anther stages. Adapted from (Vizcay-Barrena, 2005).

Bud Stage	Pollen Development Stage	Flower Stage	Anther Stage
4	Dehiscence	13	13
		13	13
	Bilocular anther containing tricellular pollen grains. Mitosis II	13	13
		11-12	12
3	Pollen mitosis I		
	Tapetum has	11-12	11
	degenerated almost completely. Septum cell degeneration initiated.	11-12	11
	Tapetum generation. Late ring stage.	11-12	10
2	Tapetum generation. Late ring stage.	11-12	10
	Ring Stage. Exine Wall formation.	10	9
		10	9
1	Ring Stage. Exine Wall formation.	10	9
	Microspores free within anther locule	10	8
	Tetrads of microspores free within anther locule	10	7

2.1.6 Transformation of *Arabidopsis thaliana* by floral dipping

Agrobacterium tumefaciens, carrying the destination vector and gene of interest, were cultured in 100ml LB at 28°C until the OD600 (optical density at a wavelength of 600nm) was between 1 and 2. 50ml of 5% (w/v) sucrose and 50ml 0.05% (w/v) Silwet L-77 were

added. 4-6 wk old newly flowered plants of *Arabidopsis* (accession *Landsberg-erecta, Ler-0*) were dipped into the solution for 1 min. The plant pots were encased in plastic sleeves which were folded down to retain humidity and the plants were placed out of direct light. 24 h later the plastic sleeves were opened and the plants were moved back into direct light.

2.1.7 Screening for transformed *Arabidopsis thaliana* seeds

One third of a 1.5ml microcentrifuge tube was filled with seeds of transformed *Arabidopsis thaliana* and 1ml 70% (v/v) ethanol was added. The ethanol and seeds were thoroughly mixed using a vortex mixer for 5 min. The tube was centrifuged for 3 min at 12,000rpm to separate the seeds and ethanol and enable the ethanol to be removed. The procedure was then repeated two more times. In a sterile laminar air flow cabinet 1ml 100% (v/v) ethanol was added before tipping the seeds onto sterile filter paper (Whatman) to dry. Dried seeds were spread evenly onto ½ MS media plates (see appendix) containing 50µg/ml kanamycin for selection and sealed with micropore tape. The transformed plants were identifiable by their more robust growth. After two weeks, transformed plantlets were transferred to 9cm diameter pots filled with Levington M3 compost (Everris). Pots were encased in plastic sleeves which were folded down to retain humidity; the sleeves were opened after 4 d. The transformed plants were grown in a glasshouse under a 22 h photoperiod in controlled conditions; temperatures of 22/20ºC (+/- 2ºC), and a light intensity of 111µmol s-1 m-2, provided by warm, white fluorescent lights.

2.2 DNA Extraction, Amplification and Purification

2.2.1 Sucrose method for crude DNA extraction from *Arabidopsis*

2-3cm young leaves of *Arabidopsis thaliana* were placed directly into individual labelled PCR tubes containing 100µl sucrose buffer (table 2.5) on ice. Samples were crushed with a yellow pipette tip then heated at 99-100°C for 10 min. The samples were micro-centrifuged briefly (5 s) at 2000-6000 x g and were either placed on ice for immediate use or stored at -20°C. 0.5-1µl of the supernatant was used for DNA amplification using the Polymerase Chain Reaction (section 2.2.3).

Table 2:5: Volume and concentration of individual components required to make 10ml sucrose buffer solution.

Component	Stock Concentration (M)	Desired Concentration (mM)	Volume required for 10ml (ml)
Tris-Cl (pH 7.5)	1	50	0.5
NaCl	4	300	0.75
Sucrose	2	300	1.5
dH_2O	-	-	7.25

2.2.2 Genomic DNA Extraction

1-2 mature leaves of *Arabidopsis thaliana* were placed into a 1.5ml Eppendorf tube and flash frozen in liquid nitrogen. Plant material was ground with a pestle in the presence of liquid nitrogen. Genomic DNA was extracted using Isolate II Plant DNA Kit (Bioline). Some changes were made to the DNA extraction protocol to maximise DNA yield. 400µl Lysis Buffer PA1 was added directly to the ground plant material and mixed thoroughly using a vortex mixer. The lysate was incubated at 65°C for 10 min. Filtration of the lysate, DNA binding and the washing and drying of the Isolate II Plant DNA Spin Column were all performed according to the manufacturer's instructions. DNA was eluted in 30µl (65°C) molecular grade water (Sigma-Aldrich).

2.2.3 DNA Amplification using the Polymerase Chain Reaction (PCR)

DNA was amplified in 10µl polymerase chain reactions (PCR) using 10-50ng template DNA and sequence specific primers. PCR reactions were performed using two different enzymes, Phusion High Fidelity Polymerase (Thermo Scientific) and Red Taq DNA Polymerase (VWR International), depending on the product to be obtained.

2.2.3.1 PCR using Phusion High Fidelity Polymerase

A single PCR reaction performed with Phusion High Fidelity Polymerase (Thermo Scientific) contained: 0.2µl (2.5mM) dNTPs, 0.15µl enzyme, 2µl 5 x GC or 5 x HF buffer (reaction specific), 0.3µl 100% DMSO (Thermo Scientific), 0.3µl (10pm/µl) forward and reverse primers and 6.64µl molecular grade water (Sigma-Aldrich). PCR conditions were; 30 s at 98ºC, 35 cycles of 30 s at 98ºC, 30 s at annealing temperature (primer specific), 30 s at 72ºC then a final 6 min extension at 72ºC.

2.2.3.2 PCR using Red Taq DNA Polymerase

A single PCR reaction performed with Red Taq DNA Polymerase (VWR International) contained: 5µl of enzyme, 0.3µl (10pm/µl) forward and reverse primers and 5µl molecular grade water (Sigma-Aldrich). PCR conditions were; 3 min at 94ºC, 35 cycles of 30 s at 94ºC, 30 s at annealing temperature (primer specific), 30 s at 72ºC then a final 6 min extension at 72ºC.

2.2.4 Agarose Gel Electrophoresis

PCR products were resolved by agarose (1-2% w/v) gel electrophoresis in 0.5 x TBE buffer (45mM Tris-borate, 1mM EDTA) by applying 100-125V for 1 h. 1µl loading buffer (Bioline) was added to each final reaction performed with Phusion High Fidelity DNA

polymerase (Thermo Scientific) prior to gel loading. The size of fragments was determined using an appropriate ladder (Bioline). The gel was stained with 500µg/ml ethidium bromide (Sigma-Aldrich) and photographed on an Ingenius^3 UV illuminator (Syngene).

2.2.5 Purification of PCR Products from Agarose Gels

DNA was extracted from agarose gels using QIAEX II Gel Extraction Kit (Qiagen) according to the manufacturer's instructions. Purified DNA was eluted in 20µl of molecular grade water (Sigma-Aldrich).

2.2.6 Purification of PCR Products

Direct purification of PCR products was performed using QIAquick purification kit (Qiagen) according to the manufacturer's instructions. The purified PCR product was eluted in 25ul of molecular grade water (Sigma-Aldrich).

2.3 Expression Analysis

2.3.1 RNA Extraction

RNA was extracted from *Arabidopsis* buds using commercially available RNeasy Plant Mini Kit (Qiagen). The RNA extraction protocol was slightly changed to maximize RNA purity. A longer incubation of 5 min at 56ºC was used to disrupt tissue after the addition of buffer RLT. The lysate, transferred to a QIAshredder spin column within a 2ml collection tube, was micro-centrifuged at full speed for 10 min to pellet cell debris. An optional On-Column DNase Digestion was performed with an RNase-Free DNase Set (Qiagen). Following the addition of the DNase 1 incubation mix to the RNeasy spin column membrane, the DNA digestion was extended to 45 min. A second application of DNase 1 incubation mix was followed by a further 45 min incubation at room temperature before the addition of Buffer RW.

30µl of molecular grade water (Sigma-Aldrich) was used to elute the purified RNA in the final stage. The concentration of extracted RNA was measured using NanoDrop Spectrophotometer 2000 (Thermo Scientific).

2.3.2 cDNA Synthesis

cDNA was synthesized using 1.5-5µg of total RNA. 1µl (0.5µg/µl) oligo (dT), 1µl (10mM) dNTP and the volume of molecular grade water required to make a final volume of 13µl, were added to a 0.6ml microcentrifuge tube. The substrates were heated at 65ºC for 5 mins then immediately incubated on ice for 1 min. 4µl 5x First Strand Buffer, 1µl (0.1M DTT), 1µl (40 units/µl) RNase OUT and 1µl (200 units/µl) Superscript3 (all Life Technologies) were added prior to a 1 h incubation at 50ºC. The reaction was deactivated by heating at 70ºC for 15 min.

2.3.3 qRT-PCR

qRT-PCR was performed in a 384 well reaction plate using SYBR green enzyme (Fermentas) and the LightCycler480 (Roche). The reaction was heated at 95ºC for 10 min, then 45 cycles of 95ºC for 30 s, 60ºC for 30 s and 72ºC for 1 min. Experiments were performed either in duplicate or triplicate and expression levels were normalised to house-keeping gene *PP2A-3* (AT2G42500). Primer pairs for reference and target genes are supplied in table A3.

2.4 Molecular Cloning using TOPO Clone® and Gateway Technology®

2.4.1 Overhanging

Overhanging is necessary to clone fragments amplified using Phusion High Fidelity DNA Polymerase (Thermo Fisher Scientific,

Loughborough, UK) into TOPO cloning vectors (Life Technologies Ltd, Paisley UK). 15µl blunt-ended PCR product was incubated at 72ºC for 15 min with 1.5µl 10x standard Taq reaction buffer (NEB), 0.5µl (2.5mM) dATP and 0.3µl (500 units/ml) qTaq. qTaq was supplied by the Genomic Facility, Plant and Crop Sciences, University of Nottingham (GF UoN) to create an 'overhanging' product for gene cloning.

2.4.2 TOPO® TA-Gene Cloning

TOPO® TA-Gene cloning was performed using vector PCR8/GW/TOPO (Life Technologies) with PCR product amplified using Phusion High Fidelity Polymerase (Thermo Scientific) and treated as described in section 2.4.1. 0.5-4µl PCR product, 1µl of the vector, 1µl salt solution (Life Technologies), and the volume of molecular grade water required to make up a final volume of 6µl, were added to a 0.6ml microcentrifuge tube and left overnight at room temperature.

2.4.3 Transformation of *Escherichia coli* using heat shock method

6µl overnight solution, described in section 2.4.1.2, was added to chemically competent DH5 alpha *E. coli* cells (supplied by GF UoN) in a 0.6ml microcentrifuge tube and incubated on ice for 30 min. Cells were heat shocked for 1 min 30 s at 42ºC in water bath and then transferred immediately to ice for 1 min. 250µl of room temperature SOC medium (see Appendix) was added. The tube containing the SOC medium and transformed cells was shaken horizontally at 200rpm, for 1 h 30 min at 37ºC.

Transformed cells were plated onto LB media selection plates (see appendix) containing the appropriate antibiotic for selection and incubated overnight at 37ºC. 10µl colony PCR reactions were performed and liquid cultures were set up for colonies containing both vector and gene of interest. Liquid cultures utilized 10ml LB media

(see Appendix) in 30ml sterile tubes, with the appropriate antibiotic for selection, and were incubated overnight at 37ºC.

2.4.4 Plasmid Extraction

Plasmid extraction was performed using Gen Elute Plasmid MiniPrep Kit (Sigma-Aldrich). 10ml of overnight liquid culture was centrifuged and the pellet used for plasmid extraction. Extracted plasmids were eluted in 50µl molecular grade water (Sigma-Aldrich).

2.4.5 Sequencing of Plasmid DNA

Plasmid samples were prepared at a concentration of 50-100ng/µl and sent for sequencing by Eurofins MWG Operon. To initiate sequencing 1.5µl of a vector specific primer was included with the sample, and water molecular grade (Sigma-Aldrich) was used to make the final volume up to 15µl.

2.4.6 LR Reaction

LR reaction was performed using 50ng of entry clone PCR8/GW/TOPO (Life Technologies) containing the gene of interest, 100ng of destination vector PGWB3 (supplied by GF UoN) and 1.5µl LR clonase enzyme (Life Technologies). Molecular grade water (Sigma-Aldrich) was used to make up a final volume of 6µl in a 0.6ml microcentrifuge tube and the reaction was left overnight at 25ºC. 1.5µl Proteinase K (Life Technologies) was added to the overnight LR reaction mixture and incubated at 37°C for 10 min. Competent *E. coli* DH5 alpha cells (supplied by GF UoN) were transformed with the LR reaction mixture, using the *E. coli* transformation protocol described in section 2.4.3.

Transformed cells were plated onto LB media selection plates, containing 50µg/ml kanamycin and incubated overnight at 37°C. 10µl colony PCR reactions were performed to identify colonies containing both vector and insert in the correction orientation. Colonies were then plated onto fresh LB media selection plates,

containing 50µg/ml spectinomycin, to confirm that they did not also contain the entry vector PCR8/GW/TOPO (Life Technologies). Liquid colonies were set up in 10ml LB media in 30ml sterile tubes, with 50µg/ml kanamycin for selection, and were incubated overnight at 37ºC prior to plasmid extraction.

2.4.7 Storage of Bacteria as Glycerol Stocks

Colonies containing the vector and gene of interest were incubated overnight (*Agrobacterium tumefaciens*; 28ºC, *E. coli*; 37ºC) in 10ml LB with the appropriate antibiotic for selection. To prepare 1ml of glycerol stock 750µl of cell culture was added to 250µl autoclaved 80% glycerol in a 2ml cryo eppendorf tube. Tubes were frozen in liquid nitrogen before storing at -80ºC.

2.4.8 Electroporation of Bacteria

Electroporation of *Agrobacterium tumefaciens* was performed using *Agrobacterium* strain GV3101 electro competent cells (supplied by GF UoN). The cells were placed inside a 2mm electroporation cuvette with 100ng of destination vector PGWB3 with insert. The cells were electroporated using Gene Pulser (Bio-rad) set at 2.5kv 25Mfd, 400 Ohms. Bacterial cells were re-suspended in 250µl of LB media inside the cuvette, before being transferred to a 1.5ml microcentrifuge tube and incubated at 28°C for 3 h. Electroporated cells were cultured on LB media selection plates containing 50µg/ml kanamycin and 30µg/ml rifampicin and incubated at 28°C for 3-4 d.

2.4.9 Cloning of GUS Reporter Constructs

2.4.9.1 Cloning of GUS Reporter Constructs for Chapter 3

The promoter sequences of *PIP1;5* and *PIP2;7* were amplified by PCR (section 2.2.3.1) and cloned into Gateway compatible destination vector PGWB3 to create *PIP1;5*pro::PGWB3 and *PIP2;7*pro::PGWB3 (see appendix for vector maps). DNA was extracted from transformed

plants (section 2.2.2) and the presence of the insert was confirmed by PCR. Primers used for cloning and the sizes of the promoter sequences are given in table 2.6. Vectors were provided by the Genomic Facility, Plant and Crop Sciences, University of Nottingham.

Table 2.6: List of primers used for cloning of GUS reporter constructs. The size of the amplicon for the promoter sequences is given in base pairs. Primers were designed using Primer 3 (Koressaar and Remm, 2007; Untergasser et al., 2012).

AGI Code	Primer Name	Primer Sequence 5'-3'	Annealing Temperature °C	Size of amplicon (bp)
AT4G23400	PIP1;5pro_F1	CCATAGTGGTCATCTTTGTA	58	1890
	PIP1;5pro_R1	ATTTGATGACTGGTGTATGT		
AT4G35100	PIP2;7pro_F1	CACTGCGTAATGTTGCCTGA	64	1949
	PIP2;7pro_R1	CGCTCACTTCTTTCGACATCTT		
AT4G23400	PIP1;5pro_F2	TCAAAAGAGACTTGAGTGCGAC	59	n/a
AT4G35100	PIP2;7pro_F2	CCCTGGCATTACAAGGGTTT	59	n/a
n/a	M13F	TGTAAAACGACGGCCAG	59	n/a
n/a	M13R	CAGGAAACAGCTATGAC	59	n/a
n/a	GUS_PGWB3_138R	AGCAATTGCCCGGCTTTCTT	59	n/a

2.4.9.2 Cloning of GUS Reporter Constructs for Chapter 4

The promoter sequence of *SUC1* was amplified by PCR (section 2.2.3.1) and cloned into Gateway compatible destination vector PGWB3 to create *SUC1*pro::PGWB3 (see appendix for vector map). DNA was extracted from transformed plants (section 2.2.2) and the presence of the insert was confirmed by PCR. Primers used for cloning and the size of the promoter sequence is given in table 2.7. Vectors were provided by the Genomic Facility, Plant and Crop Sciences, University of Nottingham.

Table 2.7: List of primers used for cloning of SUC1pro::PGWB3. The size of the amplicon for the promoter sequence is given in base pairs. Primers were designed using Primer 3 (Koressaar and Remm, 2007; Untergasser et al., 2012).

AGI Code	Primer Name	Primer Sequence 5'-3'	Annealing Temperature °C	Size of amplicon
AT1G71880	SUC1pro_F1	TCGATTCCCAAAACACGCT	64	1872
	SUC1pro_R1	GTAGGAGATGAGAGAATGGAGTT		
AT1G71880	SUC1pro_F2	CGTGTCCCTACCTTGCCATA	59	n/a
n/a	M13F	TGTAAAACGACGGCCAG	59	n/a
n/a	M13R	CAGGAAACAGCTATGAC	59	n/a
n/a	GUS_PGWB3_138R	AGCAATTGCCCGGCTTTCTT	59	n/a

2.5 Staining Methods

2.5.1 FDA Staining

Fluorescein diacetate (FDA) staining can be used to determine the viability of pollen grains. Live cells convert FDA into fluorescein, a metabolite which fluoresces green under blue light, thereby enabling

discrimination of live/dead cells by colour (Heslop-Harrison and Heslop-Harrison, 1970). 1µl FDA solution (4mg/ml) was added to 1ml BK buffer S15 MOPS (pH 7.5) (table 2.8) in a 1.5ml Eppendorf tube. Open flowers were dipped into 20µl aliquots of the solution in 0.6ml Eppendorf tubes. The second or third fully open flower of an inflorescence was used each time. Several flowers of the same stage were pooled from each plant and ten biological replicates were used. All of the solution was mounted onto a slide and the number of live/dead pollen cells were counted under blue light using a Leica DM5000 B microscope (Leica Microsystems).

Table 2:8: Components and quantities required to make up 5ml of BK buffer S15 MOPS

Component	Quantity/Volume required for required 5ml
MOPS	500µl
Sucrose	0.75g
0.1M $Ca(NO_3)_2$	6.35µl
0.1M $MgSO_4$	4.05µl
0.1M KNO_3	5µl

2.5.2 β-glucuronidase (GUS) Staining

Whole inflorescences of *Arabidopsis thaliana* GUS lines were placed directly into 0.6ml microcentrifuge tubes covered in foil and incubated overnight at 37°C in 150µl of β-glucuronidase substrate solution. The components of solutions required to make up β-glucuronidase substrate solution are given in table 2.9. Clarification of plant material was conducted by adding 150µl of the following solutions; 20% acidified methanol (HCl/methanol/water 4:20:76 (v/v)) at 55°C for 20 min, 7% (w/v) sodium hydroxide in 70% (v/v) ethanol at room temperature (RT) for 20 min, 40% (v/v) ethanol at RT for 20 min, 20% (v/v) ethanol at RT for 20 min, 10% (v/v) ethanol at RT for 10 min. At each stage of the clarification, the previous solution was carefully removed prior to adding the next substrate. Following clarification plant material was stored in 50% (v/v) glycerol until use. Floral organs were dissected under a stereo microscope and

photographed using a Leica DM5000 B microscope (Leica Microsystems).

Table 2.9: Components and quantities required to make solutions for GUS staining.

Quantity of Solution	Components	Quantity of components
Solution A (150ml)	0.2M $Na_2HPO_4.2H_2O$ water	3.56g 100ml
Solution B (150ml)	0.2M $NaH_2PO_4.H_2O$ water	2.76g 100ml
Phosphate Buffer (0.05M PO_4, pH 7.2) (150ml)	Solution A Solution B Water	30.5ml 19.5ml 100.0ml
β-glucuronidase substrate solution (5ml)	0.05M PO_4 buffer pH 7.2 33 mg/ml $K_3Fe_6(CN)_6$ in 0.05M PO_4 buffer pH7.2 43 mg/ml $K_4Fe(CN)_6.3H_2O$ in 0.05M PO_4 buffer pH 7.2 10 mg/ml X-Gluc staining solution Triton X-100	4.245ml 250µl 250µl 5µl

2.5.3 DAPI Staining

30µl of 3µg/ml 4',6-diamidino-2-phenylindole (DAPI) solution was added to dissected anthers from staged *Arabidopsis* buds (section 2.1.5) on a clean slide. The slide was mounted with a cover slip which was pressed firmly to release the pollen grains. Slides were immediately wrapped in aluminium foil because DAPI is light sensitive. Samples were examined under a Leica DM5000B fluorescence microscope after 5 minutes of staining. Centromeric heterochromatin emits a bright blue fluorescence when DAPI binds to it, which labels the nucleus and enables identification of different stages of pollen development.

2.5.4 Alexander's Staining

30µl of Alexander staining solution (Alexander, 1969) was added to dissected anthers on a clean slide. The slide was mounted with a

cover slip which was gently pressed to promote pollen release. The samples were observed under a light microscope after 30 minutes of staining. Viable pollen grains stain dark red, non-viable pollen grains stain green.

2.5.5 MTT Staining for Wheat Pollen Viability

Pollen viability assays were performed using MTT (Thiazolyl Blue Tetrazolium Bromide) staining (Khatun and Flowers, 1995; Rodriguez-Riano and Dafni, 2000). For this analysis, five plants from each genotype were used, and one floret per plant was collected. Florets were collected prior to anthesis and dehiscence. All six anthers were placed on a clean glass slide in one drop of MTT solution (0.5% MTT Sigma-Aldrich, 5% sucrose). Anthers were very carefully dissected under a stereo microscope to release the pollen grains. The solution was mounted with a coverslip and pollen was observed under a Nikon Labophot microscope (Nikon UK Limited). Purple pollen and black stained pollen was considered viable, yellow or non-stained pollen non-viable (figure 2.2) (Khatun and Flowers, 1995).

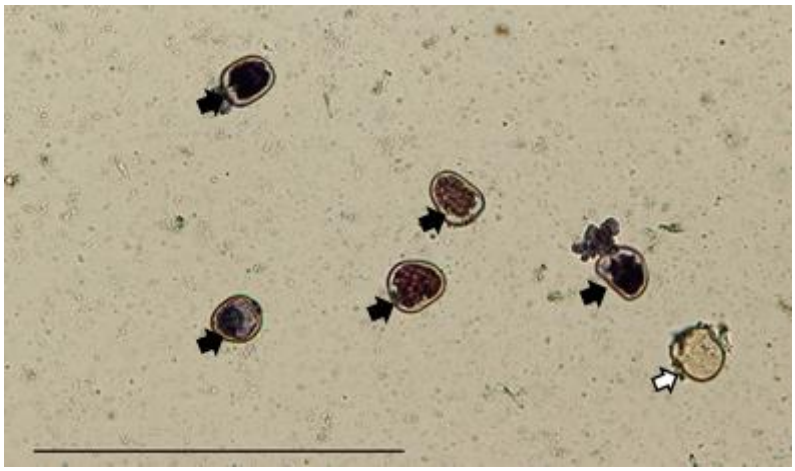

Figure 2.2 Wheat pollen grains stained for viability with Thiazolyl Blue Tetrazolium Bromide (MTT). Black arrows indicate viable pollen (stained purple or black) and the white arrow indicates non-viable pollen. Scale bar 500μm.

2.6 Microscopy Methods for Chapter 5

2.6.1 Epidermal Leaf Peels

ImpressPLUS Wash Light Body Fast Set Dental resin (BF MULLHOLLAND Ltd, Dublin) was mixed in a Petri dish and immediately applied to the abaxial side of mature *Arabidopsis* leaves using a plastic spatula, whilst they remained attached to the plant. The resin was left until hardened (a few seconds) before being carefully peeled away from the leaf. Clear nail varnish was used to paint over the impression in the dental resin. Once the nail varnish was dry, Sellotape® was placed over the nail varnish peel and used to aid its removal from the dental resin. The Sellotape® with the nail varnish peel attached was then adhered to a clean slide. The impression of the leaf epidermis was viewed under a Nikon Eclipse 50i microscope (Nikon UK Limited).

2.6.2 Confocal Microscopy

Acridine orange is a cell-permeable stain which accumulates inside acidic compartments such as the vacuole. The guard cells of anthers stained with acridine orange can be imaged by confocal microscopy. Sepals and petals were removed from *Arabidopsis* floral buds which were about to open. Anthers still attached to the pistil and pedicel were placed into PCR tubes and washed successively with 100µl 1 x PBS (pH7.2) (see appendix) containing 2% (v/v) Tween 20 and 100µl 1 x PBS before soaking in 100µl acridine orange for 1 hr. Anthers were washed three times with 100µl 1 x PBS before mounting on a slide with 50% (v/v) glycerol. Images were obtained using a Zeiss Leica TCS SP2 Confocal Microscope (Leica Microsystems). Fluorescence emissions of acridine orange were collected in the red and green channels at 616 to 666 nm and 529 to 559 nm, respectively, after excitation with a 496nm argon laser.

2.6.3 Light Microscopy

Arabidopsis anthers were dissected from stage 4 flower buds (see section 2.1.5 for staging) and placed abaxial side up on a clean microscopy slide using a stereo microscope. 30µl of water was added to the slide which was then mounted with a cover slip. Stomata were visualised, counted and images were obtained using a Nikon Eclipse 50i microscope (Nikon UK Limited). Maturing wheat florets were collected before anthesis and fixed in Clark's solution (3:1 EtOH: acetic acid). Wheat anthers swell and change from bright green, to pale green and finally to yellow, as the pollen inside ripens. Florets were collected when anthers were bright green and anthers were dissected and mounted on clean glass slides in water. Stomata were visualised and counted using a Nikon Labophot microscope (Nikon UK Limited).

CHAPTER 3 ANALYSIS OF ARABIDOPSIS AQUAPORINS EXPRESSED IN FLOWERS

3.1 Introduction

Aquaporins are ubiquitous protein membrane channels that are found in animals, plants and bacteria (Maurel et al., 2008). Belonging to the large major intrinsic proteins (MIPs) gene family, many isomers of aquaporins have been found in animals and plants (Katsuhara et al., 2008). Primarily aquaporins facilitate water transport and are associated with intercellular and transcellular water flow and the osmoregulation of cells, however some aquaporin isoforms can also transport small non-electrolytes such as CO_2 (Maurel, 2007; Tyerman et al., 2002). Aquaporins can increase water movement across membranes up to twenty-fold and are one of the fastest systems of membrane transport (Katsuhara et al., 2008; Martre et al., 2002).

In *Arabidopsis thaliana,* there are thirty-five aquaporins belonging to four subgroups: plasma membrane intrinsic proteins (PIPs), tonoplast intrinsic proteins (TIPs), nodulin-26-like intrinsic membrane proteins (NIPs) and small basic intrinsic proteins (SIPs) (figure 3.1). These four aquaporin subclasses are conserved within all land plants however the genetic events that led to species specific differences within the four subfamilies, have only happened recently in evolution (Maurel, 2007). The PIPs are the most abundant of the *Arabidopsis* aquaporins, and are further subdivided into PIP1 or PIP2 based on their phylogenetic grouping. Located in the plasma and tonoplast membranes respectively, the PIPs and TIPs help facilitate transcellular and intercellular water flow. The NIPs are not named based on their subcellular location; this subgroup of aquaporins are homologous to *Gm*NOD26, a soybean aquaporin found in the peribactoid membrane of root nodules. In *Arabidopsis*, the subcellular location of the NIPs is not certain, however in other non-leguminous

plants, NIPs have been identified in plasma and intercellular membranes. The smallest subgroup comprises of three SIP aquaporins, which are predominantly located in the endoplasmic reticulum (Maurel, 2007).

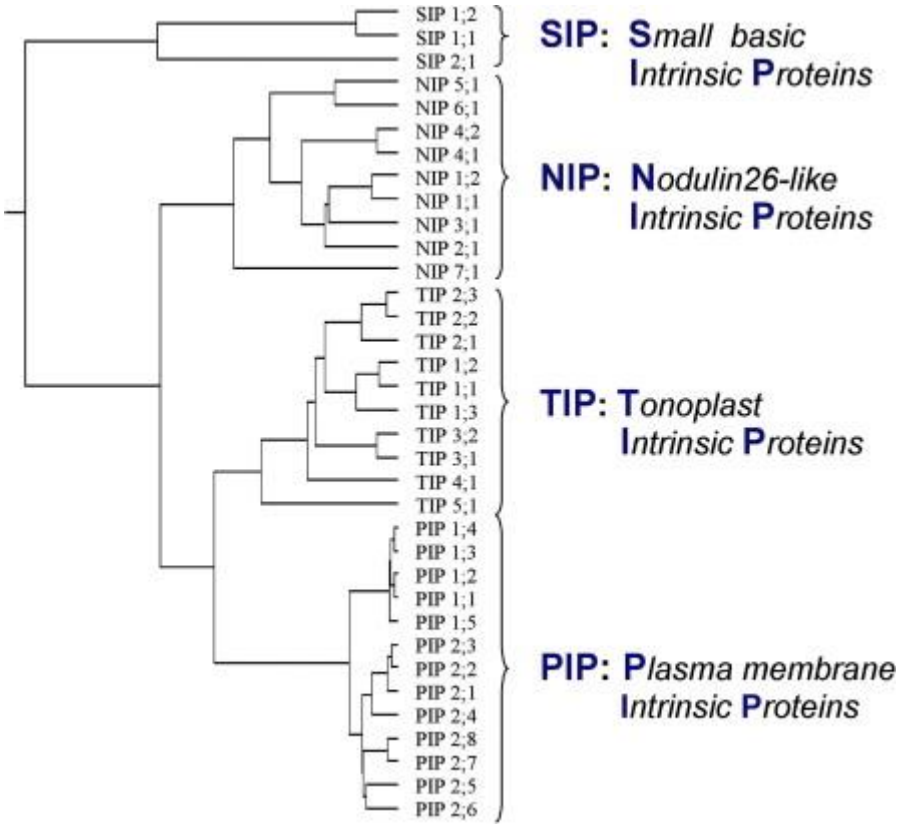

Figure 3.1: Phylogenetic tree for all thirty-five *Arabidopsis* aquaporin genes showing their position within four subgroups. Figure adapted from (Maurel, 2007).

Aquaporins are 23-31kDa hydrophobic proteins which are comprised of six transmembrane domains connected by five interconnecting loops (A-E). Loops A, C and E are located on the extra-cytoplasmic side of the membrane, while loops B, D and the N and C termini of the protein, are located on the intra-cytoplasmic side. The B and E loops have a conserved Asn-Pro-Ala (NPA) motif and dip into the centre of the molecule, and it is these, along with two of the transmembrane domains, that delineates the pore (figure 3.2) (Maurel et al., 2008). Two constrictions in the pore, (formed from the proximity of the NPA motifs and a spatial arrangement of aromatic

residues (Ar)), control transport selectivity on the basis of the size, hydrophobic interactions, and hydrogen bonding with, the molecules passing through (Li et al., 2011a; Maurel et al., 2008). The SIPs vary structurally from the other *Arabidopsis* aquaporins, the third amino acid of the NPA motif of the B loop is changed to either Thr or Leu. These changes may mean that the SIPs have altered transport selectivity (Tyerman et al., 2002).

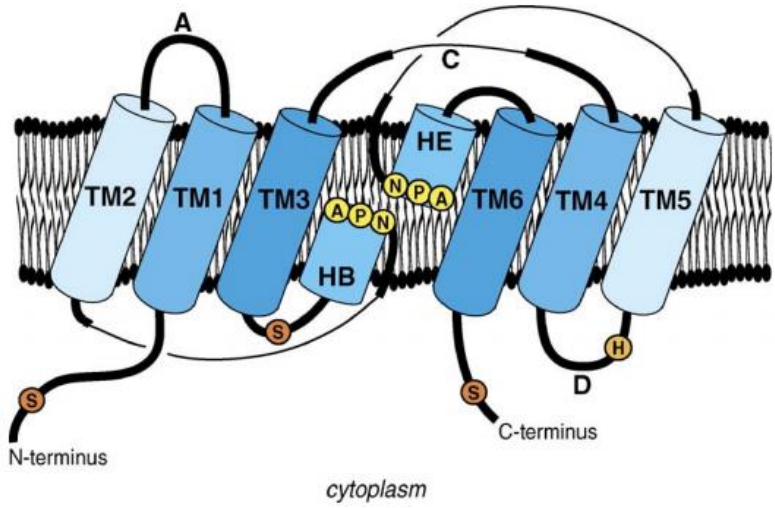

Figure 3.2: Model of an aquaporin. Figure adapted from (Hachez et al., 2006).

The six transmembrane domains (TM1-6) and the five interconnecting loops (A-E) are shown. The pore is formed by the two helical domains (HB and HE) which have the conserved NPA motif. Potentially phosphorylated serine residues (S) located on N and C termini and the B loop, are indicated. A pH sensitive histidine residue (H) in loop D is also shown.

Aquaporins form tetramers in membranes within which each monomer forms an independent channel (Chaumont and Tyerman, 2014). It has been suggested that the formation of heterotetramers between certain PIP1 and PIP2 isoforms enables the former to function. Functional studies in *xenopus* oocytes have shown that PIP2 proteins have much higher water permeability compared to PIP1s. Co-expression of *Zea mays* (maize) *ZmPIP1;2* and several different *ZmPIP2s* increased water permeability in *xenopus* oocytes and a physical interaction between PIP1 and PIP2 proteins was also demonstrated (Fetter et al., 2004). Further evidence for this was

demonstrated by Martre et al., who measured PIP activity in PIP1 and/or PIP2 antisense plants and found that whichever subgroup was not down-regulated appeared to be inactive (Martre et al., 2002). It should be noted though that transport activity of PIP1 aquaporins varies between species. Expression in oocytes has been used to show that *Arabidopsis PIP1;1*, *PIP1;2* and *PIP1;3* are active channels, whereas in maize and some other species the PIP1 isoforms are inactive (Hachez et al., 2006).

Aquaporin activity is subject to post translational regulation via phosphorylation, and the presence of protons and Ca^{2+} ions affects water permeability (Chaumont et al., 2005; Hachez et al., 2006). A conserved His residue on the D loop is the site for protonation and is responsible for pH dependant gating (opening and closing of the pore) (Törnroth-Horsefield et al., 2006). The activation effect of phosphorylating the serine residues of the B loop and N and C termini has been demonstrated in oocytes (Johansson et al., 1998; Maurel et al., 1995). Phosphorylation is affected by environmental factors such as osmotic stress and temperature, which means that aquaporin activity can be regulated in response to environmental stimuli (Hachez et al., 2006). For example, *PIP2;4* is a phosphorylation substrate of *SUCROSE INDUCED RECPETOR KINASE1* (*SIRK1),* which regulates osmotic responses to external sucrose supply (Wu et al., 2013), and the hydraulic conductivity of *Arabidopsis* rosette leaves is higher in darkness due to light dependent diphosphorylation of *PIP2;6* at Ser-280 and Ser-283 (Prado et al., 2013). Post-translational modifications can also affect aquaporin trafficking and, as the targeting of aquaporins to their subcellular destination is also sensitive to abiotic stresses, this means that gene expression levels are not always representative of aquaporin action (Li et al., 2011b; Luu and Maurel, 2013).

Plants have more aquaporin isoforms than animals (Chaumont et al., 2005). The presence of a large number of aquaporin isoforms in plants suggests a wide range of physiological roles. Various functions have been attributed to the *Arabidopsis* aquaporins that often relate

to tissue specific expression. In response to drought stress, for example, the majority of aquaporins are down regulated however those which are specifically expressed in leaves and/or flowers are not (*AtPIP1;4, AtPIP2;5* and *AtPIP2;6*). It is hypothesised that these isoforms are essential for survival/reproduction and are therefore maintained (Alexandersson et al., 2005). In seeds, *TIP3* aquaporins with seed specific expression control longevity under the influence of growth regulator ABA (Mao and Sun, 2015). Auxin co-ordinates the repression of aquaporin genes in the lateral root primordia and overexpressing *PIP2;1* delayed lateral root emergence (Péret et al., 2012). Hachez et al. suggest that the discovery that many plant aquaporins can transport a varied range of substrates, may offer an explanation for why there are so many isoforms (Hachez et al., 2006). Many of the *NIPs* are expressed in roots and the proteins have been associated with transport of boron, aluminium, lactic acid and arsenic, often in response to nutrient limiting or abiotic stress conditions (Choi and Roberts, 2007; Kamiya et al., 2009; Miwa et al., 2010; Takano et al., 2006; Wang et al., 2017; Xu et al., 2015). Another example, illustrating how broad ranging the functions of the *Arabidopsis* aquaporins are, is seen in *PIP1;2* and *PIP1;4.* Both gene products have been characterized as facilitators of CO_2 diffusion, and increase membrane permeability to CO_2 for photosynthesis (Boudichevskaia et al., 2015a, 2015b; Heckwolf et al., 2011; Li et al., 2015; Uehlein et al., 2012).

In the reproductive tissues, aquaporin expression relating to various physiological roles has been reported in different species. In *Solanum chacoense Bitt.* a *PIP2* aquaporin is expressed strongly in the elongating style and developing fruit, which implies that aquaporins aid cell expansion in developing tissues (O'Brien et al., 2002). In *Brassica oleracea,* MIPA and MIPB proteins (most closely homologous to *Arabidopsis* PIP1s) form part of the pollen coat and are hypothesized to channel water into the pollen (Ruiter et al., 1997). In anthers of *Nicotiana tabacum* it has been shown that *PIP* aquaporins of both subclasses have different but overlapping

expression patterns, which suggests that they do not function cooperatively. PIP2 proteins accumulate from anther stage eight and are concentrated in the anther walls, connective and vascular tissues. Down regulation of *PIP2* aquaporins by RNA silencing caused delayed dehiscence in tobacco, which strongly suggests that PIP2 proteins contribute to anther dehydration preceding dehiscence (Bots et al., 2005a, 2005b). In *Arabidopsis*, four aquaporins with pollen specific expression have been characterized. *NIP4;1* and *NIP4;2* are required for pollen development, germination and pollen tube growth (Di Giorgio et al., 2016; Giorgio et al., 2016), while *TIP5;1* and *TIP1;3* are very highly expressed in mature pollen, transport both water and urea, and are specific to the vegetative and sperm cells respectively (Soto et al., 2008, 2010; Wudick et al., 2014). Table 3.1 summarises expression of the *Arabidopsis* aquaporins in reproductive tissues, highlighting those with putative roles in pollen and anther development.

Table 3.1: Summary of the *Arabidopsis* aquaporin genes. The developmental map from the eFP browser was used to summarise expression levels in flower stages 12/15 and mature pollen (Winter et al., 2007). At flower stage 12, the flower bud is unopened and the petals are level with long stamens. At flower stage 15, the flower is open and stigma extends above the long anthers (Smyth et al., 1990). 1 represents masked expression and 12 represents absolute expression (Key adapted from (Winter et al., 2007)). Genes marked with * have expression levels of 5 or above in one or more of the selected tissues.

Gene	AGI Code	Expression in Flower Stages 12/15	Expression in Mature Pollen	Additional Information
SIP 1;2	AT5G18290	3/3	3	
**SIP 1;1*	AT3G04090	4/4	12	Promoter-GUS analysis showed GUS activity in the vascular tissues of the petal, stigma, stamens and pollen (Ishikawa et al., 2005)
**SIP 2;1*	AT3G56950	4/4	12	Promoter-GUS analysis showed GUS activity in the vascular tissues of the petal, stigma, stamens and pollen (Ishikawa et al., 2005)
NIP 5;1	AT4G10380	3/3	2	
NIP 6;1	AT1G80760	3/3	2	
**NIP 4;2*	AT5G37820	4/2	8	Required for pollen development, germination and pollen tube growth (Di Giorgio et al., 2016)
**NIP 4;1*	AT5G37810	4/2	8	Required for pollen development, germination and pollen tube growth (Di Giorgio et al., 2016)
NIP 1;2	AT4G18910	4/3	2	

NIP 1;1	AT4G19030	2/2	3	
NIP 3;1	AT1G31885	2/2	3	
**NIP 2;1*	AT2G34390	4/5	12	
NIP 7;1	AT3G06100	3/2	2	Boric Acid channel selectively expressed in developing pollen grains (Li et al., 2011a)
TIP 2;3	AT5G47450	2/2	2	
TIP 2;2	AT4G17340	2/2	2	
**TIP 2;1*	AT3G16240	7/5	2	
**TIP 1;2*	AT3G26520	6/7	2	
**TIP 1;1*	AT2G36830	8/8	2	
**TIP 1;3*	AT4G01470	4/2	11	Putative role in nitrogen cycling for pollen tube growth (Soto et al., 2008, 2010; Wudick et al., 2014)
TIP 3;2	AT1G17810	2/2	2	
TIP 3;1	AT1G73190	2/2	2	
TIP 4;1	AT2G25810	3/3	2	
**TIP 5;1*	AT3G47440	2/2	12	Putative role in nitrogen cycling for pollen tube growth (Soto et al., 2008, 2010; Wudick et al., 2014)
**PIP 1;4*	AT4G00430	8/9	2	

**PIP 1;3*	AT1G01620	7/6	2	
**PIP 1;2*	AT2G45960	6/8	2	
**PIP 1;1*	AT3G61430	5/7	2	
**PIP 1;5*	AT4G23400	5/6	2	
**PIP 2;3*	AT2G37180	4/5	2	
**PIP 2;2*	AT2G37170	4/5	2	
**PIP 2;1*	AT3G53420	6/6	2	
PIP 2;4	AT5G60660	2/2	2	
**PIP 2;8*	AT2G16850	9/9	2	
**PIP 2;7*	AT4G35100	9/9	2	
**PIP 2;5*	AT3G54820	5/7	2	
**PIP 2;6*	AT2G39010	6/6	2	

The large number of plant aquaporin isoforms, and the multiplicity of their methods of regulation, mean that is often difficult to determine the relationship between gene expression and function (Hachez et al., 2006). There are various known aquaporin inhibitors such as mercury chloride, silver and gold which have been used experimentally to investigate water channel activity, however reverse genetics enables a more specific approach (Hachez et al., 2006). The problem is that aquaporin mutant phenotypes are often masked by redundancy or only show when nutrients are limited (Di Giorgio et al., 2016). A

notable exception to this is *Arabidopsis TIP1;1*, where RNAi interference was reported to cause plant death in severely affected lines (Ma et al., 2004). Later studies of *TIP1;1* insertional knock-out lines however, showed that these did not have any significant phenotypic alterations, leading to the conclusion that off-target gene had silencing had occurred in the RNA interference (RNAi) lines (Beebo et al., 2009; Schüssler et al., 2008). Generally though, even the quantity of mRNA or protein level for any given aquaporin may not truly reflect its physiological importance, as aquaporins expressed in cell types that are not abundant, such as guard cells, can actually have significant impact on water transport (Chaumont and Tyerman, 2014).

3.2 Results

3.2.1 Expression analysis of the *Arabidopsis* aquaporins

3.2.1.1 Staging of *Arabidopsis thaliana* flower buds for qRT-PCR

To investigate the expression of aquaporin genes during floral development, *Arabidopsis thaliana* flower buds were staged as described in section 2.1.5. A whole inflorescence was dissected and buds were arranged in increasing size order within each stage. The staged buds were photographed under a stereo microscope in order to validate the size of buds within each stage (figure 3.3A-F). DAPI staining was used to verify the phase of pollen development within each bud stage (figure 3.3G-J). Stage 1 pollen comprised of tetrads and microspores, polarised microspores were observed at stage two, bicellular pollen at stage 3 and tricellular and mature pollen at stage 4.

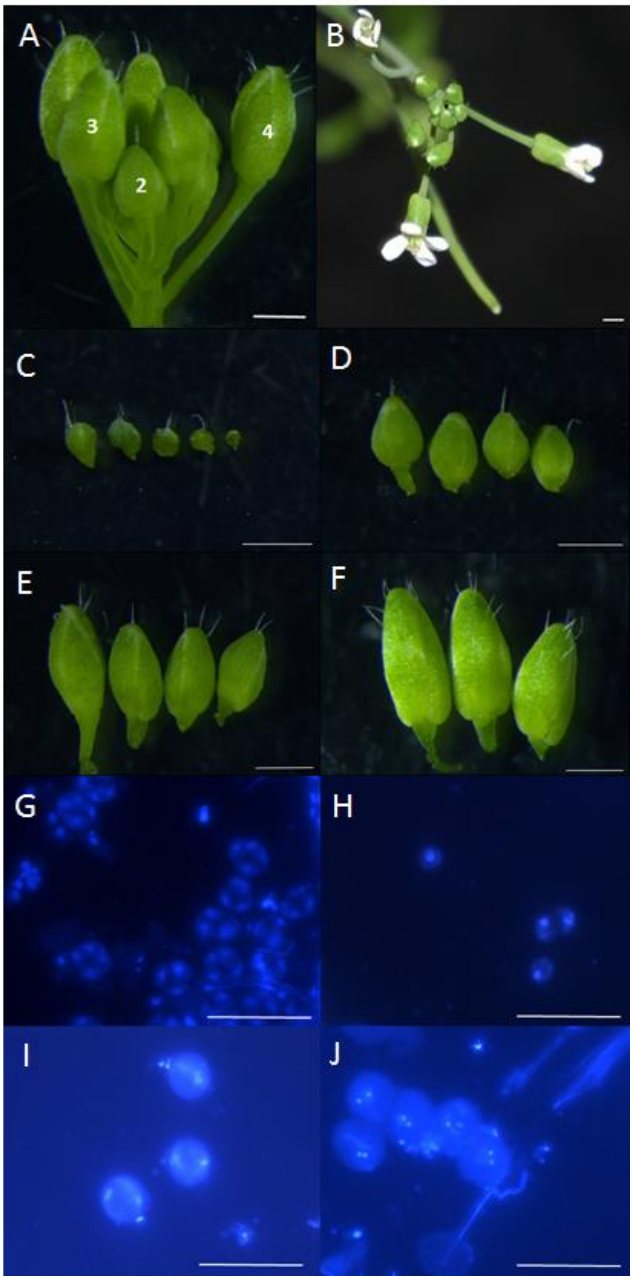

Figure 3.3: Staging of *Arabidopsis thaliana* flower buds

A: Whole inflorescence of *Arabidopsis thaliana* Columbia (Col-0). The position of stage 2, 3 and 4 buds are indicated by numbers.
B: Whole inflorescence of *Arabidopsis thaliana* Columbia (Col-0). A black dot indicates the position of stage 1 buds.
C: Col-0 stage 1 buds.
D: Col-0 stage 2 buds.
E: Col-0 stage 3 buds.
F: Col-0 stage 4 buds.
G: Tetrads from stage 1 buds.
H: Polarised microspores from stage 2 buds.
I: Bicellular pollen from stage 3 buds.
J: Tricellular pollen from stage 4 buds.

A-F scale bar, 1mm
G-J scale bar, 50μm

3.2.1.2 Expression analysis of *Arabidopsis* aquaporins expressed in flowers

Expression of *Arabidopsis* aquaporins was analysed using FlowerNet, a correlation network for *Arabidopsis* genes expressed during pollen and anther development (Pearce et al., 2015). Plots for anther related gene expression are based on previously published data sets from microarray experiments. Plots show gene expression across a developmental map as well as comparative expression in different male sterile mutants (Pearce et al., 2015). A JA time course shows changes to gene expression following treatment with jasmonic acid in a *opr3* mutant background (section 1.2.3).

A subset of fifteen *Arabidopsis* aquaporin genes (figure 3.1) was chosen for further investigation; these were selected according to their expression profiles and likely involvement in pollen and anther development. Based upon the knowledge that all *PIP1* and *PIP2* aquaporins are expressed to a moderate or high degree in flowers (table 3.1), these genes were included within the selection. *PIP2;4* is an exception because expression is highest in young roots, and there is moderate expression in the stems of flowering plants, but gene expression in flowers is low. The FlowerNet plot for *PIP2;4* correlates with the expression pattern shown in the *Arabidopsis* eFP browser (Winter et al., 2007), see figure 3.4A and B. Although some of the *SIPs*, *NIPs* and *TIPs* are highly expressed in mature pollen, the majority have low expression in flower stages 12/15 (table 3.1), and were therefore not considered for further analysis. Genes encoding tonoplast aquaporins TIP1;1, TIP1;2 and TIP2;1, are highly expressed in most flower stages and were included for expression analysis by qRT-PCR. Figure 3.5 shows the phylogenetic relationships between the selected genes and table 3.2 summarises gene expression data from the FlowerNet.

A

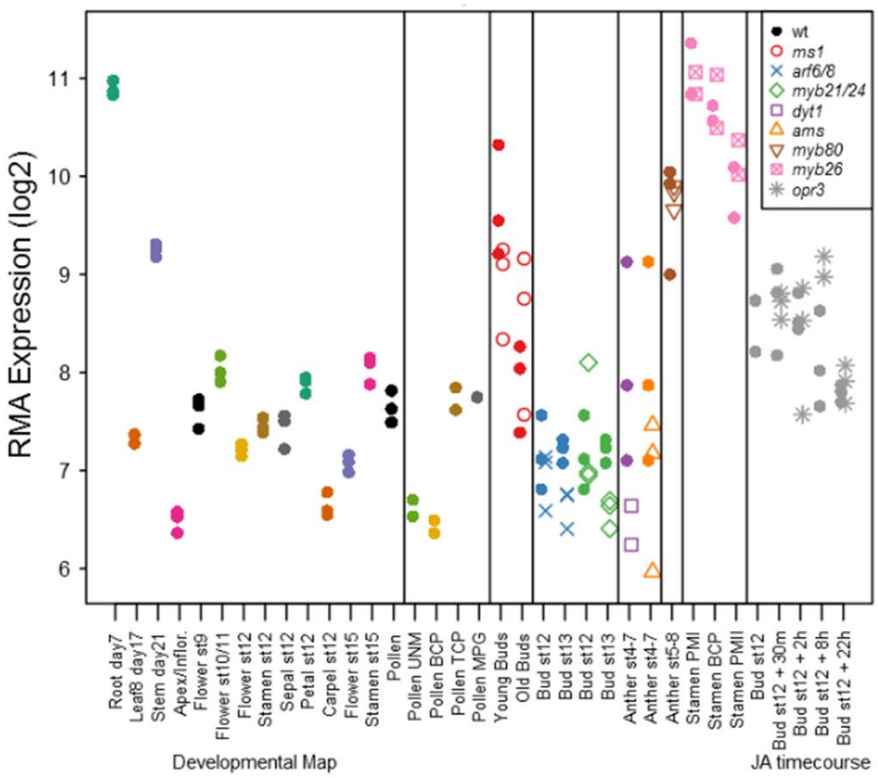
RMA Expression (log2)
wt
ms1
arf6/8
myb21/24
dyt1
ams
myb80
myb26
opr3
Root day7
Leaf8 day17
Stem day21
Apex/Inflor.
Flower st9
Flower st10/11
Flower st12
Stamen st12
Sepal st12
Petal st12
Carpel st12
Flower st15
Stamen st15
Pollen
Pollen UNM
Pollen BCP
Pollen TCP
Pollen MPG
Young Buds
Old Buds
Bud st12
Bud st13
Bud st12
Bud st13
Anther st4-7
Anther st4-7
Anther st5-8
Stamen PMI
Stamen BCP
Stamen PMII
Bud st12
Bud st12 + 30m
Bud st12 + 2h
Bud st12 + 8h
Bud st12 + 22h
Developmental Map
JA timecourse

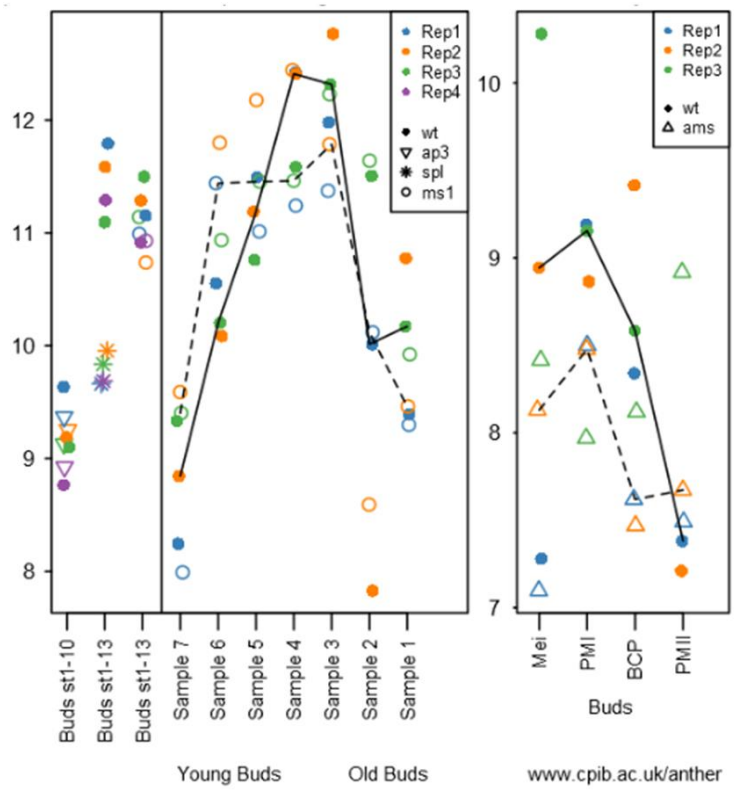
Rep1
Rep2
Rep3
Rep4
wt
ap3
spl
ms1
Buds st1-10
Buds st1-13
Buds st1-13
Sample 7
Sample 6
Sample 5
Sample 4
Sample 3
Sample 2
Sample 1
Young Buds
Old Buds
Rep1
Rep2
Rep3
wt
ams
Mei
PMI
BCP
PMII
Buds
www.cpib.ac.uk/anther

B

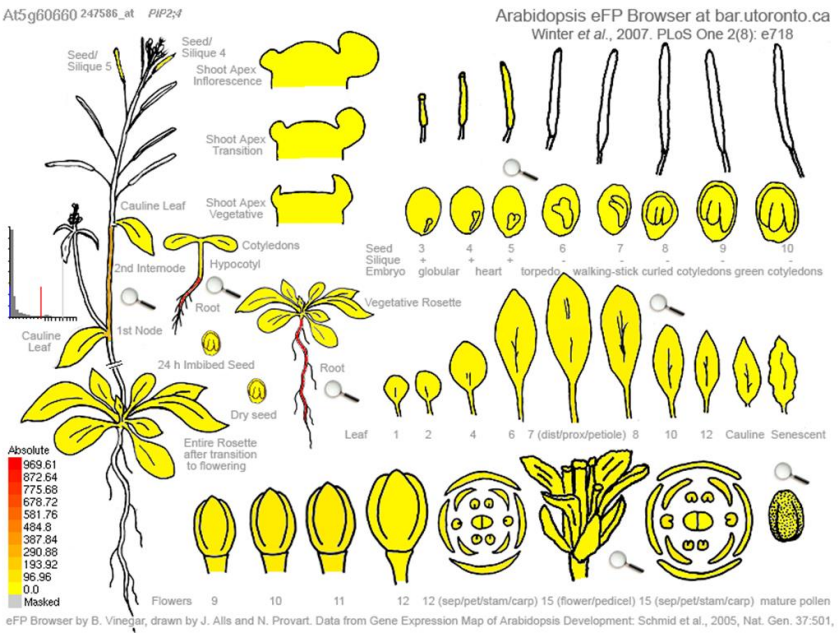

Figure 3.4: Expression data for AT5G60660 (*PIP2;4*)

A: Plot for AT5G60660 (*PIP2;4*) from FlowerNet showing gene expression from floral microarrays (Pearce et al., 2015). Plots show AT5G60660 (*PIP2;4*) expression across a developmental map, at time points following treatment with JA (in an *opr3* mutant background), and in various male sterile mutant backgrounds
B: Developmental Map for AT5G60660 (*PIP2;4*) from *Arabidopsis* eFP Browser (Winter et al., 2007)

FlowerNet groups genes that are transcriptionally co-regulated in clusters; co-expressed genes are more likely to be in the same developmental pathway and have shared functionality. *PIP2;1* and *PIP2;6* are transcriptionally co-regulated as are *PIP1;4, TIP1;1, TIP1;2*, and *TIP2;1.* Genes that are phylogenetic partners are also more likely to be redundant in function.

Table 3.2: Summary of *Arabidopsis* aquaporin genes used in qRT-PCR analysis. Actual gene expression levels are calculated from highest and lowest CP values from qRT-PCR for staged buds. Gene expression changes from the FlowerNet developmental map are summarised. High expression = RMA Expression (log2) – 10 and above. Moderate expression = RMA Expression (log2) – 8-10. Low Expression = RMA Expression(log2)- 8 and below. Changes in gene expression across the JA time course are described. Gene expression in the *myb26* background is compared relative to wild type. Columns marked * contain data from the FlowerNet (Pearce et al., 2015).

Gene	AG1 Code	Developmental Map*	Gene Expression Level	JA Time course*	Expression in *myb26* background compared to wildtype*
PIP 1;1	AT3G61430	High expression at stamen stage 15. Low expression in pollen.	514-1034	No change over time course	Slightly lower at all stages
PIP 1;2	AT2G45960	High expression at stamen stages 12 and 15. Low expression in pollen.	120-246	Slight increase over time course	Same
PIP 1;3	AT1G01620	High expression in all flower stages. Low expression in pollen.	2-4	No change over time course	Slightly lower at all stages
PIP 1;4	AT4G00430	High expression in all flower stages. Low expression in pollen.	3-6	Slight increase over time course	Same
PIP 1;5	AT4G23400	High expression at stamen stages 12 and 15. Low expression in pollen.	126-763	Increases at 30 min, then decreases over time course	Lower at all stages
PIP 2;1	AT3G53420	High expression at stamen stages 12 and 15. Low expression in pollen.	1-3	No change over time course	Same

PIP 2;2	AT2G 37170	Data not available	100-300	Data not available	Data not available
PIP 2;3	AT2G 37180	Data not available	94-247	Data not available	Data not available
PIP 2;5	AT3G 54820	High expression in flower stage 9 and carpel stage 12.	54-294	Slight increase over time course	Lower
PIP 2;6	AT2G 39010	High expression in all flower stages	655-1748	Slight increase over time course	Lower at stamen stages – pollen meiosis I and bicellular pollen
PIP 2;7	AT4G 35100	Data not available	521-3652	Data not available	Data not available
PIP 2;8	AT2G 16850	Data not available	42-521	Data not available	Data not available
TIP 1;1	AT2G 36830	High expression in all flower stages. Low expression in pollen	1073 - 5060	Slight increase over time course	Lower at all stages
TIP 1;2	AT3G 26520	High expression in all flower stages. Low expression in pollen	1948 - 5322	Slight increase 22hrs after treatment	Slightly lower at all stages
TIP 2;1	AT3G 16240	High expression in all flower stages. Low expression in pollen	Data not available	No Change over time course	Slightly lower at all stages

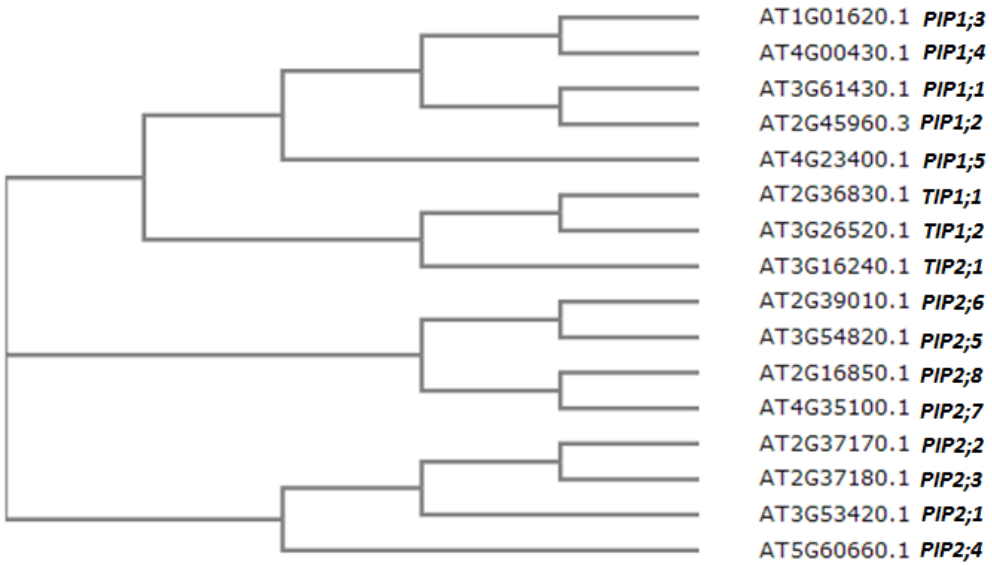

Figure 3.5: Phylogenetic tree showing relationship of *PIP* and *TIP* aquaporin genes used in qRT-PCR analysis. Figure created using Clusteral W2 from gene sequences (Larkin et al., 2007).

The expression of *Arabidopsis* aquaporin genes during pollen and anther development was investigated by qRT-PCR using staged flower buds (ecotype Ler-0). Gene expression relative to bud stage 1 is shown (figure 3.6). Due to its low expression in flowers, *PIP2;4* was not included in the analysis.

Statistical analysis was used to compare changes in gene expression levels relative to bud stage 1. Genes that showed a significant decrease ($P<0.05$) in expression at bud stage 4 relative to bud stage 1 were *PIP1;3*, *PIP2;5*, *PIP2;7* and *PIP2;8*. Genes that showed a significant increase ($P<0.05$) in expression at bud stage 4, were *PIP1;5*, *PIP2;1*, *PIP2;2*, and *PIP2;3*. The role of these aquaporin proteins during flower development is unknown, but processes requiring water transport at this developmental stage include filament and petal extension and anther dehiscence.

Genes that did not show a consistent trend between biological replicates were *PIP1;1*, *PIP1;2*, *PIP1;4* and *PIP2;6*. This may have

been caused by discrepancies between the staging of the two replicates, as gene expression changes are generally small.

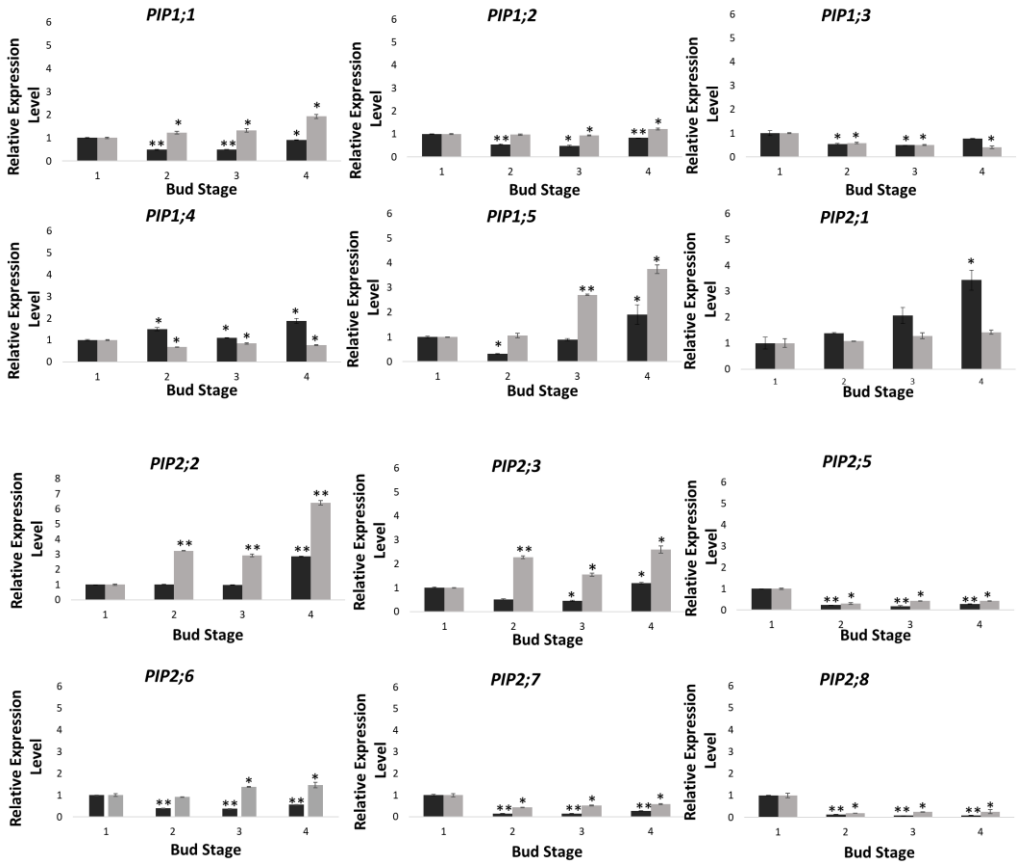

Figure 3.6: Expression of selected aquaporin genes in staged buds from wild type (Ler-0) flowers.

Gene expression is relative to stage 1. Reference gene *PP2A-3* (AT2G42500). * indicates a significant difference (P<0.05) compared to stage 1, ** indicates a significant difference (P<0.001) compared to stage 1. Error bars, standard error. Results from two separate biological replicates are shown (replicate 1 in black, replicate two in grey).

3.2.1.3 Expression analysis of selected aquaporin genes in a *myb26* background

Expression of *MYB26/MALE STERILE35 (MS35)* is essential for anther dehiscence (section 1.2.1). In order to investigate whether *MYB26/MS35* controls aquaporin gene expression during anthesis in *Arabidopsis*, an expression analysis in the *myb26* background was conducted using data available from the FlowerNet (table 3.2). The data set shows aquaporin gene expression from stamens at three

stages of pollen development (pollen mitosis I, bicellular pollen and pollen mitosis II) in *myb26* and wildtype (Ler-0) backgrounds. *MYB26* expression is highest in the anther during bud stages 2 and 3 (figure 3.7A). Out of the fifteen genes analysed, five appeared to have lower expression in the *myb26* mutant (figure 3.7B-F) and the gene with the most significant change in expression is *PIP1;5* (figure 3.7C). The FlowerNet plots (shown in figure 3.7) do show some variation between replicates at each stage of pollen development, so although there is a trend that gene is expression is lower in the *myb26* mutant, it is difficult to conclude how significant this is.

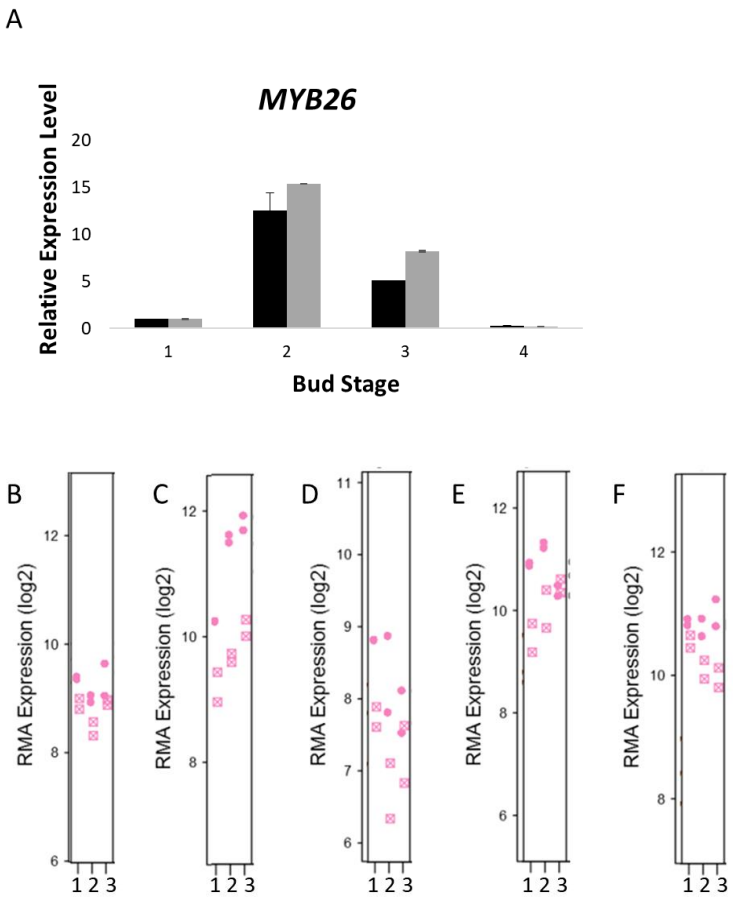

Figure 3.7: Expression analysis of selected aquaporins in a *myb26* background

A: *MYB26* expression in staged buds from wild type (Ler-0) flowers. Gene expression is relative to stage 1. Reference gene *PP2A-3* (AT2G42500). Error bars, standard error. Results from two separate biological replicates are shown (replicate 1 in black; replicate two in grey.)

B-F: Aquaporin gene expression in *myb26* (squares) and wild type (Ler-0) (circles) backgrounds at three stages of stamen development. 1= Pollen Mitosis I, 2= Bicellular Pollen, 3=Pollen Mitosis II. Adapted from (Pearce et al., 2015);

B: *PIP1;1*
C: *PIP1;5*
D: *PIP2;5*
E: *PIP2;6*
F: *TIP1;1*

In order to further investigate whether there is a link between *MYB26/MS35* and aquaporin gene expression, the expression patterns of eight aquaporin genes were investigated in *ms35* flowers by qRT-PCR (figure 3.8). Landsberg (Ler-0) plants were used as the

control, because the *ms35* mutation is in a Landsberg (Ler-0) background. A Columbia (Col-0) background was also included in the experiment to enable a more detailed analysis. Gene expression was compared between staged flower buds in two separate experiments using different biological replicates.

In the first experiment, with the exception of *PIP2;8*, all genes had significantly lower expression ($P<0.05$) in the *ms35* background compared to Ler-0, at one or more stages. In the second biological replicate, all genes have significantly higher expression ($P<0.05$) in the *ms35* background at one or more stages, although *PIP1;4* and *TIP1;2* have lower expression ($P<0.05$) at stage 1. All of the genes investigated show discrepancies in expression patterns between the two experiments, this is likely to be due to technical difficulties associated with the staging of materials and the low levels of gene expression observed. The majority of expression changes are less than 2-fold and would usually be considered as noise, however the statistics indicate some significant differences. Considering the variation in the qRT-PCR results and the data from the FlowerNet, it is currently not possible to conclude whether there is a direct link between *MS35/MYB26* and aquaporin gene expression, without further investigation.

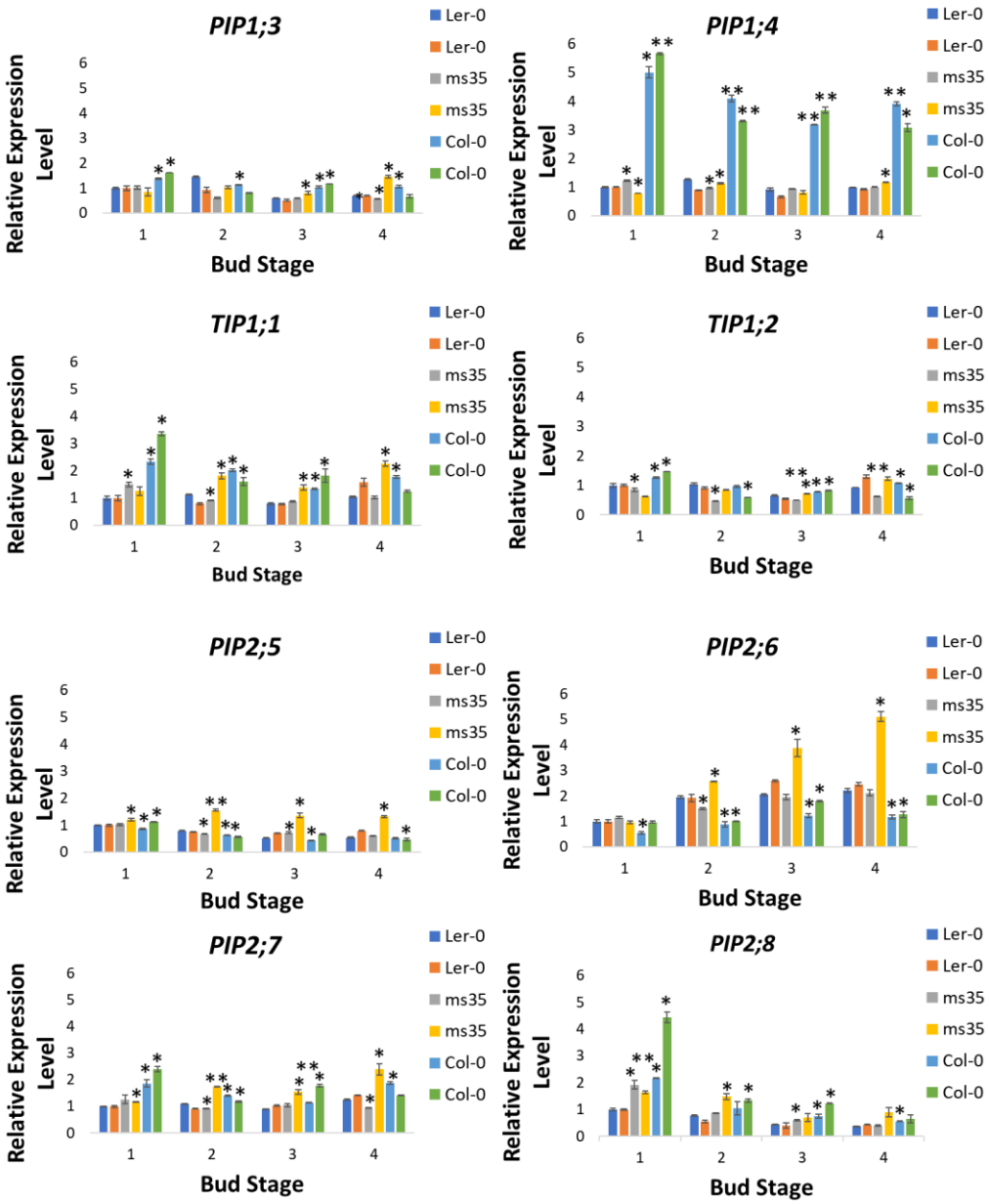

Figure 3.8: Expression of selected aquaporin genes in staged buds from Ler-0, Col-0 and *ms35* flowers.

Gene expression is relative to Ler-0 stage 1. Reference gene *PP2A-3* (AT2G42500). Error bars, standard error. Results from two separate biological replicates are shown. * above a *ms35* bar indicates a significant ($P<0.05$) difference from Ler-0 at the same stage, ** indicates ($P<0.001$). * above a Col-0 bar indicates a significant ($P<0.05$) difference from Ler-0 at the same stage, ** indicates ($P<0.001$). Dark blue, grey and light blue bars are from the same biological replicate. Red, yellow and green bars are from a second biological replicate.

Gene expression was also compared between staged buds of the Landsberg (Ler-0) and Columbia (Col-0) ecotypes. A few of the genes

had consistent changes between replicates. *PIP1;4* is much more highly expressed in Col-0 compared to Ler-0 (5-fold higher expression at bud stage 1) ($P \leq 0.001$). *TIP1;1* is also more highly expressed in the Col-0 background, while *PIP2;6* is expressed at a lower level in Col-0 ($P < 0.05$ for both).

3.2.1.4 Expression analysis of selected aquaporin genes in a *dad1* background

The plant hormone jasmonic acid is a known regulator of plant dehiscence (section 1.2.3). Eleven aquaporin genes were analysed for changes to gene expression following treatment with jasmonic acid using data available in the FlowerNet (table 3.2). The data set shows changes in gene expression in the *12-Oxophytodienoate reductase 3* (*opr3)* mutant at time points following treatment with jasmonic acid. Data from plants treated with JA is shown as circles, while data from plants mock treated with OPDA are shown as stars. Results from genes that show expression changes across the time course are shown in figure 3.9. *PIP1;2*, *PIP2;5*, *PIP2;6* and *TIP1;1* gradually increase in expression over the 22 hours following treatment with jasmonic acid (figure 3.9A, C, D, E). JA treatment caused an initial increase in expression of *PIP1;5* after 30 minutes, then expression fell during the 22 hours after treatment (figure 3.9B). In contrast, *TIP1;2* expression only notably increased at the 22-hour time point (figure 3.9F). It should be noted however that similar expression patterns occurred in the mock treated plants, therefore these changes are probably negligible.

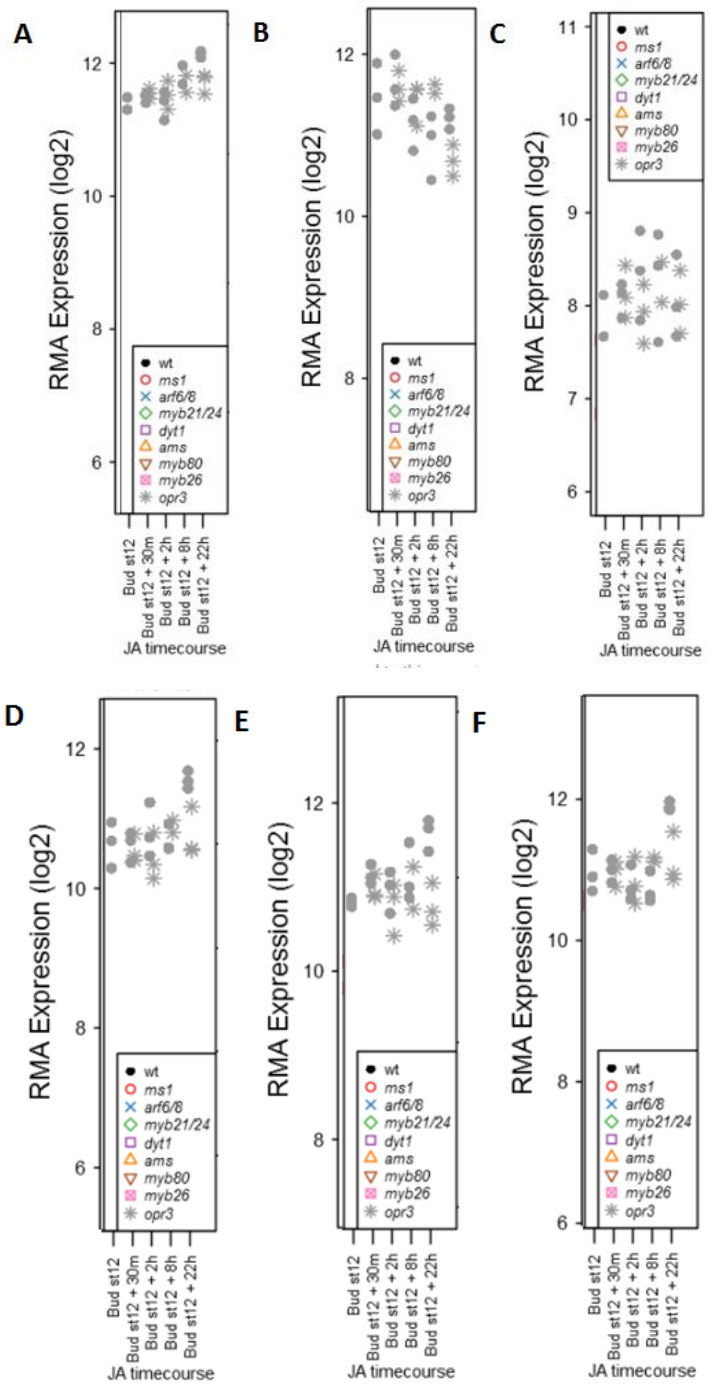

Figure 3.9: Changes to aquaporin gene expression across a JA time course. *opr3* + JA (circles), *opr3* +OPDA (stars). Figure adapted from (Pearce et al., 2015).

A: *PIP1;2*
B: *PIP1;5*
C: *PIP2;5*
D: *PIP2;6*
E: *TIP1;1*
F: *TIP1;2*

In order to further investigate whether jasmonic acid regulates aquaporin gene expression in flowers, *Arabidopsis* mutants unable to synthesise DEFECTIVE IN ANTHER DEHISCENCE1 (DAD1), a chloroplastic phospholipase A1 enzyme, were identified. DAD1 catalyses the first step of jasmonic acid biosynthesis, and *dad1* mutants are characterised by severely delayed flower opening, anther dehiscence and inviable pollen (Ishiguro et al., 2001). The single T-DNA insertion mutant SALK_138439 was grown and genotyped to identify homozygous mutants (section 2.1.1) (figure A1 A, B). qRT-PCR analysis of *DAD1* expression in staged wild type (Col-0) flowers, showed that *DAD1* expression significantly increases at bud stages 2 (polarised microspores), 3 (pollen mitosis I), and 4 (mature pollen), relative to stage 1 (tetrad stage) (figure A1 D). *DAD1* expression was reduced 0.8-fold in SALK_138439 homozygous insertion mutant flowers (figure A1 C) and it was significantly reduced at bud stages 2, 3 and 4, compared to the wild type equivalent (figure A1 D).

The expression of fourteen different aquaporins was then compared between staged wild type and SALK_138439 (*dad1*) flower buds (figure 3.10). As the *dad1* mutation is in a Columbia background, Col-0 flower buds were used as the wild type control. There were significant ($P<0.05$) changes to gene expression in the *dad1* background compared to wild type, however these changes were not consistent between the two biological replicates and may be a reflection of background noise due to very low levels of expression in many cases. *PIP2;1*, *PIP2;2* and *PIP2;3* have significantly higher expression in the *dad1* background at bud stages 3 and 4, but these results were not replicated. Overall, considering that expression changes are generally small, it seems unlikely that JA is having a major impact.

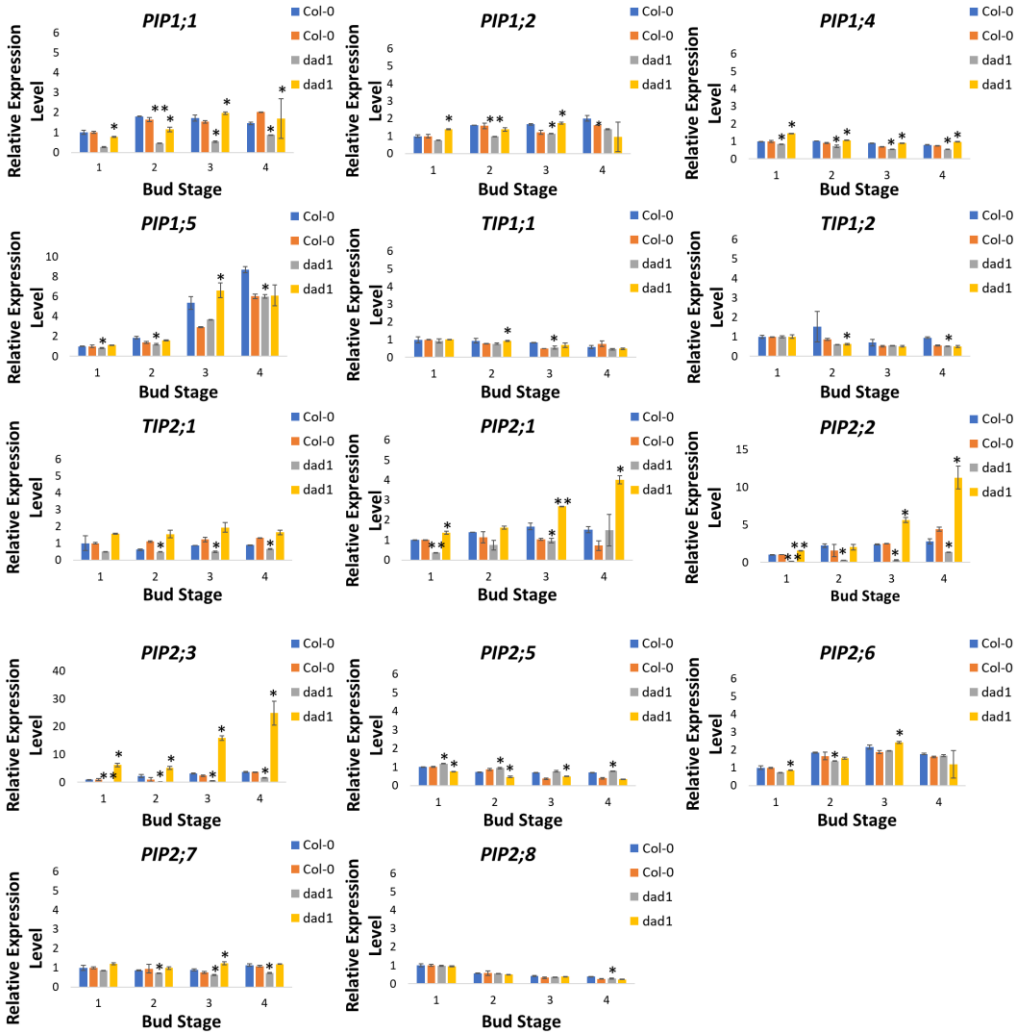

Figure 3.10: Expression of selected aquaporin genes in staged buds from wild type (Col-0) and SALK_138439 flowers. Gene expression is relative to Col-0 stage 1. Reference gene *PP2A-3* (AT2G42500). Error bars, standard error. Results from two separate biological replicates are shown. * above a *dad1* bar indicates a significant (P<0.05) difference from Col-0 at the same stage, ** indicates (P<0.001). Dark blue and grey bars are from the same biological replicate. Red and yellow bars are from a second biological replicate.

3.2.1.5 Analysis of the promoter activity of selected aquaporins using GUS reporter lines

The promoter activity of four different aquaporin genes was investigated using GUS reporter lines. Seed for *PromPIP1;2*-GFP-GUS (Postaire et al., 2010) and *PromPIP2;1*-GFP-GUS (Péret et al., 2012) was supplied by Christophe Maurel (CNRS). Both lines are in the C24 background. *PIP1;5*pro::PGWB3 and *PIP2;7*pro::PGWB3 were

generated as described in section 2.4.9.1 , and transformed into a Ler-0 background. Whole inflorescences from the transgenic lines and a Columbia control were treated with β-glucuronidase substrate (section 2.5.2) to identify regions where the promoter is active (figures 3.11 and 3.12).

GUS staining of whole inflorescences from *PromPIP1;2*-GFP-GUS and *PromPIP2;1*-GFP-GUS plants showed that expression of both genes was strongest in open flowers. Some staining can be seen within stage 1-4 buds, and this was more apparent in the *PromPIP1;2*-GFP-GUS flower buds (figure 3.11).

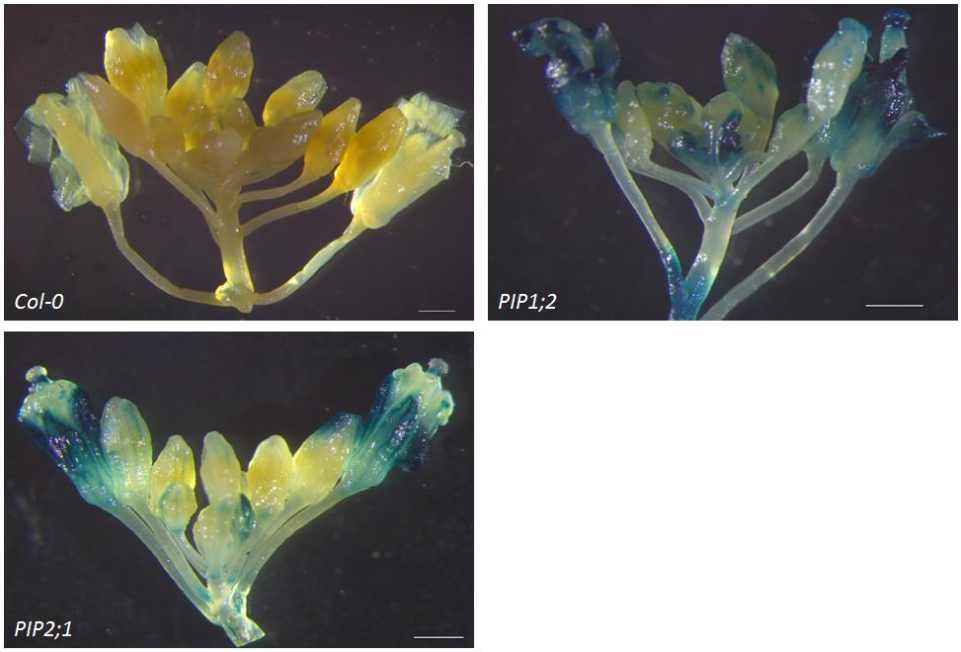

Figure 3.11: Wild type (Col-0), *PromPIP1 ;2*-GFP-GUS and *PromPIP2 ;1*-GFP-GUS whole inflorescences treated with β-glucuronidase substrate. Scale bar= 1mm.

No promoter activity was detected in early anthers (prior to dehiscence) from any of the lines (table 3.3, figure 3.12). Late anthers were taken from open flowers and had begun to dehisce. *PIP1;2* was strongly expressed in the filaments, connective and vascular tissues, and pollen of late anthers. This correlates with the high expression level indicated by eFP browser for stamen stage 15 (figure 3.13A). Although the eFP browser indicates moderate expression of *PIP1;5* at stamen stage 15, no GUS staining was

observed in any late anthers from *PIP1;5*pro::PGWB3 plants (figures 3.12 and 3.13B). *PIP2;1* has a very specific expression pattern in late anthers; expression is confined to the filament and vascular and connective tissues. Blue staining can be observed in the centre of the filament and in the centre of the anther surrounding the vascular bundle. *PIP2;7* is also strongly expressed throughout the late anther filaments. The specificity, timing and position of these expression patterns suggest that these aquaporins may facilitate water transport out of the anther walls and into the connective and vascular tissues during dehiscence (figure 3.12).

Promoter activity for *PIP1;2*, *PIP1;5* and *PIP2;1* was detected in petals (table 3.3, figure 3.12). Promoter activity was strongest in *PIP1;5* petals, which correlates with the expression pattern shown in the developmental map from the eFP browser. The eFP browser indicates that *PIP1;2*, *PIP2;1* and *PIP2;7* are all expressed in petals of open flowers, although no GUS staining was observed in petals from *PIP2;7*pro::PGWB3 plants. GUS staining indicated that *PIP1;2*, *PIP1;5* and *PIP2;1* are also expressed strongly in sepals of open flowers (figure 3.12). These aquaporins may facilitate the transport of water for floral organ extension.

PIP1;2 and *PIP2;1* promoter activity was detected in stigmas from open flowers. Expression of *PIP1;2* was wide spread throughout the stigma, whereas expression of *PIP2;1* was confined to the lower region of the stigma (at the top of the style). Very faint staining was detected in stigmas from early buds (prior to anthesis) of *PIP2;7*pro::PGWB3 plants. No promoter activity was detected in stigmas from *PIP1;5*pro::PGWB3 flowers.

Table 3.3: Summary table for the promoter activity of *PIP1;2*, *PIP1;5*, *PIP2;1* and *PIP2;7* in floral organs detected by GUS staining. X indicates that promoter activity was detected within that organ.

Organ	*PIP1;2*	*PIP1;5*	*PIP2;1*	*PIP2;7*
Early Anther				
Late Anther	X		X	X
Petal	X	X	X	
Sepal	X	X	X	
Stigma	X		X	X

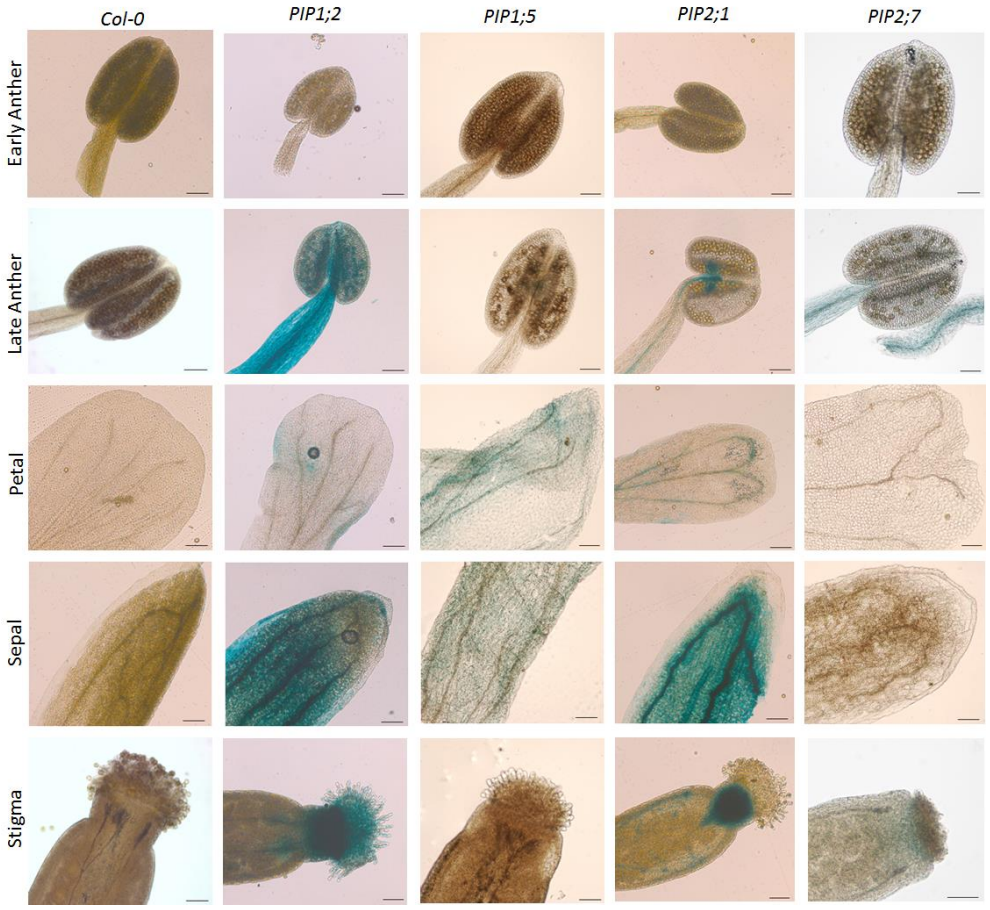

Figure 3.12: GUS staining of floral organs

GUS staining showing promoter activity of *PIP1;2*, *PIP1;5*, *PIP2;1* and *PIP2;7* in sepals, petals, stigmas and anthers. Early anthers were taken from flower buds before anthesis and late anthers are taken from open flowers. Scale bars = 100μm.

A

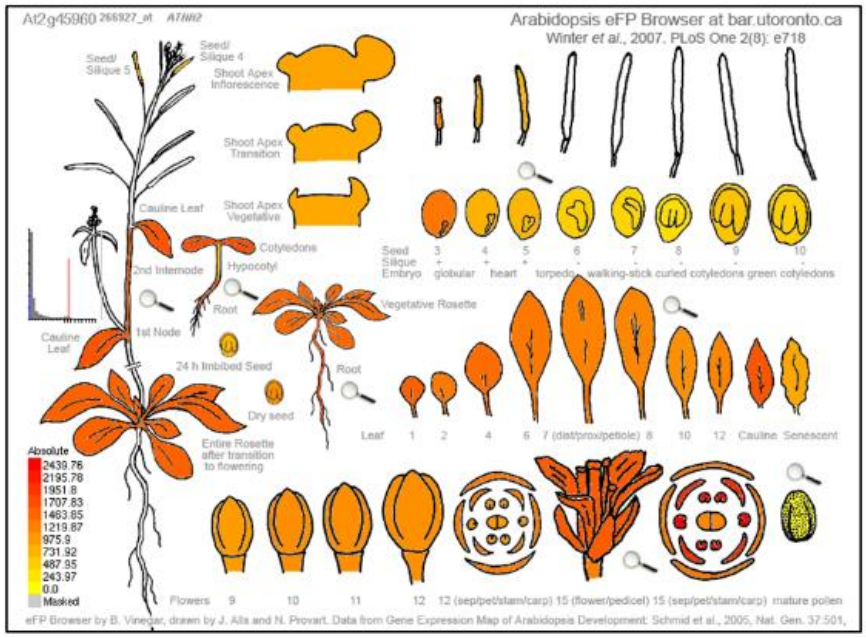
At2g45960 266927_at ATNI2
Arabidopsis eFP Browser at bar.utoronto.ca
Winter et al., 2007. PLoS One 2(8): e718
Seed/ Silique 5
Seed/ Silique 4
Shoot Apex Inflorescence
Shoot Apex Transition
Shoot Apex Vegetative
Cauline Leaf
Cotyledons
Hypocotyl
2nd Internode
Root
1st Node
Cauline Leaf
24 h Imbibed Seed
Dry seed
Entire Rosette after transition to flowering
Vegetative Rosette
Seed 3 4 5 6 7 8 9 10
Silique + + + - - - - -
Embryo globular heart torpedo walking-stick curled cotyledons green cotyledons
Leaf 1 2 4 6 7 (dist/prox/petiole) 8 10 12 Cauline Senescent
Flowers 9 10 11 12 12 (sep/pet/stam/carp) 15 (flower/pedicel) 15 (sep/pet/stam/carp) mature pollen
Absolute
2439.76
2195.78
1951.8
1707.83
1463.85
1219.87
975.9
731.92
487.95
243.97
0.0
Masked
eFP Browser by B. Vinegar, drawn by J. Alls and N. Provart. Data from Gene Expression Map of Arabidopsis Development: Schmid et al., 2005, Nat. Gen. 37:501,

B

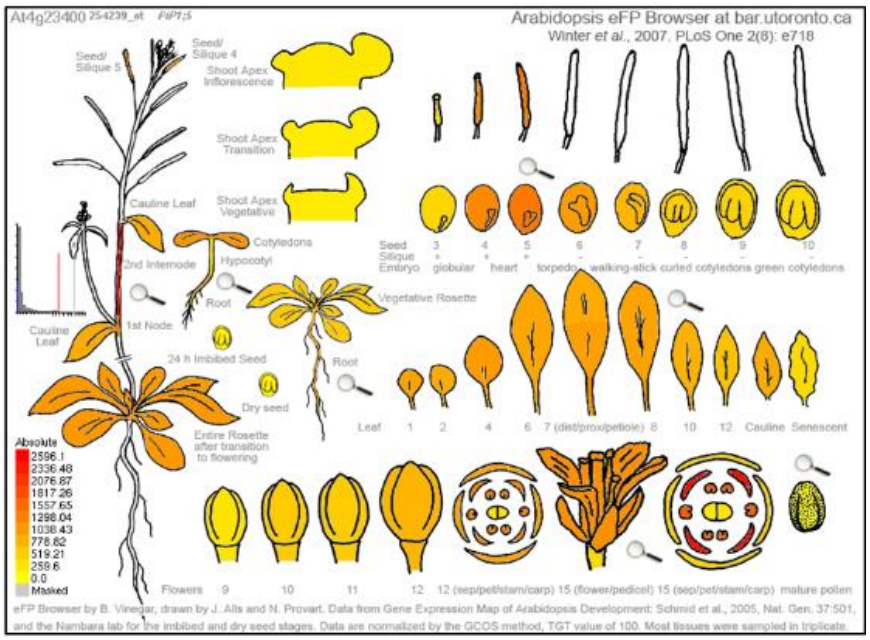
At4g23400 254239_at PAP75
Arabidopsis eFP Browser at bar.utoronto.ca
Winter et al., 2007. PLoS One 2(8): e718
Seed/ Silique 5
Seed/ Silique 4
Shoot Apex Inflorescence
Shoot Apex Transition
Shoot Apex Vegetative
Cauline Leaf
Cotyledons
Hypocotyl
2nd Internode
Root
1st Node
Cauline Leaf
24 h Imbibed Seed
Dry seed
Entire Rosette after transition to flowering
Vegetative Rosette
Seed 3 4 5 6 7 8 9 10
Silique + + + - - - - -
Embryo globular heart torpedo walking-stick curled cotyledons green cotyledons
Leaf 1 2 4 6 7 (dist/prox/petiole) 8 10 12 Cauline Senescent
Flowers 9 10 11 12 12 (sep/pet/stam/carp) 15 (flower/pedicel) 15 (sep/pet/stam/carp) mature pollen
Absolute
2596.1
2336.48
2076.87
1817.26
1557.65
1298.04
1038.43
778.82
519.21
259.6
0.0
Masked
eFP Browser by B. Vinegar, drawn by J. Alls and N. Provart. Data from Gene Expression Map of Arabidopsis Development: Schmid et al., 2005, Nat. Gen. 37:501,
and the Nambara lab for the imbibed and dry seed stages. Data are normalized by the GCOS method, TGT value of 100. Most tissues were sampled in triplicate.

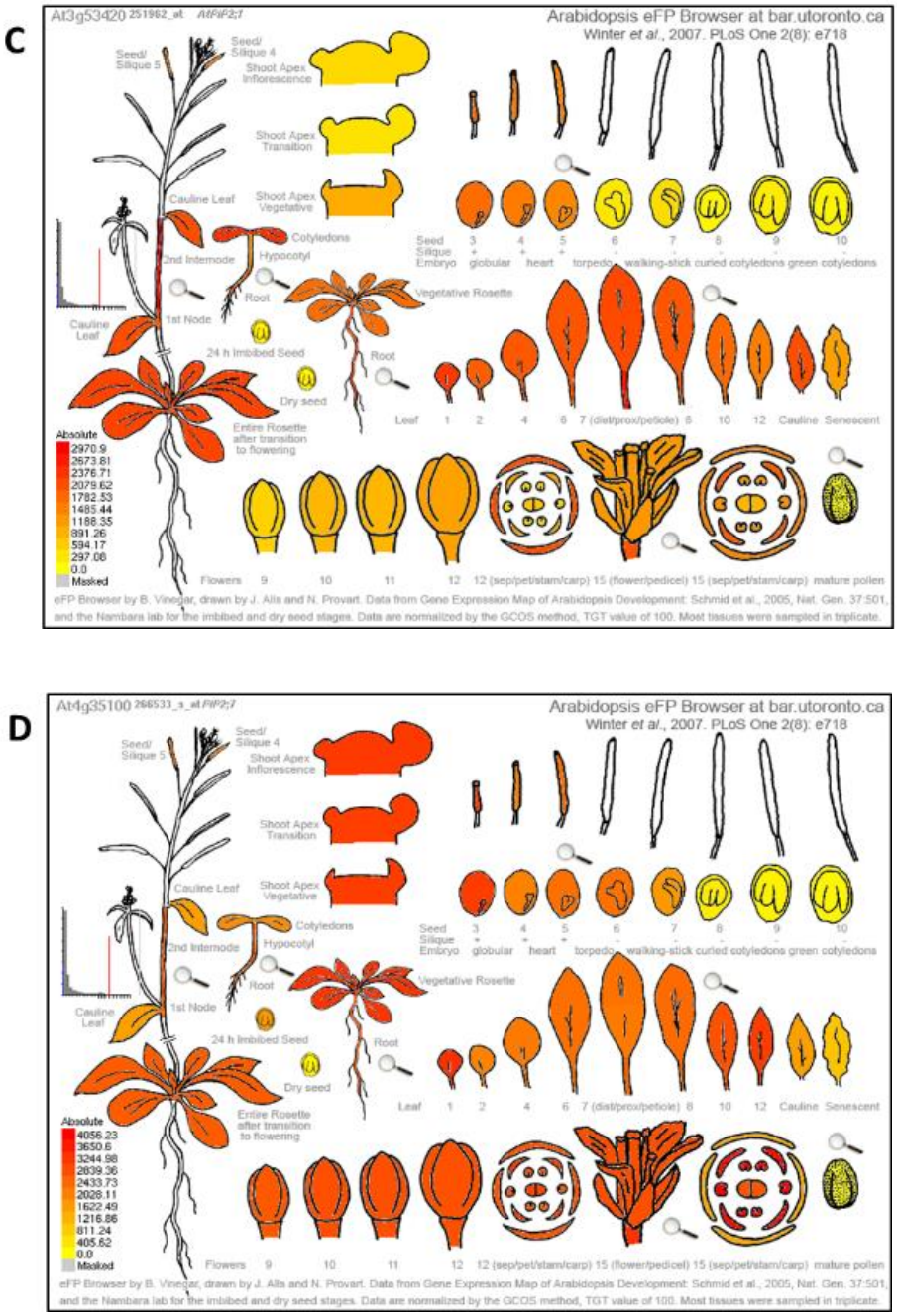

Figure 3.13: Developmental Maps for AT2G45960 (*PIP1;2*), AT4G2340 (*PIP1;5*), AT3G53420 (*PIP2;1*), AT4G35100 *(PIP2;7*) from *Arabidopsis* eFP Browser (Winter et al., 2007).

A: *PIP1;2*
B: *PIP1;5*
C: *PIP2;1*
D: *PIP2;7*

3.2.2 Analysis of *PIP2;5* and *PIP2;6*

In order to study the putative function of *PIP2;5* and *PIP2;6* in flowers, single T-DNA insertion lines were obtained for *PIP2;5* and *PIP2;6* from NASC and genotyped to identify homozygous mutants (figure A2 B, E). Lines SALK_072405 and SALK_118213 have single T-DNA insertions located within the third and fourth exons of *PIP2;5* and *PIP2;6* respectively (figure A2 A, D). Expression of *PIP2;5* was reduced 0.93-fold in flowers, and expression of *PIP2;6* was completely knocked out (figure A2 C, F).

The expression of various *PIP* genes in SALK_118213 (*pip2;6*) flowers was compared relative to wild type (Col-0) (figure 3.14). Changes to the expression levels of *PIP2;7* and *PIP2;8* were not significant ($P>0.05$), however relative expression of *PIP1;4* and *PIP2;3* was significantly lower ($P<0.05$) in the mutant background. Relative expression of *PIP2;2* was also significantly reduced ($P<0.001$), while expression of *PIP2;5* was significantly elevated ($P<0.05$) in *pip2;6* flowers compared to the wild type equivalent. Due to their close evolutionary relationship (figure 3.5), it may be that PIP2;5 and PIP2;6 have a similar function in flowers and that *PIP2;5* gene expression is increased in *pip2;6* flowers to compensate for *PIP2;6* being knocked out. Overall these changes in gene expression levels suggest that the *Arabidopsis* aquaporins may be part of a complex gene regulatory network, where changes to expression of a single gene results in over/under compensation by others.

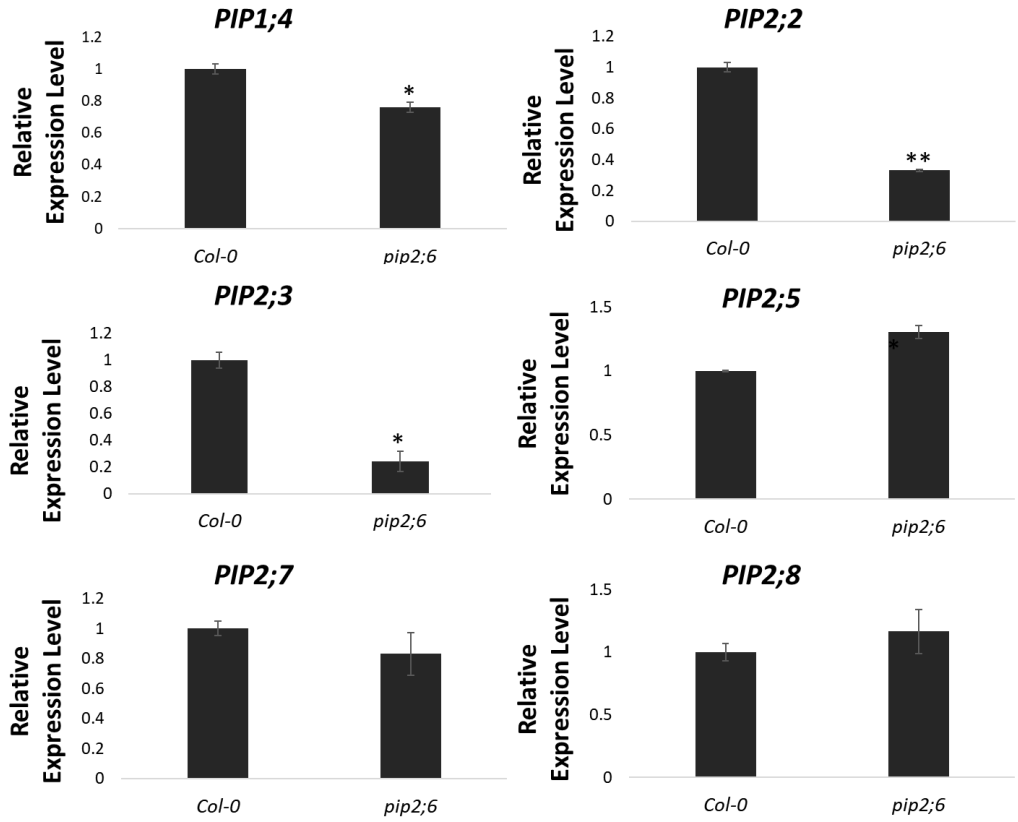

Figure 3.14: Expression of various aquaporin genes in SALK_118213 (*pip2;6* mutant) flowers (whole inflorescence), relative to wild type (Col-0). Reference gene *PP2A-3* (AT2G42500). * indicates a significant difference in expression ($P<0.05$), ** ($P<0.001$). Error bars, standard error.

Pollen viability of the *PIP2;5* and *PIP2;6* mutants was assessed using Alexander's stain (figure 3.15A) and FDA staining. Statistical analysis from FDA staining showed that the viability of pollen from mutant genotypes does not differ significantly from wild type ($P>0.05$) (figure 3.15B). The length of siliques on the main stem and the number of sterile siliques, were used as measures of plant fertility (figure 3.15C, D). Siliques were measured from base to tip. Sterile siliques were completely flat as they contained no seeds, and were always 3-4mm in length.

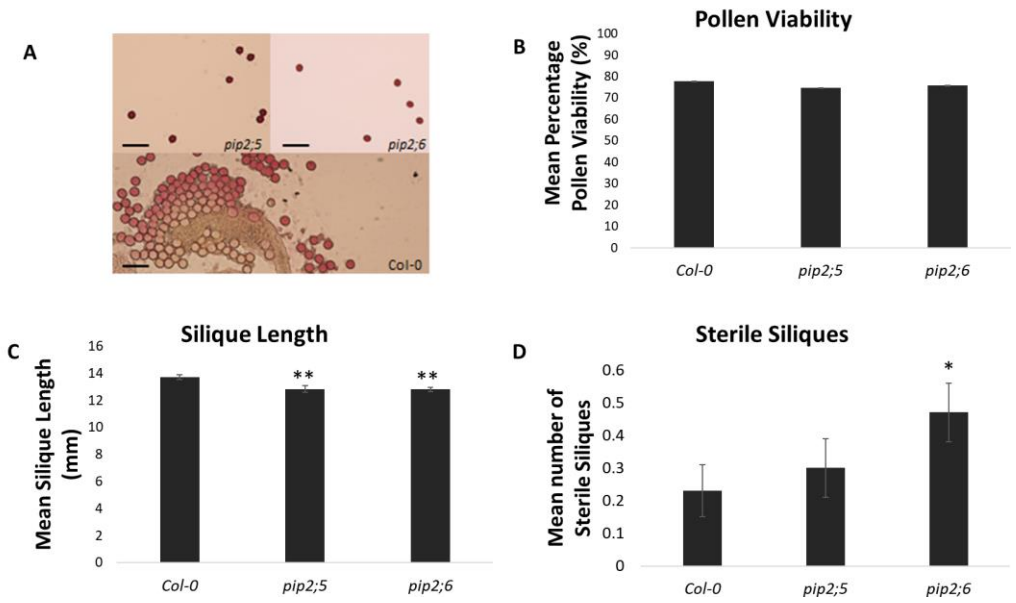

Figure 3.15: Characterisation of *pip2;5* and *pip2;6*

A: Alexander's staining for pollen viability.
B: Percentage pollen viability of the *pip2;5* (SALK_072405) and *pip2;6* (SALK_118213) mutants and wild type (Col-0) calculated from FDA staining. The effect of genotype is not significant, P>0.05, error bars, standard error.
C: Silique length of the *pip2;5* (SALK_072405) and *pip2;6* (SALK_118213) mutants and wild type (Col-0). Silique length of the 1st to 6th siliques on the main stem was measured. ** indicates significant variation (P<0.001) from the wild type control, error bars, standard error. The combined results from two biological replicates are shown.
D: Number of sterile siliques on the main stem of the *pip2;5* (SALK_072405) and *pip2;6* (SALK_118213) mutants and wild type (Col-0). * indicates significant variation (P<0.05) from the wild type control, error bars, standard error. The combined results from two biological replicates are shown.

Both of the T-DNA insertions lines, *pip2;5* (SALK_072405) and *pip2;6* (SALK_118213), had a significant reduction in the length of siliques formed on the main stem (*P<0.001*). This suggests that *PIP2;5* and *PIP2;6* gene expression is required for normal full fertility. The number of sterile siliques on the main stem of *pip2;5* plants did not vary significantly from wildtype (*P>0.05*), however there was a significant increase in the number of sterile siliques on the main stems of *pip2;6* plants (P<0.05).

In order to investigate possible functional redundancy between closely related genes (figure 3.5), homozygous mutants of *pip2;5* and *pip2;6* were crossed in order to generate a *pip2;5pip2;6* double

mutant. Plants which were homozygous for both mutations were identified in the F2 generation. Seed from one of the plants identified was re-sown and genotyping confirmed that this line was stable for the double mutation. qRT-PCR was used to confirm that expression of both genes was reduced in the flowers of *pip2;5pip2;6* plants (figure 3.16A). A wider spectrum qRT-PCR compared relative expression of various aquaporins in *pip2;5pip2;6* flowers against the wild type (Col-0) equivalent (figure 3.16B). Expression of *PIP1;5* and *PIP2;3* was significantly ($P<0.05$) reduced in the mutant, while relative expression levels of *PIP1;2* and *PIP2;7* were significantly ($P<0.05$) increased. *PIP2;3* expression is reduced in both *pip2;6* and *pip2;5pip2;6*, which suggests there is a regulatory relationship between these genes.

Table 3.4: Summary of aquaporin gene expression in *pip2;6* and *pip2;5pip2;6* flowers. 'Lower' indicates that relative gene expression is significantly lower than it is in wild type flowers (Col-0) ($P<0.05$), 'higher' indicates that relative gene expression is significantly higher than it is wild type flowers (Col-0) ($P<0.05$).

Gene	*pip2;6* background	*pip2;5pip2;6* background
PIP1;2		Higher
PIP1;4	Lower	
PIP1;5		Lower
PIP2;2	Lower	
PIP2;3	Lower	Lower
PIP2;5	Higher	
PIP2;7		Higher

Nevertheless, no significant change in fertility was observed in the *pip2;5pip2;6* double mutant. Pollen viability analysed by FDA staining did not differ significantly from Columbia ($P>0.05$). Seed set of the *pip2;5pip2;6* double mutant did not vary significantly from a wild type control (figure 3.16C, D). It may be that there is widespread functional redundancy within the aquaporin gene family and that upregulation of other aquaporins in the double mutant compensates for any effects caused. Alternatively, the fertility changes observed in the *pip2;5, pip2;6* single mutants may have been due to an interplay

between environmental stress and the altered aquaporin gene expression.

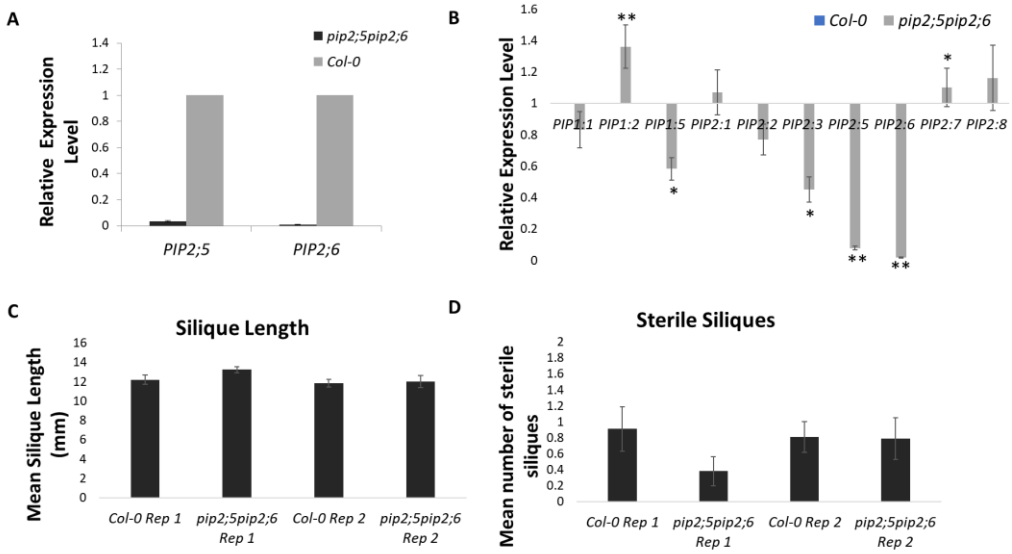

Figure 3.16: Characterisation of the *pip2;5pip2;6* double mutant

A: Expression of genes *PIP2;5* and *PIP2;6* in *pip2;5pip2;6* flowers (whole inflorescence), relative to wild type (Col-0). Reference gene *PP2A-3* (AT2G42500). Error bars, standard error.
B: Expression of selected aquaporin genes in *pip2;5pip2;6* flowers (whole inflorescence), relative to wild type (Col-0). Expression in wild type flowers has been set at a reference value of 1. * indicates a significant difference in expression ($P<0.05$), ** ($P<0.001$). Reference gene *PP2A-3* (AT2G42500). Error bars, standard error.
C: Silique length of *pip2;5pip2;6* double mutant plants and wild type (Col-0). Silique length of the 1st to 6th siliques on the main stem was measured. The effect of genotype is not significant, $P>0.05$, error bars, standard error, results for two biological replicates are shown.
D: Number of sterile siliques on the main stem of *pip2;5pip2;6* double mutant plants and wild type (Col-0). The effect of genotype is not significant, $P>0.05$, error bars, standard error, results for two biological replicates are shown.

In order to investigate the relationship between floral organ growth and fertility, the lengths of floral organs were measured in flowers at two different developmental stages (named flower stages 1 and 2). Flowers of the *pip2;5pip2;6* double mutant and wild type (Col-0) plants were photographed with several sepals and petals removed, and measurements of floral organ length were taken using Image J. Petal length was measured from the tip to the base, while stamen length was measured from the apical tip of the anther to the base of

the filament. Only the length of long stamens was measured. Pistils were measured from the base to the underside of the stigma.

Stage one flowers were defined as the first bud in the inflorescence from which the petal is clearly protruding (figure 3.17A). Anthers of stage one flowers are very close to the point of dehiscence and sometimes filament extension and dehiscence of one or two anthers had occurred within stage 1 flowers. It is very difficult to stage unopened buds, therefore some variability at stage 1 is inevitable. Stage two flowers were defined as the first fully open flower of the inflorescence. In stage two flowers of wild type plants, the filaments have extended so that the long anthers are positioned above the stigma (which is receptive), most or all of the anthers have dehisced, and petals have significantly extended compared to petals of stage one flowers (figure 3.17C). Flower stages 1 and 2 were chosen to investigate changes to the timing of dehiscence and extension of the floral organs. An initial analysis showed that the difference between organ lengths at stage 1 and stage 2 was significant ($P<0.001$).

Timing of filament extension is critical for positioning the anther so that the pollen is deposited onto the receptive stigma. The stigmatic papillae (protuberances comprised of cells which are receptive to the pollen) start to appear before anthesis at flower stage 11. When the flower bud opens at the end of flower stage 12, the surface of the stigma is densely packed with papillae (Smyth et al., 1990). Petal extension is also important as it ensures the correct timing of flower opening. The developmental stages described above (flower stages 1 and 2) respectively correspond to late flower stage 12 and flower stage 14 described by Symth et al. (Smyth et al., 1990) It is possible that changes to floral organ lengths measured at these developmental stages could affect fertility.

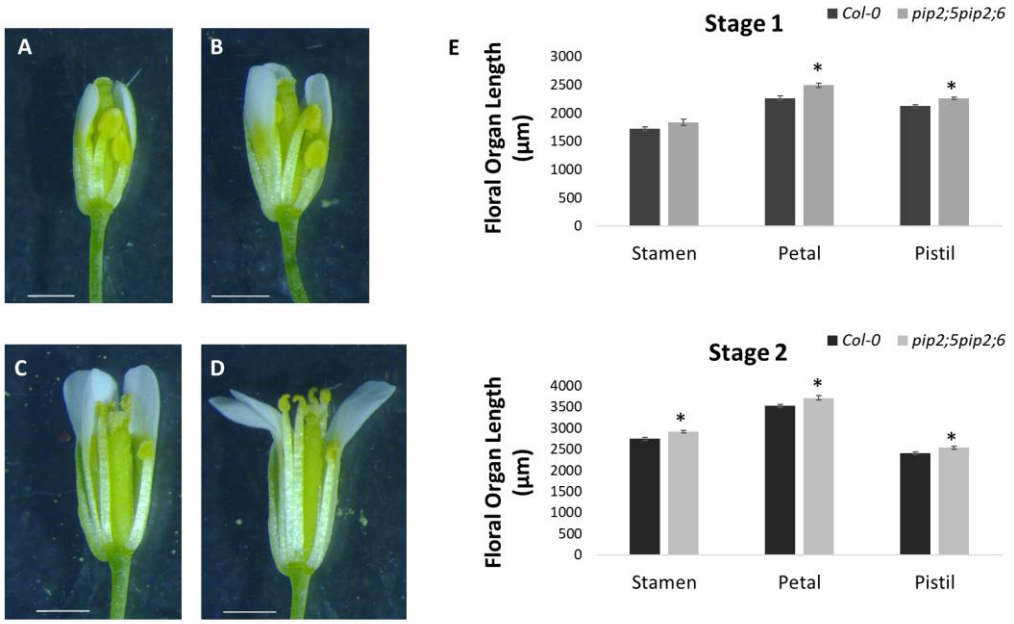

Figure 3.17: Analysis of *pip2;5pip2;6* flower development

A: Col-0 Stage 1 flower
B: *pip2;5pip2;6* Stage 1 flower
C: Col-0 Stage 2 flower
D: *pip2;5pip2;6* Stage 2 flower
E: Length of floral organs of *pip2;5pip2;6* double mutant plants and wild type (Col-0), at two stages of flower development. The results for two biological replicates are averaged. * indicates significant variation from wild type measurements of the same organ ($P<0.05$), error bars, standard error.

All scale bars = 1mm.

Analysis of the length of floral organs of the *pip2;5pip2;6* double mutant showed some variation from the equivalent wild type (Col-0) measurements. At stage 1, the lengths of petals and pistils was significantly increased ($P<0.001$). At stage 2, there was a significant ($P<0.05$) increase in the length of petals, pistils and stamens compared to wild type (figure 3.17A-E). These changes did not result in a decrease in fertility (figure 3.16E, F). Statistical analysis showed that the ratio of stamen length to pistil length did not vary significantly ($P>0.05$) between mutant and wild type plants. This suggests that, despite changes in length, the position of the anthers in relation to the stigma may still be optimal for pollen release in *pip2;5pip2;6* flowers.

3.2.3 Analysis of *PIP2;7* and *PIP2;8*

Single T-DNA insertions lines were ordered for genes *PIP2;7* and *PIP2;8* and plants were genotyped to identify homozygous mutants (figure A3 B, E). Line SALK_068839 has a T-DNA insertion located in the promoter (figure A3 A), and expression of *PIP2;7* was reduced 0.47-fold in flowers (figure A3 C). Line SALK_099098 has a T-DNA insertion disrupting exons 1 and 2 (figure A3 D), and expression of *PIP2;8* was reduced 0.37-fold in flowers (figure A3 F).

The expression of *PIP1;4*, *PIP2;2*, *PIP2;3*, *PIP2;5*, *PIP2;6* and *PIP2;7* was investigated in SALK_099098 (*pip2;8*) flowers, and compared relative to expression in wild type (Col-0) flowers (figure 3.18). Although *PIP2;8* was not knocked out in SALK_099098 flowers, significant changes to gene expression levels were observed. The expression level of *PIP1;4* was significantly reduced ($P<0.05$), while expression of *PIP2;5* was significantly increased ($P<0.05$). There was also a significant reduction in the expression levels of *PIP2;2* and *PIP2;3* ($P<0.001$). Despite *PIP2;7* being closely related to *PIP2;8* (figure 3.5), the expression level of *PIP2;7* was not significantly altered in the *pip2;8* mutant. It may be that these genes are not functionally redundant, and therefore reduced expression of *PIP2;8* is not compensated for by increased expression of *PIP2;7*. Alternatively, it is possible that in SALK_099098 flowers, expression of *PIP2;8* is not sufficiently reduced to cause a significant change to *PIP2;7* expression levels. In both the *pip2;6* and *pip2;8* single mutants, there was a significant reduction in the expression levels of *PIP1;4*, *PIP2;2* and *PIP2;3*, which suggests that these genes may be co-regulated with other aquaporins.

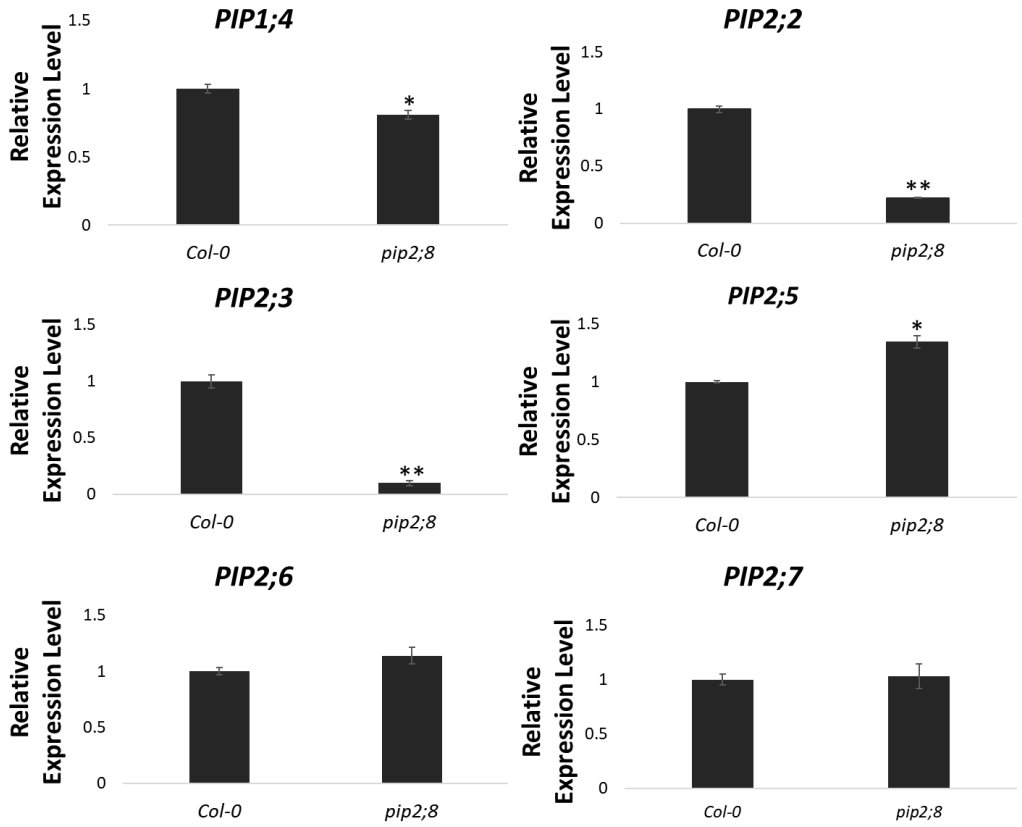

Figure 3.18: Expression of various aquaporin genes in SALK_099098 (*pip2;8* mutant) flowers (whole inflorescence), relative to wild type (Col-0). Reference gene *PP2A-3* (AT2G42500). * indicates a significant difference in expression ($P<0.05$), ** ($P<0.001$). Error bars, standard error.

Alexander's stain was used to assess pollen viability of the T-DNA insertion mutants (figure 3.19A) and FDA staining was used for a statistical analysis (figure 3.19B). The pollen viability of *pip2;7* and *pip2;8* single mutants did not differ significantly from wildtype ($P>0.05$). Seed set was used as a measure of plant fertility (figure 3.19C, D) and both of the T-DNA insertion lines had a significant reduction in the length of siliques formed on the main stem ($P=0.001$). There was a significant increase ($P<0.05$) in the number of sterile siliques on the main stem of *pip2;8* plants, compared to the wild type control.

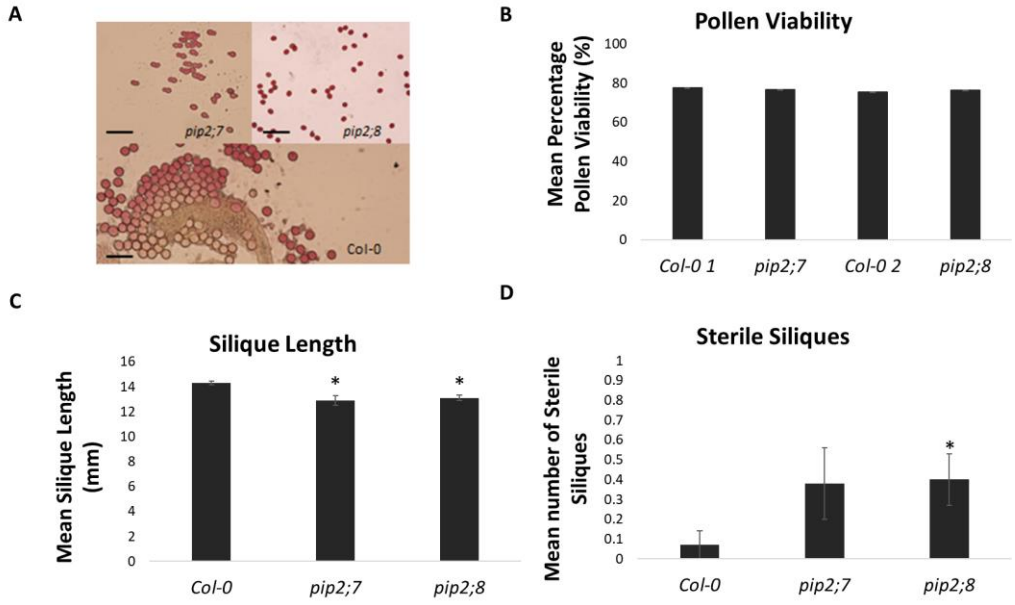

Figure 3.19: Characterisation of *pip2;7* and *pip2;8* mutants

A: Alexander's staining for pollen viability.
B: Percentage pollen viability of *pip2;7* (SALK_068839) and *pip2;8* (SALK_099098) mutants and wild type (Col-0) calculated from FDA staining. The effect of genotype is not significant, P>0.05, error bars, standard error.
C: Silique length of *pip2;7* (SALK_068839) and *pip2;8* (SALK_099098) mutants and wild type (Col-0). Silique length of the 1st to 6th siliques on the main stem was measured. * indicates significant variation from the wild type control (P=0.001), error bars, standard error.
D: Number of sterile siliques on the main stem of *pip2;7* (SALK_068839) and *pip2;8* (SALK_099098) mutants and wild type (Col-0). * indicates significant variation from the wild type control (P<0.05), error bars, standard error.

While attempting to generate a *pip2;7pip2;8* double mutant a male sterile phenotype was identified. Plants with the phenotype had filaments that did not extend at all and indehiscent anthers. The unidentified mutation causing the phenotype will be referred to as *short anther* from hereon in. Statistical analysis of floral organ lengths within stage 1 and 2 flowers confirmed that there is a significant reduction in stamen length at both stages compared to wild type (P<0.001), and this is clearly visible by eye at stage 2 (figure 3.20D). There was no change to the petal length of mutant flowers while pistil length was significantly longer at stage 1 (P<0.05) (figure 3.20E). FDA staining was used to assess viability of pollen from plants with the phenotype. There was a significant reduction in the percentage of

viable pollen from *short anther* plants compared to wild type (P<0.05) (figure 3.20F).

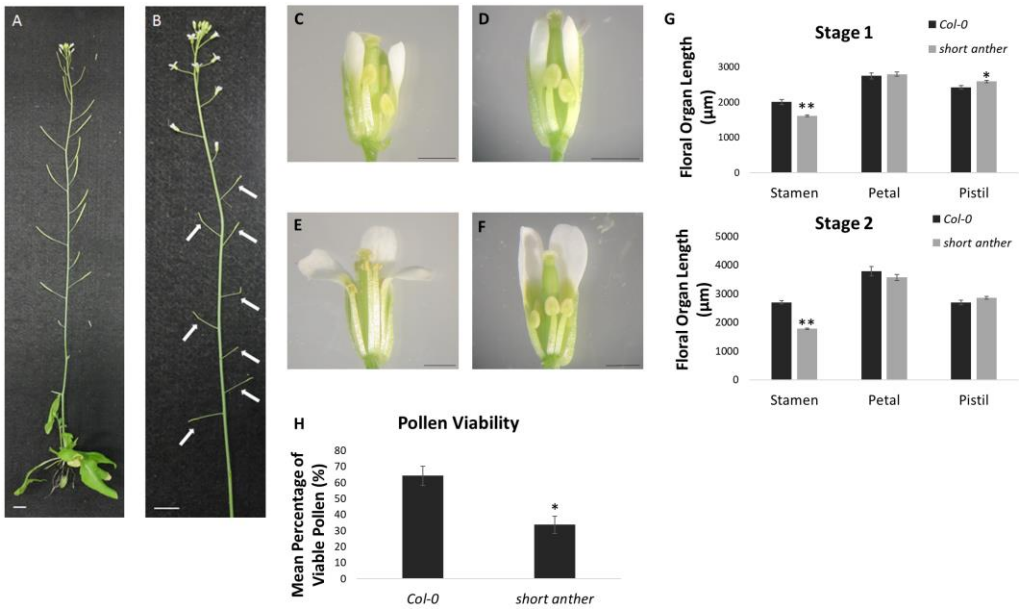

Figure 3.20: Analysis of *short anther* flower development

A: Main stem of Columbia
B: Main stem of *short anther*. White arrows indicate the position of sterile siliques
C: Col-0 Stage 1 Flower
D: *short anther* Stage 1 Flower
E: Col-0 Stage 2 Flower
F: *short anther* Stage 2 Flower
G: Length of floral organs of *short anther* plants and wild type (Col-0), at two stages of flower development. * indicates significant variation from wildtype measurements of the same organ (P<0.05), ** indicates P<0.001, error bars, standard error.
H: Percentage pollen viability of *short anther* plants and wild type (Col-0) calculated from FDA staining. * indicates significant variation from the wild type control (P<0.05), error bars, standard error.

A, B scale bars = 1cm
C, D, E, F scale bars = 1mm

In order to maintain the mutation, the plant showing the phenotype was crossed with wild type (Col-0) pollen. The F1 seed was collected and sown and the phenotype was observed within the segregating population. The population was genotyped for the SALK_068839 (*pip2;7*) and SALK_099098 (*pip2;8*) T-DNA insertions (figure 3.21). Genotyping revealed that plants were a mix of wild type and *pip2;8* single mutants (both heterozygous and homozygous). The male

sterile phenotype did not appear to be segregating with the *pip2;8* mutation (table 3.5). This observation is also supported by the previous phenotyping of *pip2;8* plants (figure 3.19).

Table 3.5: Genotyping and phenotyping of the segregating F1 population. The silique length of the first six siliques on the main stem was averaged. The mean number of sterile siliques on the main stem was averaged.

Plant	Genotype	Mean Silique Length (mm)	Mean number of sterile siliques	Phenotype
1	*pip2;8* (Hm)	11.67	1	N
2	*pip2;8* (Hm)	12.5	1	N
9	*pip2;8* (Hm)	10.5	1	N
13	*pip2;8* (Hm)	3.33	9	Y
16	Wt	14	0	N
18	Wt	11.67	0	N
19	*pip2;8* (Hm)	12.17	0	N
20	Wt	13	0	N
21	*pip2;8* (Hm)	3	3	Y
22	*pip2;8* (Hm)	3	4	Y
24	*pip2;8* (Ht)	12.33	0	N

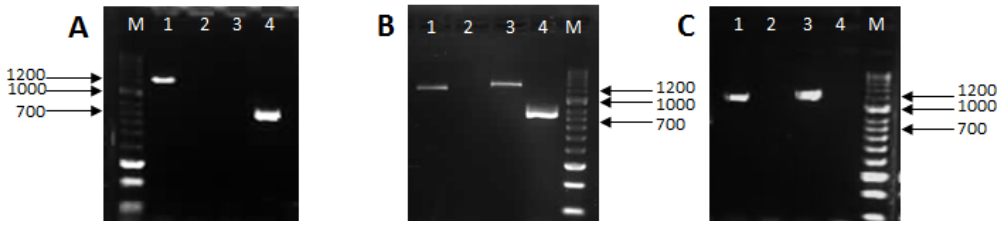

Figure 3.21: Genotyping examples from a population segregating for the *short anther* phenotype

A: Genotyping example for plant identified as *pip2;8* (Hm).
B: Genotyping example for plant identified as *pip2;8* (Ht).
C: Genotyping example for plant identified as Wt.

All PCRs performed using primer pairs;

Lane 1 = SALK_068839F/ SALK_068839R (1065bp)
Lane 2 = LBlb.3F/SALK_068839R (493-793bp)
Lane 3 = SALK_099098F/SALK_099098R (1166bp)
Lane 4 = LB1b.3F/SALK_099098R (580-880bp)
M, hyperladder™ 50bp.

It is possible that the phenotype detected was caused by a contaminant – possibly from cross pollination with another male

sterile mutant. Several previously characterised male sterile mutants share phenotypic features with this unidentified mutant. The *ams* mutant also has reduced filament extension, and anthers are positioned below the stigma at anthesis. However, the *ams* mutant does not produce mature pollen although desiccation of the anthers occurs as normal (Sorensen et al., 2003) (figure 3.22E, F). Another male sterile mutant that does not produce viable pollen is *ms1*, although the phenotype of the plants is otherwise normal (Wilson et al., 2001). Despite an overall reduction in the viability of pollen from *short anther* plants, some viable pollen grains were observed, which suggests that neither *ams* or *ms1* is the contaminant. This mutation could also have been the result of an independent mutation during T-DNA insertion during the SALK line generation.

The anthers of *short anther* plants did not dehisce, even in older open flowers. This phenotype is concurrent with the phenotype of other dehiscence mutants such as *myb26* or *nst1nst2*. Failure of dehiscence in these mutants is caused by defective formation of secondary thickening in the endothecium however filaments extend normally and, if mechanically opened, the anthers contain viable pollen (Mitsuda et al., 2005; Steiner-Lange et al., 2003).

Jasmonic acid mutants are the class of male sterile mutants with the phenotype closest to what was observed. Jasmonic acid mutants are characterised by delayed filament extension, delayed dehiscence or indehiscent anthers, and non-viable pollen. Treatment of JA biosynthesis mutants with jasmonates, results in recovered fertility (Ishiguro et al., 2001; Wilson et al., 2011). Anthers of JA mutants do not undergo normal desiccation, and unopened anthers remain turgid (figure 3.22D). The anthers of plants displaying the *short anther* phenotype remained turgid after anthesis, when compared against *ams* and *myb26* anthers, which appear desiccated (figure 3.22B, C, E). This suggests that anther dehydration does not occur normally in plants with the *short anther* mutation.

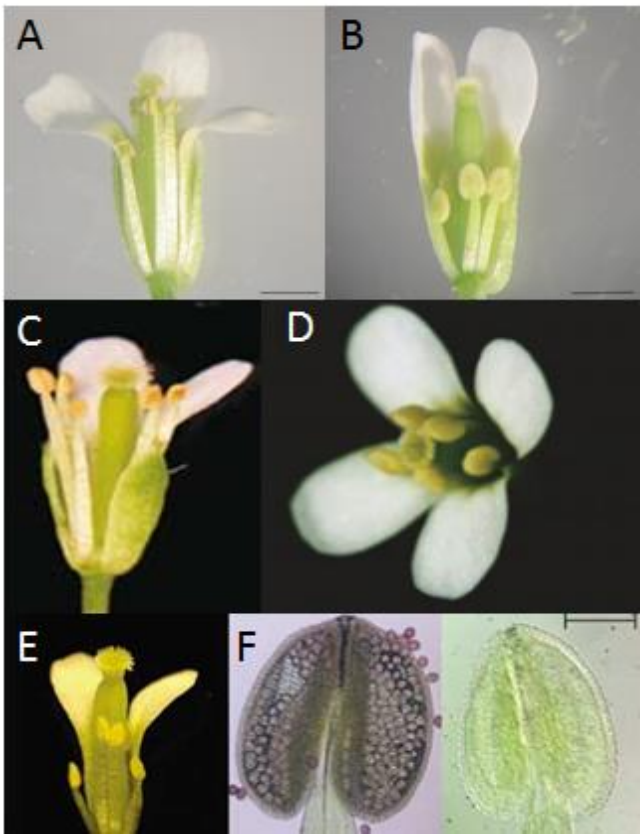

Figure 3.22: Comparison between open flowers of male sterile mutants. Figure adapted from (Ishiguro et al., 2001; Sorensen et al., 2003; Steiner-Lange et al., 2003).

A: Wild type (Col-0) open flower. Bar = 1mm.
B: *short anther* open flower. Bar = 1mm.
C: *myb26* open flower.
D: *dad1* open flower.
E: *ams* open flower.
F: Wild type (left) and *ams* (right) anthers. Bar = 200μm.

Although some features of the *short anther* phenotype were consistent with those of a jasmonic acid mutant, there were some discrepancies. Filament extension did not occur in *short anther* flowers, even after anthesis and anthers remained indehiscent. Pollen from indehiscent anthers of open flowers contained a mix of viable and non-viable grains. It is therefore possible that this phenotype has been caused by a novel mutation. In order to determine whether the observed phenotype is novel, a full spectrum qRT-PCR could be used to check expression of genes that commonly cause male sterility. If the expression level of the genes investigated is normal compared to

wild type, then this information can be used to eliminate possible contaminants.

3.2.4 Analysis of *pip1;2pip2;1* and *pip1;2pip2;1pip2;6* double and triple mutants

Seed for aquaporin double and triple mutants *pip1;2pip2;1* and *pip1;2pip2;1pip2;6* was obtained from Christophe Maurel (CNRS). Molecular characterisation of these knockout lines is described in (Prado et al., 2013). The contribution of *PIP1;2, PIP2;1* and *PIP2;6* to water transport within rosette leaves has been studied, however affects to the fertility of knockout lines was not investigated. FDA staining was used to assess pollen viability of the double and triple mutants and no significant change was detected compared to the wild type control ($P>0.05$).

Analysis of seed set showed that both double and triple mutant plants had reduced fertility compared to Columbia. There was a significant reduction in the length of siliques on the main stems of *pip1;2pip2;1* and *pip1;2pip2;1pip2;6* plants compared to wild type (Col-0) (figure 3.23A-D). The double and triple mutants also had a higher proportion of sterile siliques on the main stem (figure 3.23A-C and E). Sterile siliques tended to result from early flowers, suggesting that fertility is recovered later on.

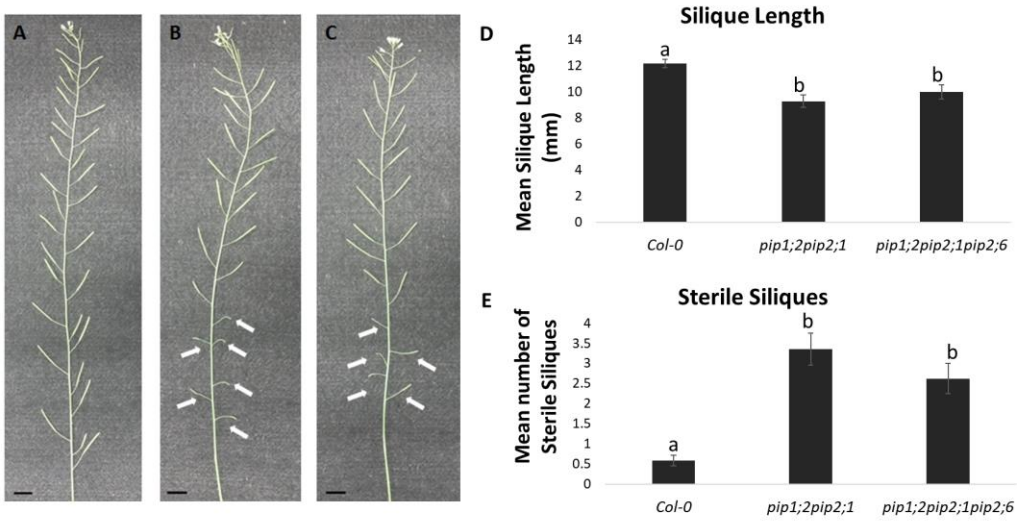

Figure 3.23: Characterisation of *pip1;2pip2;1* and *pip1;2pip2;1pip2;6* mutants

A: Main stem of Columbia
B: Main stem of *pip1;2pip2;1*. White arrows indicate position of sterile flowers.
C: Main stem of *pip1;2pip2;1pip2;6*. White arrows indicate position of sterile flowers.
D: Silique length of the *pip1;2pip2;1*and *pip1;2pip2;1pip2;6* mutants and wild type (Col-0). Silique length of the 1st to 6th siliques on the main stem was measured. Bars marked with different letters vary significantly (P=0.001), error bars, standard error.
E: Number of sterile siliques on the main stem of the *pip1;2pip2;1*and *pip1;2pip2;1pip2;6* mutants and wild type (Col-0). Bars marked with different letters vary significantly (P<0.001), error bars, standard error.

All scale bars = 1cm.

The *pip1;2pip2;1pip2;6* triple mutant showed a significant increase (P<0.05) in the length of floral organs compared to wild type in both stage 1 and stage 2 flowers (figure 3.24). With the exception of increased pistil length at stage 2 (P<0.001), floral organ lengths of *pip1;2pip2;1* flowers did not vary significantly from the control. Although the three genes are not phylogenetically close, this result suggests that there is a degree of functional redundancy between them which is overcome by knocking out a third PIP aquaporin. The student's t-test was used to compare the ratios of stamen: pistil length. There was no significant difference between the ratios at stage 1 (P>0.05) for *pip1;2pip2;1pip2;6* and wildtype, however the ratio of *pip1;2pip2;1pip2;6* stamen: pistil length was lower

(P<0.001) at stage 2. The ratio of *pip1;2pip2;1* stamen: pistil length was also significantly lower (P<0.001) at stage 2. At stage 2 all stamens (mutant and wild type) are positioned above the pistil. A lower ratio indicates that stamens are closer to the pistil which is unlikely to cause a decrease in fertility.

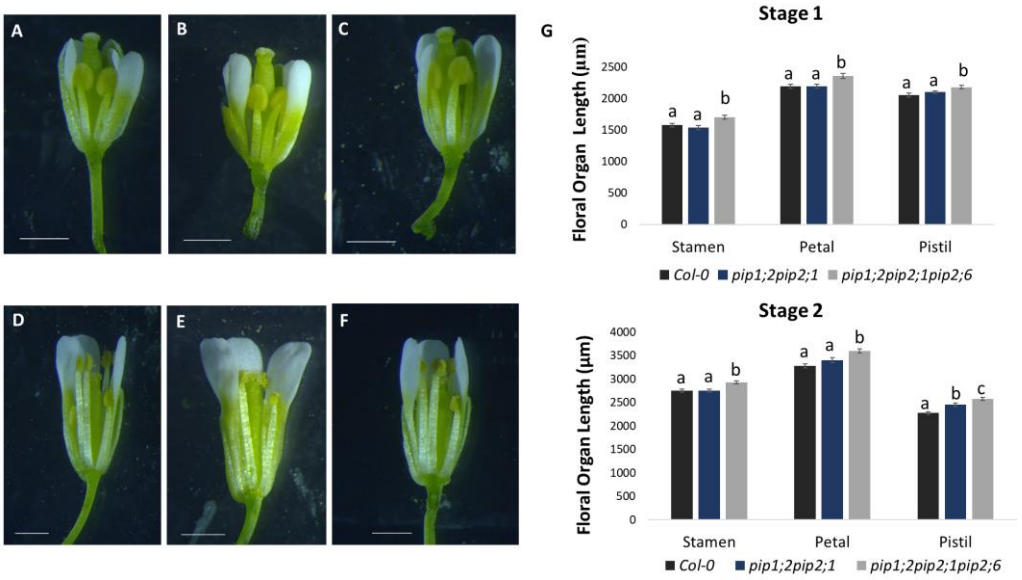

Figure 3.24: Analysis of *pip1;2pip2;1* and *pip1;2pip2;1pip2;6* flower development

A: Col-0 Stage 1 flower
B: *pip1;2pip2;1* Stage 1 flower
C: *pip1;2pip2;1pip2;6* Stage 1 flower
D: Col-0 Stage 2 flower
E: *pip1;2pip2;1* Stage 2 flower
F: *pip1;2pip2;1pip2;6* Stage 2 flower
G: Length of floral organs of *pip1;2pip2;1, pip1;2pip2;1pip2;6* plants and wild type (Col-0), at two stages of flower development. The results for two biological replicates are averaged. Bars marked with different letters vary significantly for that organ (P<0.05), error bars, standard error.

All scale bars = 1mm.

In order to further investigate the observed fertility changes in the *pip1;2pip2;1* and *pip1;2pip2;1pip2;6* mutants, the number of dehisced anthers were counted at stage 1 and 2 (figure 3.25). The student's t-test was used to compare the results from each of the insertion mutant lines against the wild type control. There was no significant difference between the number of dehisced anthers at each stage (P>0.05).

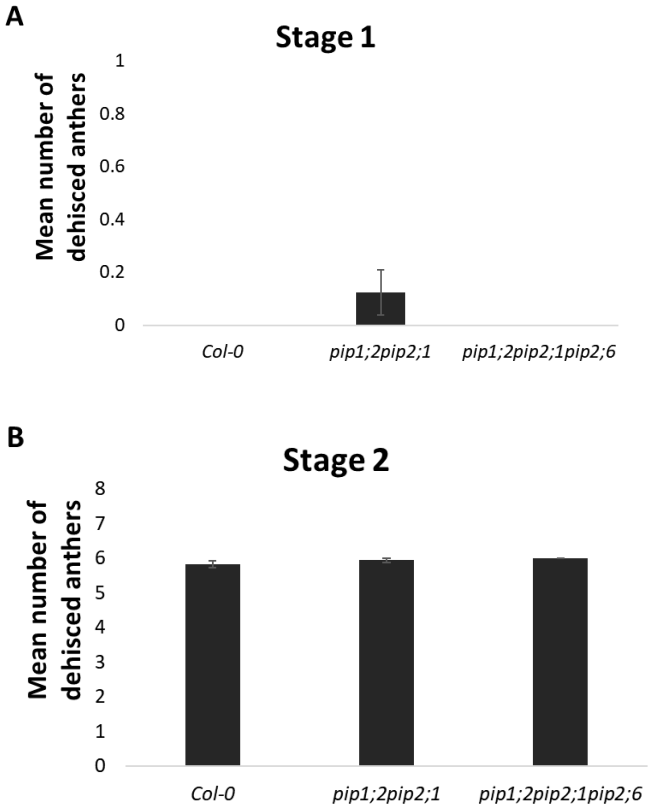

Figure 3.25: Analysis of *pip1;2pip2;1* and *pip1;2pip2;1pip2;6* dehiscence

A: Mean number of anther dehisced within Stage 1 flowers, error bars, standard error.
B: Mean number of anthers dehisced within Stage 2 flowers, error bars, standard error.

Stigma receptivity was then compared between the double and triple mutants and wild type at each stage. Figure 3.26 shows that stigma receptivity appears normal in both of the mutant lines, the papillae are present and stage 2 flowers contain receptive stigmas coated in pollen.

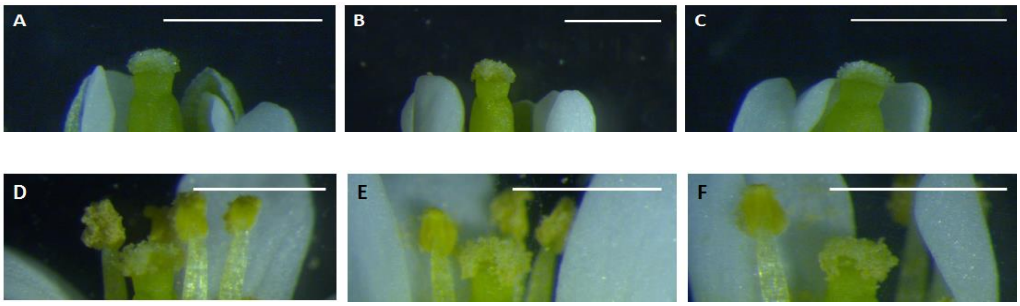

Figure 3.26: Analysis of *pip1;2pip2;1* and *pip1;2pip2;1pip2;6* stigma receptivity

A: Col-0 Stage 1 stigma
B: *pip1;2pip2;1* Stage 1 stigma
C: *pip1;2pip2;1pip2;6* Stage 1 stigma
D: Col-0 Stage 2 stigma
E: *pip1;2pip2;1* Stage 2 stigma
F: *pip1;2pip2;1pip2;6* Stage 2 stigma
All scale bars = 1mm.

It is difficult to conclude what is causing the reduction in fertility observed in the *pip1;2pip2;1* and *pip1;2pip2;1pip2;6* mutant lines. Pollen viability, stigma receptivity and dehiscence appear to be normal, and although there are some changes to floral organ lengths, these seem unlikely to cause such a severe reduction in fertility. It is possible that other unexplored factors are the cause – for example pollen germination, or pollen tube growth.

3.3 Discussion

3.3.1 The majority of *Arabidopsis PIP1* and *PIP2* aquaporin genes are highly expressed during anther dehiscence

Analysis of publicly available microarray data (see tables 3.1 and 3.2) showed that all of the *PIP1 Arabidopsis* aquaporin genes are highly expressed in the late flower stages. With the exception of *PIP2;4*, all of the *PIP2* aquaporins are also highly expressed during flower stages 12/15, as are three *TIP* genes. Jang et al. calculated transcript levels for *PIP* aquaporins in aerial parts of the two-week-old seedlings relative to actin (Jang et al., 2004). The analysis showed that RNA transcripts levels varied significantly from gene to gene. Gene

expression levels calculated from qRT-PCR CP values (table 3.2) also showed this, and although the results are not comparable as different tissues and a different reference gene were used, some similarities were observed – in particular the low relative expression of *PIP1;4* and *PIP2;1* and the high relative expression of *PIP2;7* and *PIP1;1,* in comparison to the other *PIPs* (Jang et al., 2004).

Table 3.6 summarises gene expression data from qRT-PCR experiments and analysis of GUS-promoter lines. Only genes that showed significant ($P<0.05$) changes in expression are included in the summary table. Staged buds were used to investigate gene expression changes during pollen and anther development (section 2.1.5). It is possible that aquaporin genes significantly upregulated at bud stage 4 relative to bud stage 1, could be required for processes such as filament and petal extension or facilitating the targeted removal of water from the anther walls prior to dehiscence. qRT-PCR analysis identified four genes (*PIP1;5/PIP2;1/PIP2;2/PIP2;3*) which are upregulated during bud stage 4. Analysis of *PIP1;5* and *PIP2;1* promoter activity using GUS reporter constructs (see table 3.3 and section 3.2.1.5) showed tissue specific expression patterns relevant to the aforementioned processes.

Ecotype specific variation in gene expression was observed for three genes (table 3.6). This was particularly notable for *PIP1;4*, where gene expression was significantly higher ($P<0.001$), in the Columbia background at all four bud stages (see figure 3.8). Ecotype specific expression has previously been reported in *Arabidopsis,* for example the Epithiospecifier protein (ESP), which affects defence against insect herbivory, has varying levels between the Martuba (Mt-0) and Columbia (Col-0) ecotypes (Kissen et al., 2012). Analysis revealed the gene is regulated differently and a mis-spliced transcript could be responsible for lower levels of ESP in Columbia (Kissen et al., 2012). This was also the case for genes encoding sucrose transporter *SUC6/7*, which are only correctly spliced in Wassilewskaija (Ws) and classed as pseudogenes in C24, Ler-0 and Col-0 (see section 4.1) (Sauer et al., 2004). Further analysis, including examination of

transcript sequences and protein levels in both Ler-0 and Col-0, would be necessary to explain the differences observed in figure 3.8.

Table 3.6: Summary of expression analysis data for the *Arabidopsis* aquaporins. In staged buds, expression at bud stage 4 was compared against expression at bud stage 1 (background Ler-0). Ecotype specific variation was analysed by comparing gene expression in a Col-0 background against gene expression in a Ler-0 background. In the *pip2;6*, *pip2;5pip2;6* and *pip2;8* backgrounds, gene expression was compared against expression in a wild type background (Col-0). Promoter activity detected using GUS reporter lines is summarised. ^=higher expression, ˅=lower expression.

Gene	Staged Buds	Ecotype Specific Variation	*pip 2;6*	*pip2;5 pip2;6*	*pip 2;8*	GUS Activity
PIP 1;2				^		Filaments/ vascular and connective tissue/pollen /petals/sepal/ stigma of open flowers
PIP 1;3	˅					
PIP 1;4		^ Col-0	˅		˅	
PIP 1;5	^			˅		Petals/sepals of open flowers
PIP 2;1	^					Filaments/ vascular and connective tissue/ /petals/sepal/ stigma of open flowers
PIP 2;2	^		˅		˅	
PIP 2;3	^		˅	˅	˅	
PIP 2;5	˅		^		^	
PIP 2;6		˅ Col-0				
PIP 2;7	˅			^		Filaments of open flowers/ stigma of early buds
PIP 2;8	˅					
TIP 1;1		^ Col-0				

3.3.2 Complex regulatory relationships may exist between aquaporin isoforms

Changes to aquaporin gene expression in the *myb26* and *dad1* mutant backgrounds varied between replicates. A possible cause for the observed variation could be the growth conditions of the plants. The majority of the *PIP* aquaporins are down regulated in response to drought stress (Alexandersson et al., 2005), therefore changes in temperature and/or watering patterns could have had an effect. Changes in temperature caused by growing plants at different times of year could be avoided by using a growth room. Other environmental stresses, such as insect infestation, may also have affected gene expression.

Ishiguro et al. hypothesise that JA controls anther dehydration by regulating expression of genes required for water transport (Ishiguro et al., 2001). Some aquaporin genes show expression changes in the JA time course in the FlowerNet (figure 3.10), and if aquaporin gene expression is regulated by JA then application of exogenous JA would be expected to affect gene expression. The data shown in the FlowerNet plots is inconclusive however, because expression patterns are similar in both the *opr3* + JA and mock treated controls. As previously discussed (section 3.1), aquaporin gene expression is not always reflective of protein activity as aquaporins are often subject to post-translational regulation. It is possible that JA could control aquaporin activity indirectly via regulation of genes that control post-translational regulation. This could also be true of *MYB26*, although this seems less likely as evidence suggests that secondary thickening and anther dehydration are separately controlled processes. Treatment of the *myb26* mutant with JA does not recover the mutant phenotype and *MYB26* has not been identified as a jasmonate induced gene (Mandaokar et al., 2006; Steiner-Lange et al., 2003).

Analysis of gene expression in the *pip2;6, pip2;5pip2;6* and *pip2;8* mutant backgrounds suggests that complex regulatory relationships exist between the aquaporins. Upregulation of *PIP2;5* in the *pip2;6*

mutant background implies that these two genes may be functionally redundant, although the *pip2;5pip2;6* mutant did not have an additive phenotype (section 3.2.2). It seems that changes in expression of one aquaporin isoform, influences the expression of others (table 3.6). Jang et al. showed that constitutive expression of *PIP1;4* and *PIP2;5* led to altered expression of different *PIP*s under different abiotic stresses, and concluded that overexpressing an aquaporin affects expression of other endogenous aquaporins under stress conditions (Jang et al., 2007). Although the changes reported in the different mutant backgrounds (table 3.6) were not recorded under stress conditions, these observations support the possibility of complex regulatory relationships between the *PIP* aquaporins. Interestingly, Jang et al. reported levels of *PIP2;3* to be downregulated under osmotic and dehydration stress (Jang et al., 2004, 2007), and *PIP2;3* expression was also lower in all three mutant backgrounds (table 3.6). It would be intriguing to see how expression of other aquaporins is altered in a *pip2;3* mutant background.

3.3.3 The promoter activity of certain aquaporins is confined to specific parts of the flower

Analysis of the promoter activity of *PIP1;2, PIP1;5, PIP2;1* and *PIP2;7* showed that gene expression is confined to specific parts of the flower (section 3.2.1.5). To date, no role for the *PIP1* and *PIP2* aquaporins has been characterised in flowers, however the expression patterns identified suggest distinct but overlapping functions for these aquaporins in flower development. All four genes are expressed highly during flower stages 12/15 (table 3.1) and qRT-PCR analysis using staged buds showed that *PIP1;5* and *PIP2;1* were significantly upregulated at bud stage 4 relative to bud stage 1 (table 3.6), which correlates with their expression in open flowers. *PIP2;7*, which had significantly lower expression at bud stage 4 relative to bud stage 1,

showed faint GUS staining in the stigmas from buds prior to anthesis (figure 3.12).

Based on the very specific gene expression patterns observed for *PIP1;2*, *PIP1;5, PIP2;1* and *PIP2;7* by GUS staining, it is possible to predict functions for these aquaporins in flower development. These are only speculations however and further evidence, such as identification of corresponding mutant phenotypes, would be needed to confirm them. The expression of *PIP1;2*, *PIP1;5* and *PIP2;1* in the sepals and petals of open flowers, suggests that these aquaporins could facilitate water transport for organ expansion. As aquaporins mediate most of the water movement across the plasma membrane they play a critical role in controlling turgor pressure for cell expansion (Beauzamy et al., 2014). The growth and movement of organs such as the petals, relies on osmoregulation and cell expansion (section 1.3). Similarly, expression of *PIP1;2*, *PIP2;1* and *PIP2;7* within the filaments of open flowers could mean that these aquaporins are required for filament extension. While *PIP1;2* and *PIP2;7* are expressed throughout the filament as a whole, *PIP2;1* has a very specific expression pattern in the anther connective tissue and vascular bundle (figure 3.12). This distinct pattern of expression supports the theory proposed by Botts et. al (section 1.3), who hypothesise that PIP2 aquaporins are present in the anther connective tissue to enhance water flow towards the vascular bundle during anther dehydration (Bots et al., 2005a). Finally, GUS staining was observed in the pollen grains of anthers from *PromPIP1;2*-GFP-GUS flowers (figure 3.12) and although, according to the *Arabidopsis* eFP browser, all of the *PIP1* and *PIP2* aquaporins have low expression in mature pollen (table 3.1), roles for NIP and TIP aquaporins in pollen development have been described (section 3.1).

3.3.4 Combinations of single, double and triple *Arabidopsis* aquaporin mutants showed changes to fertility

Analysis of mutant phenotypes showed that aquaporins are required for normal fertility in *Arabidopsis*. The majority of the lines investigated showed a reduction in seed set however the phenotype was most noticeable in the *pip1;2pip2;1* and *pip1;2pip2;1pip2;6* double and triple mutants. For both of these lines, the increase in sterile siliques and reduction in overall silique length, compared to wild type, was highly significant ($P \leq 0.001$). Changes in floral organ lengths were detected in *pip2;5pip2;6* and *pip1;2pip2;1pip2;6* flowers. In both lines the lengths of pistils, petals and stamens were significantly increased ($P < 0.05$) compared to wild type (see figures 3.18 and 3.25). Changes in floral organ lengths are likely to be linked to changes in water movement within the flower, as in *dad1* flowers both stamen and petal elongation is delayed (Ishiguro et al., 2001). A putative role for *PIP* aquaporins in petal growth for flower opening has been described in carnations (Morita et al., 2017) and the expression patterns observed by GUS staining for *PIP1;2* and *PIP2;1* suggest roles in petal and filament expansion. Why downregulation of these genes results in increased organ length is puzzling, as a reduction in the number of plasma-membrane located aquaporin channels would be expected to restrict water flow into cells. It could be that knocking out certain aquaporin genes increases the expression of others (section 3.3.1), which overcompensate for the function of those knocked out. A full spectrum qRT-PCR analysis of the mutant lines would help determine this, as would a broader investigation of aquaporin expression patterns in floral organs using GUS reporter lines.

In jasmonic acid mutants, dehiscence is delayed because removal of water from the endothecium, connective tissues and anther locules to the vascular tissue is blocked (see section 1.2.1) (Ishiguro et al., 2001). Although the expression pattern of *PIP2;1* in the anthers of open flowers (figure 3.12) suggests it may play a role in the targeted

removal of water for anther opening, delayed dehiscence was not observed in either of the *pip1;2pip2;1* or *pip1;2pip2;1pip2;6* mutants (figure 3.26). Dehiscence occurs just before anthesis and subtle delays are difficult to detect, it is also possible that functional redundancy with other aquaporin isotopes masked any effect.

It is not possible to conclude what caused the fertility changes reported for the aquaporin mutant lines. Although pollen viability appeared normal for all of the lines, it is recommended that further analysis, examining germination rates and pollen tube growth, is conducted. The possibility that fertility changes are caused by disruption to plant female reproduction should also not be discounted. GUS staining showed that *PIP1;2* was expressed in the style and stigma and *PIP2;1* in the stigma below the style (figure 3.12), suggesting a possible function for these aquaporins in female floral organs.

3.3.5 A novel phenotype was identified

The *short anther* phenotype identified in section 3.2.3 may be caused by a novel mutation. Flowers have indehiscent anthers that remain turgid after anthesis and filaments that do not extend. A notable reduction in pollen viability was also observed. This phenotype most closely resembles that of a jasmonic acid mutant, where pollen viability is reduced, filament extension and anther opening are delayed, and unopened anthers remain turgid. In order to establish whether the *short anther* phenotype is caused by a mutation in the JA biosynthesis pathway, it is recommended plants are treated with exogenous JA. If the phenotype is a result of a mutation that affects JA perception, then it will not be recovered by the application of JA. Further characterisation would require gene identification by mapping, genomic sequencing and transcriptomic analysis.

CHAPTER 4 ANALYSIS OF *ARABIDOPSIS* SUCROSE TRANSPORTERS EXPRESSED IN FLOWERS

4.1 Introduction

Osmoregulation is the adjustment of cytosolic and vacuolar concentrations of ions, amino acids and sugars, which enables a cell to control its water content. The resultant changes in turgor pressure are essential for many developmental processes inside plants including pollen tube growth, flower opening and anther dehiscence (Beauzamy et al., 2014). The reallocation of water during anther dehiscence has been attributed to the active transport of sugars. Keijzer documented a sudden depletion of starch in *Gasteria verrucosa* anthers which was accompanied by movement of water from the anthers to the filament (Keijzer, 1987). A depletion of starch deposits in the connective tissue was also observed in *Lycopersicon esculentum* during anther dehydration (Bonner and Dickinson, 1990). In *Petunia hybrida* down regulation of the *NEC1* gene caused early anther opening (Ge et al., 2000). *NEC1* is expressed predominantly in the nectaries but also in the stomium cells and upper part of the filament. In the *nec1* mutant the stomium ruptures early and in young flower buds some anthers were open, resulting in ineffective release of immature pollen. In the nectaries *NEC1* is assumed to play a role in sugar hydrolysis, and in the anthers it appears that *NEC1* is required for stomium function, however the exact role of *NEC1* during anther dehiscence remains unclear (Ge et al., 2000, 2001).

Sucrose/H^+ symporters rely on ATP-ases which use energy to pump H^+ against its electrochemical gradient. H^+ ions then flow down their electrochemical potential through sucrose/H^+ symporters, driving a flux of sucrose molecules in the same direction (Bush, 1993; Zhou et al., 1997). Plant sucrose transporters are transport proteins that belong to the major facilitator superfamily. The plant sucrose transporters form a distinct group have been classified into four sub-groups based on protein sequence analysis (figure 4.1A). Groups 1

and 2 contain sequences from monocots and dicots respectively, while groups 3 and 4 contain a mixture of both monocot and dicot sequences. Out of the nine *Arabidopsis* sucrose transporters, the majority (SUC1, SUC2, SUC5, SUC8 and SUC9) are classified as group 2 transporters, while only one belongs to group 3 (SUC3) and one to group 4 (SUT4) (Sauer, 2007). *SUC6* and *SUC7*, which have high sequence homology to *SUC8*, have been classified as pseudogenes because they encode truncated proteins in the *Arabidopsis* ecotypes C24, Columbia (Col-0) and Landsberg *erecta* (Ler-0) (Sauer et al., 2004).

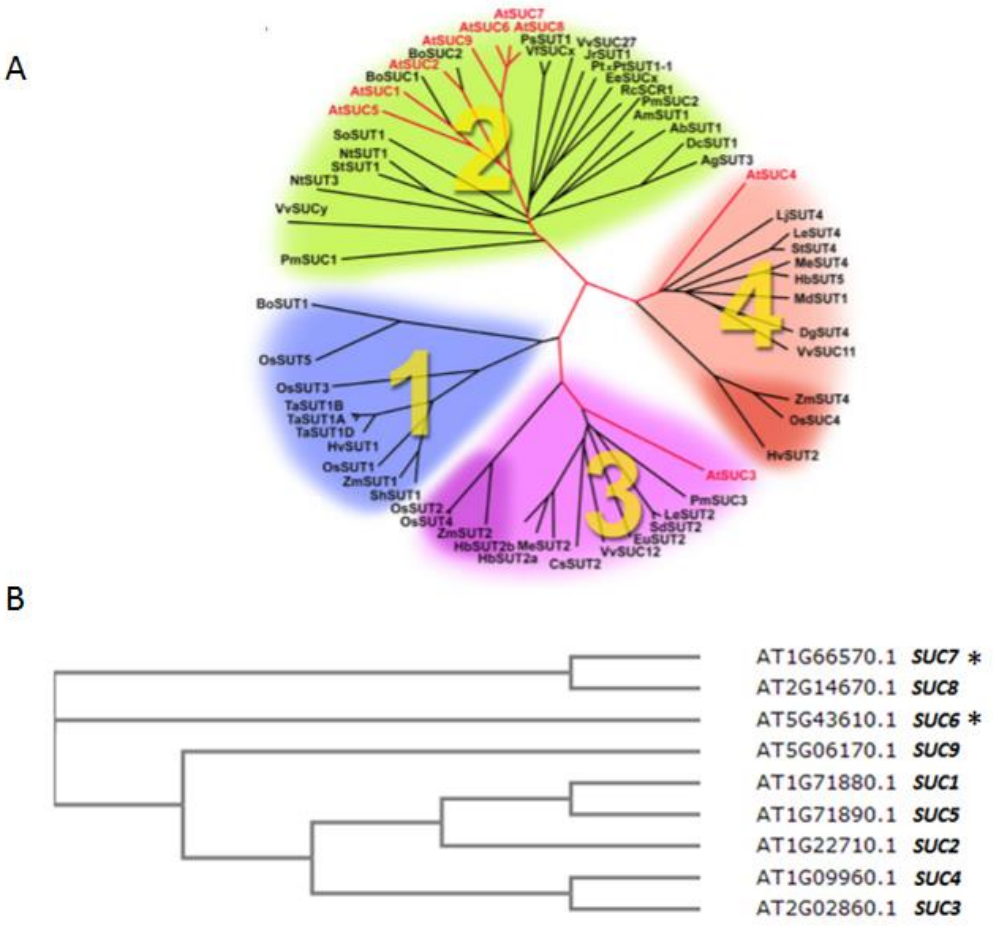

Figure 4.1: Classification of plant sucrose transporters.

A: Phylogenetic tree for 62 plant sucrose transporters based on protein sequences. *Arabidopsis* sucrose transporters are shown in red. Figure adapted from (Sauer, 2007).
B: Phylogenetic tree for genes encoding *Arabidopsis* sucrose transporters based on gene sequences. Figure created using Clusteral W2 (Larkin et al., 2007). * indicates classified as pseudogenes.

Plant sucrose transporters are comprised of twelve transmembrane helices arranged into two halves and originating from a gene duplication event (Sauer, 2007). Sucrose transporters belonging to groups one, two and three, are located within plasma membranes and it has been demonstrated that the N and C termini of the proteins are on the cytoplasmic side of the membrane. Sequence variation amongst the different groups is predominately confined to the linker sequences between the transmembrane helices and to the N and C terminal ends. The group three transporters are characterised by an elongated N-terminus and a much larger cytoplasmic loop. Group four

transporters are predicted to be located in the vacuole and have a shorter C-terminus and linker sequence between helices VII-VIII. A model for how the transmembrane helices may be arranged to form the substrate pore is shown (figure 4.2) (Sauer, 2007).

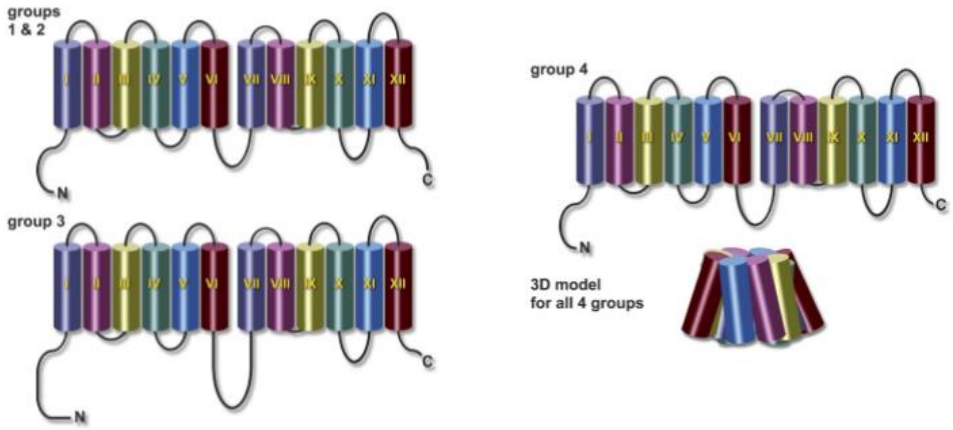

Figure 4.2: The structure of plant sucrose transporters

Predicted 2D models for the four groups of plant sucrose transporters. Variations in the length of the N and C terminal ends and linker sequences between the transmembrane helices are shown. A 3D model of pore structure for all four groups is based on available crystal structure data for other major facilitator superfamily members. Figure adapted from (Sauer, 2007).

Stadler et al. identified the AtSUC1 protein in the cells of anther connective tissue just before dehiscence (Stadler et al., 1999). They propose that the protein's physiological role in the anther is to create an osmotic gradient via the accumulation of sucrose, which draws water from the adjacent anther walls and signals the start of dehiscence. AtSUC1 was also found in germinating pollen and pollen tubes, suggesting that it imports sugar for pollen metabolism. Interestingly *SUC1* mRNA was detected in pollen at a much earlier stage of anther development than the AtSUC1 protein, so it seems that mRNA translation is only initiated after pollination. *SUC1* mRNA was also detected in cells surrounding the transmitting tissue of the style and in the funiculi. Due to this very specific expression in the style and funiculi, a role for SUC1 in pollen tube guidance was speculated. It seemed unlikely that, if only required for carbohydrate metabolism, expression would be confined to these tissues (Stadler et al., 1999).

Stadler et al. described *SUC1* expression as flower specific, however previously Sauer and Stolz. had detected *SUC1* mRNA in roots and leaves (Sauer and Stolz, 1994; Stadler et al., 1999). Sivitz et al. showed that *SUC1* is expressed in trichomes (which accounts for activity detected in leaves), roots and anthers, which was in agreement with publicly available microarray data (Sivitz et al., 2007). Expression in trichomes was not originally detected because the trichome-less *Arabidopsis* ecotype C24 was used. Expression in roots is controlled by intragenic sequences rather than the *SUC1* promoter, therefore use of a *SUC1*-promoter GUS construct did not reveal root specific expression. Control by regulatory elements outside of the promoter region was also shown for *SUC9* gene. (Sivitz et al., 2007, 2008).

Feuerstein et al. investigated ecotype specific differences in *SUC1* expression (Feuerstein et al., 2010). They detected *SUC1* expression in the funicular epidermis of C24, Ler and Wassilewskaija (Ws) but not Col-0 plants, and showed that expression in this tissue is pollination induced. In contrast, no *SUC1* expression was detected in Ws pollen and expression in Col-0 pollen was higher than in C24 or Ler-0 pollen (Feuerstein et al., 2010). Aside from a putative role in pollen metabolism and pollen tube growth, *SUC1* is also required for sucrose signalling in vegetative tissues and anthocyanin accumulation in the hypocotyls (Sivitz et al., 2008). Furthermore, it seems that *SUC1* may facilitate cross talk between sucrose and ABA signalling pathways. *SUC1* transcript levels are limited in the hypocotyls by the binding of ABA-dependant transcription factor AB15 to the *SUC1* promotor in the presence of high sucrose, which prevents overaccumulation of anthocyanin (Hoth et al., 2010).

Other group 2 *Arabidopsis* sucrose transporters have diverse functions: the SUC2 sucrose-H^+ symporter is essential for phloem loading (Gottwald et al., 2000; Sauer and Stolz, 1994; Srivastava et al., 2008), *SUC5* is expressed in the endosperm and associated with seed development (Baud et al., 2005; Pommerrenig et al., 2013), while *SUC8* and *SUC9* are predominantly expressed in flowers (Sivitz

et al., 2007). The early flowering phenotype of *suc9* plants has led to the suggestion that *SUC9* prevents premature flowering by maintaining uptake of extracellular sucrose (Sivitz et al., 2007). SUT2/SUC3, the only *Arabidopsis* group 3 sucrose transporter, is characterized by an unusually large open reading frame with many introns, a feature that it shares with its dicot homologues (Meyer et al., 2000, 2004). Protein interactions between AtSUC2, AtSUC3 and AtSUC4 have been demonstrated via a yeast-based split ubiquitin system and a putative sucrose sensor function for SUT2/SUC3-type transporters has been suggested (Barker et al., 2000; Schulze et al., 2003). AtSUC3 is specifically found in the sieve elements of the phloem, but *AtSUC3* is also widely expressed in sink tissues including germinating pollen, which suggests that it may function to import sucrose into these tissues (Meyer et al., 2004). The AtSUT4 transporter, unlike other *Arabidopsis* sucrose/H^+ symporters, is located in the tonoplast rather than the plasma membrane (Endler et al., 2006). *AtSUT4* is expressed in the roots, developing anthers and all aerial meristematic tissues, and overexpression of *AtSUT4* resulted in enhanced release of sucrose from *AtSUT4-OX* vacuoles (Schneider et al., 2012). *AtSUT4*, along with *AtSUC2*, have recently been identified as important for abiotic stress tolerance via ABA, and may also be regulated by *AtSUC3* for sucrose signalling under abiotic stress conditions (Gong et al., 2015). Table 4.1 summarises expression of the *Arabidopsis* sucrose transporters in reproductive tissues, highlighting those with putative roles in pollen and anther development.

Table 4.1: Summary of the *Arabidopsis* sucrose transporter genes. The developmental map from the *Arabidopsis* eFP browser was used to summarise expression levels in flower stages 12/15 and mature pollen. 1 represents masked expression and 12 represents absolute expression (Key adapted from (Winter et al., 2007)). Genes marked with * have expression levels of 5 or above in one or more of the selected tissues.

Gene	AGI Code	Expression in Flower Stages 12/15	Expression in Mature Pollen	Additional Information
**SUC1*	AT1G71880	4/3	5	Putative role in anther dehiscence, pollen development and pollen tube growth (Feuerstein et al., 2010; Sivitz et al., 2008; Stadler et al., 1999)
**SUC2*	AT1G22710	3/6	2	
**SUC3*	AT2G02860	5/5	5	AtSUC3-promoter::reporter gene plants revealed expression in pollen before and after dehiscence and in pollen tubes (Meyer et al., 2004)
SUC4	AT1G09960	4/4	3	*AtSUT4* expression detected in anthers and floral meristems (Schneider et al., 2012)
SUC5	AT1G71890	2/3	3	
**SUC8*	AT2G14670	4/5	5	
**SUC9*	AT5G06170	5/6	9	Mutants have an early flowering phenotype (Sivitz et al., 2007)

4.2 Results

4.2.1 Expression analysis of *Arabidopsis* sucrose transporters

Microarray data from the FlowerNet, for the *SUC1-5* sucrose transporter genes, is summarised in table 4.2. Of the five genes analysed, *SUC1* and *SUC2* have the highest expression in the late flower stages. *SUC2*, *SUC3*, *SUT4* and *SUC5* showed some expression level changes in the *myb26* mutant background but there is variation between replicates, so without further investigation it is not possible to conclude whether there is a regulatory relationship between *MYB26* and the *Arabidopsis* sucrose transporters (figure 4.3).

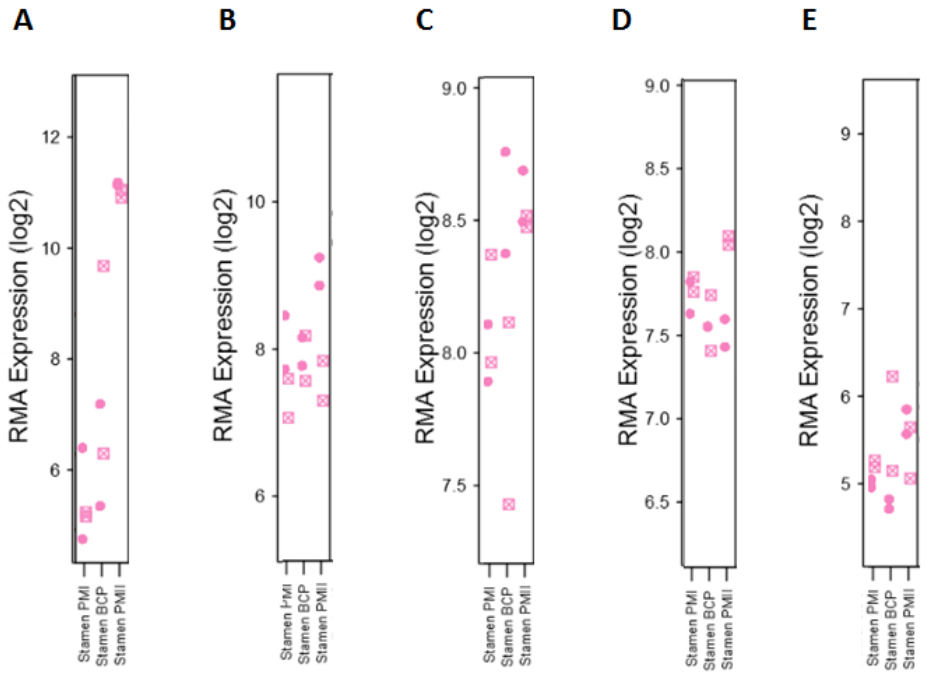

Figure 4.3: Sucrose transporters gene expression in *myb26* (squares) and wild type (Ler-0) (circles) backgrounds at three stages of stamen development. PMI, pollen mitosis I, BCP, bicellular pollen, PMII, pollen mitosis II. Adapted from (Pearce et al., 2015).

A: *SUC1*
B: *SUC2*
C: *SUC3*
D: *SUT4*
E: *SUC5*

The JA time course from the FlowerNet shows very little change to *SUC1-5* expression levels following treatment with jasmonic acid in an *opr3* mutant background (figure 4.4). These results suggest that it is unlikely that the expression of these sucrose transporter genes is regulated by jasmonic acid, however further analysis by qRT- PCR analysis was conducted (figure 4.5).

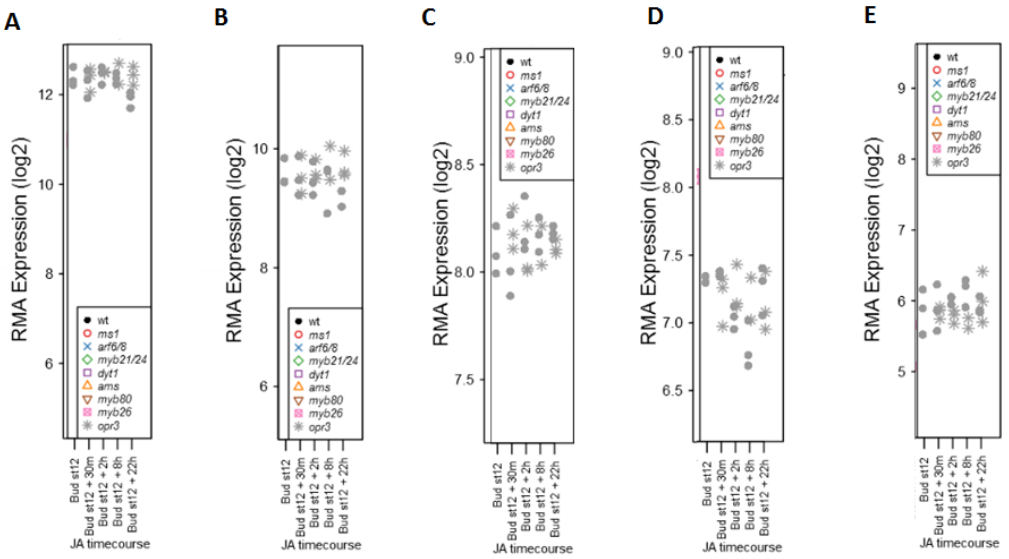

Figure 4.4: Changes to sucrose transporter gene expression across a JA time course; *opr3* + JA (circles), *opr3* +OPDA (stars). Adapted from (Pearce et al., 2015).

A: *SUC1*
B: *SUC2*
C: *SUC3*
D: *SUT4*
E: *SUC5*

The expression of the *SUC1-5 Arabidopsis* sucrose transporter genes was investigated by qRT-PCR as described in section 2.3.3. *SUC6* and *SUC7* were not included for analysis as these have been classed as pseudogenes in several *Arabidopsis* ecotypes. *SUC8* and *SUC9* are expressed in flowers, and roles in flowering and pollen tube growth have been discussed for these genes (section 4.1). It was not possible however to design specific qRT-PCR primers for *SUC8* and *SUC9* due to the extremely high degree of homology between the *Arabidopsis* sucrose transporter genes.

The relative expression of sucrose transporter genes *SUC1-5* was investigated in staged wild type (Col-0) and SALK_138439 (*dad1*) flower buds (figure 4.5). The single T-DNA insertion mutant SALK_138439 was grown and genotyped to identify homozygous mutants as described in section 2.1.2. Staging was performed as

previously described (section 2.1.5). Expression in the stage 1 Columbia background was set as a reference value of 1. Statistical analysis was used to compare changes in gene expression levels. In the Columbia background, expression at bud stage 4 was compared relative to stage 1. *SUC1*, *SUC2*, *SUC3* and *SUC5* all significantly increased in expression at bud stage 4 relative to bud stage 1 ($P<0.05$), and this result was the same for two biological replicates (figure 4.5). Data from the developmental map from the FlowerNet also indicates that these genes are upregulated in the later stages of flower development.

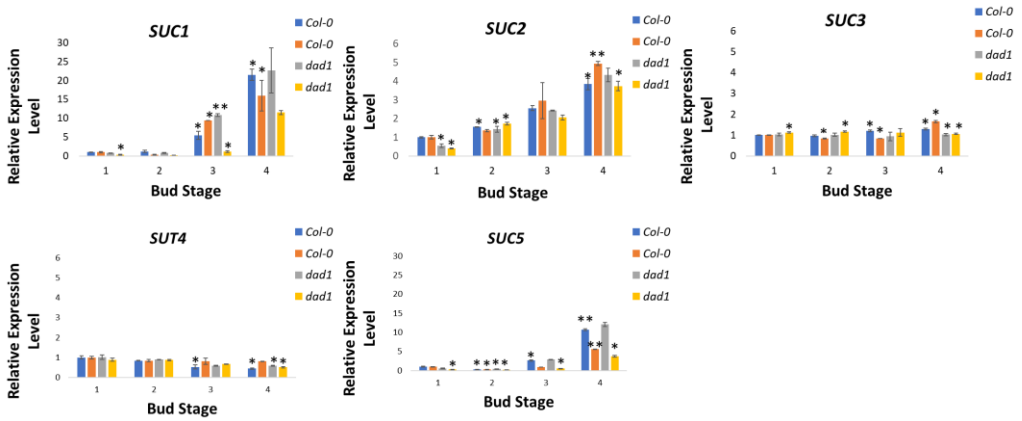

Figure 4.5: Expression of selected sucrose transporter genes in staged buds from wild-type (Col-0) and SALK_138439 flowers. Gene expression is relative to Col-0 stage 1. Reference gene *PP2A-3* (AT2G42500). Error bars, standard error. Results from two separate biological replicates are shown. * above a Col-0 bar indicates a significant ($P<0.05$) difference from stage one, ** indicates ($P<0.001$). * above a *dad1* bar indicates a significant ($P<0.05$) difference from Col-0 at the same stage, ** indicates ($P<0.001$). Blue and grey bars are from the same biological replicate, orange and yellow bars are from a second biological replicate.

Statistical analysis was also used to compare the relative expression of *SUC1-5* in SALK_138439 (*dad1*) flower buds against wild type (Col-0). In the *dad1* background, expression of *SUC2* was significantly lower at bud stage 1 ($P<0.05$), and expression of *SUC3* was significantly lower at bud stage 4 ($P<0.05$), for two biological replicates. Other significant changes to relative expression levels were observed between the *dad1* and Columbia backgrounds, however these were not consistent between two biological replicates. Data from the FlowerNet (figure 4.4) supports that JA is not a regulator of sucrose transporter gene expression, and it may be that

the changes shown in figure 4.5 are a result of noise in gene expression levels. Table 4.2 summarises the FlowerNet data for *SUC1-5* and also includes gene expression levels calculated from qRT-PCR data.

Table 4.2: Summary of *Arabidopsis* sucrose transporter genes analysed by qRT-PCR. Gene expression levels are calculated from highest and lowest CP values from qRT-PCR for staged buds. Gene expression changes from the FlowerNet developmental map are summarised. High expression = RMA Expression (log2) – 10 and above. Moderate expression = RMA Expression (log2) – 8-10. Low Expression = RMA Expression(log2)- 8 and below. Changes in gene expression across the JA time course are described. Gene expression in the *myb26* background is compared relative to wild type at three stages of pollen development. Columns marked with * contain data from the FlowerNet (Pearce et al., 2015). PMI, pollen mitosis I, BCP, bicellular pollen, PMII, pollen mitosis II.

Gene	AGI Code	Developmental Map*	Gene Expression Level	JA Time Course*	*myb26**
SUC1	AT1G71880	High expression in pollen and stamen stage 12.	1-30	No change over time course	Same
SUC2	AT1G22710	High expression in late flower stages, also in petals and sepals.	103-192	No change over time course	Slightly Lower at PMI, BCP, PMII
SUC3	AT2G02860	Moderate expression in stamens, petals and sepals at Stage 12.	14-19	No change over time course	Lower at BCP
SUT4	AT1G09960	Low expression in flowers and pollen. Moderate expression at stamen stage 15.	7-29	Slightly lower expression 8 hrs after treatment	Higher at PMII
SUC5	AT1G71890	Low expression in flowers and pollen.	0.5-4	No Change over time course	Higher at BCP

4.2.2 Analysis of *SUC1*

The promoter activity of *SUC1* was investigated using the GUS reporter line *SUC1*pro::PGWB3, which was generated as previously described (section 2.4.9.2). Whole inflorescences from *SUC1*pro::PGWB3 and a Columbia control were treated with β-glucuronidase substrate (section 2.5.2) to identify regions of expression (figure 4.6).

No expression was detected in early anthers (prior to dehiscence) from *SUC1*pro::PGWB3 flowers, however strong dark blue staining was observed in the pollen of late anthers (collected after anthesis). Blue staining was also visible in the pollen tubes from germinated pollen grains on the stigma, however there was no *SUC1* promoter activity in either the sepals or petals of *SUC1*pro::PGWB3 flowers. The developmental map in the *Arabidopsis* eFP browser only shows strong expression of *SUC1* in mature pollen (table 4.1). The results of GUS staining floral material from the *SUC1*pro::PGWB3 line confirm that *SUC1* is expressed strongly in mature pollen and continues to be expressed after pollen germination.

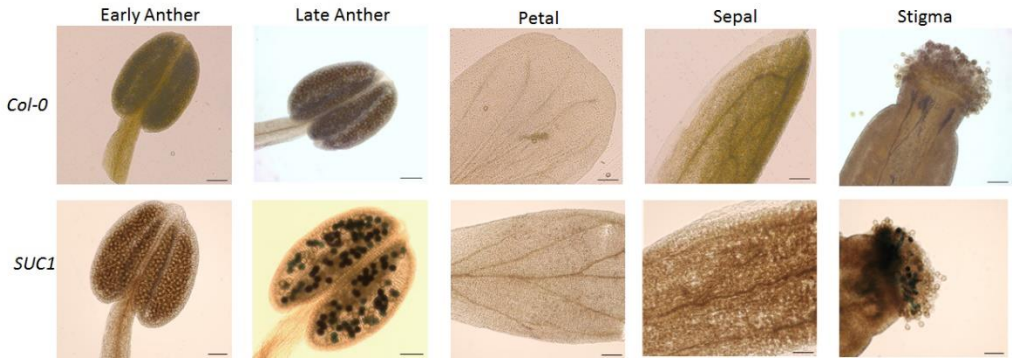

Figure 4.6: GUS staining of wild type (Columbia) and SUC1pro::PGWB3 floral organs. Bars = 100μm.

In order to study the putative function of *SUC1* in flowers, seed for the single T-DNA insertion line SALK_123324 was ordered from NASC. Plants were genotyped to identify those homozygous for the mutation (figure A4 B). SALK_123324 plants have a single T-DNA

insertion located within the *SUC1* promoter (figure A4 A). Expression of *SUC1* is reduced 0.64-fold in whole inflorescences (figure A4 C).

SALK_123324 plants, homozygous for the *suc1* mutation, were investigated for changes in fertility. Pollen viability was assessed quantitatively using FDA staining and did not vary significantly from the wild type control (P>0.05) (figure 4.7C). Similarly, measurements of seed set (figure 4.7A, B) did not vary notably from the wild type control (P>0.05).

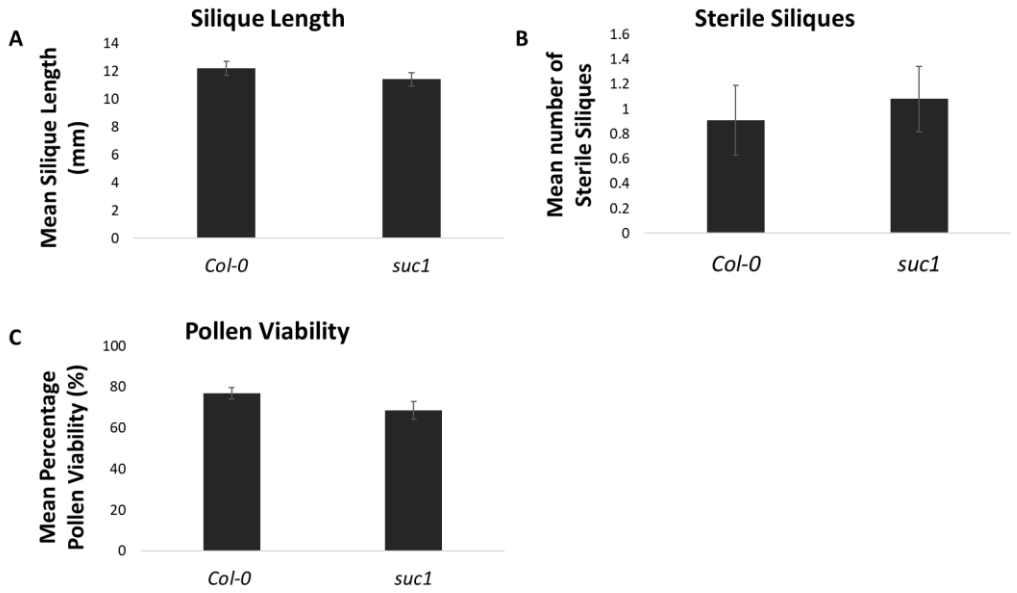

Figure 4.7: Characterisation of the *suc1* hm mutant

A: Average silique length of *suc1* hm (SALK_123324) and wild type (Col-0) plants. The length of the 1st to 6th siliques on the main stem was measured. The effect of genotype is not significant, P>0.05, error bars, standard error.
B: Average number of sterile siliques on the main stem of *suc1* hm (SALK_123324) and wild type (Col-0) plants. The effect of genotype is not significant, P>0.05, error bars, standard error.
C: Percentage of viable pollen from *suc1* hm (SALK_123324) and wild type (Col-0) flowers calculated from FDA staining. The effect of genotype is not significant, P>0.05, error bars, standard error.

The lengths of stamens, petals and pistils were measured at two stages of flower development as previously described (section 3.2.2). No changes in floral organ length were detected compared to a wild type control at either stage (P>0.05) (figure 4.8). It seems therefore, that the SUC1 protein transports sucrose specifically required for pollen germination and pollen tube growth. The *SUC1* gene may act

redundantly within the anther, as no fertility changes were observed in the *suc1* mutant.

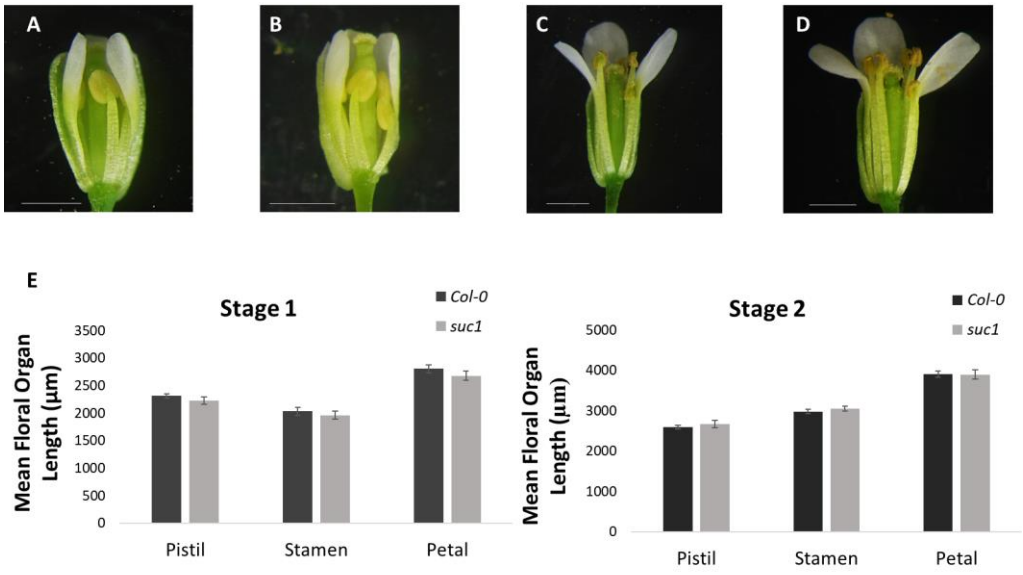

Figure 4.8: Analysis of staged wild type (Col-0) and *suc1* (hm) flowers

A: Col-0 Stage 1 flower
B: *suc1* Stage 1 flower
C: Col-0 Stage 2 flower
D: *suc1* Stage 2 flower
E: Length of floral organs of *suc1* plants and wild type (Col-0), at two stages of flower development. The effect of genotype is not significant, P>0.05, error bars, standard error
All scale bars = 1mm.

4.2.3 Analysis of *SUC2* and *SUC5*

Seed for single T-DNA insertion lines SALK_087046 and SAIL_365_D07 was ordered from NASC. SALK_087046 plants have a single T-DNA insertion in exon 1 of the *SUC2* gene, and expression of *SUC2* was reduced 0.78-fold in heterozygous SALK_087046 flowers (figure A5 A, C). SAIL_365_D07 plants have a single T-DNA insertion disrupting the first and second exons of the *SUC5* gene, and expression of *SUC5* is completely knocked out in homozygous SAIL_365_D07 flowers (figure A5 D, F). Plants of both lines were genotyped to identify homozygous mutants (figure A5 B, E). No

homozygous plants were identified for the SALK_087046 line; it is assumed that the homozygous *suc2* mutation is embryo lethal.

SALK_087046 and SAIL_365_D07 plants were investigated for changes to fertility and in both lines seed set was significantly reduced. The silique length of the first six siliques on the main stem was measured and averaged. The mean silique length of both SALK_087046 and SAIL_365_D07 plants was significantly reduced compared to wildtype ($P<0.001$) (figure 4.9A, B). The number of sterile siliques on the main stem was also counted for each line, and SALK_087046 and SAIL_365_D07 plants had a significant increase in the number of sterile siliques on the main stem ($P<0.001$), compared to the Columbia control (figure 4.9B, D, E, F). An assessment of pollen viability using FDA staining however, showed that the percentage pollen viability of the mutant lines did not vary from wild type ($P>0.05$).

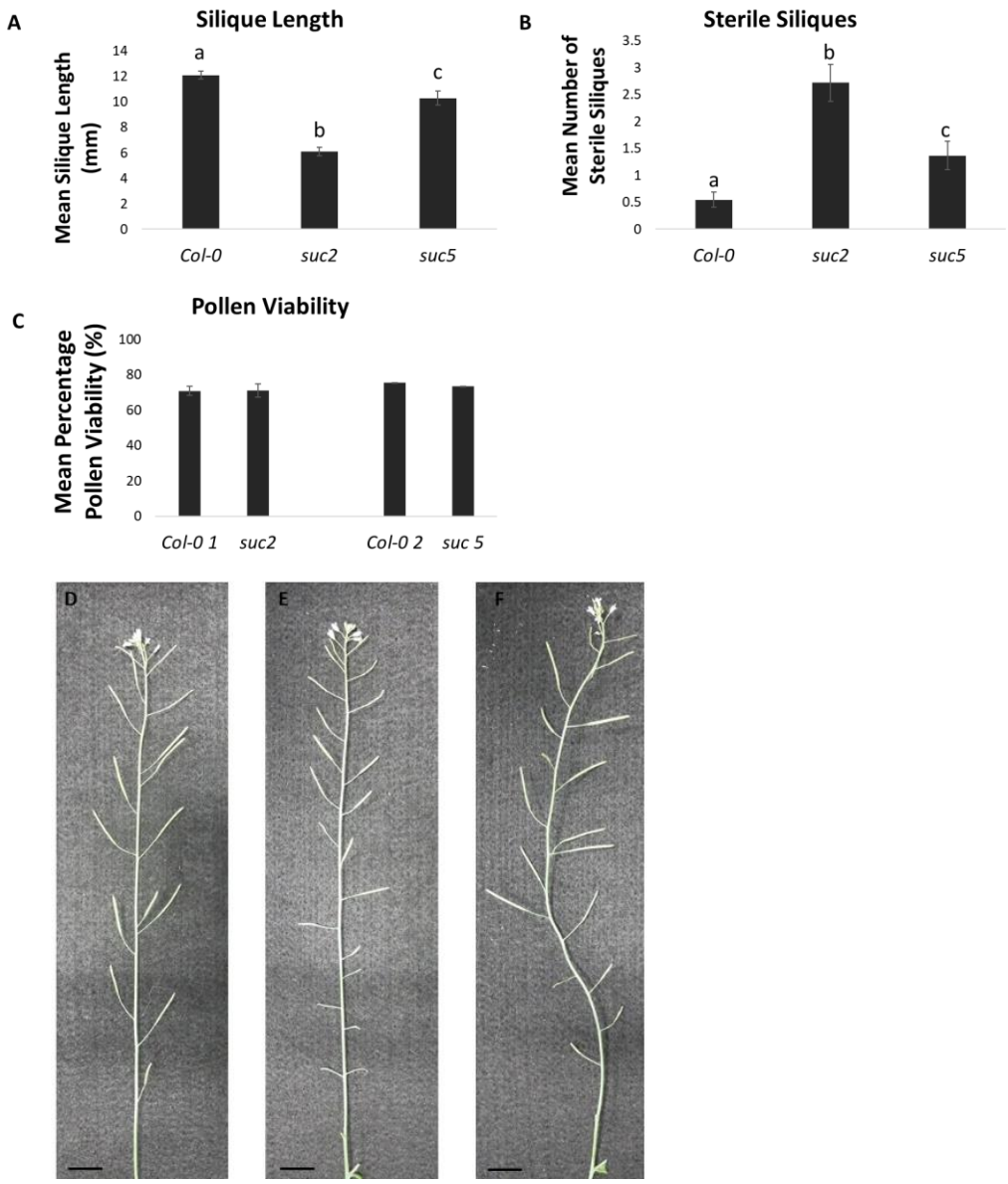

Figure 4.9: Fertility analysis of *suc2* (het) and *suc5* (hm) mutants

A: Silique length of the *suc2* (SALK_087046) and *suc5* (SAIL_365_D07) mutants and wild type (Col-0). Silique length of the 1st to 6th siliques on the main stem was measured. Different letters indicate significant variation ($P<0.001$), error bars, standard error. The combined results from two biological replicates are shown.
B: Number of sterile siliques on the main stem of the *suc2* (SALK_087046) and *suc5* (SAIL_365_D07) mutants and wild type (Col-0). Different letters indicate significant variation ($P<0.001$), error bars, standard error. The combined results from two biological replicates are shown.
C: Percentage pollen viability of the *suc2* (SALK_087046) and *suc5* (SAIL_365_D07) mutants and wild type (Col-0) calculated from FDA staining. The effect of genotype is not significant, $P>0.05$, error bars, standard error.
D: Main stem of Columbia
E: Main stem of het *suc2* plant
F: Main stem of hm *suc5* plant

All scale bars = 1 cm

To further investigate the changes to fertility, the lengths of floral organs of *suc2* and *suc5* plants were measured (as described in section 3.2.2) and compared against a wild type control (figure 4.10). The petal length of *suc5* flowers was significantly increased in stage 1 flower buds ($P<0.05$). No other significant changes were detected within *suc2* or *suc5* stage 1 flower buds. At stage 2, there was a significant increase in the lengths of stamens ($P<0.001$) and pistils ($P<0.05$) of *suc5* flowers compared to wildtype. There was also a significant reduction in the length of stamens and petals of *suc2* flowers compared to wildtype ($P<0.001$). Further statistical analysis showed that the ratio of stamen length: pistil length is not significantly altered in *suc5* flowers compared to wildtype ($P>0.05$), however the ratio of stamen length: pistil length is significantly reduced in *suc2* flowers ($P=0.001$), as a result of the reduced length of the stamens.

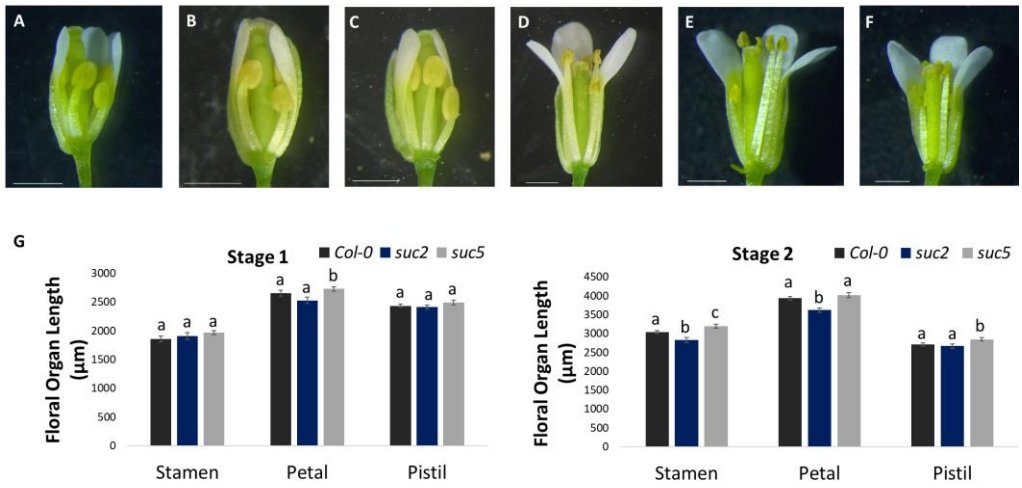

Figure 4.10: Analysis of staged *suc2* (het), *suc5* (hm) and wild type (Col-0) flowers

A: *Col-0* Stage 1 flower
B: *suc2* Stage 1 flower
C: *suc5* Stage 1 flower
D: C*ol-0* Stage 2 flower
E: *suc2* Stage 2 flower
F: *suc5* Stage 1 flower
G: Length of floral organs of *suc2, suc5* plants and wild type (Col-0), at two stages of flower development. The results for two biological replicates are averaged. Bars marked with different letters vary significantly for that organ ($P<0.05$), error bars, standard error

All scale bars = 1mm

In wild type flowers at stage 2 the ratio of the stamen length to the pistil length was always greater than 1. In *suc2* flowers the ratio of the stamen length to the pistil length was sometimes lower than 1, meaning that sometimes the dehisced anthers were positioned just below the receptive stigma (figure 4.11E). This may be responsible for the reduction in seed set, as less pollen is deposited on the stigma while it is receptive. Petal elongation is important for flower opening, therefore it is possible that *suc2* flower opening may also be delayed, although this was not observed.

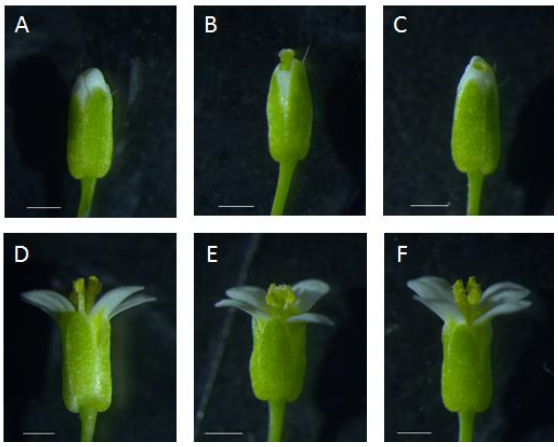

Figure 4.11: Staged *suc2* (het) *suc5* (hm) and wild type (Col-0) flowers

A: Col-0 Stage 1 flower
B: *suc2* Stage 1 flower
C: *suc5* Stage 1 flower
D: Col-0 Stage 2 flower
E: *suc2* Stage 2 flower
F: *suc5* Stage 2 flower

All scales bars = 1mm

In order to further investigate why *suc2* and *suc5* plants had a severe reduction in fertility, dehiscence and stigma receptivity were also investigated. The mean number of dehisced anthers were counted within stage 1 and 2 flowers. Dehisced anthers were counted as those where pollen could be seen outside of the anther. Although *suc2* and *suc5* flowers had a greater mean number of dehisced anthers at stage 1 (figure 4.12A), this was not significant ($P>0.05$) and no other significant changes to dehiscence at either stage were detected.

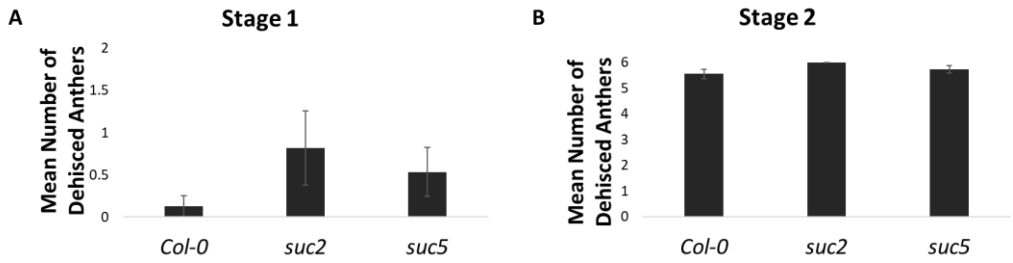

Figure 4.12: Analysis of dehiscence in staged *suc2* (het), *suc5* (hm) and wild type (Col-0) flowers

A: Mean number of anthers dehisced within Stage 1 flowers, error bars, standard error.
B: Mean number of anthers dehisced within Stage 2 flowers, error bars, standard error.

Close up images of the stigmas of *suc2* and *suc5* flowers at stages 1 and 2, showed no noticeable change to stigma receptivity compared to wild type, however there was less pollen on some of the *suc2* stigmas (figure 4.13E), presumably as a result of the reduction in filament length.

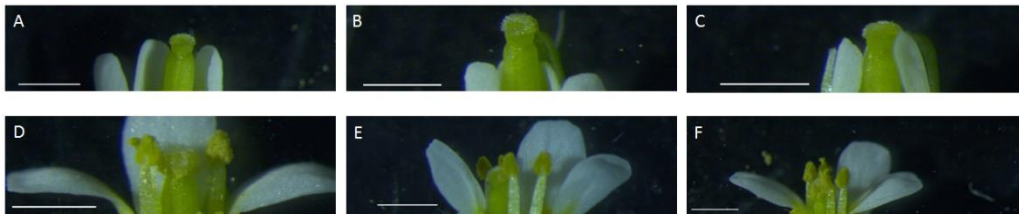

Figure 4.13: Close ups of *suc2* (het) *suc5* (hm) and wild type (Col-0) pistils, within staged flowers

A: Col-0 Stage 1 pistil
B: *suc2* Stage 1 pistil
C: *suc5* Stage 1 pistil
D: Col-0 Stage 2 pistil
E: *suc2* Stage 2 pistil
F: *suc5* Stage 2 pistil

All scale bars = 1mm

4.3 Discussion

4.3.1 *SUC1* is expressed in mature pollen and pollen tubes

qRT-PCR analysis showed that expression of *SUC1* is significantly increased at bud stage 4 relative to bud stage 1 ($P<0.05$). Data from both the FlowerNet (table 4.2) and the *Arabidopsis* eFP browser (table 4.1) indicate that *SUC1* is highly expressed in the stamens at flower stage 12 and in mature pollen. GUS staining of *SUC1*pro::PGWB3 flowers revealed expression in mature pollen and growing pollen tubes however no expression was observed in anthers from buds prior to anthesis (figure 4.6). Stadler et al. also analysed GUS staining in *SUC1* promoter-GUS *Arabidopsis* plants and reported seeing blue staining in pollen grains released from the anthers and in the growing pollen tubes. Faint staining was also observed in the styles of older ovaries. No staining was observed in any other floral tissue, including pollen of developing anthers (Stadler et al., 1999). The discrepancies between the publicly available microarray data and the promoter::GUS results may be due to intragenic regulatory elements controlling *SUC1* expression (section 4.1) (Sivitz et al., 2007).

suc1 plants had no reduction in fertility, no change to floral organ lengths and *suc1* pollen tested viable by FDA staining. Sivitz et al. showed that a lower percentage of *suc1* pollen germinated compared to wild type, however it was still capable of fertilization and no fertility defects were reported for homozygous mutants (Sivitz et al., 2008). Stadler et al. suggest that SUC1 imports sucrose to support pollen germination and pollen tube growth, although it is not known whether the sucrose is required for metabolism or to create an osmotic driving force for water transport (Stadler et al., 1999). Based on the fact that the SUC1 protein isn't present in the pollen of developing anthers (section 4.1), Sivitz et al. propose that it plays a specific role in pollen germination, reasoning that if it were required for metabolism the protein would be present at an earlier stage (Sivitz et al., 2008). Feuerstein et al. also conjecture that, as *SUC1* is not essential in

pollen grains and its expression in reproductive tissues varies between ecotypes (section 4.1), uptake of sucrose for metabolism is unlikely to be its only role (Feuerstein et al., 2010). They hypothesise that the presence or absence of *SUC1* in the pollen and funicular epidermis of certain ecotypes may influence extracellular sucrose levels, which in turn positively or negatively influence pollen tube growth of one ecotype along the placenta of another (Feuerstein et al., 2010).

Stadler et al. identified the SUC1 protein in the anther connective tissue just before dehiscence and suggested that it created an osmotic gradient required for anther dehydration (section 4.1) (Stadler et al., 1999). There are no reports of delayed dehiscence in *suc1* mutants however, although it is possible that the effects are too subtle to observe or else are masked by functional redundancy. The fact that fertility is unaltered in *suc1* mutants, despite a proven lower pollen germination rate (Sivitz et al., 2008), supports that the *SUC1* gene may be functionally redundant. *SUC3*, *SUC8* and *SUC9* are also highly expressed in pollen and it is possible that one or more of these proteins overlaps in function with SUC1. It would be interesting to investigate the phenotypes of multiple mutants.

4.3.2 *SUC2* and *SUC5* are expressed during anther dehiscence and *suc2* (het) and *suc5* (hm) mutants show a reduction in fertility

SUC2 and *SUC5* are expressed during anther dehiscence. qRT-PCR analysis showed that expression of both genes increased significantly at bud stage 4 relative to bud stage 1 ($P<0.001$). To date, *SUC5* has only been characterised in seeds, and microarray data from both the FlowerNet and the *Arabidopsis* eFP browser indicate that gene expression in pollen and anthers is low (relative to expression of the other *Arabidopsis* sucrose transporters) (tables 4.1 and 4.2). Seed set in *suc5* homozygous mutants was significantly reduced ($P<0.001$) however, which implies that *SUC5* is required for normal fertility. *suc2*

heterozygous mutants also had a significant reduction in seed set ($P<0.001$). No *suc2* homozygous mutants were identified within a segregating population (figure A5B), which suggests that the homozygous *suc2* mutation is embryo lethal. Gottwald et al. characterised three independent *suc2* T-DNA insertion lines and showed that all three independent mutant alleles had the same phenotype; homozygous mutants did not survive past the cotyledon expansion stage unless germinated on media with supplementary sucrose (Gottwald et al., 2000). It seems likely therefore, that when sown on soil (see section 2.1.4 for conditions), *suc2* homozygous seed did not germinate.

Apoplastic sinks are tissues that are not connected symplastically to the phloem, but require sucrose from the apoplast for energy. Apoplastic sink tissues include guard cells, the developing seed embryo, developing pollen grains and pollen tubes (Sauer, 2007). In the apoplast, sucrose is either taken up by sink specific sucrose transporters, or else split into glucose and fructose by cell-wall bound invertases (Sauer, 2007). In *Arabidopsis*, SUC1 and SUC5 are examples of sink specific sucrose transporters while SUC2 is essential for phloem loading and sucrose transport (Gottwald et al., 2000; Sauer, 2007; Sauer and Stolz, 1994; Srivastava et al., 2008). *suc2* mutants are unable to export sucrose from source leaves, so plants accumulate soluble carbohydrates and starch in the source leaves and development of sinks tissues is affected, leading to an overall reduction in growth. Homozygous *suc2* plants are unable to produce viable seed (Gottwald et al., 2000). A previous analysis of *SUC2* promoter activity, using GUS reporter constructs, showed that *SUC2* is strongly expressed in the sepals and filaments (but not anthers) of younger and older flowers (figure 4.14B, C), and within the vascular bundle of developing siliques (figure 4.14D,E) (Truernit and Sauer, 1995). No GUS activity was detected in the petals at any stage, although in the developmental map from the *Arabidopsis* eFP browser, high expression in petals is indicated (figure 4.14A). Truernit et al. suggest a role for SUC2 in phloem unloading in sink

tissues (Truernit and Sauer, 1995). It is not possible to conclude if the fertility changes observed in *suc2* heterozygous mutants were caused by a limited sucrose supply to developing sink tissues, or whether *SUC2* has another role in the reproductive organs. The use of immunolocalization techniques to resolve the specific location of the SUC2 protein in floral tissues, may help to elucidate its function.

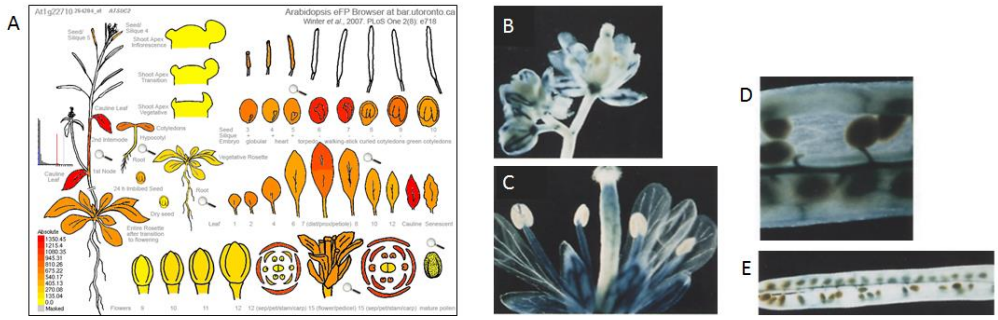

Figure 4.14: *SUC2* (AT1G22710) expression in floral organs. Figure adapted from (Truernit and Sauer, 1995; Winter et al., 2007).

A: Developmental map for AT1G22710 (*SUC2*) from the *Arabidopsis* eFP browser
B: SUC2-GUS activity in young flower buds
C: SUC2-GUS activity in an older flower with elongating ovary
D: SUC2-GUS activity in a developing silique (opened)
E: Close up of SUC2-GUS activity within the same silique

In order to further investigate the fertility changes observed for the *suc2* (het) and *suc5* (hm) mutants, floral organ lengths were measured in staged flowers. In *suc2* stage 2 flowers), the average lengths of stamens and petals were significantly reduced ($P<0.001$) (figure 4.10). This affected the ratio of stamen: pistil lengths at this developmental stage, and may explain the observed reduction in seed set, as in some flowers the anthers dehisced just below the stigma. In *suc5* stage 2 flowers however, the average lengths of pistils and stamens were increased (figure 4.10) relative to wild type flowers of the same stage. As this did not significantly affect the ratio of stamen: pistil lengths ($P>0.05$), it seems unlikely that this affected fertilization. Pollen viability, anther dehiscence and stigma receptivity of *suc2* (het) and *suc5* (hm) mutants appeared to be normal, therefore it is not possible to conclude what caused the fertility change in the *suc5* mutant without further analysis. Previous studies

of the SUC5 protein revealed that it transports biotin (a co-factor for fatty acid biosynthesis) in addition to sucrose (Ludwig et al., 2000). Pommerrenig et al. conducted a detailed analysis of developing seeds and embryos from *suc5* siliques, and compared the morphology, fatty acid content and seed weight of dried seeds (Pommerrenig et al., 2013). The study revealed no significant changes to seed and embryo development in *suc5* mutants despite reduced biotin uptake, however developmental defects common to biotin synthesis mutants (*bio1/bio2*) were augmented in *suc5bio1/suc5bio2* double mutants, suggesting that *SUC5* is essential for biotin uptake under biotin limiting conditions (Pommerrenig et al., 2013). Sucrose uptake into *suc5* embryos was not altered compared to wild type, which suggests that another embryo expressed sucrose transporter contributes to sucrose loading into the embryo (Pommerrenig et al., 2013). Although previous reports state that *SUC5* expression is specifically induced in the endosperm between 4 and 9 days after flowering (Baud et al., 2005) and that seed and embryo development is not significantly altered in *suc5* mutants (Pommerrenig et al., 2013), the increased expression of *SUC5* in stage 4 flower buds and the reduction in seed set of the *suc5* mutant suggests that *SUC5* may play an additional, currently uncharacterised, role in plant reproduction.

CHAPTER 5 ANALYSIS OF THE ROLE OF ANTHER STOMATA

5.1 Introduction

Located on the epidermes of aerial structures in higher plants, stomatal pores enable plants to control gas exchange via pore opening and density (Casson and Hetherington, 2010; Doheny-Adams et al., 2012). The intake of CO_2 for photosynthesis is a trade off against transpirational water loss, so plants respond to a range of environmental signals in order to optimise gas exchange within their current environment. (Casson and Hetherington, 2010; Doheny-Adams et al., 2012). For example, during stomatal development, the fate of epidermal cells can be influenced by high levels of light or atmospheric CO_2, resulting in either an increase or decrease in stomatal density, respectively (Casson and Hetherington, 2010). With future climate predictions of more frequent and longer lasting droughts, manipulating stomatal density to reduce transpiration rates and enhance water use efficiency is currently of interest (Franks et al., 2015; Hepworth et al., 2015).

Stomatal patterning in young *Arabidopsis* leaves arises from a series of asymmetric cell divisions and a single symmetric division (Bergmann and Sack, 2007). Firstly, meristemoid mother cells (MMC) derived from protodermal cells in the epidermis, divide asymmetrically to produce a smaller meristemoid and larger sister cell. This division defines the start of a stomatal lineage and is referred to as the entry division. The resulting meristemoid can then either become a guard mother cell (GMC), which divides symmetrically to produce two guard cells (GCs), or it can undergo up to three further asymmetric amplifying divisions (figure 5.1B). These amplifying divisions generate daughter cells which will either become pavement cells or divide via an asymmetric 'spacing' division to produce new meristemoids, thus generating new stomata. Spacing divisions ensure a 'one cell spacing rule' which means that stomata do not form adjacent to each other. The majority of cells in the

epidermis are derived from the stomatal lineage however it is the frequency of entry and spacing divisions that determines the number of stomata formed (Bergmann and Sack, 2007). Five basic helix-loop-helix (bHLH) transcription factors positively regulate the stomatal lineage (figure 5.1A) (Pillitteri and Dong, 2013). Three of these, *SPEECH-LESS (SPCH), MUTE* and *FAMA*, act independently at specific points, while *SCREAM* (SCRM) and *SCRM2* act more broadly; they heterodimerize with the former three to promote cell fate transitions (Pillitteri and Dong, 2013). Stomatal number varies in different parts of the plant, in response to environmental stimuli and between different taxa (Casson and Gray, 2008).

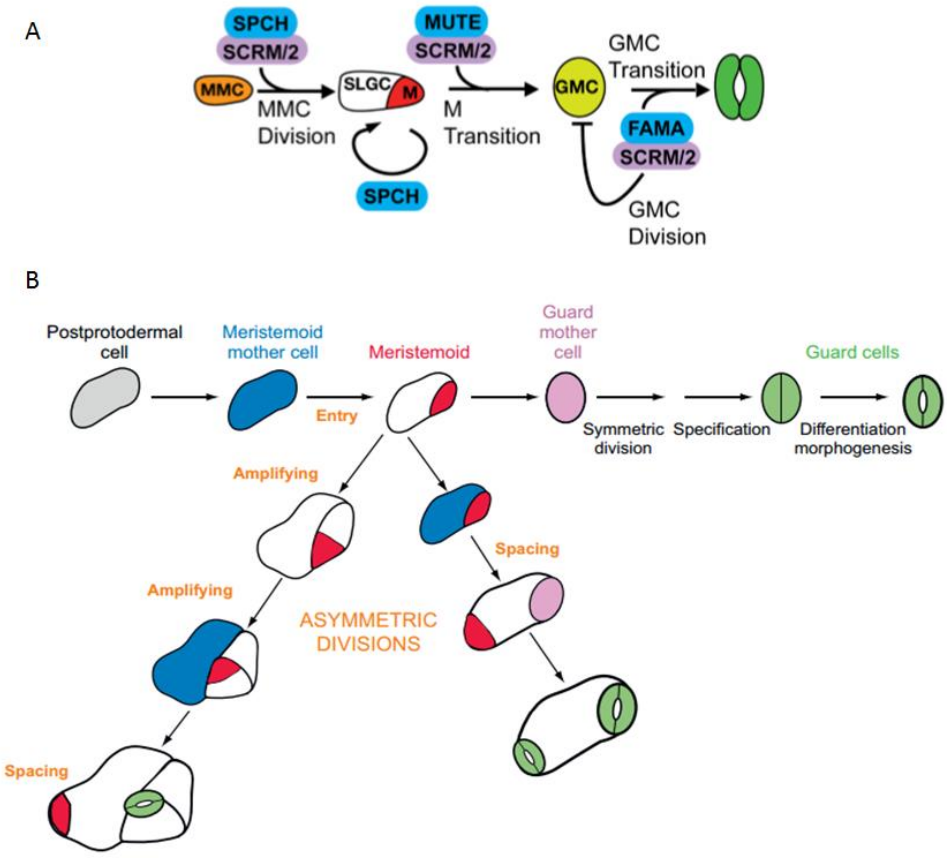

Figure 5.1: The cell types and transitions of the stomatal lineage. Figure adapted from (Bergmann and Sack, 2007; Pillitteri and Dong, 2013).

A: Five types of bHLH proteins control cell transitions through the stomatal lineage. SPCH and SCRM/2 act together to promote division of MMCs, MUTE and SCRM/2 direct GMC transition and FAMA and SCRM/2 cause the transition of GCs.
B: Three types of asymmetric division: entry, amplifying and spacing, determine the stomatal cell lineage from a meristemoid mother cell (MMC). A single symmetric division marks the formation of the guard cells.

Two small secretory peptides expressed during stomatal development have been identified as negative regulators of stomatal density and patterning. *EPIDERMAL PATTERNING FACTOR* (*EPF*) 1 and 2, belong to a family of eleven secretary peptides that have six to eight conserved cysteine residues at the C-terminal domain. *EPF2* is secreted from the meristemoids and prevents neighbouring cells from undergoing asymmetric divisions, thereby reducing the number of cells entering the stomatal lineage (Hara et al., 2009; Hunt and Gray, 2009). *EPF1* acts slightly later than *EPF2*, and in an independent manner. *EPF1* controls asymmetric spacing divisions to ensure one cell spacing between neighbouring stomata and the *epf1* mutant has pairs of adjacent stomata (Hara et al., 2007). Conversely a third family member, *EPF-like 9* (*EPFL9* or *STOMAGEN*), has been established as a positive regulator of stomatal development that acts independently of both *EPF1* and *2*. *STOMAGEN* is produced in the mesophyll cells and its function requires the same cell surface receptor as *EPF1* and *2* (*TOO MANY MOUTHS* (*TMM*)), which has led several authors to suggest that these peptides compete for the same receptor (Hunt et al., 2010; Kondo et al., 2010; Sugano et al., 2010).

TOO MANY MOUTHS (*TMM*) is an early component of a MAP kinase (MAPK) signalling cascade which negatively regulates stomatal development (Bhave et al., 2009; Geisler et al., 1998, 2000; Yang and Sack, 1995). *SPCH* has a MAPK target domain and is likely to be a downstream target of the signalling cascade, whereas *MUTE*, *FAMA* and *SCRM* do not and are only putative targets for phosphorylation. TMM is a LRR-RLP and lacks a kinase domain; evidence suggests that interactions with the closely related ERECTA family (ERf) of LRR-RLKs facilitates the signalling cascade (figure 5.2) (Pillitteri and Dong, 2013). The *tmm* mutant has a very unusual phenotype, in which the number of stomatal units varies in an organ specific manner. While the cotyledons have a significant increase in clustered stomata (caused by a reduction in amplifying cells divisions and early

conversion of meristemoids to GMCs), the inflorescence stem has no stomata at all (compared to 24± 2 in wild type plants) and the flower stalk exhibits a gradient of increasing number of stomatal units at the floral end (Bhave et al., 2009; Geisler et al., 1998, 2000; Yang and Sack, 1995). Characterisation of a fourth EPF family member, *CHALLAH (CHAL),* helped shed some light on this, as *CHAL* is a negative repressor of stomatal production that acts through the ER family of receptors. *CHAL* is highly expressed in the mesophyll tissue of young stems and its expression is upregulated in the *tmm* mutant, suggesting that TMM represses CHAL signalling in the inflorescence stem and hypocotyls (Abrash and Bergmann, 2010; Rowe and Bergmann, 2010).

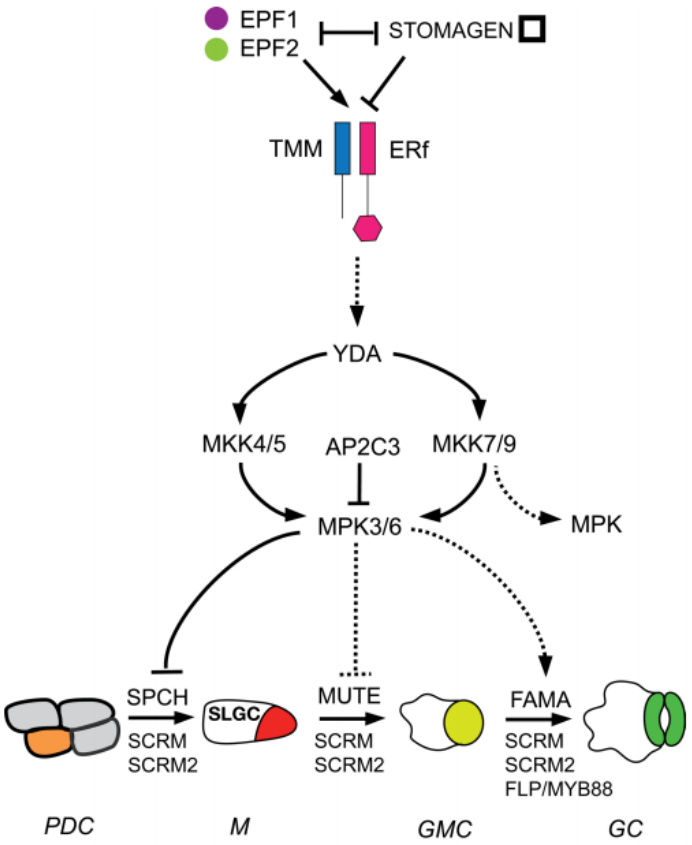

Figure 5.2: Diagram of the signal transduction pathway regulating stomatal development.

EPF1, EPF2 and STOMAGEN inhibit or activate a MAPK signalling cascade via TMM and the ERf. MPK3/6 inactivates SPCH through phosphorylation which reduces the number of entry divisions. Horizontal lines denote inhibition, arrows denote activation. Solid lines show where there is supporting experimental evidence, dashed lines show predicted interactions. Figure adapted from (Pillitteri and Dong, 2013).

BREAKING OF ASYMMETRY IN THE STOMATAL LINEAGE (BASL) encodes a protein which accumulates inside stomatal lineage cells and is required for their asymmetric division (Dong et al., 2009). Reduction of *BASL* expression results in more symmetric divisions and increased numbers of stomata. In mature leaves, the *basl* mutation did not cause a significant increase in stomata yet clustered stomata were observed. *BASL* acts independently of *TMM* and the double mutant *basl tmm* has an additive phenotype (Dong et al., 2009; Hunt and Gray, 2010).

STOMATAL DENSITY AND DISTRIBUTION1 (SDD1) encodes a subtilisin-like serine protease which is thought to act within the same signalling pathway as *TMM* and the ERfs, but functions independently from the EPF proteins (Berger and Altmann, 2000; Von Groll et al., 2002). It has been suggested that *SDD1* may activate an unknown proteinaceous signalling substrate (Berger and Altmann, 2000). The *sdd1* mutant has up to a four-fold increase in stomatal density and exhibits stomatal clustering. The percentage of stomata that are clustered does not directly relate to the increase in stomatal density and both of these factors vary in different organs. Unlike the *tmm* mutant which has large clusters of adjacent stomata, in *sdd1,* clusters predominantly consist of two paired stomata (Berger and Altmann, 2000; Casson and Hetherington, 2010; Von Groll et al., 2002).

A guard cell expressed, and secreted, extensin-like protein FUSED OUTER CUTICULAR LEDGE1 (FOCL1), has been shown to be required for the correct formation of the outer cuticular ledge (OCL) (Hunt et al., 2017). The OCL is a lip which forms around the stomatal pore and may help to seal the pore when closed, or improve its orientation when open. Immature stomata are covered by a cuticular layer, which tears open as the guard cells mature and forms the OCL. In *focl1* mutant plants, the stomatal pore of mature stomata remains covered by a membrane of cuticular material and as a result transpiration from stomata is reduced. *focl1* stomata had a larger stomatal aperture and were impaired in their ability to close, which may be a result of defective guard cell wall formation and function (Hunt et al., 2017). *focl1* plants also had retarded growth, probably caused by a reduced CO_2 intake, but tolerance under drought stress was improved (Hunt et al., 2017).

While the function of stomata in the leaves is well documented, the occurrence of stomata on anthers is less widely reported. Geisler et al. recorded an average of twenty stomata per anther in wild type *Arabidopsis*, which is significantly less than the number on other floral

organs such as the sepals and siliques, which equals hundreds (Geisler et al., 1998). *Allium cepa* is a species which lacks stomata on its anthers. Before dehiscence occurs in *A. cepa*, the anthers are lifted outside of the opening bud by extension of the filament, presumably to induce desiccation via direct transpiration. Dehiscence happens slowly in *A. cepa*, and dehiscence of different anthers within the same whorl sometimes occurs over many hours (Keijzer et al., 1987). In *Gasteria verrucosa* and *Lilium hybrida* stomata on the anthers remain open during dehydration, suggesting that their presence contributes to water loss through evaporation. The addition of Vaseline® onto the surface of anthers of *G. verrucosa* caused anthers to remain closed for many hours, whereas untreated anthers started to dehisce within one hour (Keijzer et al., 1987). Such evidence suggests a correlation between the presence of stomata on anthers and the speed of anther dehiscence.

5.2 Results

5.2.1 Analysis of stomatal patterning and density in *Arabidopsis* leaves

Stomatal patterning on the abaxial side of mature *Arabidopsis* rosette leaves was investigated as previously described (section 2.6.1). Previous work has shown a significant increase in the stomatal density of *STOMAGEN* overexpressing lines while constitutive overexpression of *EPF2* resulted in plants with a five-fold reduction in stomatal density, caused by a decreased number of cells entering the stomatal lineage (Hunt and Gray, 2009; Hunt et al., 2010; Kondo et al., 2010; Sugano et al., 2010). *Arabidopsis* has nine homologues of *EPF1*, two of which (*EPFL3* and *EPFL7*) were previously unpredicted genes (Hara et al., 2009). *EPFL7* has not been studied in detail to date. Like the other EPF1 homologues, EPFL7 has six conserved cysteine residues at its C-terminal end and a predicted secretory signal sequence (Hara et al., 2009). It also shares conservation of

two additional cysteine residues with *EPF1* and *EPF2* and is closest phylogenetically to *EPF2* within the *EPF* gene family (figure 5.3) (Rowe and Bergmann, 2010; Rychel et al., 2010). Therefore, it is likely that *EPFL7* is also a negative regulator of stomatal development and that an overexpression line will be characterised by a reduced number of stomata.

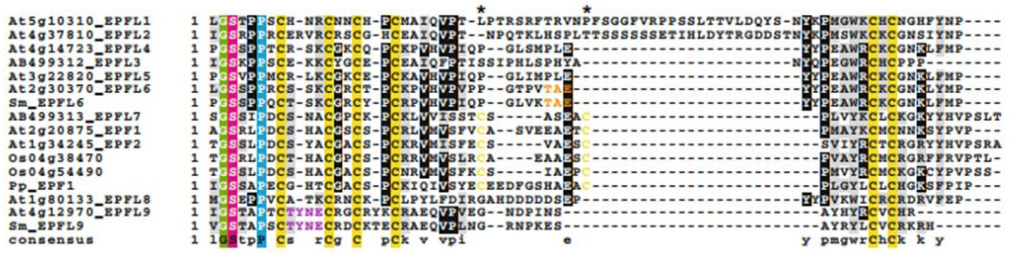

Figure 5.3: Alignments of amino acid sequences for *EPFL* genes in *Arabidopsis thaliana* (At) and homologous sequences from other species. Figure adapted from (Rychel et al., 2010).

Pp, moss *Physcomitrella patens*, Sm, lycophyte *Selaginella moellendorffii*, Os, rice, *Oryza sativa*. Conserved cysteine residues are highlighted in yellow. The EPF1, EPF2, and EPFL7 family members of *Arabidopsis*, *O. sativa*, *and P. patens*, have two extra conserved cysteine residues which are shown in yellow and marked by asterisks.

Epidermal leaf peels showed that *tmm, sdd1, STOMAGEN OE* and double mutant *basl tmm* all had an increased number of stomata on the abaxial side of rosette leaves, compared to wild type (figure 5.4B, C, F, and G). The increase in stomatal number was most apparent in the *tmm* and *sdd1* lines. All four lines also had stomatal clustering-groups of adjacent guard cell pairs caused by abnormalities in stomatal patterning. The largest clusters were observed in the *tmm* line, where up to 6-8 stomata were grouped adjacently (figure 5.4C). Hunt et al. report a moderate degree of stomatal clustering in *STOMAGEN* overexpressing lines (Hunt et al., 2010), and although pairs of adjacent stomata were commonly observed in the leaf peels (figure 5.4F), larger clusters were less common. Where multiple stomata were closely clustered, they were generally smaller than paired or single stomata which is in agreement with previous observations (Doheny-Adams et al., 2012). The phenotypes observed

in *tmm* and *sdd1* epidermal leaf peels were consistent with those reported in the literature (Berger and Altman, 2000; Bhave et al., 2009; Geisler et al., 1998, 2000; Von Groll et al., 2002). Previous studies have shown that the *basl tmm* phenotype is additive in comparison to the single mutants (Hunt and Gray, 2010). Clusters of stomata were observed in the epidermal leaf peels of *basl tmm* plants, however the majority of these were formed of pairs of adjacent stomata, similar to those seen in the *STOMAGEN OE* and *sdd1* leaf peels (figure 5.4B, F, G).

EPF2 and *EPFL7* overexpressing lines had few stomata which were spaced widely apart compared to wild type (figure 5.4D, E). This suggests that like family members *EPF1* and *EPF2*, *EPFL7* is also a negative regulator of stomatal density. Epidermal leaf peels for *focl1_1* and *focl1_2* showed stomatal patterning and density that was similar to wild type (figure 5.4A, I, J). Hunt et al. reported an increase in stomatal index in *focl1_1* and *focl1_2*, however this was caused by a reduction in pavement cell density, rather than an increase in stomatal density (Hunt et al., 2017). Hunt et al. also showed a significant increase in the length, width and area of *focl1_1* stomata, compared to a Columbia control (Hunt et al., 2017).

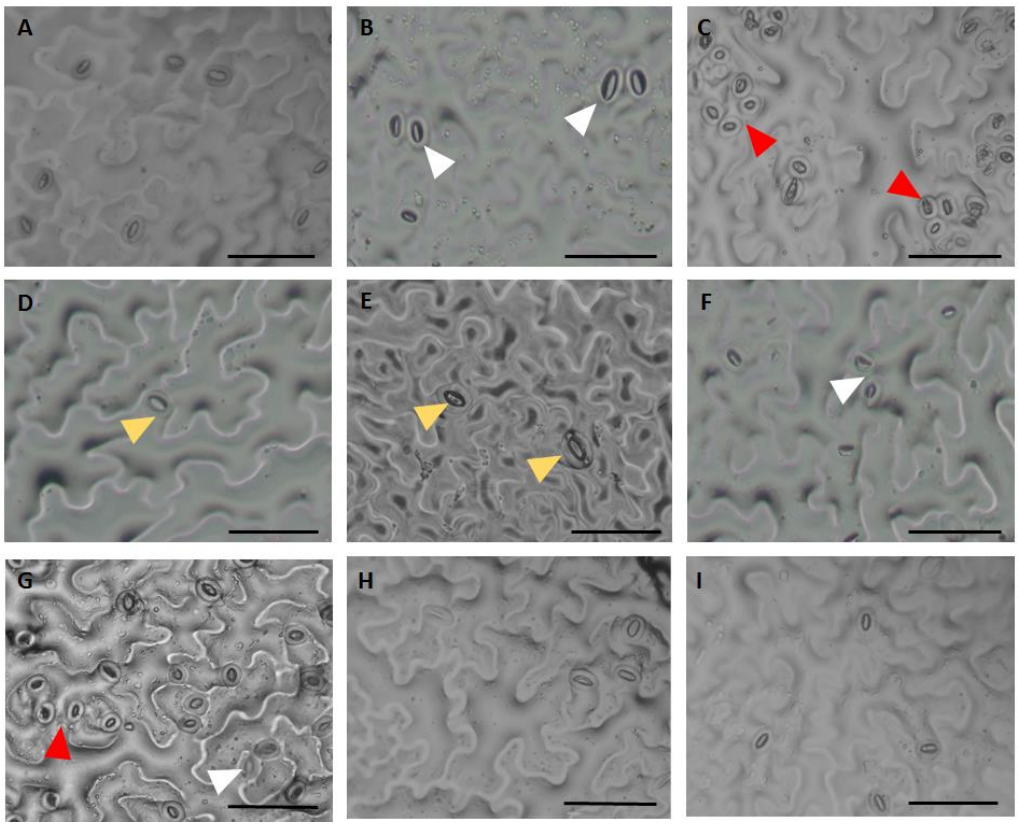

Figure 5.4: Epidermal leaf peels from *Arabidopsis* lines with altered stomatal development.

White arrows indicate pairs of adjacent stomata. Red arrows indicate clusters of adjacent stomata. Yellow arrows indicate where stomata are widely spaced compared to wild type (Col-0). All scale bars =100μm.
A: Col-0 (wt)
B: *basl tmm*
C: *tmm*
D*: EPF2 OE*
E: *EPFL7 OE*
F: *STOMAGEN OE*
G: *sdd1*
H: *focl1_1*
I: *focl1_2*

5.2.2 Analysis of stomatal number and patterning in *Arabidopsis* anthers

The FlowerNet was used to confirm that all of the genes described in table 2.5 are expressed in flowers. Gene expression at flower stages 12/15 was low (RMA Expression(log2) 8 or below) for all of the genes. Confocal microscopy was used to investigate stomatal patterning on

anthers. Anthers from *Arabidopsis* floral buds that were about to open were stained with acridine orange and then imaged. Buds from five separate plants were examined for the *EPF2*, *EPLF7* and *STOMAGEN* overexpressing lines, and the *basl tmm* double mutant and a Columbia control (figure 5.5). Stomata are located on the abaxial surface of anthers and are predominantly positioned along the connective tissue between the end of the filament and the tip of the anther. Occasionally stomata were observed on the back of the lobes. No stomata were observed on any anthers of *EPF2 OE* and *EPFL7 OE* plants (figure 5.5E, F). Clusters of adjacent stomata were visible on the anthers from *basl tmm* plants (figure 5.5C). The staining within the images suggests that the majority of stomata are open; the guard cells of closed stomata have many small vacuoles whereas the guard cells of open stomata have fewer large vacuoles (figure 5.5B) (Gao et al., 2005).

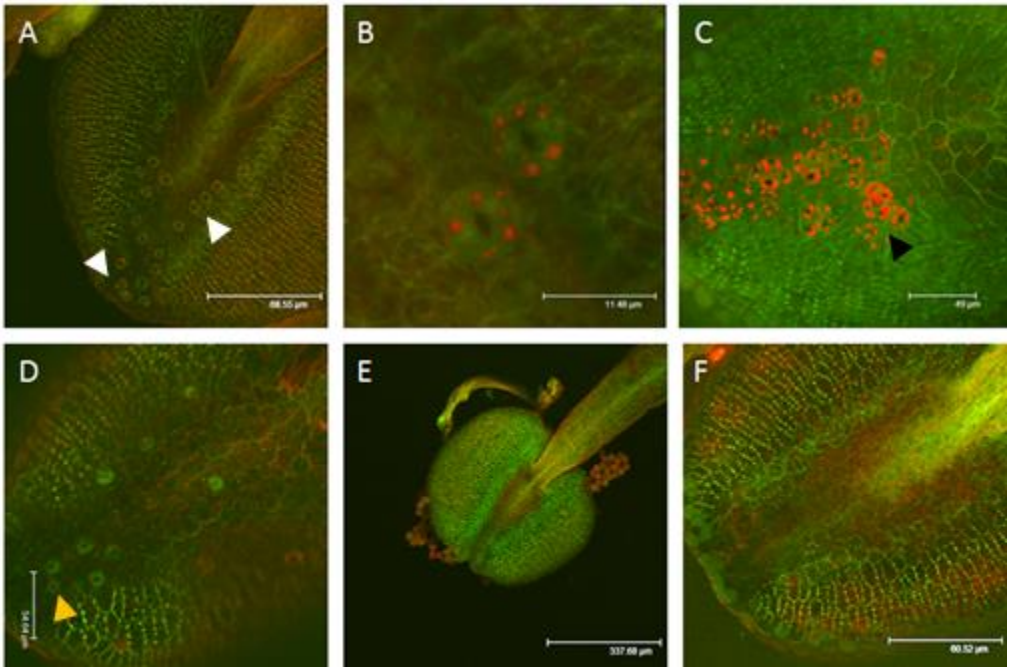

Figure 5.5: The abaxial side of *Arabidopsis* anthers stained with acridine orange.

A: Col-0 (wt) anther showing rows of stomata along the connective tissue and at the anther tip (white arrows), scale bar 68.55μm
B: Close up of stomata on a Col-0 anther, scale bar 11.48μm
C: *basl tmm* anther showing clustered stomata (black arrow), scale bar 49μm
D: *STOMAGEN OE* anther showing a pair of adjacent stomata (yellow arrow), scale bar 54.64μm
E: *EPF2 OE* anther with no stomata, scale bar 337.68μm
F: *EPFL7 OE* anther with no stomata, scale bar 60.52μm

To further investigate stomatal patterning on anthers, light microscopy was used to image the abaxial side of anthers as described in section 2.6.3. The total number of stomata visible on the abaxial side of entire anthers was counted for the eight lines, described in table 5.1, and a Columbia control (figure 5.6). The total number of stomata on two to four anthers per bud were counted. Two buds from different inflorescences were counted per plant and a minimum of five biological replicates were used per line. The number of stomata per anther was compared statistically for the different lines. All of the lines varied significantly ($P<0.001$) in the number of stomata per anther compared to wild type, with the exception of *focl1_1* (figure 5.6). No stomata were observed on any anthers of *EPF2* OE and *EPFL7* OE plants. Hunt and Gray had previously showed

that overexpressing *EPF2* results in a 5-fold reduction in stomatal density in leaves (Hunt and Gray, 2009). Figure 5.4 shows that some stomata were observed in the leaf epidermises of both *EPF2* OE and *EPFL7* OE plants. Another line where the phenotype varied between leaves and anthers was the *STOMAGEN* overexpression line. Hunt et al. characterise *STOMAGEN* as a positive regulator of stomatal density and showed that overexpressing *STOMAGEN* promotes stomatal development in the leaf epidermis (Hunt et al., 2010). Counts of the number of stomata per anther however, were significantly lower than wildtype ($P<0.001$). The *sdd1*, *tmm* and *basl tmm* mutant lines, all had an increased number of stomata compared to wild type, which was concurrent with the phenotypes observed in leaves. The two *focl1* mutant lines (*focl1_1* and *focl1_2*) both had an increased number of stomata on the anthers compared to wild type, however the difference was only significant for the *focl1_2* line ($P<0.001$). Hunt et al. concluded that there was no significant alteration to stomatal density in *focl1_1* and *focl1_2* leaf epidermises, and no clustered stomata were observed (Hunt et al., 2017).

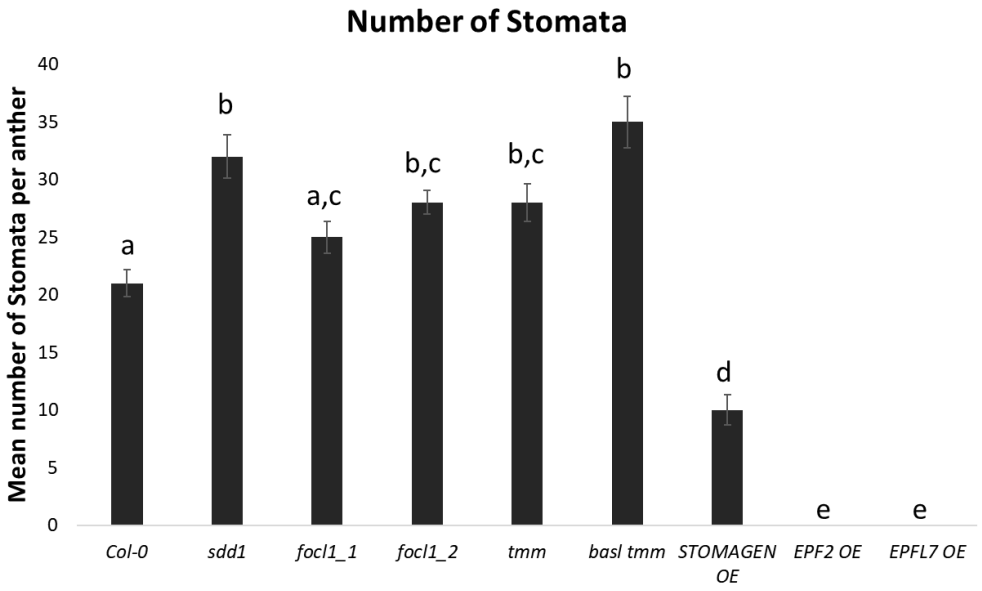

Figure 5.6: Mean number of stomata per anther for eight *Arabidopsis* lines with altered stomatal development and a wild type control (Col-0). Bars marked with different letters vary significantly (P<0.001), bars sharing a letter do not, error bars, standard error.

Images of the abaxial side of anthers taken with a light microscope showed that some of the lines had differences in stomatal patterning between leaves and anthers (figure 5.8). Clusters of two adjacent stomata were commonly observed in the *STOMAGEN OE* leaf epidermis, and clusters of multiple stomata were more infrequent. On *STOMAGEN OE* anthers however, only pairs of adjacent stomata were observed (figure 5.8K, L). *tmm* and *basl tmm* both had clusters and pairs of adjacent stomata in both leaves and anthers, however the additive effect of the *tmm* and *basl* mutations was more apparent in anthers, where large clusters of adjacent stomata were observed in the double mutant (figure 5.8C, D, E, F). *focl1_1* and *focl1_2* stomata appeared equivalently spaced to Columbia in both anthers and leaves, and no clustered stomata were observed in either organ (figure 5.8O, P, Q, R). The *sdd1* mutant had clusters of two adjacent stomata in both leaves and anthers (figure 5.8M, N). Table 5.1 summarises the differences between stomatal patterning of leaves and anthers for all of the lines.

The position of stomata on the anthers varied slightly between the lines. In Columbia, the stomata tended to line up along either side of

the connective tissue and go quite far back towards the filament with few at the tip. In contrast, the stomata on anthers of *basl tmm* plants, were often clustered at the tip, with fewer towards the filament end (figure 5.8C, D). *tmm* anthers had stomata which were spread across the connective tissue, and there were many that were immature (figure 5.7). Mature, open stomata can be easily identified by the pore and the two surrounding guard cells. Immature stomata are more rounded with a pore that is still covered by the cuticular layer (Hunt et al., 2017), however these were still identifiable by the chloroplasts in the guard cells. *focl1_2* anthers had stomata positioned quite far back towards the filament and also had stomata positioned across the anther lobes (figure 5.8Q, R). In *sdd1* anthers, stomata were spread quite widely across the connective tissue and also the anther lobes (figure 5.8M and N).

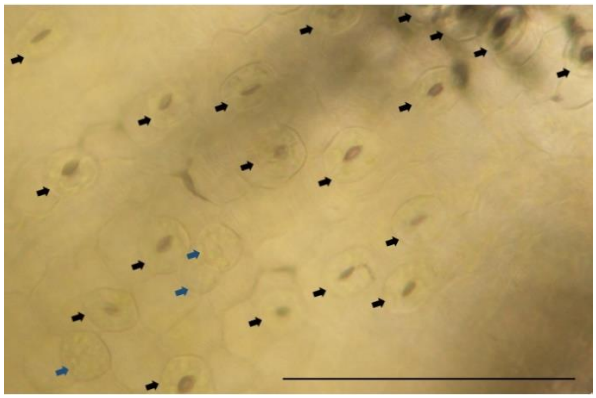

Figure 5.7: *tmm* anther showing a mixture of immature and mature stomata. Immature stomata are indicated with blue arrows, mature stomata are indicated by black arrows. Scale bar 100μm.

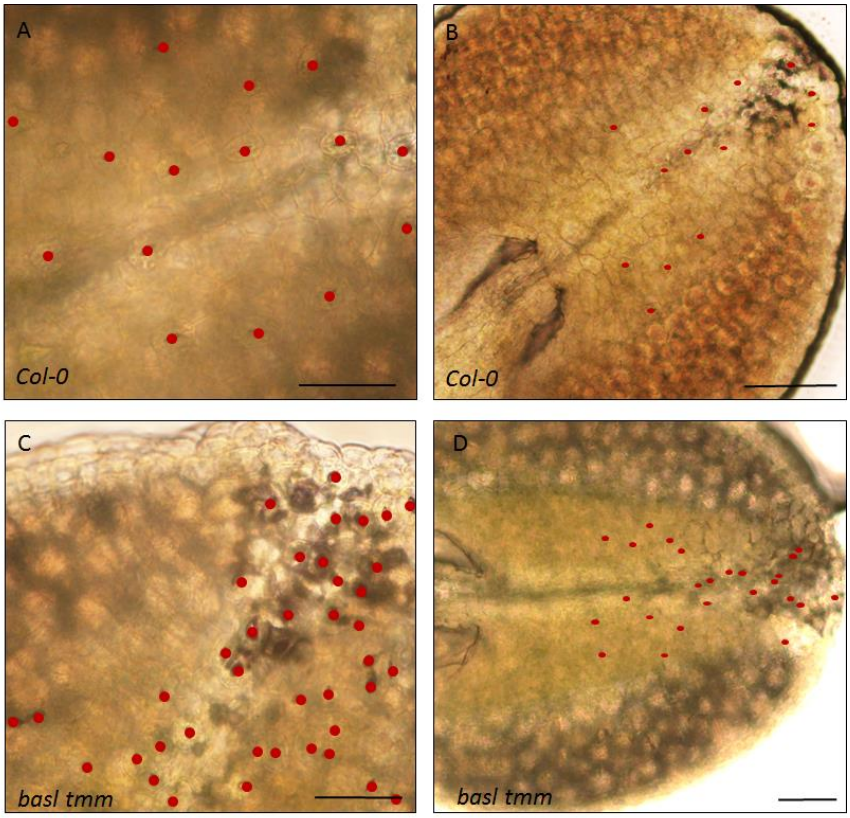
A
Col-0
B
Col-0
C
basl tmm
D
basl tmm

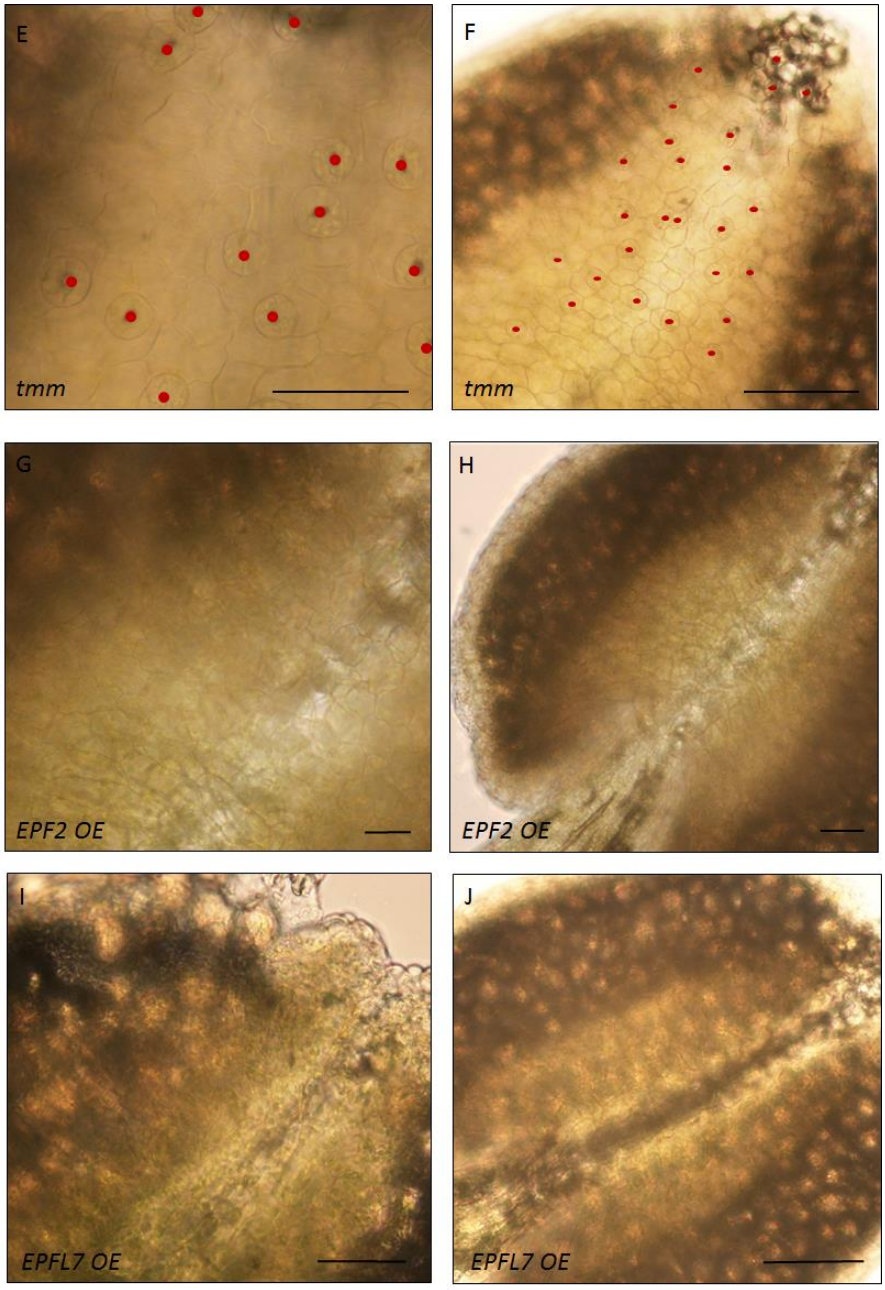
E
tmm
F
tmm
G
EPF2 OE
H
EPF2 OE
I
EPFL7 OE
J
EPFL7 OE

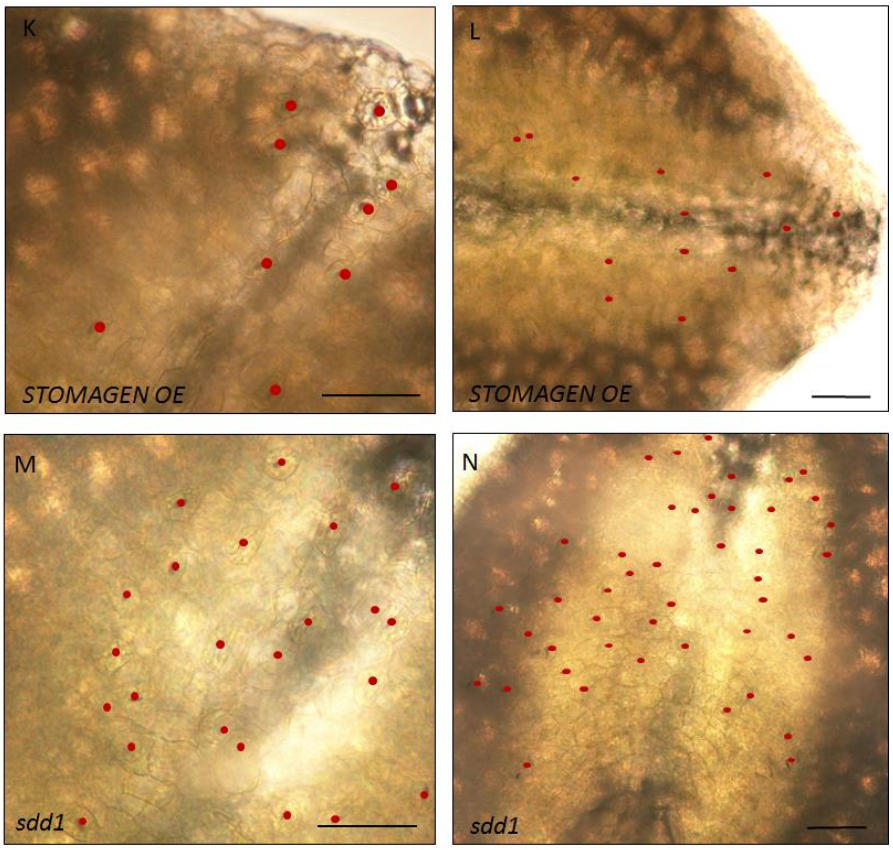
K
STOMAGEN OE
L
STOMAGEN OE
M
sdd1
N
sdd1

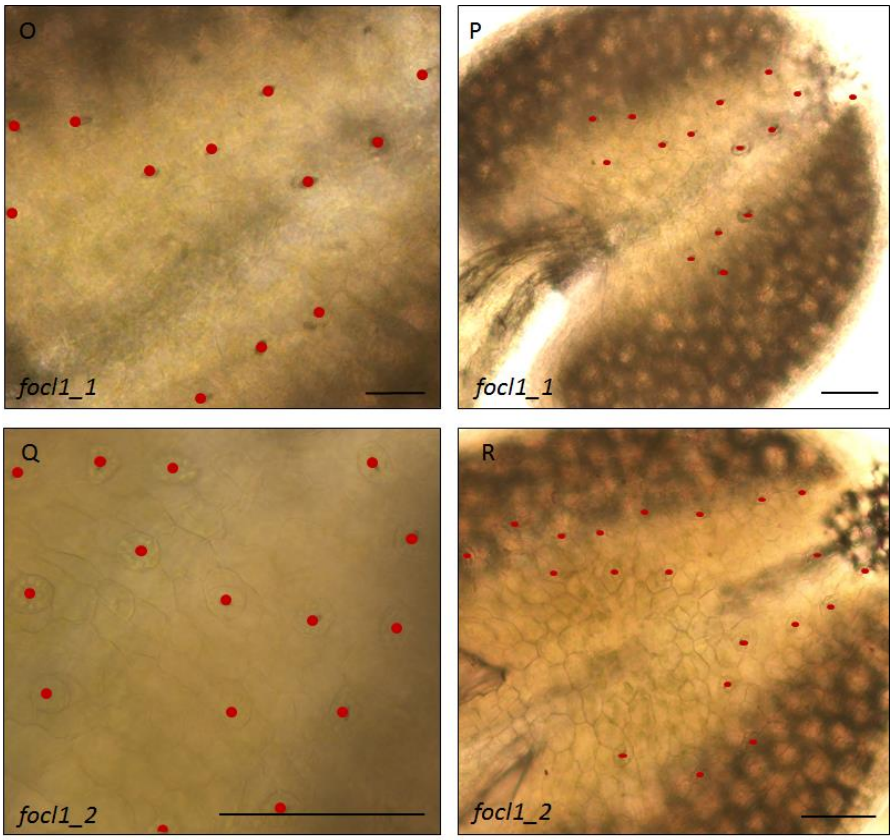

Figure 5.8: Stomatal patterning on *Arabidopsis* anthers.

Images show the distribution and spacing of anther stomata for *Arabidopsis* lines with altered stomatal development. Red dots indicate the position of stomata.

A: Columbia anther close up
B: Columbia anther
C: *basl tmm* anther close up
D: *basl tmm* anther
E: *tmm* anther close up
F: *tmm* anther
G: *EPF2 OE* anther close up
H: *EPF2 OE* anther
I: *EPFL7 OE* anther close up
J: *EPFL7 OE* anther
K: *STOMAGEN OE* anther close up
L: *STOMAGEN OE* anther
M: *sdd1* anther close up
N: *sdd1* anther
O: *focl1_1* anther close up
P: *focl1_1* anther
Q: *focl1_2* anther close up
R: *focl1_2* anther

A, C, G, I, K, M, O Scale bar 50μm
B, D, E, F, H, J, L, N, P, Q, R Scale bar 100 μm

Table 5.1: Summary of stomatal phenotypes in leaves and anthers. * based on observations only. ǂ based on statistical analysis. Pairs = two adjacent stomata, clusters = three or more adjacent stomata, large clusters = clusters of 8 or more adjacent stomata.

Line	Number of stomata Leaves*	Number of stomata in anthers ǂ	Patterning in leaves*	Patterning in anthers*
sdd1	Increased	Increased	Pairs	Pairs
tmm	Increased	Increased	Large Clusters, clusters and Pairs	Clusters and Pairs
basl tmm	Increased	Increased	Clusters and Pairs	Large Clusters, clusters and Pairs
STOMAGEN OE	Increased	Decreased	Clusters and Pairs	Pairs, no clusters
EPF2 OE	Reduced	None	Widely spaced stomata	N/A
EPFL7 OE	Reduced	None	Widely spaced stomata	N/A
focl1_1	Equivalent to Col-0	No significant difference to Col-0	Equivalent to Col-0	Equivalent to Col-0
focl1_2	Equivalent to Col-0	Increased	Equivalent to Col-0	Equivalent to Col-0

5.2.3 Fertility analysis of *Arabidopsis* stomatal development mutants

All eight stomatal mutant lines, were analysed for fertility changes. Seed set was used as an indicator of fertility as previously described (section 3.2.2). *EPF2* OE and *EPFL7* OE plants showed a severe reduction in fertility; *EPFL7 OE* plants were completely sterile and *EPF2 OE* plants had a significantly larger number of sterile siliques on the main stem ($P<0.001$). The *STOMAGEN* overexpressing line did not vary significantly from wild type, while the double mutant *basl tmm* only varied significantly for mean silique length which was

slightly reduced compared to Columbia (figure 5.9A, B). Both of the *focl1* mutant lines also showed a severe reduction in fertility compared to the Columbia controls. Both lines had a significant reduction in the mean length of siliques and an increased number of sterile siliques on the main stem (P<0.001). *sdd1* plants had a higher mean silique length compared to *Col-01* (figure 5.9C), otherwise *sdd1* and *tmm* plants did not vary significantly from the *Col-01* control (figure 5.9C, D).

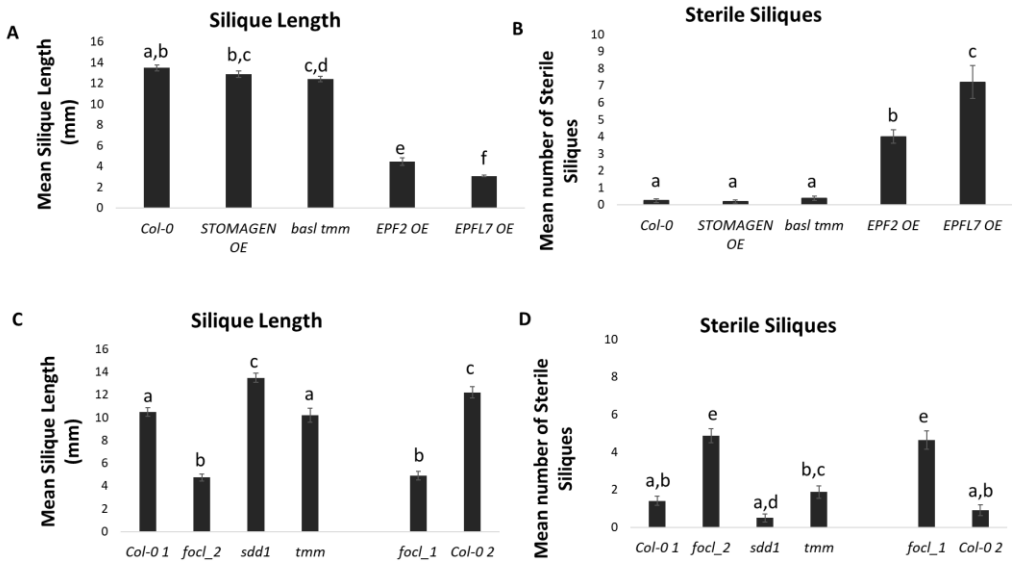

Figure 5.9: Characterisation of *Arabidopsis* lines with altered stomatal development

A: Mean silique length of *STOMAGEN OE, basl tmm, EPF2 OE, EPFL7 OE* and wild type (Col-0). Silique length of the 1st to 6th siliques on the main stem was measured. Bars marked with different letters vary significantly (P<0.001), bars sharing a letter do not, error bars, standard error.
B: Mean number of sterile siliques on the main stem of *STOMAGEN OE, basl tmm, EPF2 OE, EPFL7 OE* and wild type (Col-0). Bars marked with different letters vary significantly (P<0.001), bars sharing a letter do not, error bars, standard error.
C: Mean silique length of *focl1_2, sdd1, tmm, focl1_1.* Measurements were taken at two separate time points using two different wild type controls (Col-0 1 and Col-0 2). Silique length of the 1st to 6th siliques on the main stem was measured. Bars marked with different letters vary significantly (P<0.001), bars sharing a letter do not, error bars, standard error.
D: Mean number of sterile siliques on the main stem of *focl1_2, sdd1, tmm, focl1_1.* Measurements were taken at two separate time points using two different wild type controls (Col-0 1 and Col-0 2). Bars marked with different letters vary significantly (P<0.001), bars sharing a letter do not, error bars, standard error.

Pollen viability was assessed using FDA staining as previously described (section 2.5.1). None of the lines varied significantly from the Columbia control for the mean percentage of viable pollen (table 5.2). It may therefore be assumed that the reduction in fertility observed for *EPF2 OE, EPFL7 OE, focl1_1, focl1_2* plants was not caused by inviable pollen.

Table 5.2: Summary table for the statistical analysis of pollen viability for lines varying in stomatal development. The students' t-test was used to compare mean percentage pollen viability against a Columbia control. D.F = degrees of freedom.

Genotype	Mean percentage of viable pollen (%)	Mean percentage of viable pollen (%) Columbia Control	*t* stat	D.F	*P* value
basl tmm	76.0	81.1	1.67	18	>0.05
tmm	81.3	78.8	-0.85	18	>0.05
STOMAGEN OE	77.1	81.1	1.28	18	>0.05
sdd1	76.4	78.8	0.66	18	>0.05
focl_1	67.7	76.9	-1.82	17	>0.05
focl_2	77.1	78.8	0.46	18	>0.05
EPF2 OE	68.0	71.5	1.10	18	>0.05
EPFL7 OE	71.2	80.1	-1.86	18	>0.05

Delayed dehiscence was observed in both the *EPF2 OE* and *EPFL7 OE* lines (figure 5.10). The phenotype was more severe in *EPFL7 OE* flowers where the majority of anthers were indehiscent, even in older flowers. The *EPF2 OE* line sometimes had one or two dehisced anthers in just opened flowers and in older flowers all anthers eventually opened. Moving the plants from a growth chamber to the glasshouse, caused an increase in the number of dehisced anthers for both lines. From these observations, it seems probable that stomata facilitate water loss via evaporation from anthers which is required for anther opening. For plants that have no stomata on anthers, delayed dehiscence may be partially overcome in a drier environment, presumably because direct transpiration from the anthers is increased. Interestingly, although the *focl1_1* and *focl1_2* lines had a severe reduction in fertility, delayed dehiscence was not observed in

these lines. *focl1* mutants have occluded stomata and reduced stomatal conductance from leaves (Hunt et al., 2017). It may be that dehiscence is delayed in these lines, however at a subtler level.

Figure 5.10: Open flowers of Columbia, *EPF2 OE*, *EPFL7 OE*. One petal and sepal has been removed to show the anthers.

A: A young Columbia flower, all anthers dehisced
B: A young *EPF2 OE* flower, one dehisced anther is visible
C: An older *EPFL7 OE* flower, all anthers are indehiscent
All scale bars = 1mm

5.2.4 Analysis of wheat *TaEPFL1* overexpression lines

5.2.4.1 Analysis of stomatal number and patterning on wheat anthers

To investigate stomatal number and patterning in wheat anthers, light microscopy was used to image the abaxial side of anthers, as described in section 2.6.3. The images showed that, in wild type anthers, stomata line up on either side of the connective tissue and no stomata were observed on either of the anther lobes (figure 5.11B, C). The total number of stomata observed on whole anthers were counted for multiple anthers from five different biological replicates. The mean number of stomata per wild type anther was 8.1. No stomata were observed on the anthers of the *TaEPFL1* overexpression line, *TaEPFL1* 2.7 (figure 5.11A).

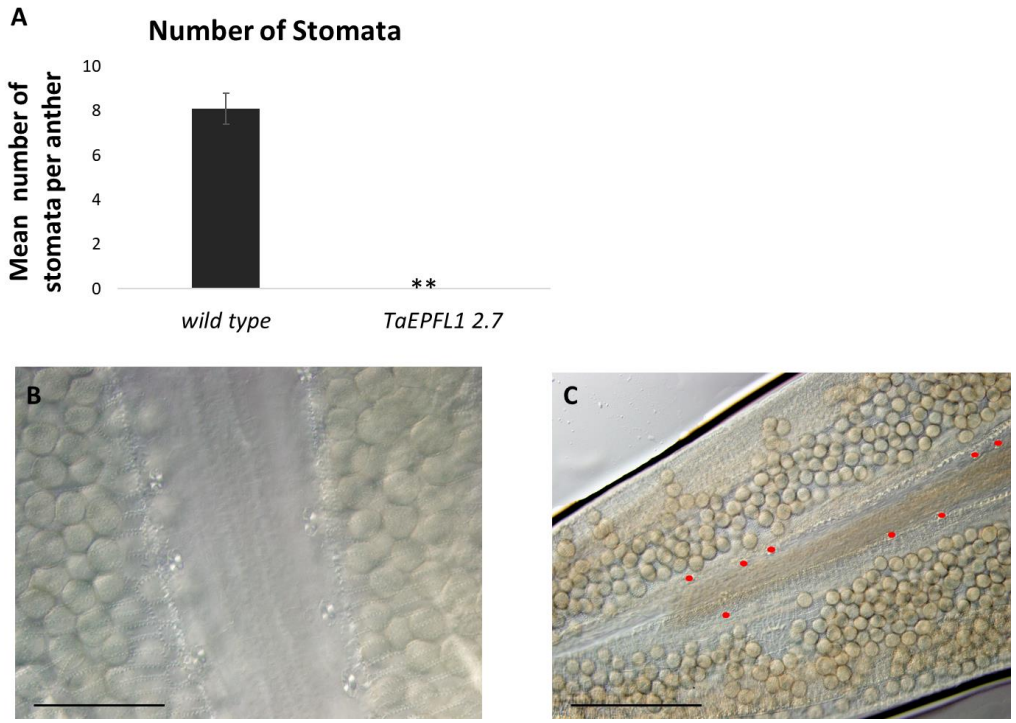

Figure 5.11: Analysis of stomatal number and patterning on wheat anthers

A: Mean number of stomata per anther for wild type (Fielder) and *TaEPFL1* 2.7 wheat lines. ** indicates a significant (P<0.001) variation from the wild-type control, error bars, standard error.
B: Wild type anther. Scale bar 100μm.
C: Wild type anther. Scale bar 200μm. Red dots indicate the position of stomata.

5.2.4.2 Analysis of seed yield and pollen viability of wheat *TaEPFL1* overexpression lines

To investigate whether over-expressing *TaEPFL1* affected fertility, the mean seed yield was calculated for three different *TaEPFL1* over-expression lines. The total weight of all the seeds from all the ears were counted per plant. The mean seed yield from five plants per genotype is shown (figure 5.12A). All of the lines had a lower seed yield compared to wild type although the reduction was only significant for the *TaEPFL1* 2.7 line (P<0.05) (figure 5.12A). MTT staining was used to investigate pollen viability of the same lines as described in section 2.5.5. The *TaEPFL1* 2.7 overexpression line had a significant reduction (P<0.05) in the number of viable pollen grains

compared to wild type, however the *TaEPFL1* 2.9 and *TaEPFL1* 4.5 lines did not differ significantly from the control (P>0.05) (figure 5.12B). When examining *TaEPFL1* 2.7 anthers by light microscopy (described in section 2.6.3), it was noticed that sometimes one or both lobes of the anther lacked any pollen grains (figure 5.12C, D, E). Therefore, it seems that overexpression of *TaEPFL1* may affect pollen development in wheat.

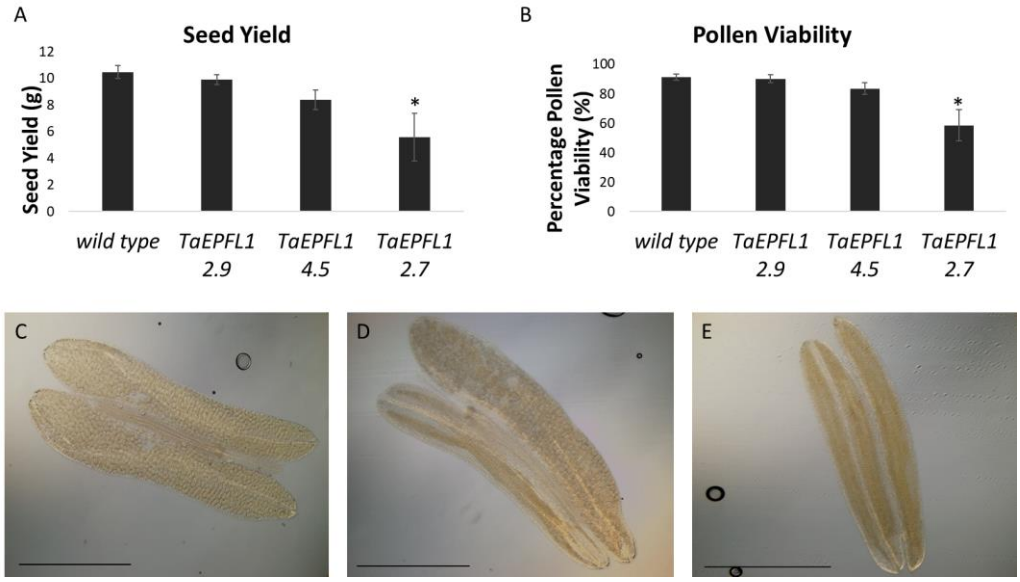

Figure 5.12: Characterisation of wheat *TaEPFL1* overexpression lines

A: Mean seed yield of wheat lines. * indicates significant variation from the wild type control (P<0.05), error bars, standard error.
B: Mean percentage pollen viability of wheat lines calculated from MTT staining. * indicates significant variation from the wild type control (P<0.05), error bars, standard error.
C: Wild-type anther. Scale bar 1000μm.
D: *TaEPFL1* 2.7 anther. Scale bar 1000μm.
E: *TaEPFL1* 2.7 anther. Scale bar 1000μm.

5.2.5 Analysis of the effect of varying environmental conditions on dehiscence and fertility

To investigate whether the presence of stomata on anthers affects dehiscence and fertility under different environmental conditions, four *Arabidopsis* lines with varying stomatal densities were selected. The lines selected were *STOMAGEN OE*, *basl tmm*, *focl1_1* and *EPF2 OE* (see table 5.1 for details of stomatal numbers and patterning). Plants

were grown under the conditions described in section 2.1.4 and then transferred into the experimental conditions (table 5.3) at flowering stage 6.10 (when 10% of the flowers to be produced have opened) (Boyes et al., 2001). Pots containing five replicates of each genotype were positioned in each condition by random design. Measurements of dehiscence, seed set and pollen viability were taken after one week in the new conditions.

Table 5.3: Experimental set up for analysis of the effect of varying environmental conditions on dehiscence and fertility (experiment1). Readings of temperature and relative humidity were taken at multiple time points over several days. A one-off reading of light intensity was taken for each condition (in the morning).

Condition	Experimental Set Up	Temperature (°C)	Light Intensity (umol)	Relative Humidity (%)
Normal	Plants placed in a glasshouse in still air	18-28	78.38	37-46
Fan	Plants placed in a glasshouse 25cm from a rotating free-standing fan	17-28	79.06	26-46
Humidity	Plants placed inside a small plastic greenhouse within a glasshouse. Two trays, each containing 1L of water, were used to create humid conditions inside the greenhouse.	18-28	81.43	87-92

The number of dehisced anthers in the first open flower of the primary inflorescence was counted for each plant (figure 5.13A). Statistical analysis showed both the effect of the environmental conditions and the genotype of the plants, affected dehiscence ($P<0.001$) and that the interaction between these two factors was also significant ($P=0.006$). With the exception of the wild type control (Col-0) and *basl tmm*, all genotypes had significantly fewer dehisced anthers in

humid conditions. In *EPF2 OE* flowers, none of the anthers dehisced under humid conditions but a higher number of anthers dehisced when plants were grown in front of the fan.

The mean percentage of viable pollen was calculated using FDA staining (section 2.5.1.) (figure 5.13B). Pollen viability was significantly affected by changes in the environmental conditions ($P=0.008$), however pollen viability did not differ significantly between genotypes ($P=0.085$) and the interaction between the two factors was not significant either ($P=0.908$). The viability of pollen from *basl tmm*, *focl1_1* and *EPF2 OE* flowers was significantly reduced in high humidity and none of the pollen from *EPF2 OE* flowers was viable under humid conditions.

The length of the first fifteen siliques on the main stem was measured and the averages compared for all plants (figure 5.13C). Statistical analysis showed that both the environmental conditions, and the genotype of the plants, significantly affected seed set ($P<0.001$) and that the interaction between these two factors was also significant ($P=0.004$). The mean silique length was significantly lower for all genotypes in humid conditions. The seed set of *focl1_1* and *EPF2 OE* plants was also reduced when plants were grown in front of the fan.

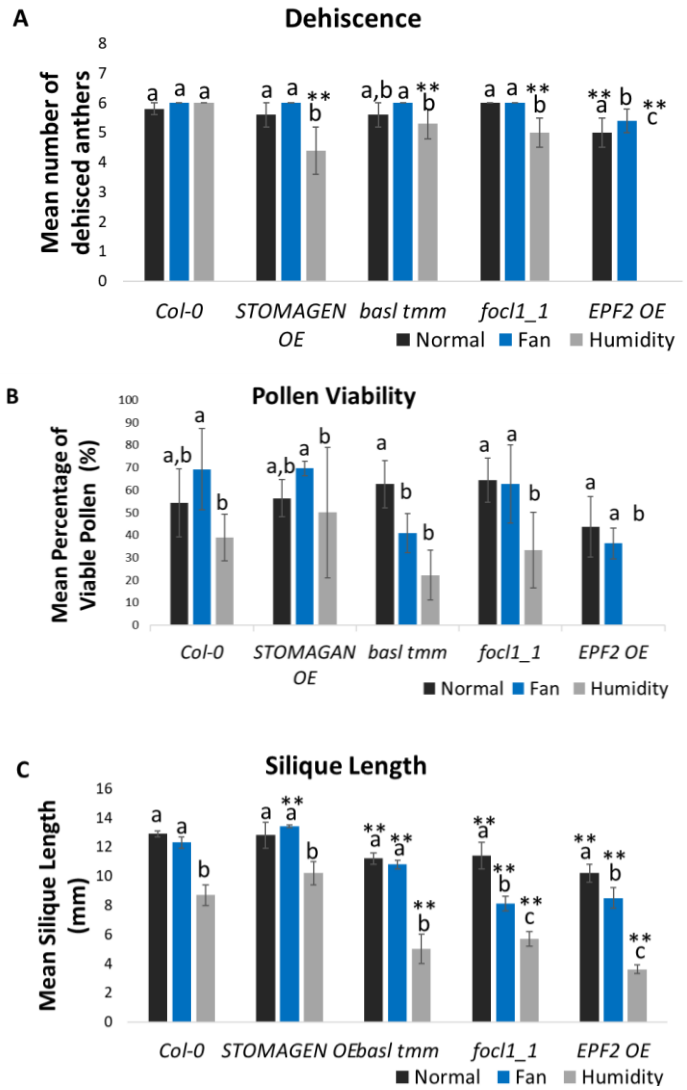

Figure 5.13: The effect of varying environmental conditions on dehiscence, pollen viability and silique length (experiment 1).

A: Mean number of dehisced anthers within the first open flower of the inflorescence for Col-0, *STOMAGEN OE, basl tmm, focl1*_1 and *EPF2 OE* flowers. Within each genotype, Bars marked with different letters vary significantly (P<0.001), bars sharing a letter do not, error bars, standard error. ** indicates a significant variation (P<0.001) from the wild type (Col-0) control for that condition.
B: Mean percentage of viable pollen for Col-0, *STOMAGEN OE, basl tmm, focl1*_1 and *EPF2 OE* plants in varying environmental conditions. Within each genotype, Bars marked with different letters vary significantly (P<0.001), bars sharing a letter do not, error bars, standard error.
C: Mean length of siliques on the main stem of Col-0, *STOMAGEN OE, basl tmm, focl1_1* and *EPF2 OE* plants in varying environmental conditions. The first fifteen siliques on the main stem were measured. Within each genotype, bars marked with different letters vary significantly (P<0.001), bars sharing a letter do not, error bars, standard error. ** indicates a significant variation (P<0.001) from the wild type (Col-0) control for that condition.

The experiment was repeated to confirm the observed trends. The environmental conditions for the repeated experiment are described in table 5.4. Due to external weather conditions, higher temperatures were recorded during the second experiment. Some of the *focl1_1* plants grown in high humidity did not form siliques at all and eventually the main stems wilted. It is presumed that this was caused by heat stress under humid conditions.

Table 5.4: Experimental set up for analysis of the effect of varying environmental conditions on dehiscence and fertility (experiment 2). Readings of temperature and relative humidity were taken at multiple time points over several days. A one-off reading of light intensity was taken for each condition (in the morning).

Condition	Experimental Set Up	Temperature (°C)	Light Intensity (umol)	Relative Humidity (%)
Normal	Plants placed in a glasshouse in still air	20 - 32	54.85	29-31
Fan	Plants placed in a glasshouse 25cm from a rotating free-standing fan	20 - 32	64.16	26-46
Humidity	Plants placed inside a small plastic greenhouse within a glasshouse. Two trays, each containing 1L of water, were used to create humid conditions inside the greenhouse.	20 - 34	44.16	89-90

Analysis of dehiscence in the repeated experiment showed that both the genotype of the plants and the environmental conditions significantly affected the number of dehisced anthers ($P<0.001$) (figure 5.14A), however in this experiment the interaction between the two factors was not significant ($P=0.839$). All of the genotypes had a significant reduction in the number of dehisced anthers in humid conditions. The percentage of viable pollen was also significantly affected by the environmental conditions ($P<0.001$), and

was reduced for all genotypes in high humidity (figure 5.14B). In this experiment, none of the pollen from the wild type control was viable under humid conditions. The genotype of the plants did not affect the pollen viability ($P=0.084$), however the interaction between the environmental conditions and the different genotypes was significant ($P<0.001$). Finally, both the environmental conditions and the genotype of the plants had a significant effect on silique length ($P<0.001$) (figure 5.14C), although the interaction between the two factors was not significant ($P=0.2$). All of the genotypes had reduced seed set under humid conditions. *basl tmm, focl1_1* and *EPF2 OE* plants, all had significantly longer siliques when grown in front of the fan.

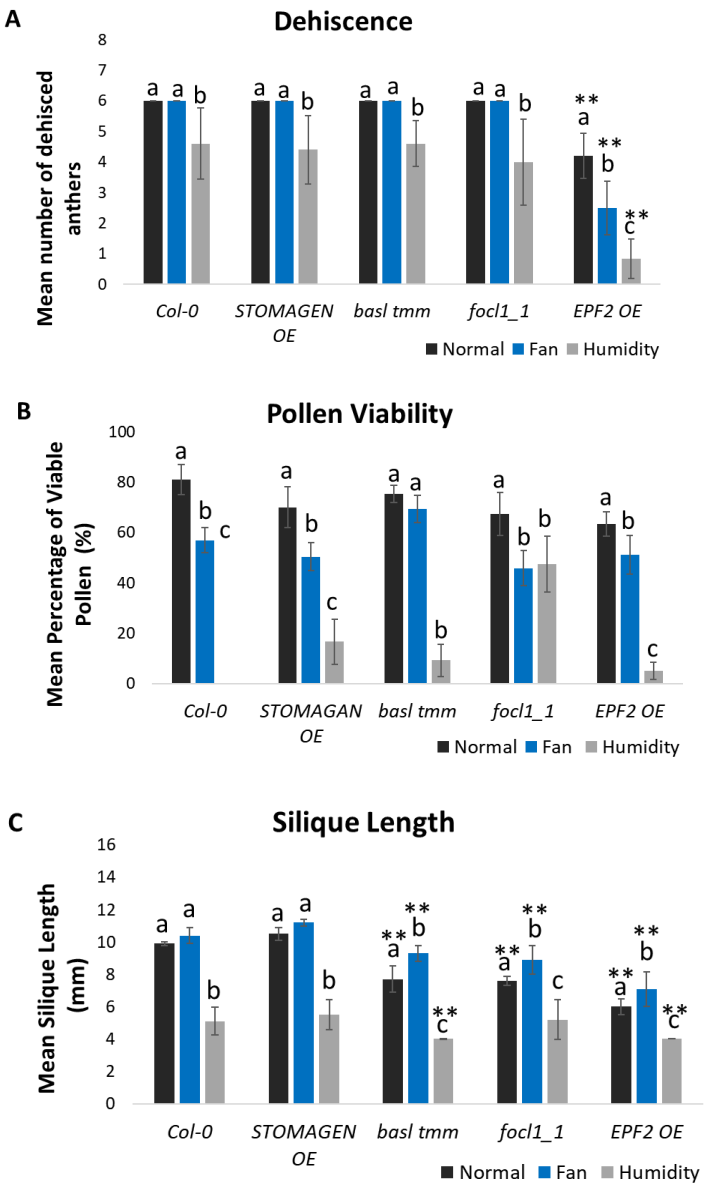

Figure 5.14: The effect of varying environmental conditions on dehiscence, pollen viability and silique length (experiment 2).

A: Mean number of dehisced anthers within the first open flower of the inflorescence for Col-0, *STOMAGEN OE, basl tmm, focl1*_1 and *EPF2 OE* flowers. Within each genotype, Bars marked with different letters vary significantly (P<0.001), bars sharing a letter do not, error bars, standard error. ** indicates a significant variation (P<0.001) from the wild type (Col-0) control for that condition.
B: Mean percentage of viable pollen for Col-0, *STOMAGEN OE, basl tmm, focl1*_1 and *EPF2 OE* plants in varying environmental conditions. Within each genotype, Bars marked with different letters vary significantly (P<0.001), bars sharing a letter do not, error bars, standard error.
C: Mean length of siliques on the main stem of Col-0, *STOMAGEN OE, basl tmm, focl1_1* and *EPF2 OE* plants in varying environmental conditions. The first fifteen siliques on the main stem were measured. Within each genotype, bars marked with different letters vary significantly (P<0.001), bars sharing a letter do not, error bars, standard error. ** indicates a significant variation (P<0.001) from the wild type (Col-0) control for that condition.

The two experiments showed that placing plants in conditions of high humidity affected dehiscence, pollen viability and seed set. It is likely that the reduction in seed set is a direct result of delayed dehiscence and reduced pollen viability although, as previously shown in figures 5.9A and C, mean silique length already varied between the genotypes. The genotype of the plants does not affect their pollen viability (which is consistent with the results in table 5.2), however the environmental conditions do affect the amount of viable pollen. The relative humidity of the air in front of the fan was quite variable (tables 5.3 and 5.4) and opposite effects on seed set were observed for *EPF2 OE* plants grown in front of the fan between the two experiments. Placing plants inside an enclosed environment containing silica gel, may be a more effective way to reduce the relative humidity. Overall the data suggests that water loss via evaporation is important for anther opening as this is significantly reduced under humid conditions. It seems likely that the presence of stomata on anthers facilitates this process as *EPF2 OE* anther dehiscence was the most severely affected under humid conditions (figures 5.13A, 5.14A).

5.3 Discussion

5.3.1 Stomatal patterning and number varies between leaves and anthers for some *Arabidopsis* lines with altered stomatal development

Analysis of stomatal patterning on leaves and anthers revealed that, for some *Arabidopsis* lines with altered stomatal density, the number and distribution of stomata varied between organs. The most striking difference was observed between leaves and anthers of *STOMAGEN* overexpressing plants. While it is well documented that *STOMOGEN* is a positive regulator of stomatal development and overexpression increases stomatal density in leaves (Hunt et al., 2010; Kondo et al.,

2010; Sugano et al., 2010), *STOMAGEN OE* anthers had fewer stomata than wild type (figure 5.6). It is possible that *STOMAGEN* regulates stomatal development in an organ specific manner, similar to its EPF family member *CHAL* (section 5.1). *CHAL* and *EPF1/2* are all negative regulators of stomatal density in a wild type background however overexpression of these factors in a *tmm* mutant background results in different phenotypes: *EPF1/2* overexpression ceases to reduce stomatal number, whereas in tissues where *CHAL* is expressed (inflorescence stem and hypocotyls), no stomata are produced (Abrash and Bergmann, 2010). Therefore, it seems that *TMM* has opposite effects on *CHAL* and *EPF1/2* signalling via the ER family of receptors (figure 5.15A). The TMM/CHAL interaction doesn't explain all of the *tmm* mutant phenotypes, therefore it is possible that other EPF family members also control stomatal development, and that this may occur in an organ specific manner (Abrash and Bergmann, 2010). While *EPF1/2* are expressed within the stomatal lineage, *STOMAGEN* and *CHAL* are responsible for signalling between the epidermis and the internal tissue of the leaf and stem respectively (Pillitteri and Dong, 2013). *STOMAGEN* is widely expressed in plants however, including in the early flower stages (figure 5.15B). *STOMAGEN* signalling also requires interaction with the TMM receptor, and it is thought that STOMAGEN competes against EPF1/2 for TMM in order to positively regulate stomatal density (Kondo et al., 2010). The correct folding of the STOMAGEN protein is essential for its bioactivity and it is likely all of the EPF proteins undergo post-translational modifications (Kondo et al., 2010; Ohki et al., 2011; Pillitteri and Dong, 2013). Therefore, it is possible that the differences in stomatal density observed between *STOMAGEN OE* leaves and anthers, are caused by differences in the levels of competing proteins, possibly controlled via post-translational processing.

A

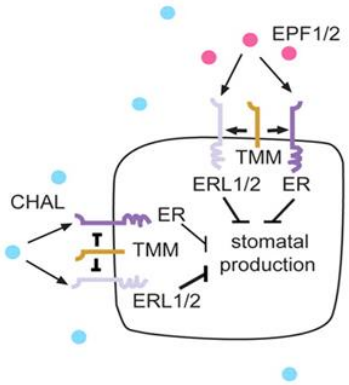

B

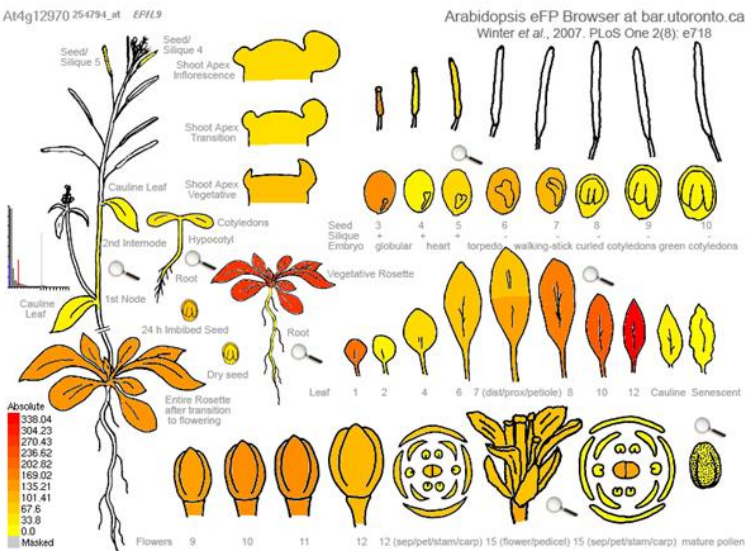

Figure 5.15: Model for *TMM* and *CHAL/EPF1/2* interactions and the Developmental map for *STOMAGEN* expression

A: *TMM* enhances *EPF1/2* signalling via the ER family of receptors, but reduces *CHAL* signalling. It is possible that *CHAL* may also act through other unidentified receptors. Figure adapted from (Abrash and Bergmann, 2010). B: Developmental map for AT4G12970 *(STOMAGEN)* from the *Arabidopsis* eFP browser (Winter et al., 2007)

The *EPF2* and *EPFL7* overexpression lines also showed differences in stomatal development between leaves and anthers. While overexpressing *EPF2* and *EPFL7* significantly reduces the number of stomata in the leaf epidermis, no stomata were observed on any *EPF2 OE* or *EPFL7 OE* anthers (figures 5.4 and 5.8). Furthermore, leaves and anthers of the *tmm*, *basl tmm* and *STOMAGEN OE* lines, varied for the number of adjacent stomata observed on the epidermises

(table 5.1). The frequency of clustered stomata varies in different organs of the *sdd1* mutant (Berger and Altmann, 2000), so it may be that the frequency and number of clustered stomata is affected in an organ specific manner in different stomatal development mutants.

5.3.2 *focl1_1, focl1_2, EPF2 OE* and *EPFL7 OE* lines all had reduced fertility, and overexpressing *EPF2* and *EPFL7* delayed dehiscence

Four out of the eight *Arabidopsis* lines with changes to stomatal development, had a significant reduction in seed set ($P<0.001$). *focl1_1*, *focl1_2*, *EPF2 OE* and *EPFL7 OE* plants all had an increased number of sterile siliques and a reduction in mean silique length, compared to wildtype (figure 5.9). Open flowers of *EPF2 OE* and *EPFL7 OE* plants had many indehiscent anthers, however moving plants to a drier environment caused more anthers to open (section 5.2.3). Anthers of *EPF2 OE* and *EPFL7 OE* plants had no stomata, so these observations suggest that the presence of stomata on anthers facilitates water loss via evaporation required for anther opening and successful fertilisation. It is surprising therefore, that delayed dehiscence was not observed in *focl1* plants, as these have occluded stomata and reduced transpiration rates (Hunt et al., 2017). There are a few possible explanations for this. Firstly, it could be that the *focl1* phenotype varies between leaves and anthers. Hunt et al. used scanning electron microscopy to show that in the leaf epidermis, *focl1* stomatal pores can remain totally blocked even when stomata are fully mature (Hunt et al., 2017). It could be that changes in turgor pressure, and the resultant biomechanical forces on the anther walls during dehydration, cause the cuticular membranous material covering the *focl1* stomatal pores to tear. *focl1* guard cells are presumed to have defective cell walls, which means they have increased turgor pressure compared to wild type guard cells, and this affects the shape and size of the *focl1* stomatal pore. The altered morphology of the *focl1* stomata mean they are unable to close as fully as wild type stomata (Hunt et al., 2017), which suggests a

rigidity that could be significant as the epidermis dehydrates. Alternatively, it could be that the *focl1* anther stomata remain obstructed and subsequently dehiscence is delayed, however this occurs at a subtler level than in *EPF2/EPFL7 OE* flowers. The photosynthetic capacity of *focl1* plants has not been investigated to date, therefore it is not possible to say what caused the reduction in fertility of *focl1* plants without further investigation. Checking the phenotype of *focl1* anther stomata is recommended as a next step.

5.3.3 *TaEPFL1 OE* wheat anthers had no stomata and plants had reduced pollen viability and seed set

Anthers from the wheat *TaEPFL1* 2.7 line were analysed for stomatal number and patterning, however no stomata were observed (figure 5.11A). Pollen formation appears to be affected in this line, as anther lobes completely lacking pollen were sometimes observed (figure 5.12D, E).

Three independent *TaEPFL1* overexpression lines were analysed for changes to fertility. All three lines had a reduction in seed yield and pollen viability, however these changes were only significant for the *TaEPFL1 2.7* line (figure 5.12). The *TaEPFL1* 2.7 line has a greater reduction in stomatal density in the leaves than the other two lines, so the fertility phenotype may be directly related to that, or could be a consequence of the increased number of gene copies (4+) in this line (personal communication, Dr Lee Hunt, The University of Sheffield). A significant reduction in grain filling was also recorded for a rice line overexpressing the rice *EPF2* homologue (Mohammed, 2017).

There has been considerable interest in manipulating the *EPF* genes to improve water use efficiency (WUE), particularly as mutations in other genes of the stomatal developmental pathway have proved to be deleterious to the plant (Franks et al., 2015). Stomatal density (*D*) and size (*S*) are negatively correlated, and although it is thought that a larger number of smaller stomata would enable more efficient and

better controlled gas exchange, plants with fewer larger stomata grow advantageously under conditions of high CO_2 (Doheny-Adams et al., 2012). *Arabidopsis* plants overexpressing *EPF2* had reduced stomatal conductance of water vapour (g_w), but this did not significantly affect their photosynthetic capacity and resulted in improved WUE (Franks et al., 2015). Furthermore, nutrient uptake from the soil which is driven by transpiration was not significantly affected in *Arabidopsis EPF2 OE* plants (Hepworth et al., 2015). It has been questioned why such advantageous traits have not evolved in the natural population (Doheny-Adams et al., 2012) however, given that a reduction in fertility has been reported for three species overexpressing the *EPF2* gene under normal growth conditions, it seems that reducing stomatal density comes at a price. While it appears that in *Arabidopsis*, the reduction in seed set is caused by delayed dehiscence, it is not possible to conclude what caused the fertility changes in wheat and rice without further analysis. Seed set and pollen viability was only significantly affected in the wheat *TaEPFL1*2.1 line (figure 5.12), which had the greatest reduction in stomatal density. It seems therefore, that there may be a threshold value below which reducing stomatal density induces negative traits.

5.3.4 High humidity affects fertility, dehiscence and pollen viability in *Arabidopsis*

High humidity affected dehiscence, pollen viability and seed set of *Arabidopsis* lines with altered stomatal development and wild type plants (section 5.2.5). Open flowers of all lines had significantly fewer dehisced anthers under humid conditions and for the *EPF2 OE* lines, this reduction was highly significant ($P<0.001$) (figures 5.13A, 5.14A). These results suggest that water loss via evaporation is important for anther opening in *Arabidopsis* and that the presence of stomata on the abaxial side of anthers facilitates this. Other evidence, supporting a correlation between the presence of stomata on anthers and the speed of anther dehiscence, has been discussed in section 5.1. Yates and Sparks demonstrated that high temperatures and low

humidity showed a positive interaction and promoted dehiscence of anthers removed from pecan trees (*Carya illinoinensis*) (Yates and Sparks, 1993). Furthermore increasing temperature could partially overcome the negative effect of humidity on anther dehiscence (Yates and Sparks, 1993). It is now known that environmental signals can influence stomatal development directly. The *Arabidopsis HIGH CARBON DIOXIDE (HIC)* gene encodes a negative regulator of stomatal development that controls stomatal density in response to elevated CO_2 (Gray et al., 2000), and MAPK pathways (figure 5.1) are activated in response to stresses including drought and low humidity (Ichimura et al., 2000). Changes to stomatal density in response to environmental conditions have only been studied in leaves, so an analysis of stomatal numbers on anthers of *Arabidopsis* plants grown under different conditions would be interesting.

All of the *Arabidopsis* lines had a reduction in seed set under conditions of high relative humidity (RH) (figures 5.13C, 5.14C), which is assumed to be a result of delayed dehiscence and reduced pollen viability (figures 5.13A, B, 5.14A, B). The reduction in pollen viability may have been caused by the pollen being retained in the anther, however none of the genotypes varied significantly from wild type for pollen viability under normal conditions (table 5.2 and section 5.2.5). As *EPF2 OE* and *EPFL7 OE* anthers had delayed dehiscence under normal conditions, this suggests that it is the effect of the environmental conditions which led to reduced pollen viability. Experiments to test the effect of high RH (>95%) and temperature stress on pollen viability and pollen vigour (classed as the time for germination and pollen tube growth), showed that the effect of these conditions varied significantly between species, and that vigour was affected more than viability (Shivanna et al., 1991). Changes to pollen water status during pollen development are predominantly regulated by osmoregulation (see section 1.3), therefore further analysis would be required to understand how and why the viability of *Arabidopsis* pollen is reduced under conditions of high RH.

CHAPTER 6 GENERAL DISCUSSION

Plants optimise the timing of pollen release in order to maximise the chance of successful fertilization. Anther dehiscence is multi-step process comprised of a number of tightly regulated phases. Key stages including secondary thickening of the endothecium, rupture of the septum, and changes in water status that result in bending of the locule wall and splitting of the stomium, are conserved between species. Dehydration of the anther walls is a critical last step in the dehiscence process yet the genetic factors underlying water movement in the anther are not known. Evidence from research in different species suggests that both passive and active processes take place and a number of complementary theories have been suggested (sections 1.2.3 and 1.3) (Nelson et al., 2012). Separate work, focusing on the importance of water loss by evaporation during anther opening, has shown a correlation between the presence of anther stomata and the speed of anther dehiscence (Keijzer et al., 1987).

This project aimed to use the model plant *Arabidopsis thaliana* to elucidate the process of anther dehydration and the genetic factors controlling it. Not only does this contribute to fundamental knowledge of how the anther opens but it also has applications for plant breeding. Hybrid plant breeding has many advantages including improved trait values caused by heterosis and larger and more stable yields, however in autogamous crops it requires an effective male sterility system to prevent self-fertilization (Longin et al., 2012). Hybrid breeding in rice has been particularly successful due to exploitation of a naturally occurring cytoplasmic male sterility (CMS), however such traits are not available in all species and emasculation processes are often time consuming and expensive. Controlling the process of pollen release is of commercial interest because it can be applied to hybrid and selective breeding programs and can be used to restrict the spread of GM pollen (Wilson and Zhang, 2009). Furthermore, there is growing interest in manipulating stomatal

density to optimise plant growth for changing environmental conditions, however the importance of stomata on reproductive organs has not previously been considered.

6.1 *Arabidopsis PIP1* and *PIP2* aquaporins have specific temporal and spatial expression patterns in flowers

A wide range of tissue specific, physiological roles have been described for the *Arabidopsis* aquaporins. Despite the fact that the majority of *Arabidopsis PIP1* and *PIP2* genes are expressed during the late stages of flower development, their function in flowers is unknown. qRT-PCR expression analysis identified four aquaporin genes, *PIP1;5*, *PIP2;1*, *PIP2;2* and *PIP2;3,* which are significantly upregulated during bud stage 4. Bud stage 4 is equivalent to flower stage 12, which is just before anthesis (Smyth et al., 1990). At this stage of flower development, water movement is essential for organ expansion, flower opening and anther dehiscence. Furthermore, analysis of GUS reporter lines for *PIP1;2, PIP1;5, PIP2;1* and *PIP2;7* revealed overlapping spatial expression patterns that could easily relate to roles in the aforementioned processes. The majority of expression was observed in open flowers and was confined to the filaments (*PIP1;2, PIP2;1, PIP2;7*), vascular and connective tissues (*PIP1;2, PIP2;1*), petals and sepals (*PIP1;2, PIP1;5, PIP2;1*) and pistils (*PIP1;2, PIP2;1*). Overlapping, but not identical, spatial and temporal expressions patterns were also identified for *PIP1* and *PIP2* aquaporins in tobacco (Bots et al., 2005b). There are a number of possible reasons for having a large number of isoforms with overlapping expression patterns. Firstly, it is possible that the different aquaporin proteins all perform the same function in the flower, however differential expression means that certain isoforms contribute to specific developmental stages. Alternatively, the multiple isoforms may exist to confer functional redundancy, or else different aquaporins may have different transport properties (see section 3.1) (Bots et al., 2005b).

There are other instances where spatial and temporal control of aquaporins seems to be important for their function. For example, *PIP1;4* and *PIP2;5* are upregulated under drought stress, however constitutive expression of these genes had a deleterious effect under dehydration stress. This suggests that the specificity of where and when these genes are expressed is important for their function under water limiting conditions (Jang et al., 2004, 2007). The role of *PIP2;1* in lateral root emergence (LRE) provides another example. *PIP2;1* is gradually excluded from the lateral root primordia during LRE but maintained in the underlying tissues. *pip2;1* mutants have altered water transport within the primordia which reduces its emergence rate, while overexpression of *PIP2;1* causes increased water flow into the overlaying tissue which is normally repressed during LRE. Both the loss-of-function and gain-of-function mutants have delayed LRE (Péret et al., 2012). Given the possibility that complex regulatory relationships exist between the aquaporins particularly under stress (section 3.3.2), it may be that the temporal and spatial expression patterns of different aquaporins overlap in floral organs to ensure water transport is optimised under different conditions.

6.2 *Arabidopsis* aquaporin and sucrose transporter mutants have reduced fertility

Combinations of *Arabidopsis* aquaporin single, double and triple mutants and sucrose transporter single mutants showed changes in fertility. Seed set was reduced although no alteration in pollen viability was observed. The *suc2* (het) and *pip1;2pip2;1*, *pip1;2pip2;1pip2;6* phenotypes were the most severe and many of the early siliques on the main stems of these plants were completely sterile. Generally, the sucrose transporters had lower expression in flowers than the aquaporins (tables 3.1, 3.2, 4.1 and 4.2), however single *suc2* (het) and *suc5* (hm) mutants had stronger phenotypes than the aquaporin single mutants. This may be due to functional redundancy among the aquaporin isoforms. Silencing of multiple *PIP2* aquaporins in tobacco caused delayed dehiscence, however plant

growth was normal and dehiscence was only slightly delayed (Bots et al., 2005a). Bots et al. consider that the purpose of aquaporins in facilitating water movement across plasma membranes is subsidiary to the proteins that create osmotic gradients that drive water flux (Bots et al., 2005a), and this could also explain the strong phenotype of the single sucrose transporter mutants.

Both aquaporin and sucrose transporter mutants had various changes to lengths of petals, stamens and pistils at two different developmental stages however no changes to dehiscence or stigma receptivity were observed. These results suggest a role in controlling water transport for cell expansion and organ growth, which is supported by the specific expression of certain aquaporins in filaments and petals at a time when these organs extend. These changes cannot explain the reduction in seed set however, as generally floral organ lengths were increased compared to wild type and the ratio of stamen to pistil lengths were not significantly altered. The *suc2* (het) mutant was the exception to this, which had significantly shorter stamens and petals in open flowers. Further work is required to determine the exact role of aquaporins and sucrose transporters in *Arabidopsis* flowers.

6.3 The presence of stomata on anthers is important for anther dehiscence in *Arabidopsis*

In *Arabidopsis* stomata are found not only on the abaxial and adaxial side of leaves, but also on both sides of the sepals, the abaxial side of anthers, on siliques and on the flower stalk and inflorescence stem. The number of stomata per organ varies greatly and is probably reflective of the size of the organ and its capacity for photosynthesis. For example, cauline leaves have thousands of stomata, whereas cotyledons, sepals and siliques have hundreds, and the inflorescence stem and anthers have less than thirty (Geisler et al., 1998). Flower organs can be divided into two types depending on the type of photosynthesis that they do. Leaves, green stems and sepals are

optimised for light harvesting and use atmospheric CO_2 for net carbon assimilation, while most fruit and fertile flower organs use CO_2 released from respiration to perform carbon refixation and recycling (Aschan and Pfanz, 2003). It is not known whether anthers have stomata primarily for carbon refixation, or if stomata are present to aid anther dehydration.

Arabidopsis plants with no anther stomata had delayed dehiscence, which supports previous work in *G. verrucosa* (described in section 5.1) (Keijzer et al., 1987). Furthermore, humid conditions reduced the rate of anther opening in wild type plants, which suggests that water loss via evaporation is integral to anther dehydration in *Arabidopsis*. Wheat plants with no anther stomata had reduced seed set however, it is not known whether this was caused by delayed dehiscence and reduced pollen viability was also observed. Wild type wheat anthers are considerably larger than *Arabidopsis* anthers, yet have far fewer stomata per anther. It's likely that the function of anther stomata varies between species depending on the mechanism of flower and anther opening. Some species do not have anther stomata, and evaporation is unlikely to be the primary means of anther dehydration in cleistogamous flowers (Bonner and Dickinson, 1989; Keijzer et al., 1987).

6.4 The role of phytohormones in anther dehiscence

Jasmonic acid mutants are characterised by reduced filament extension, delayed dehiscence or completely indehiscent anthers. While phenotypes of the JA biosynthesis mutants can be rescued by the application of endogenous JA, phenotypes of the signalling mutants cannot be (Feys et al., 1994; Ishiguro et al., 2001; von Malek et al., 2002; McConn and Browse, 1996; Park et al., 2002; Sanders et al., 2000; Stintzi and Browse, 2000; Xie et al., 1998). Ishiguro et al. proposed that JA acts as a master regulator for water transport in flowers, promoting both anther dehydration and the uptake of water required for petal and filament expansion (see figure

1.5) (Ishiguro et al., 2001). qRT-PCR analysis showed that *Arabidopsis* aquaporin and sucrose transporter genes expressed in flowers showed negligible expression changes in a jasmonic acid deficient background (sections 3.2.1.4 and 4.2.1). It seems unlikely therefore, that JA regulates water transport in *Arabidopsis* flowers via the aquaporin and sucrose transporter genes investigated. Furthermore, with the exception of the *short anther* phenotype (section 3.2.3), the phenotypes of the aquaporin and sucrose transporter mutants were not typical of the jasmonic acid mutants.

The role of phytohormones in anther dehiscence is complex. In tobacco ethylene controls the timing of anther dehiscence and ethylene insensitive mutants show defects in anther dehydration that are very similar to the *Arabidopsis dde1* mutant (Rieu et al., 2003). Both hormones co-ordinate dehiscence with flower opening and may act as interorgan signalling molecules. It is not known whether ethylene and jasmonic acid have partially redundant or homologous functions in tobacco and *Arabidopsis*, however ethylene insensitive *Arabidopsis* mutants do not have delayed dehiscence (Rieu et al., 2003). *YUC* genes, required for auxin biosynthesis, are essential for normal floral development in *Arabidopsis* and show spatial and temporal expression patterns in reproductive organs (Cheng et al., 2006). Moreover, auxin is an upstream negative regulator of both *MYB26* and JA (section 1.2.3), and in the auxin perception mutant *afb1-3* endothecium lignification and anther dehiscence occur early (Cecchetti et al., 2013). The *afb1-3opr3* double mutant however, has the combined phenotypic features of the two single mutants; secondary thickening of the endothecium occurs early and anthers are indehiscent due to defective stomium opening as seen in the *opr3* mutant. This suggests that auxin does not control stomium opening in the absence of JA however it does control stomium opening through JA (Cecchetti et al., 2013).

Gibberellin (GA) is synthesised in developing stamens and is important for pollen development and tapetum function as well as filament elongation and anther dehiscence. GA acts partially, but not

exclusively, through interaction with the JA biosynthesis pathway (Plackett et al., 2011). *Arabidopsis* SWEET proteins have been identified as multifunctional transporters of both sucrose and GA (Chen et al., 2012; Kanno et al., 2016). Double mutant *sweet13sweet14* had normal filament extension but delayed dehiscence which could be recovered by the application of exogenous GA. Interestingly, the bulk GA content of *sweet13sweet14* anthers was similar to wild type. It seems that loss of protein function results in reduced GA uptake into cells and affects GA distribution rather than bulk content (Kanno et al., 2016).

Abscisic acid (ABA) regulates many aspects of plant growth yet mutant phenotypes are often subtle in the absence of abiotic stress. One well known response to ABA is stomatal closure (Brocard-Gifford et al., 2004). Recent evidence suggests that aquaporins and sucrose transporters may contribute to osmoregulation for the control of stomatal aperture. *SUC2* is one of several *Arabidopsis* sugar transporters which is strongly expressed in guard cells and *sugar transporters1* and *4* (*STP1/4*) were shown to be ABA responsive (Daloso et al., 2016; Wang et al., 2011). Aquaporins are also expressed in guard cells and it has recently been shown that in *Arabidopsis, PIP2;1* is important for ABA-mediated stomatal closure (Grondin et al., 2015; Heinen et al., 2014). *Open Stomata1* (*OST1*) (a protein kinase involved in ABA signalling in guard cells) activates *PIP2;1* via phosphorylation at Ser-121, and increases guard cell water permeability required for stomatal closure (Grondin et al., 2015). In other organs ABA can inhibit *PIP2;1* via dephosphorylation at Ser-280, which illustrates how a single PIP isoform can have opposite responses to the same stimulus (Grondin et al., 2015; Kline et al., 2010).

These examples highlight the complexity of hormonal control of anther dehiscence. Further work is required to fully understand the roles played by different phytohormones. Crossing mutants of interest into different hormone deficient backgrounds, and

experimenting with applying hormones exogenously, could help to establish links.

6.5 Future Work

6.5.1 Defining the roles of *Arabidopsis* aquaporins and sucrose transporters in flowers

A large number of *Arabidopsis* aquaporin and sucrose transporters genes are expressed during flower stages 12/15. Nearly all of the mutants characterised had a reduction in seed set, which implies that these genes are required for normal fertility. Analysis of GUS reporter lines revealed overlapping spatial and temporal expression patterns for some of the aquaporins. The expression of certain aquaporins in floral organs just before anthesis, combined with changes to stamen, petal and pistil lengths in some of the mutant lines, suggests that they facilitate water transport for organ expansion. Expanding the analysis of GUS reporter lines and correlating this with the characterisation of relevant mutants, would help to elucidate gene function. For example, *PIP1;5* and *PIP2;7* had specific expression in the petals/sepals and anther filaments of open flowers respectively. Analysis of the lengths of petals, sepals and filaments in the respective mutant backgrounds may reveal changes. As aquaporin single mutant phenotypes are often masked under normal conditions, it may be necessary to make multiple mutants. If genes are closely positioned on a chromosome it will not be possible to generate multiple T-DNA insertion mutants, but RNAi silencing could be used as an alternative. Generating double and triple mutants for *PIP2;1*, *PIP2;2* and *PIP2;3* would be interesting, as these are all genes which are upregulated during bud stage 4. As these genes are phylogenetically close (figure 3.5), they may overlap in function. Using reporter lines to compare the expression patterns of *PIP2;2* and *PIP2;3* against *PIP2;1* would be of interest.

The physiological roles of *SUC2* and *SUC5* have been characterised in the phloem and endosperm respectively. Both genes are required for normal fertility, however their function in flowers remains unclear. It is possible that the *Arabidopsis* aquaporins and sucrose transporters function co-operatively in floral organs to control water flow. Stadler et al. localised the SUC1 protein to a ring of cells surrounding the connective tissue and this complements *PIP2;1* expression in the connective tissue surrounding the vascular bundle (figure 3.12) (Stadler et al., 1999). It may be useful to expand the analysis to include other sucrose transporters expressed in flowers (*SUC3/SUC8/SUC9*), in order to generate a comprehensive overview of gene expression patterns.

6.5.2 Establishing the importance of water loss via evaporation for anther opening

Stomatal number and patterning on anthers was characterised for *Arabidopsis* lines with altered stomatal density. Some organ specific differences were observed (section 5.3.1) and lines which had occluded stomata or no anther stomata had reduced fertility (section 5.3.2). In order to establish whether anther stomata facilitate water loss via evaporation, it would be useful to establish the rate of stomatal conductance from anthers with varying numbers of stomata. Infrared thermography has been used as a proxy measure of transpiration rates in leaves, as transpiration causes evaporative cooling (Hunt et al., 2017). It would be interesting to know if anthers are hotter under humid conditions as this could impact pollen development and explain the observed reduction in pollen viability (section 5.3.4). It may be difficult to visualise temperature changes with a thermal camera because *Arabidopsis* flowers are so small. Alternative options could be to use a thermocouple or look for expression changes in heat stress induced genes. For measurements of leaf gas exchange a leaf cuvette attached to an Infra-red gas analyser (IRGA) is usually used, but systems with multiple whole plant chambers are also available (Kölling et al., 2015). To measure

gas exchange from flowers, flowering stems of *Arabidopsis* lines with varying stomatal density could be chambered separately and then compared.

Anther dehiscence was delayed under conditions of high humidity (section 5.3.4). It would be interesting to analyse whether stomatal development in wild type anthers is influenced by the environment, as this can occur in leaves. It is tempting to speculate that plants could fine tune the timing of dehiscence in response to environmental conditions via the anther stomata. *Arabidopsis* plants overexpressing *EPF2* had delayed dehiscence and reduced seed set, and wheat plants overexpressing the wheat homologue also had reduced grain yield (section 5.3.3). Investigating the timing of dehiscence in *TaEPFL1* plants would help to clarify why plants overexpressing *EPF2* have reduced fertility.

6.6 Conclusion

Many *Arabidopsis* aquaporins and sucrose transporters genes are expressed during the later stages of pollen and anther development. Mutants from both gene families showed a reduction in seed set, however no changes to pollen viability or dehiscence were detected. Analysis of GUS reporter lines revealed overlapping temporal and spatial expression patterns for certain aquaporins in floral organs. The expression patterns identified suggest that different aquaporin isoforms enhance hydraulic conductivity in different parts of the flower, which may facilitate water transport required for petal and filament extension and anther dehiscence. It is possible that sucrose transporters create osmotic gradients required to drive the movement of water through floral organs, and changes to floral organ lengths were observed in both aquaporin and sucrose transporter mutants. Further analysis of gene expression patterns and characterisation of mutant phenotypes, should help to elucidate the exact function of aquaporins and sucrose transporters in *Arabidopsis* flowers.

Arabidopsis mutants with altered stomatal development were characterised. Plants which had occluded stomata or no anther stomata had reduced fertility and plants overexpressing *EPF2* and *EPFL7* had delayed dehiscence. Wheat plants overexpressing the wheat homologue of *EPF2* also had reduced grain yield. Dehiscence was delayed under conditions of high humidity and the *EPF2 OE* line, which has no anther stomata, was most severely affected. These results suggest that water loss via evaporation is facilitated by anther stomata and that this is pivotal to anther opening in *Arabidopsis*. Reducing stomatal density to improve agronomic traits such as WUE should be treated cautiously, as these may be counterbalanced by negative effects to fertility. Targeting modifications to the leaf stomata only could be a solution, and continuing research in different species will help to further understanding.

REFERENCES

Abrash, E.B., and Bergmann, D.C. (2010). Regional specification of stomatal production by the putative ligand CHALLAH. Dev. Camb. Engl. *137*, 447–455.

Albrecht, C., Russinova, E., Hecht, V., Baaijens, E., and de Vries, S. (2005). The Arabidopsis thaliana SOMATIC EMBRYOGENESIS RECEPTOR-LIKE KINASES1 and 2 Control Male Sporogenesis. Plant Cell *17*, 3337–3349.

Alexander, M.P. (1969). Differential staining of aborted and nonaborted pollen. Stain Technol. *44*, 117–122.

Alexandersson, E., Fraysse, L., Sjövall-Larsen, S., Gustavsson, S., Fellert, M., Karlsson, M., Johanson, U., and Kjellbom, P. (2005). Whole gene family expression and drought stress regulation of aquaporins. Plant Mol. Biol. *59*, 469–484.

Alonso, J.M., Stepanova, A.N., Leisse, T.J., Kim, C.J., Chen, H., Shinn, P., Stevenson, D.K., Zimmerman, J., Barajas, P., Cheuk, R., et al. (2003). Genome-wide insertional mutagenesis of Arabidopsis thaliana. Science *301*, 653–657.

Alves-Ferreira, M., Wellmer, F., Banhara, A., Kumar, V., Riechmann, J.L., and Meyerowitz, E.M. (2007). Global expression profiling applied to the analysis of Arabidopsis stamen development. Plant Physiol. *145*, 747–762.

Ariizumi, T., and Toriyama, K. (2011). Genetic regulation of sporopollenin synthesis and pollen exine development. Annu. Rev. Plant Biol. *62*, 437–460.

Aschan, G., and Pfanz, H. (2003). Non-foliar photosynthesis – a strategy of additional carbon acquisition. Flora - Morphol. Distrib. Funct. Ecol. Plants *198*, 81–97.

Bassil, E., Tajima, H., Liang, Y.-C., Ohto, M.-A., Ushijima, K., Nakano, R., Esumi, T., Coku, A., Belmonte, M., and Blumwald, E. (2011). The Arabidopsis Na+/H+ antiporters NHX1 and NHX2 control vacuolar pH and K+ homeostasis to regulate growth, flower development, and reproduction. Plant Cell *23*, 3482–3497.

Baud, S., Wuillème, S., Lemoine, R., Kronenberger, J., Caboche, M., Lepiniec, L., and Rochat, C. (2005). The AtSUC5 sucrose transporter specifically expressed in the endosperm is involved in early seed development in Arabidopsis. Plant J. Cell Mol. Biol. *43*, 824–836.

Beals, T.P., and Goldberg, R.B. (1997). A novel cell ablation strategy blocks tobacco anther dehiscence. Plant Cell *9*, 1527–1545.

Beauzamy, L., Nakayama, N., and Boudaoud, A. (2014). Flowers under pressure: ins and outs of turgor regulation in development. Ann. Bot. *114*, 1517–1533.

Beebo, A., Thomas, D., Der, C., Sanchez, L., Leborgne-Castel, N., Marty, F., Schoefs, B., and Bouhidel, K. (2009). Life with and without AtTIP1;1, an Arabidopsis aquaporin preferentially localized in the apposing tonoplasts of adjacent vacuoles. Plant Mol. Biol. *70*, 193–209.

Berger, D., and Altmann, T. (2000). A subtilisin-like serine protease involved in the regulation of stomatal density and distribution in Arabidopsis thaliana. Genes Dev. *14*, 1119–1131.

Bergmann, D.C., and Sack, F.D. (2007). Stomatal development. Annu. Rev. Plant Biol. *58*, 163–181.

Bernhardt, P. (1996). The anther, form, function and phylogeny. (Cambridge: Cambridge University Press).

Bhave, N.S., Veley, K.M., Nadeau, J.A., Lucas, J.R., Bhave, S.L., and Sack, F.D. (2009). TOO MANY MOUTHS promotes cell fate progression in stomatal development of Arabidopsis stems. Planta *229*, 357–367.

Bianchini, M., and Pacini, E. (1996). Explosive Anther Dehiscence in Ricinus communis L. Involves Cell Wall Modifications and Relative Humidity. Int. J. Plant Sci. *157*, 739–745.

Bonner, L.J., and Dickinson, H.G. (1989). Anther dehiscence in Lycopersicon esculentum Mill. I. Structural aspects. New Phytol. *113*, 97–115.

Bonner, L.J., and Dickinson, H.G. (1990). Anther dehiscence in Lycopersicon esculentum. New Phytol. *115*, 367–375.

Bots, M., Vergeldt, F., Wolters-Arts, M., Weterings, K., van As, H., and Mariani, C. (2005a). Aquaporins of the PIP2 Class Are Required for Efficient Anther Dehiscence in Tobacco. Plant Physiol. *137*, 1049–1056.

Bots, M., Feron, R., Uehlein, N., Weterings, K., Kaldenhoff, R., and Mariani, T. (2005b). PIP1 and PIP2 aquaporins are differentially expressed during tobacco anther and stigma development. J. Exp. Bot. *56*, 113–121.

Boudichevskaia, A., Heckwolf, M., and Kaldenhoff, R. (2015a). T-DNA insertion in aquaporin gene AtPIP1;2 generates transcription profiles reminiscent of a low CO2 response. Plant Cell Environ. *38*, 2286–2298.

Boudichevskaia, A., Heckwolf, M., Althaus, L., and Kaldenhoff, R. (2015b). Transcriptome analysis of the aquaporin AtPIP1;2 deficient line in Arabidopsis thaliana. Genomics Data *4*, 162–164.

Boyes, D.C., Zayed, A.M., Ascenzi, R., McCaskill, A.J., Hoffman, N.E., Davis, K.R., and Görlach, J. (2001). Growth stage-based phenotypic analysis of Arabidopsis: a model for high throughput functional genomics in plants. Plant Cell *13*, 1499–1510.

Brocard-Gifford, I., Lynch, T.J., Garcia, M.E., Malhotra, B., and Finkelstein, R.R. (2004). The Arabidopsis thaliana ABSCISIC ACID-INSENSITIVE8 Locus Encodes a Novel Protein Mediating Abscisic Acid and Sugar Responses Essential for Growth. Plant Cell *16*, 406–421.

Bush, D.R. (1993). Proton-Coupled Sugar and Amino Acid Transporters in Plants. Annu. Rev. Plant Physiol. Plant Mol. Biol. *44*, 513–542.

Bush, S.M., and Krysan, P.J. (2007). Mutational evidence that the Arabidopsis MAP kinase MPK6 is involved in anther, inflorescence, and embryo development. J. Exp. Bot. *58*, 2181–2191.

Canales, C., Bhatt, A.M., Scott, R., and Dickinson, H. (2002). EXS, a putative LRR receptor kinase, regulates male germline cell number and tapetal identity and promotes seed development in Arabidopsis. Curr. Biol. CB *12*, 1718–1727.

Carrizo García, C., Matesevach, M., and Barboza, G. (2008). Features related to anther opening in Solanum species (Solanaceae). Bot. J. Linn. Soc. *158*, 344–354.

Casson, S., and Gray, J.E. (2008). Influence of environmental factors on stomatal development. New Phytol. *178*, 9–23.

Casson, S.A., and Hetherington, A.M. (2010). Environmental regulation of stomatal development. Curr. Opin. Plant Biol. *13*, 90–95.

Causier, B., Schwarz-Sommer, Z., and Davies, B. (2010). Floral organ identity: 20 years of ABCs. Semin. Cell Dev. Biol. *21*, 73–79.

Cecchetti, V., Altamura, M.M., Falasca, G., Costantino, P., and Cardarelli, M. (2008). Auxin regulates Arabidopsis anther dehiscence, pollen maturation, and filament elongation. Plant Cell *20*, 1760–1774.

Cecchetti, V., Altamura, M.M., Brunetti, P., Petrocelli, V., Falasca, G., Ljung, K., Costantino, P., and Cardarelli, M. (2013). Auxin controls Arabidopsis anther dehiscence by regulating endothecium lignification and jasmonic acid biosynthesis. Plant J. Cell Mol. Biol. *74*, 411–422.

Chaumont, F., and Tyerman, S.D. (2014). Aquaporins: highly regulated channels controlling plant water relations. Plant Physiol. *164*, 1600–1618.

Chaumont, F., Moshelion, M., and Daniels, M.J. (2005). Regulation of plant aquaporin activity. Biol. Cell *97*, 749–764.

Chen, L.-Q., Qu, X.-Q., Hou, B.-H., Sosso, D., Osorio, S., Fernie, A.R., and Frommer, W.B. (2012). Sucrose efflux mediated by SWEET proteins as a key step for phloem transport. Science *335*, 207–211.

Cheng, H., Song, S., Xiao, L., Soo, H.M., Cheng, Z., Xie, D., and Peng, J. (2009). Gibberellin acts through jasmonate to control the expression of MYB21, MYB24, and MYB57 to promote stamen filament growth in Arabidopsis. PLoS Genet. *5*, e1000440.

Cheng, Y., Dai, X., and Zhao, Y. (2006). Auxin biosynthesis by the YUCCA flavin monooxygenases controls the formation of floral organs and vascular tissues in Arabidopsis. Genes Dev. *20*, 1790–1799.

Choi, W.-G., and Roberts, D.M. (2007). Arabidopsis NIP2;1, a major intrinsic protein transporter of lactic acid induced by anoxic stress. J. Biol. Chem. *282*, 24209–24218.

Colcombet, J., Boisson-Dernier, A., Ros-Palau, R., Vera, C.E., and Schroeder, J.I. (2005). Arabidopsis SOMATIC EMBRYOGENESIS RECEPTOR KINASES1 and 2 are essential for tapetum development and microspore maturation. Plant Cell *17*, 3350–3361.

Daloso, D.M., Dos Anjos, L., and Fernie, A.R. (2016). Roles of sucrose in guard cell regulation. New Phytol. *211*, 809–818.

Dawson, J., Sözen, E., Vizir, I., Van Waeyenberge, S., Wilson, Z.A., and Mulligan, B.J. (1999). Characterization and genetic mapping of a mutation (ms35) which prevents anther dehiscence in Arabidopsis thaliana by affecting secondary wall thickening in the endothecium. New Phytol. *144*, 213–222.

Di Giorgio, J.A.P., Bienert, G.P., Ayub, N.D., Yaneff, A., Barberini, M.L., Mecchia, M.A., Amodeo, G., Soto, G.C., and Muschietti, J.P. (2016). Pollen-Specific Aquaporins NIP4;1 and NIP4;2 Are Required for Pollen Development and Pollination in Arabidopsis thaliana. Plant Cell *28*, 1053–1077.

Doheny-Adams, T., Hunt, L., Franks, P.J., Beerling, D.J., and Gray, J.E. (2012). Genetic manipulation of stomatal density influences stomatal size, plant growth and tolerance to restricted water supply across a growth carbon dioxide gradient. Philos. Trans. R. Soc. B Biol. Sci. *367*, 547–555.

Dong, J., MacAlister, C.A., and Bergmann, D.C. (2009). BASL controls asymmetric cell division in Arabidopsis. Cell *137*, 1320–1330.

Doorn, V., G, W., and van Meeteren, U. (2003). Flower opening and closure: a review. J. Exp. Bot. *54*, 1801–1812.

Endler, A., Meyer, S., Schelbert, S., Schneider, T., Weschke, W., Peters, S.W., Keller, F., Baginsky, S., Martinoia, E., and Schmidt, U.G. (2006). Identification of a vacuolar sucrose transporter in barley and Arabidopsis mesophyll cells by a tonoplast proteomic approach. Plant Physiol. *141*, 196–207.

Feng, X., and Dickinson, H.G. (2010). Cell-cell interactions during patterning of the Arabidopsis anther. Biochem. Soc. Trans. *38*, 571–576.

Feng, B., Lu, D., Ma, X., Peng, Y., Sun, Y., Ning, G., and Ma, H. (2012). Regulation of the Arabidopsis anther transcriptome by DYT1 for pollen development. Plant J. Cell Mol. Biol. *72*, 612–624.

Ferguson, A.C., Pearce, S., Band, L.R., Yang, C., Ferjentsikova, I., King, J., Yuan, Z., Zhang, D., and Wilson, Z.A. (2017). Biphasic regulation of the transcription factor ABORTED MICROSPORES (AMS) is essential for tapetum and pollen development in Arabidopsis. New Phytol. *213*, 778–790.

Fetter, K., Van Wilder, V., Moshelion, M., and Chaumont, F. (2004). Interactions between plasma membrane aquaporins modulate their water channel activity. Plant Cell *16*, 215–228.

Feuerstein, A., Niedermeier, M., Bauer, K., Engelmann, S., Hoth, S., Stadler, R., and Sauer, N. (2010). Expression of the AtSUC1 gene in the female gametophyte, and ecotype-specific expression differences in male reproductive organs. Plant Biol. Stuttg. Ger. *12 Suppl 1*, 105–114.

Feys, B.J.F., Benedetti, C.E., Penfold, C.N., and Turner, J.G. (1994). Arabidopsis Mutants Selected for Resistance to the Phytotoxin Coronatine Are Male Sterile, Insensitive to Methyl Jasmonate, and Resistant to a Bacterial Pathogen. Plant Cell *6*, 751–759.

Firon, N., Nepi, M., and Pacini, E. (2012). Water status and associated processes mark critical stages in pollen development and functioning. Ann. Bot. *109*, 1201–1214.

Franks, P.J., W Doheny-Adams, T., Britton-Harper, Z.J., and Gray, J.E. (2015). Increasing water-use efficiency directly through genetic manipulation of stomatal density. New Phytol. *207*, 188–195.

Gao, X.-Q., Li, C.-G., Wei, P.-C., Zhang, X.-Y., Chen, J., and Wang, X.-C. (2005). The Dynamic Changes of Tonoplasts in Guard Cells Are Important for Stomatal Movement in Vicia faba. Plant Physiol. *139*, 1207–1216.

García, C.C., Nepi, M., and Pacini, E. (2006). Structural aspects and ecophysiology of anther opening in Allium triquetrum. Ann. Bot. *97*, 521–527.

Garrett, J.J.T., Meents, M.J., Blackshaw, M.T., Blackshaw, L.C., Hou, H., Styranko, D.M., Kohalmi, S.E., and Schultz, E.A. (2012). A novel, semi-dominant allele of MONOPTEROS provides insight into leaf initiation and vein pattern formation. Planta *236*, 297–312.

Ge, Y.X., Angenent, G.C., Wittich, P.E., Peters, J., Franken, J., Busscher, M., Zhang, L.M., Dahlhaus, E., Kater, M.M., Wullems, G.J., et al. (2000). NEC1, a novel gene, highly expressed in nectary tissue of Petunia hybrida. Plant J. Cell Mol. Biol. *24*, 725–734.

Ge, Y.X., Angenent, G.C., Dahlhaus, E., Franken, J., Peters, J., Wullems, G.J., and Creemers-Molenaar, J. (2001). Partial silencing of the NEC1 gene results in early opening of anthers in Petunia hybrida. Mol. Genet. Genomics MGG *265*, 414–423.

Geisler, M., Yang, M., and Sack, F.D. (1998). Divergent regulation of stomatal initiation and patterning in organ and suborgan regions of the Arabidopsis mutants too many mouths and four lips. Planta *205*, 522–530.

Geisler, M., Nadeau, J., and Sack, F.D. (2000). Oriented asymmetric divisions that generate the stomatal spacing pattern in arabidopsis are disrupted by the too many mouths mutation. Plant Cell *12*, 2075–2086.

Giorgio, J.A.P.D., Barberini, M.L., Amodeo, G., and Muschietti, J.P. (2016). Pollen aquaporins: What are they there for? Plant Signal. Behav. *11*, e1217375.

Goldberg, R.B., Beals, T.P., and Sanders, P.M. (1993). Anther development: basic principles and practical applications. Plant Cell *5*, 1217–1229.

Gong, X., Liu, M., Zhang, L., Ruan, Y., Ding, R., Ji, Y., Zhang, N., Zhang, S., Farmer, J., and Wang, C. (2015). Arabidopsis AtSUC2 and AtSUC4, encoding sucrose transporters, are required for abiotic stress tolerance in an ABA-dependent pathway. Physiol. Plant. *153*, 119–136.

Gottwald, J.R., Krysan, P.J., Young, J.C., Evert, R.F., and Sussman, M.R. (2000). Genetic evidence for the in planta role of phloem-specific plasma membrane sucrose transporters. Proc. Natl. Acad. Sci. U. S. A. *97*, 13979–13984.

Gray, J.E., Holroyd, G.H., van der Lee, F.M., Bahrami, A.R., Sijmons, P.C., Woodward, F.I., Schuch, W., and Hetherington, A.M. (2000). The HIC signalling pathway links CO2 perception to stomatal development. Nature *408*, 713–716.

Grondin, A., Rodrigues, O., Verdoucq, L., Merlot, S., Leonhardt, N., and Maurel, C. (2015). Aquaporins Contribute to ABA-Triggered Stomatal Closure through OST1-Mediated Phosphorylation. Plant Cell *27*, 1945–1954.

Gu, J.-N., Zhu, J., Yu, Y., Teng, X.-D., Lou, Y., Xu, X.-F., Liu, J.-L., and Yang, Z.-N. (2014). DYT1 directly regulates the expression of TDF1 for tapetum development and pollen wall formation in Arabidopsis. Plant J. Cell Mol. Biol. *80*, 1005–1013.

Hachez, C., Zelazny, E., and Chaumont, F. (2006). Modulating the expression of aquaporin genes in planta: A key to understand their physiological functions? Biochim. Biophys. Acta *1758*, 1142–1156.

Hara, K., Kajita, R., Torii, K.U., Bergmann, D.C., and Kakimoto, T. (2007). The secretory peptide gene EPF1 enforces the stomatal one-cell-spacing rule. Genes Dev. *21*, 1720–1725.

Hara, K., Yokoo, T., Kajita, R., Onishi, T., Yahata, S., Peterson, K.M., Torii, K.U., and Kakimoto, T. (2009). Epidermal cell density is autoregulated via a secretory peptide, EPIDERMAL PATTERNING FACTOR 2 in Arabidopsis leaves. Plant Cell Physiol. *50*, 1019–1031.

Heckwolf, M., Pater, D., Hanson, D.T., and Kaldenhoff, R. (2011). The Arabidopsis thaliana aquaporin AtPIP1;2 is a physiologically relevant CO_2 transport facilitator. Plant J. Cell Mol. Biol. *67*, 795–804.

Heinen, R.B., Bienert, G.P., Cohen, D., Chevalier, A.S., Uehlein, N., Hachez, C., Kaldenhoff, R., Thiec, D.L., and Chaumont, F. (2014). Expression and characterization of plasma membrane aquaporins in stomatal complexes of Zea mays. Plant Mol. Biol. *86*, 335–350.

Hepworth, C., Doheny-Adams, T., Hunt, L., Cameron, D.D., and Gray, J.E. (2015). Manipulating stomatal density enhances drought tolerance without deleterious effect on nutrient uptake. New Phytol. *208*, 336–341.

Heslop-Harrison, J., and Heslop-Harrison, Y. (1970). Evaluation of pollen viability by enzymatically induced fluorescence; intracellular hydrolysis of fluorescein diacetate. Stain Technol. *45*, 115–120.

Hord, C.L.H., Chen, C., Deyoung, B.J., Clark, S.E., and Ma, H. (2006). The BAM1/BAM2 receptor-like kinases are important regulators of Arabidopsis early anther development. Plant Cell *18*, 1667–1680.

Hord, C.L.H., Sun, Y.-J., Pillitteri, L.J., Torii, K.U., Wang, H., Zhang, S., and Ma, H. (2008). Regulation of Arabidopsis early anther development by the mitogen-activated protein kinases, MPK3 and MPK6, and the ERECTA and related receptor-like kinases. Mol. Plant *1*, 645–658.

Hoth, S., Niedermeier, M., Feuerstein, A., Hornig, J., and Sauer, N. (2010). An ABA-responsive element in the AtSUC1 promoter is involved in the regulation of AtSUC1 expression. Planta *232*, 911–923.

Huang, J., Zhang, T., Linstroth, L., Tillman, Z., Otegui, M.S., Owen, H.A., and Zhao, D. (2016). Control of Anther Cell Differentiation by the Small Protein Ligand TPD1 and Its Receptor EMS1 in Arabidopsis. PLoS Genet. *12*, e1006147.

Hunt, L., and Gray, J.E. (2009). The signaling peptide EPF2 controls asymmetric cell divisions during stomatal development. Curr. Biol. CB *19*, 864–869.

Hunt, L., and Gray, J.E. (2010). BASL and EPF2 act independently to regulate asymmetric divisions during stomatal development. Plant Signal. Behav. *5*, 278–280.

Hunt, L., Bailey, K.J., and Gray, J.E. (2010). The signalling peptide EPFL9 is a positive regulator of stomatal development. New Phytol. *186*, 609–614.

Hunt, L., Amsbury, S., Baillie, A., Movahedi, M., Mitchell, A., Afsharinafar, M., Swarup, K., Denyer, T., Hobbs, J.K., Swarup, R., et al. (2017). Formation of the Stomatal Outer Cuticular Ledge Requires a Guard Cell Wall Proline-Rich Protein. Plant Physiol. *174*, 689–699.

Ichimura, K., Mizoguchi, T., Yoshida, R., Yuasa, T., and Shinozaki, K. (2000). Various abiotic stresses rapidly activate Arabidopsis MAP kinases ATMPK4 and ATMPK6. Plant J. Cell Mol. Biol. *24*, 655–665.

Ishiguro, S., Kawai-Oda, A., Ueda, J., Nishida, I., and Okada, K. (2001). The DEFECTIVE IN ANTHER DEHISCENCE1 Gene Encodes a Novel Phospholipase A1 Catalyzing the Initial Step of Jasmonic Acid Biosynthesis, Which Synchronizes Pollen Maturation, Anther Dehiscence, and Flower Opening in Arabidopsis. Plant Cell *13*, 2191–2210.

Ishikawa, F., Suga, S., Uemura, T., Sato, M.H., and Maeshima, M. (2005). Novel type aquaporin SIPs are mainly localized to the ER membrane and show cell-specific expression in Arabidopsis thaliana. FEBS Lett. *579*, 5814–5820.

Ito, T., and Shinozaki, K. (2002). The MALE STERILITY1 gene of Arabidopsis, encoding a nuclear protein with a PHD-finger motif, is expressed in tapetal cells and is required for pollen maturation. Plant Cell Physiol. *43*, 1285–1292.

Ito, T., Nagata, N., Yoshiba, Y., Ohme-Takagi, M., Ma, H., and Shinozaki, K. (2007a). Arabidopsis MALE STERILITY1 encodes a PHD-type transcription factor and regulates pollen and tapetum development. Plant Cell *19*, 3549–3562.

Ito, T., Ng, K.-H., Lim, T.-S., Yu, H., and Meyerowitz, E.M. (2007b). The homeotic protein AGAMOUS controls late stamen development by regulating a jasmonate biosynthetic gene in Arabidopsis. Plant Cell *19*, 3516–3529.

Iwano, M., Entani, T., Shiba, H., Takayama, S., and Isogai, A. (2004). Calcium crystals in the anther of Petunia: the existence and biological significance in the pollination process. Plant Cell Physiol. *45*, 40–47.

Jang, J.Y., Kim, D.G., Kim, Y.O., Kim, J.S., and Kang, H. (2004). An Expression Analysis of a Gene Family Encoding Plasma Membrane Aquaporins in Response to Abiotic Stresses in Arabidopsis Thaliana. Plant Mol. Biol. *54*, 713–725.

Jang, J.Y., Lee, S.H., Rhee, J.Y., Chung, G.C., Ahn, S.J., and Kang, H. (2007). Transgenic Arabidopsis and tobacco plants overexpressing an aquaporin respond differently to various abiotic stresses. Plant Mol. Biol. *64*, 621–632.

Jia, G., Liu, X., Owen, H.A., and Zhao, D. (2008). Signaling of cell fate determination by the TPD1 small protein and EMS1 receptor kinase. Proc. Natl. Acad. Sci. U. S. A. *105*, 2220–2225.

Jiang, J., Zhang, Z., and Cao, J. (2013). Pollen wall development: the associated enzymes and metabolic pathways. Plant Biol. Stuttg. Ger. *15*, 249–263.

Johansson, I., Karlsson, M., Shukla, V.K., Chrispeels, M.J., Larsson, C., and Kjellbom, P. (1998). Water transport activity of the plasma membrane aquaporin PM28A is regulated by phosphorylation. Plant Cell *10*, 451–459.

Kamiya, T., Tanaka, M., Mitani, N., Ma, J.F., Maeshima, M., and Fujiwara, T. (2009). NIP1;1, an aquaporin homolog, determines the arsenite sensitivity of Arabidopsis thaliana. J. Biol. Chem. *284*, 2114–2120.

Kanno, Y., Oikawa, T., Chiba, Y., Ishimaru, Y., Shimizu, T., Sano, N., Koshiba, T., Kamiya, Y., Ueda, M., and Seo, M. (2016). AtSWEET13 and AtSWEET14 regulate gibberellin-mediated physiological processes. Nat. Commun. *7*, ncomms13245.

Katsuhara, M., Hanba, Y.T., Shiratake, K., and Maeshima, M. (2008). Expanding roles of plant aquaporins in plasma membranes and cell organelles. Funct. Plant Biol. *35*, 1–14.

Keijzer, C.J. (1987). The Processes of Anther Dehiscence and Pollen Dispersal. New Phytol. *105*, 487–498.

Keijzer, C.J., Hoek, I.H.S., and Willeemse, M.T.M. (1987). The Processes of Anther Dehiscence and Pollen Dispersal Iii. the Dehydration of the Filament Tip and the Anther in Three Monocotyledonous Species. New Phytol. *106*, 281–287.

Keijzer, C.J., Klooster, H.B.L.-T., and Reinders, M.C. (1996). The Mechanics of the Grass Flower: Anther Dehiscence and Pollen Shedding in Maize. Ann. Bot. *1*, 15–21.

Kepinski, S., and Leyser, O. (2002). Ubiquitination and Auxin Signaling. Plant Cell *14*, s81–s95.

Khatun, S., and Flowers, T.J. (1995). The estimation of pollen viability in rice. J. Exp. Bot. *46*, 151–154.

Kim, Y.Y., Jung, K.W., Jeung, J.U., and Shin, J.S. (2012). A novel F-box protein represses endothecial secondary wall thickening for anther dehiscence in Arabidopsis thaliana. J. Plant Physiol. *169*, 212–216.

Kissen, R., Hyldbakk, E., Wang, C.-W.V., Sørmo, C.G., Rossiter, J.T., and Bones, A.M. (2012). Ecotype dependent expression and alternative splicing of epithiospecifier protein (ESP) in Arabidopsis thaliana. Plant Mol. Biol. *78*, 361–375.

Kline, K.G., Barrett-Wilt, G.A., and Sussman, M.R. (2010). In planta changes in protein phosphorylation induced by the plant hormone abscisic acid. Proc. Natl. Acad. Sci. U. S. A. *107*, 15986–15991.

Kölling, K., George, G.M., Künzli, R., Flütsch, P., and Zeeman, S.C. (2015). A whole-plant chamber system for parallel gas exchange measurements of Arabidopsis and other herbaceous species. Plant Methods *11*, 48.

Kondo, T., Kajita, R., Miyazaki, A., Hokoyama, M., Nakamura-Miura, T., Mizuno, S., Masuda, Y., Irie, K., Tanaka, Y., Takada, S., et al. (2010). Stomatal density is controlled by a mesophyll-derived signaling molecule. Plant Cell Physiol. *51*, 1–8.

Koressaar, T., and Remm, M. (2007). Enhancements and modifications of primer design program Primer3. Bioinforma. Oxf. Engl. *23*, 1289–1291.

Larkin, M.A., Blackshields, G., Brown, N.P., Chenna, R., McGettigan, P.A., McWilliam, H., Valentin, F., Wallace, I.M., Wilm, A., Lopez, R., et al. (2007). Clustal W and Clustal X version 2.0. Bioinforma. Oxf. Engl. *23*, 2947–2948.

Li, L., Wang, H., Gago, J., Cui, H., Qian, Z., Kodama, N., Ji, H., Tian, S., Shen, D., Chen, Y., et al. (2015). Harpin Hpa1 Interacts with Aquaporin PIP1;4 to Promote the Substrate Transport and Photosynthesis in Arabidopsis. Sci. Rep. *5*, 17207.

Li, T., Choi, W.-G., Wallace, I.S., Baudry, J., and Roberts, D.M. (2011a). Arabidopsis thaliana NIP7;1: an anther-specific boric acid transporter of the aquaporin superfamily regulated by an unusual tyrosine in helix 2 of the transport pore. Biochemistry (Mosc.) *50*, 6633–6641.

Li, X., Wang, X., Yang, Y., Li, R., He, Q., Fang, X., Luu, D.-T., Maurel, C., and Lin, J. (2011b). Single-molecule analysis of PIP2;1 dynamics and partitioning reveals multiple modes of Arabidopsis plasma membrane aquaporin regulation. Plant Cell *23*, 3780–3797.

Longin, C.F.H., Mühleisen, J., Maurer, H.P., Zhang, H., Gowda, M., and Reif, J.C. (2012). Hybrid breeding in autogamous cereals. TAG Theor. Appl. Genet. Theor. Angew. Genet. *125*, 1087–1096.

Ludwig, A., Stolz, J., and Sauer, N. (2000). Plant sucrose-H+ symporters mediate the transport of vitamin H. Plant J. Cell Mol. Biol. *24*, 503–509.

Luu, D.-T., and Maurel, C. (2013). Aquaporin trafficking in plant cells: an emerging membrane-protein model. Traffic *14*, 629–635.

Ma, H. (2005). Molecular genetic analyses of microsporogenesis and microgametogenesis in flowering plants. Annu. Rev. Plant Biol. *56*, 393–434.

Ma, S., Quist, T.M., Ulanov, A., Joly, R., and Bohnert, H.J. (2004). Loss of TIP1;1 aquaporin in Arabidopsis leads to cell and plant death. Plant J. Cell Mol. Biol. *40*, 845–859.

von Malek, B., van der Graaff, E., Schneitz, K., and Keller, B. (2002). The Arabidopsis male-sterile mutant dde2-2 is defective in the ALLENE OXIDE SYNTHASE gene encoding one of the key enzymes of the jasmonic acid biosynthesis pathway. Planta *216*, 187–192.

Mandaokar, A., and Browse, J. (2009). MYB108 acts together with MYB24 to regulate jasmonate-mediated stamen maturation in Arabidopsis. Plant Physiol. *149*, 851–862.

Mandaokar, A., Thines, B., Shin, B., Lange, B.M., Choi, G., Koo, Y.J., Yoo, Y.J., Choi, Y.D., Choi, G., and Browse, J. (2006). Transcriptional regulators of stamen development in Arabidopsis identified by transcriptional profiling. Plant J. Cell Mol. Biol. *46*, 984–1008.

Mao, Z., and Sun, W. (2015). Arabidopsis seed-specific vacuolar aquaporins are involved in maintaining seed longevity under the control of ABSCISIC ACID INSENSITIVE 3. J. Exp. Bot. *66*, 4781–4794.

Martre, P., Morillon, R., Barrieu, F., North, G.B., Nobel, P.S., and Chrispeels, M.J. (2002). Plasma membrane aquaporins play a significant role during recovery from water deficit. Plant Physiol. *130*, 2101–2110.

Matsui, T., Omasa, K., and Horie, T. (1999a). Rapid Swelling of Pollen Grains in Response to Floret Opening Unfolds Anther Locules in Rice (Oryza sativa L.). Plant Prod. Sci. *2*, 196–199.

Matsui, T., Omasa, K., and Horie, T. (1999b). Mechanism of Anther Dehiscence in Rice (Oryza sativa L.). Ann. Bot. *84*, 501–506.

Matsui, T., Omasa, K., and Horie, T. (2000). Rapid Swelling of Pollen Grains in the Dehiscing Anther of Two-rowed Barley (Hordeum distichum L. emend. L AM .). Ann. Bot. *85*, 345–350.

Maurel, C. (2007). Plant aquaporins: novel functions and regulation properties. FEBS Lett. *581*, 2227–2236.

Maurel, C., Kado, R.T., Guern, J., and Chrispeels, M.J. (1995). Phosphorylation regulates the water channel activity of the seed-specific aquaporin alpha-TIP. EMBO J. *14*, 3028–3035.

Maurel, C., Verdoucq, L., Luu, D.-T., and Santoni, V. (2008). Plant aquaporins: membrane channels with multiple integrated functions. Annu. Rev. Plant Biol. *59*, 595–624.

McConn, M., and Browse, J. (1996). The Critical Requirement for Linolenic Acid Is Pollen Development, Not Photosynthesis, in an Arabidopsis Mutant. Plant Cell *8*, 403–416.

Meyer, S., Melzer, M., Truernit, E., Hümmer, C., Besenbeck, R., Stadler, R., and Sauer, N. (2000). AtSUC3, a gene encoding a new Arabidopsis sucrose transporter, is expressed in cells adjacent to the vascular tissue and in a carpel cell layer. Plant J. Cell Mol. Biol. *24*, 869–882.

Meyer, S., Lauterbach, C., Niedermeier, M., Barth, I., Sjolund, R.D., and Sauer, N. (2004). Wounding enhances expression of AtSUC3, a sucrose transporter from Arabidopsis sieve elements and sink tissues. Plant Physiol. *134*, 684–693.

Mitsuda, N., Seki, M., Shinozaki, K., and Ohme-Takagi, M. (2005). The NAC transcription factors NST1 and NST2 of Arabidopsis regulate secondary wall thickenings and are required for anther dehiscence. Plant Cell *17*, 2993–3006.

Miwa, K., Tanaka, M., Kamiya, T., and Fujiwara, T. (2010). Molecular mechanisms of boron transport in plants: involvement of Arabidopsis NIP5;1 and NIP6;1. Adv. Exp. Med. Biol. *679*, 83–96.

Mizuno, S., Osakabe, Y., Maruyama, K., Ito, T., Osakabe, K., Sato, T., Shinozaki, K., and Yamaguchi-Shinozaki, K. (2007). Receptor-like protein kinase 2 (RPK 2) is a novel factor controlling anther development in Arabidopsis thaliana. Plant J. Cell Mol. Biol. *50*, 751–766.

Mohammed, U. (2017). The improvement of drought tolerance in rice. Thesis. The University of Nottingham.

Morita, S., Sugiyama, S., Tateishi, A., and Satoh, S. (2017). Identification and Characterization of Plasma Membrane Intrinsic Protein (PIP) Aquaporin Genes in Petals of Opening Carnation Flowers. Hortic. J. *86*, 78–86.

Murmu, J., Bush, M.J., DeLong, C., Li, S., Xu, M., Khan, M., Malcolmson, C., Fobert, P.R., Zachgo, S., and Hepworth, S.R. (2010). Arabidopsis basic leucine-zipper transcription factors TGA9 and TGA10 interact with floral glutaredoxins ROXY1 and ROXY2 and are redundantly required for anther development. Plant Physiol. *154*, 1492–1504.

Nagpal, P., Ellis, C.M., Weber, H., Ploense, S.E., Barkawi, L.S., Guilfoyle, T.J., Hagen, G., Alonso, J.M., Cohen, J.D., Farmer, E.E., et al. (2005). Auxin response factors ARF6 and ARF8 promote jasmonic acid production and flower maturation. Dev. Camb. Engl. *132*, 4107–4118.

Nelson, M.R., Band, L.R., Dyson, R.J., Lessinnes, T., Wells, D.M., Yang, C., Everitt, N.M., Jensen, O.E., and Wilson, Z.A. (2012). A biomechanical model of anther opening reveals the roles of dehydration and secondary thickening. New Phytol. *196*, 1030–1037.

O'Brien, M., Bertrand, C., and Matton, D.P. (2002). Characterization of a fertilization-induced and developmentally regulated plasma-membrane aquaporin expressed in reproductive tissues, in the wild potato Solanum chacoense Bitt. Planta *215*, 485–493.

Ohki, S., Takeuchi, M., and Mori, M. (2011). The NMR structure of stomagen reveals the basis of stomatal density regulation by plant peptide hormones. Nat. Commun. *2*, 512.

Pacini, E. (2000). From anther and pollen ripening to pollen presentation. Plant Syst. Evol. *222*, 19–43.

Park, J.-H., Halitschke, R., Kim, H.B., Baldwin, I.T., Feldmann, K.A., and Feyereisen, R. (2002). A knock-out mutation in allene oxide synthase results in male sterility and defective wound signal transduction in Arabidopsis due to a block in jasmonic acid biosynthesis. Plant J. Cell Mol. Biol. *31*, 1–12.

Pearce, S., Ferguson, A., King, J., and Wilson, Z.A. (2015). FlowerNet: a gene expression correlation network for anther and pollen development. Plant Physiol. *167*, 1717–1730.

Peng, Y.-J., Shih, C.-F., Yang, J.-Y., Tan, C.-M., Hsu, W.-H., Huang, Y.-P., Liao, P.-C., and Yang, C.-H. (2013). A RING-type E3 ligase controls anther dehiscence by activating the jasmonate biosynthetic pathway gene DEFECTIVE IN ANTHER DEHISCENCE1 in Arabidopsis. Plant J. Cell Mol. Biol. *74*, 310–327.

Péret, B., Li, G., Zhao, J., Band, L.R., Voß, U., Postaire, O., Luu, D.-T., Da Ines, O., Casimiro, I., Lucas, M., et al. (2012). Auxin regulates aquaporin function to facilitate lateral root emergence. Nat. Cell Biol. *14*, 991–998.

Pillitteri, L.J., and Dong, J. (2013). Stomatal Development in Arabidopsis. Arab. Book Am. Soc. Plant Biol. *11*.

Plackett, A.R.G., Thomas, S.G., Wilson, Z.A., and Hedden, P. (2011). Gibberellin control of stamen development: a fertile field. Trends Plant Sci. *16*, 568–578.

Pommerrenig, B., Popko, J., Heilmann, M., Schulmeister, S., Dietel, K., Schmitt, B., Stadler, R., Feussner, I., and Sauer, N. (2013). SUCROSE TRANSPORTER 5 supplies Arabidopsis embryos with biotin and affects triacylglycerol accumulation. Plant J. Cell Mol. Biol. *73*, 392–404.

Postaire, O., Tournaire-Roux, C., Grondin, A., Boursiac, Y., Morillon, R., Schäffner, A.R., and Maurel, C. (2010). A PIP1 Aquaporin Contributes to Hydrostatic Pressure-Induced Water Transport in Both the Root and Rosette of Arabidopsis1[C][W]. Plant Physiol. *152*, 1418–1430.

Prado, K., Boursiac, Y., Tournaire-Roux, C., Monneuse, J.-M., Postaire, O., Da Ines, O., Schäffner, A.R., Hem, S., Santoni, V., and Maurel, C. (2013). Regulation of Arabidopsis leaf hydraulics involves light-dependent phosphorylation of aquaporins in veins. Plant Cell *25*, 1029–1039.

Rieu, I., Wolters-Arts, M., Derksen, J., Mariani, C., and Weterings, K. (2003). Ethylene regulates the timing of anther dehiscence in tobacco. Planta *217*, 131–137.

Rodriguez-Riano, T., and Dafni, A. (2000). A new procedure to asses pollen viability. Sex. Plant Reprod. *12*, 241–244.

Rowe, M.H., and Bergmann, D.C. (2010). Complex signals for simple cells: the expanding ranks of signals and receptors guiding stomatal development. Curr. Opin. Plant Biol. *13*, 548–555.

Ruiter, R.K., van Eldik, G.J., van Herpen, M.M., Schrauwen, J.A., and Wullems, G.J. (1997). Expression in anthers of two genes encoding Brassica oleracea transmembrane channel proteins. Plant Mol. Biol. *34*, 163–168.

Rychel, A.L., Peterson, K.M., and Torii, K.U. (2010). Plant twitter: ligands under 140 amino acids enforcing stomatal patterning. J. Plant Res. *123*, 275–280.

Sanders, P.M., Bui, A.Q., Weterings, K., McIntire, K.N., Hsu, Y.-C., Lee, P.Y., Truong, M.T., Beals, T.P., and Goldberg, R.B. (1999).

Anther developmental defects in Arabidopsis thaliana male-sterile mutants. Sex. Plant Reprod. *11*, 297–322.

Sanders, P.M., Lee, P.Y., Biesgen, C., Boone, J.D., Beals, T.P., Weiler, E.W., and Goldberg, R.B. (2000). The Arabidopsis DELAYED DEHISCENCE1 Gene Encodes an Enzyme in the Jasmonic Acid Synthesis Pathway. Plant Cell *12*, 1041–1062.

Sanders, P.M., Bui, A.Q., Le, B.H., and Goldberg, R.B. (2005). Differentiation and degeneration of cells that play a major role in tobacco anther dehiscence. Sex. Plant Reprod. *17*, 219–241.

Sauer, N. (2007). Molecular physiology of higher plant sucrose transporters. FEBS Lett. *581*, 2309–2317.

Sauer, N., and Stolz, J. (1994). SUC1 and SUC2: two sucrose transporters from Arabidopsis thaliana; expression and characterization in baker's yeast and identification of the histidine-tagged protein. Plant J. Cell Mol. Biol. *6*, 67–77.

Sauer, N., Ludwig, A., Knoblauch, A., Rothe, P., Gahrtz, M., and Klebl, F. (2004). AtSUC8 and AtSUC9 encode functional sucrose transporters, but the closely related AtSUC6 and AtSUC7 genes encode aberrant proteins in different Arabidopsis ecotypes. Plant J. Cell Mol. Biol. *40*, 120–130.

Schneider, S., Hulpke, S., Schulz, A., Yaron, I., Höll, J., Imlau, A., Schmitt, B., Batz, S., Wolf, S., Hedrich, R., et al. (2012). Vacuoles release sucrose via tonoplast-localised SUC4-type transporters. Plant Biol. Stuttg. Ger. *14*, 325–336.

Schüssler, M.D., Alexandersson, E., Bienert, G.P., Kichey, T., Laursen, K.H., Johanson, U., Kjellbom, P., Schjoerring, J.K., and Jahn, T.P. (2008). The effects of the loss of TIP1;1 and TIP1;2 aquaporins in Arabidopsis thaliana. Plant J. Cell Mol. Biol. *56*, 756–767.

Scott, R.J., Spielman, M., and Dickinson, H.G. (2004). Stamen structure and function. Plant Cell *16 Suppl*, S46-60.

Selinski, J., and Scheibe, R. (2014). Pollen tube growth: where does the energy come from? Plant Signal. Behav. *9*.

Senatore, A., Trobacher, C.P., and Greenwood, J.S. (2009). Ricinosomes predict programmed cell death leading to anther dehiscence in tomato. Plant Physiol. *149*, 775–790.

Shih, C.-F., Hsu, W.-H., Peng, Y.-J., and Yang, C.-H. (2014). The NAC-like gene ANTHER INDEHISCENCE FACTOR acts as a repressor that controls anther dehiscence by regulating genes in the jasmonate biosynthesis pathway in Arabidopsis. J. Exp. Bot. *65*, 621–639.

Shivanna, K.R., Linskens, H.F., and Cresti, M. (1991). Pollen viability and pollen vigor. Theor. Appl. Genet. *81*, 38–42.

Shpak, E.D., Lakeman, M.B., and Torii, K.U. (2003). Dominant-negative receptor uncovers redundancy in the Arabidopsis ERECTA Leucine-rich repeat receptor-like kinase signaling pathway that regulates organ shape. Plant Cell *15*, 1095–1110.

Shpak, E.D., Berthiaume, C.T., Hill, E.J., and Torii, K.U. (2004). Synergistic interaction of three ERECTA-family receptor-like kinases controls Arabidopsis organ growth and flower development by promoting cell proliferation. Dev. Camb. Engl. *131*, 1491–1501.

Sivitz, A.B., Reinders, A., Johnson, M.E., Krentz, A.D., Grof, C.P.L., Perroux, J.M., and Ward, J.M. (2007). Arabidopsis sucrose transporter AtSUC9. High-affinity transport activity, intragenic control of expression, and early flowering mutant phenotype. Plant Physiol. *143*, 188–198.

Sivitz, A.B., Reinders, A., and Ward, J.M. (2008). Arabidopsis Sucrose Transporter AtSUC1 Is Important for Pollen Germination and Sucrose-Induced Anthocyanin Accumulation. Plant Physiol. *147*, 92–100.

Smyth, D.R., Bowman, J.L., and Meyerowitz, E.M. (1990). Early flower development in Arabidopsis. Plant Cell *2*, 755–767.

Sorensen, A.-M., Kröber, S., Unte, U.S., Huijser, P., Dekker, K., and Saedler, H. (2003). The Arabidopsis ABORTED MICROSPORES (AMS) gene encodes a MYC class transcription factor. Plant J. Cell Mol. Biol. *33*, 413–423.

Soto, G., Alleva, K., Mazzella, M.A., Amodeo, G., and Muschietti, J.P. (2008). AtTIP1;3 and AtTIP5;1, the only highly expressed Arabidopsis pollen-specific aquaporins, transport water and urea. FEBS Lett. *582*, 4077–4082.

Soto, G., Fox, R., Ayub, N., Alleva, K., Guaimas, F., Erijman, E.J., Mazzella, A., Amodeo, G., and Muschietti, J. (2010). TIP5;1 is an aquaporin specifically targeted to pollen mitochondria and is probably involved in nitrogen remobilization in Arabidopsis thaliana. Plant J. Cell Mol. Biol. *64*, 1038–1047.

Srivastava, A.C., Ganesan, S., Ismail, I.O., and Ayre, B.G. (2008). Functional characterization of the Arabidopsis AtSUC2 Sucrose/H+ symporter by tissue-specific complementation reveals an essential role in phloem loading but not in long-distance transport. Plant Physiol. *148*, 200–211.

Stadler, R., Truernit, E., Gahrtz, M., and Sauer, N. (1999). The AtSUC1 sucrose carrier may represent the osmotic driving force for anther dehiscence and pollen tube growth in Arabidopsis. Plant J. Cell Mol. Biol. *19*, 269–278.

Steiner-Lange, S., Unte, U.S., Eckstein, L., Yang, C., Wilson, Z.A., Schmelzer, E., Dekker, K., and Saedler, H. (2003). Disruption of Arabidopsis thaliana MYB26 results in male sterility due to non-dehiscent anthers. Plant J. Cell Mol. Biol. *34*, 519–528.

Stintzi, A., and Browse, J. (2000). The Arabidopsis male-sterile mutant, opr3, lacks the 12-oxophytodienoic acid reductase required for jasmonate synthesis. Proc. Natl. Acad. Sci. U. S. A. *97*, 10625–10630.

Sugano, S.S., Shimada, T., Imai, Y., Okawa, K., Tamai, A., Mori, M., and Hara-Nishimura, I. (2010). Stomagen positively regulates stomatal density in Arabidopsis. Nature *463*, 241–244.

Tabata, R., Ikezaki, M., Fujibe, T., Aida, M., Tian, C., Ueno, Y., Yamamoto, K.T., Machida, Y., Nakamura, K., and Ishiguro, S. (2010). Arabidopsis auxin response factor6 and 8 regulate jasmonic acid biosynthesis and floral organ development via repression of class 1 KNOX genes. Plant Cell Physiol. *51*, 164–175.

Takano, J., Wada, M., Ludewig, U., Schaaf, G., von Wirén, N., and Fujiwara, T. (2006). The Arabidopsis major intrinsic protein NIP5;1 is essential for efficient boron uptake and plant development under boron limitation. Plant Cell *18*, 1498–1509.

Taylor, L.P., and Hepler, P.K. (1997). Pollen Germination and Tube Growth. Annu. Rev. Plant Physiol. Plant Mol. Biol. *48*, 461–491.

Theissen, G., and Saedler, H. (2001). Plant biology. Floral quartets. Nature *409*, 469–471.

Törnroth-Horsefield, S., Wang, Y., Hedfalk, K., Johanson, U., Karlsson, M., Tajkhorshid, E., Neutze, R., and Kjellbom, P. (2006). Structural mechanism of plant aquaporin gating. Nature *439*, 688–694.

Truernit, E., and Sauer, N. (1995). The promoter of the Arabidopsis thaliana SUC2 sucrose-H+ symporter gene directs expression of β-glucuronidase to the phloem: Evidence for phloem loading and unloading by SUC2. Planta *196*, 564–570.

Tyerman, S.D., Niemietz, C.M., and Bramley, H. (2002). Plant aquaporins: multifunctional water and solute channels with expanding roles. Plant Cell Environ. *25*, 173–194.

Uehlein, N., Sperling, H., Heckwolf, M., and Kaldenhoff, R. (2012). The Arabidopsis aquaporin PIP1;2 rules cellular CO(2) uptake. Plant Cell Environ. *35*, 1077–1083.

Untergasser, A., Cutcutache, I., Koressaar, T., Ye, J., Faircloth, B.C., Remm, M., and Rozen, S.G. (2012). Primer3—new capabilities and interfaces. Nucleic Acids Res. *40*, e115.

Vizcay-Barrena, G. (2005). Functional Analysis of ms1 during Anther Development in Arabidopsis. Thesis. University of Nottingham.

Vizcay-Barrena, G., and Wilson, Z.A. (2006). Altered tapetal PCD and pollen wall development in the Arabidopsis ms1 mutant. J. Exp. Bot. *57*, 2709–2717.

Von Groll, U., Berger, D., and Altmann, T. (2002). The subtilisin-like serine protease SDD1 mediates cell-to-cell signaling during Arabidopsis stomatal development. Plant Cell *14*, 1527–1539.

Wang, R.-S., Pandey, S., Li, S., Gookin, T.E., Zhao, Z., Albert, R., and Assmann, S.M. (2011). Common and unique elements of the ABA-regulated transcriptome of Arabidopsis guard cells. BMC Genomics *12*, 216.

Wang, Y., Li, R., Li, D., Jia, X., Zhou, D., Li, J., Lyi, S.M., Hou, S., Huang, Y., Kochian, L.V., et al. (2017). NIP1;2 is a plasma membrane-localized transporter mediating aluminum uptake, translocation, and tolerance in Arabidopsis. Proc. Natl. Acad. Sci. *114*, 5047–5052.

Wasternack, C., and Hause, B. (2013). Jasmonates: biosynthesis, perception, signal transduction and action in plant stress response, growth and development. An update to the 2007 review in Annals of Botany. Ann. Bot. *111*, 1021–1058.

Wilson, Z.A., and Zhang, D.-B. (2009). From Arabidopsis to rice: pathways in pollen development. J. Exp. Bot. *60*, 1479–1492.

Wilson, Z.A., Morroll, S.M., Dawson, J., Swarup, R., and Tighe, P.J. (2001). The Arabidopsis MALE STERILITY1 (MS1) gene is a transcriptional regulator of male gametogenesis, with homology to the PHD-finger family of transcription factors. Plant J. Cell Mol. Biol. *28*, 27–39.

Wilson, Z.A., Song, J., Taylor, B., and Yang, C. (2011). The final split: the regulation of anther dehiscence. J. Exp. Bot. *62*, 1633–1649.

Winter, D., Vinegar, B., Nahal, H., Ammar, R., Wilson, G.V., and Provart, N.J. (2007). An "Electronic Fluorescent Pictograph" Browser for Exploring and Analyzing Large-Scale Biological Data Sets. PLOS ONE *2*, e718.

Wu, X.N., Sanchez Rodriguez, C., Pertl-Obermeyer, H., Obermeyer, G., and Schulze, W.X. (2013). Sucrose-induced receptor kinase SIRK1 regulates a plasma membrane aquaporin in Arabidopsis. Mol. Cell. Proteomics MCP *12*, 2856–2873.

Wudick, M.M., Luu, D.-T., Tournaire-Roux, C., Sakamoto, W., and Maurel, C. (2014). Vegetative and sperm cell-specific aquaporins of Arabidopsis highlight the vacuolar equipment of pollen and contribute to plant reproduction. Plant Physiol. *164*, 1697–1706.

Xie, D.X., Feys, B.F., James, S., Nieto-Rostro, M., and Turner, J.G. (1998). COI1: an Arabidopsis gene required for jasmonate-regulated defense and fertility. Science *280*, 1091–1094.

Xing, S., and Zachgo, S. (2008). ROXY1 and ROXY2, two Arabidopsis glutaredoxin genes, are required for anther development. Plant J. Cell Mol. Biol. *53*, 790–801.

Xu, J., Yang, C., Yuan, Z., Zhang, D., Gondwe, M.Y., Ding, Z., Liang, W., Zhang, D., and Wilson, Z.A. (2010). The ABORTED MICROSPORES regulatory network is required for postmeiotic male reproductive development in Arabidopsis thaliana. Plant Cell *22*, 91–107.

Xu, J., Ding, Z., Vizcay-Barrena, G., Shi, J., Liang, W., Yuan, Z., Werck-Reichhart, D., Schreiber, L., Wilson, Z.A., and Zhang, D. (2014). ABORTED MICROSPORES Acts as a Master Regulator of Pollen Wall Formation in Arabidopsis. Plant Cell *26*, 1544–1556.

Xu, W., Dai, W., Yan, H., Li, S., Shen, H., Chen, Y., Xu, H., Sun, Y., He, Z., and Ma, M. (2015). Arabidopsis NIP3;1 Plays an Important Role in Arsenic Uptake and Root-to-Shoot Translocation under Arsenite Stress Conditions. Mol. Plant *8*, 722–733.

Yang, M., and Sack, F.D. (1995). The too many mouths and four lips mutations affect stomatal production in Arabidopsis. Plant Cell Online *7*, 2227–2239.

Yang, C., Vizcay-Barrena, G., Conner, K., and Wilson, Z.A. (2007a). MALE STERILITY1 is required for tapetal development and pollen wall biosynthesis. Plant Cell *19*, 3530–3548.

Yang, C., Xu, Z., Song, J., Conner, K., Vizcay Barrena, G., and Wilson, Z.A. (2007b). Arabidopsis MYB26/MALE STERILE35 regulates secondary thickening in the endothecium and is essential for anther dehiscence. Plant Cell *19*, 534–548.

Yang, C., Song, J., Ferguson, A., Klisch, D., Simpson, K., Mo, R., Taylor, B., Mitsuda, N., and Wilson, Z.A. (2017). Transcription factor MYB26 is key to spatial specificity in anther secondary thickening formation. Plant Physiol. pp.00719.2017.

Yang, S.-L., Xie, L.-F., Mao, H.-Z., Puah, C.S., Yang, W.-C., Jiang, L., Sundaresan, V., and Ye, D. (2003). Tapetum determinant1 is required for cell specialization in the Arabidopsis anther. Plant Cell *15*, 2792–2804.

Yang, S.-L., Jiang, L., Puah, C.S., Xie, L.-F., Zhang, X.-Q., Chen, L.-Q., Yang, W.-C., and Ye, D. (2005). Overexpression of TAPETUM DETERMINANT1 Alters the Cell Fates in the Arabidopsis Carpel and Tapetum via Genetic Interaction with EXCESS MICROSPOROCYTES1/EXTRA SPOROGENOUS CELLS. Plant Physiol. *139*, 186–191.

Yang, W.C., Ye, D., Xu, J., and Sundaresan, V. (1999). The SPOROCYTELESS gene of Arabidopsis is required for initiation of sporogenesis and encodes a novel nuclear protein. Genes Dev. *13*, 2108–2117.

Yates, I.E., and Sparks, D. (1993). Environmental Regulation of Anther Dehiscence and Pollen Germination in Pecan. J. Am. Soc. Hortic. Sci. *118*, 699–706.

Zhang, W., Sun, Y., Timofejeva, L., Chen, C., Grossniklaus, U., and Ma, H. (2006). Regulation of Arabidopsis tapetum development and function by DYSFUNCTIONAL TAPETUM1 (DYT1) encoding a putative bHLH transcription factor. Dev. Camb. Engl. *133*, 3085–3095.

Zhao, D. (2009). Control of anther cell differentiation: a teamwork of receptor-like kinases. Sex. Plant Reprod. *22*, 221–228.

Zhao, D., and Ma, H. (2000). Male fertility: a case of enzyme identity. Curr. Biol. CB *10*, R904-907.

Zhao, D.-Z., Wang, G.-F., Speal, B., and Ma, H. (2002). The excess microsporocytes1 gene encodes a putative leucine-rich repeat receptor protein kinase that controls somatic and reproductive cell fates in the Arabidopsis anther. Genes Dev. *16*, 2021–2031.

Zhao, F., Zheng, Y.-F., Zeng, T., Sun, R., Yang, J.-Y., Li, Y., Ren, D., Ma, H., Xu, Z.-H., and Bai, S.-N. (2017). Phosphorylation of SPOROCYTELESS/NOZZLE by the MPK3/6 kinase is Required for Anther Development. Plant Physiol. pp.01765.2016.

Zhou, J., Theodoulou, F., Sauer, N., Sanders, D., and Miller, A.J. (1997). A kinetic model with ordered cytoplasmic dissociation for SUC1, an Arabidopsis H+/sucrose cotransporter expressed in Xenopus oocytes. J. Membr. Biol. *159*, 113–125.

Zhu, J., Lou, Y., Xu, X., and Yang, Z.-N. (2011). A genetic pathway for tapetum development and function in Arabidopsis. J. Integr. Plant Biol. *53*, 892–900.

Zhu, Q.-H., Ramm, K., Shivakkumar, R., Dennis, E.S., and Upadhyaya, N.M. (2004). The ANTHER INDEHISCENCE1 gene encoding a single MYB domain protein is involved in anther development in rice. Plant Physiol. *135*, 1514–1525.

APPENDIX

Analysis of T-DNA insertion mutants for Chapter 3

Table A1: Summary of primers used to genotype single T-DNA insertion lines. The wild type gene was identified using the SALK forward/reverse primers and the T-DNA insertion was identified using the left border primer of the T-DNA insertion (LB1b.3F) and the SALK reverse primer. F, forward primer, R, reverse primer. All primer pairs were used with an annealing temperature of 59°C.

AG1 Code	Primer Name	Primer Sequence 5'-3'	Size of amplicon (no. of base pairs)
AT3G54820	SALK_072405F	GAAAGTGACGTTG GTGAGAGC	1107
	SALK_072405R	AGCCCTCAACACA AACTGATG	
AT2G39010	SALK_118213F	TGAAAACGATGTC GTCTAGCC	992
	SALK_118213R	TTGTTACACACAA ACCTCCCC	
AT4G35100	SALK_068839F	AAAAATTGCCGCG AATATACC	1065
	SALK_068839R	AACTCAGCGATGA GAGCTCTG	
AT2G16850	SALK_099098F	AAGCAACACACAA GATGCAAG	1166
	SALK_099098R	AAAATCCATGTCA AACCCTACG	
AT2G44810	SALK_138439F	AACTTTGGTGATG ACGTCGTC	1063
	SALK_138439R	CTCTCTTTCTCCC GTACGTCC	
n/a	LB1b.3F	ATTTTGCCGATTTC GGAAC	n/a

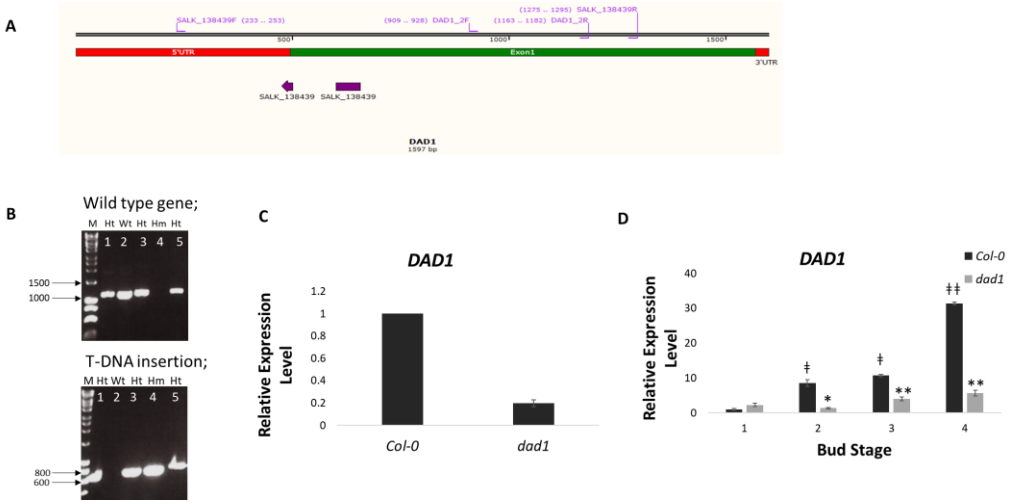

Figure A1: Analysis of T-DNA insertion mutant SALK_138439

A: Map of gene *DAD1* (AT2G44810) showing the position and direction of the T-DNA insert for line SALK_138439 (purple arrow). The position of primers used for genotyping and qRT-PCR are shown.
B: Genotyping example of the T-DNA insertion mutant SALK_138439. M, hyperladder^{TM} 1kb, Wt, wild type, Hm, homozygous, Het, heterozygous. PCR was performed using primer pairs SALK_138439F/SALK_138439R (top gel) and LB1b.3F/ SALK_138439R (bottom gel).
C: Expression of gene *DAD1* in SALK_138439 and wild type (Col-0) flowers (whole inflorescence). Reference gene *PP2A-3* (AT2G42500). Error bars, standard error.
D: Expression of gene *DAD1* in staged SALK_138439 and wild type (Col-0) flowers. Gene expression is relative to Col-0 stage 1. Reference gene *PP2A-3* (AT2G42500). ǂ indicates a significant difference in expression relative to Col-0 stage 1 ($P<0.05$), ǂǂ ($P<0.001$). * indicates a significant difference in expression relative to Col-0 for the equivalent stage ($P<0.05$), ** ($P<0.001$), Error bars, standard error.

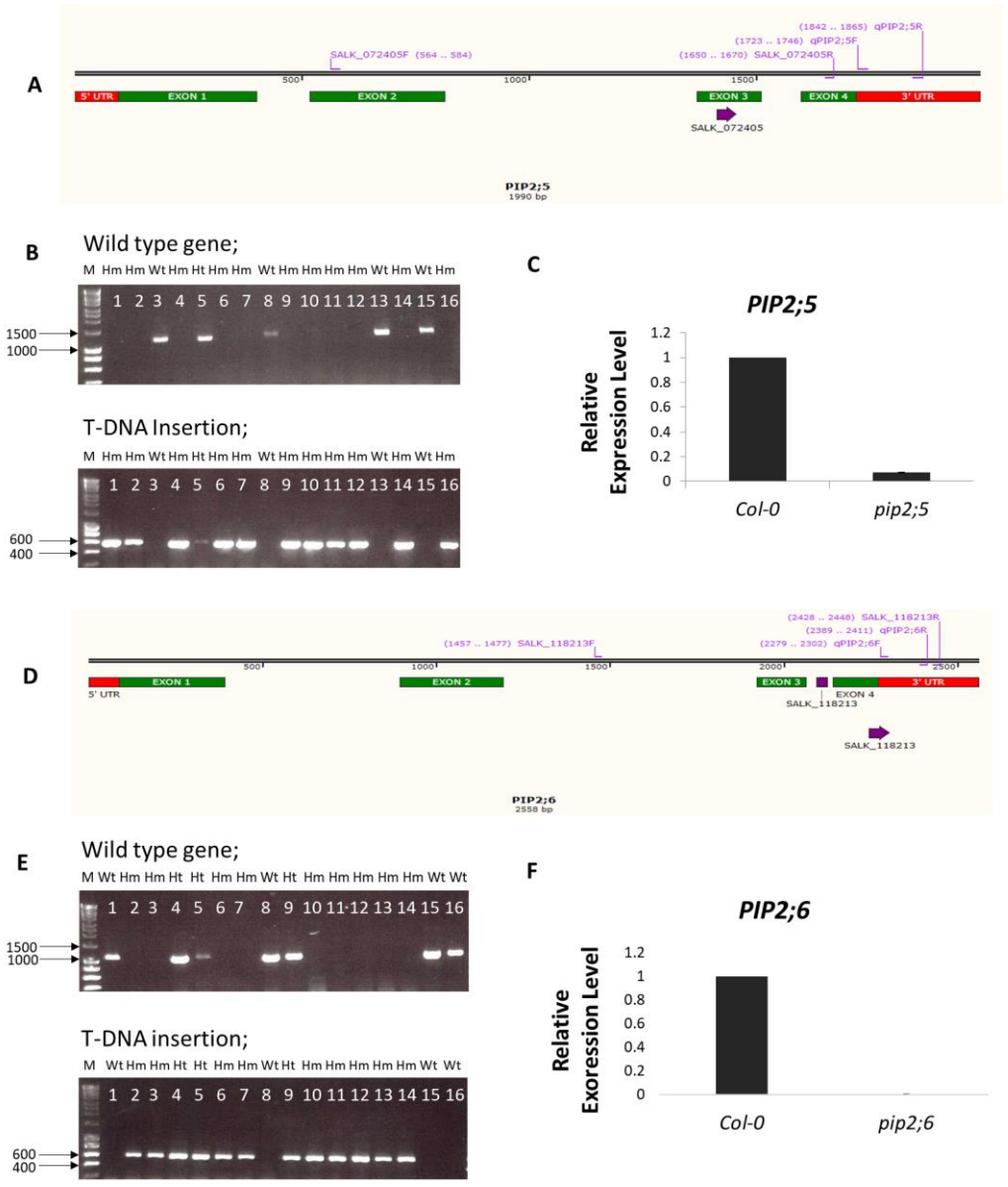

Figure A2: Analysis of T-DNA insertion mutants SALK_072405 and SALK_118213

A: Map of gene *PIP2;5* (AT3G54820) showing the position and direction of the T-DNA insert for line SALK_072405 (purple arrow). The position of primers used for genotyping and qRT-PCR are shown.
B: Genotyping example of the T-DNA insertion mutant SALK_072405. M, hyperladder^{TM} 1kb, Wt, wild type, Hm, homozygous, Het, heterozygous. PCR was performed using primer pairs SALK_072405F/SALK_072405R (top gel) and Lb1b.3F/SALK_072405R (bottom gel).
C: Expression of gene *PIP2;5* in SALK_072505 flowers (whole inflorescence) relative to wild type (Col-0). Reference gene *PP2A-3* (AT2G42500). Error bars, standard error.
D: Map of gene *PIP2;6* (AT2G39010) showing the position and direction of the T-DNA insert for line SALK_118213 (purple box/arrow). The position of primers used for genotyping and qRT-PCR are shown.

E: Genotyping example of the T-DNA insertion mutant SALK_118213. M, hyperladder™ 1kb, Wt, wild type, Hm, homozygous, Het, heterozygous. PCR was performed using primer pairs SALK_118213F/SALK_118213R (top gel) and Lb1b.3F/SALK_118213R (bottom gel).
F: Expression of gene *PIP2;6* in SALK_118213 flowers (whole inflorescence), relative to wild type (Col-0). Reference gene *PP2A-3* (AT2G42500). Error bars, standard error.

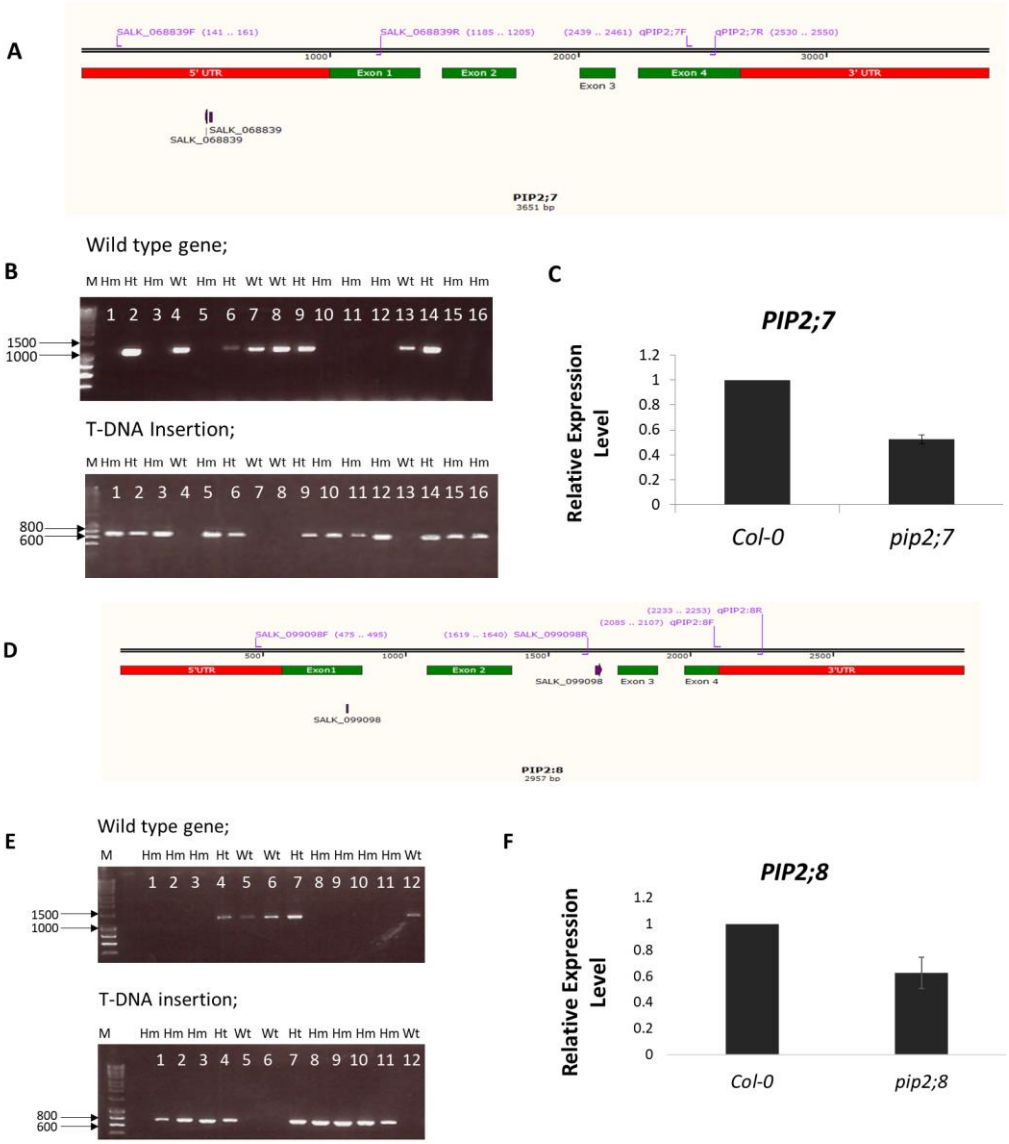

Figure A3: Analysis of T-DNA insertion mutants SALK_068839 and SALK_099098

A: Map of gene *PIP2;7* (AT4G35100) showing the position and direction of the T-DNA insert for line SALK_068839 (purple arrow). The position of primers used for genotyping and qRT-PCR are shown.
B: Genotyping example of the T-DNA insertion mutant SALK_068839. M, hyperladder™ 1kb, Wt, wild type, Hm, homozygous, Het, heterozygous. PCR was performed using primer pairs SALK_068839F/SALK_068839R (top gel) and LB1b.3F/SALK_068839R (bottom gel).
C: Expression of gene *PIP2;7* in SALK_068839 and wild type (Col-0) flowers. Reference gene *PP2A-3* (AT2G42500).
D: Map of gene *PIP2;8* (AT2G16850) showing the position and direction of the T-DNA insert for line SALK_099098 (purple box/arrow). The position of primers used for genotyping and qRT-PCR are shown.
E: Genotyping example of the T-DNA insertion mutant SALK_099098. M, hyperladder™ 1kb, Wt, wild type, Hm, homozygous, Het, heterozygous. PCR was performed using primer pairs SALK_099098F/SALK_099098R (top gel) and LB1b.3F/SALK_099098R (bottom gel).
F: Expression of gene *PIP2;8* in SALK_099098 and wild type (Col-0) flowers (whole inflorescence). Reference gene *PP2A-3* (AT2G42500).

Analysis of T-DNA insertion mutants for Chapter 4

Table A2: List of primers used for genotyping. All primer pairs were used with an annealing temperature of 59°C.

AG1 Code	Primer Name	Primer Sequence 5′-3′	Size of amplicon (no. of base pairs)
AT1G22710	SALK_087046F	TTTACCTGAGGGACGACAATG	1014
	SALK_087046R	GTTTTTCGGAGAAATCTTCGG	
AT1G71880	SALK_123324F	GACCACAGAGCCAAATGAGAG	1008
	SALK_123324R	TGTTGCCCTGAACCATCTATC	
AT1G71890	SAIL_365_D07F	AGGTGCATGAATGATGAAACC	1150
	SAIL_365_D07R	ATGACAAAAGCTTGCGACATC	
AT2G44810	SALK_138439F	AACTTTGGTGATGACGTCGTC	1063
	SALK_138439R	CTCTCTTTCTCCCGTACGTCC	
n/a	Lb1b.3F	ATTTTGCCGATTTCGGAAC	n/a
n/a	LB3F	TAGCATCTGAATTTCATAACCAATCTCGATACAC	n/a

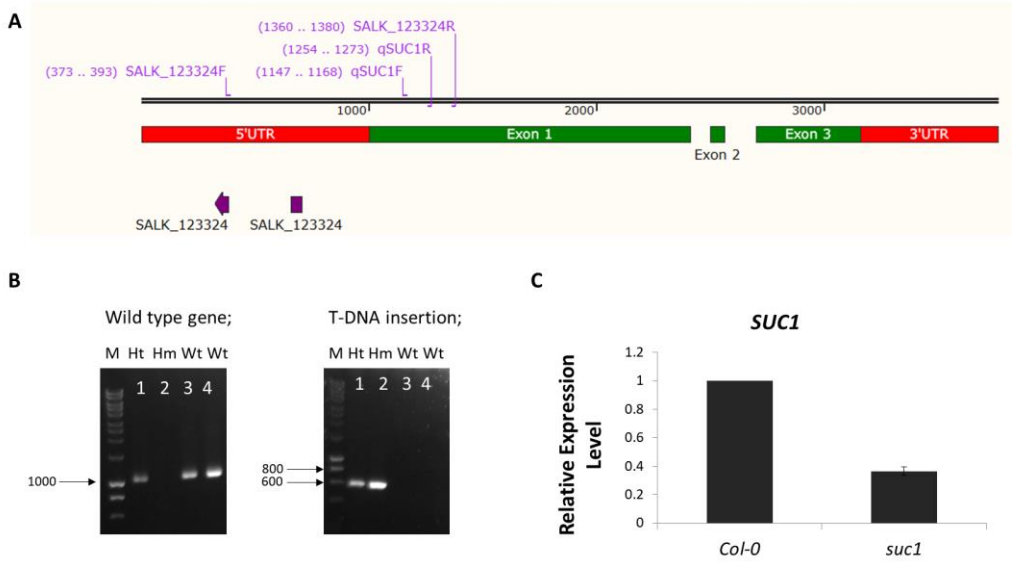

Figure A4: Analysis of the T-DNA insertion mutant SALK_123324

A: Map of gene *SUC1* (AT1G71880) showing the position and direction of the T-DNA insert for line SALK_ 123324 (purple arrow). The position of primers used for genotyping and RT-QPCR are shown.
B: Genotyping example of the *suc1* T-DNA insertion mutant SALK_123324. M, hyperladder™ 1kb, Wt, wild type, Hm, homozygous, Ht, heterozygous. PCR was performed using primer pairs SALK_123324F/SALK_123324R (left-hand side gel) and Lb1b.3F/ SALK_123324R (right-hand side gel).
C: Expression of gene *SUC1* in SALK_123324 and wild type (Col-0) flowers (whole inflorescence). Reference gene *PP2A-3* (AT2G42500). Error bars, standard error.

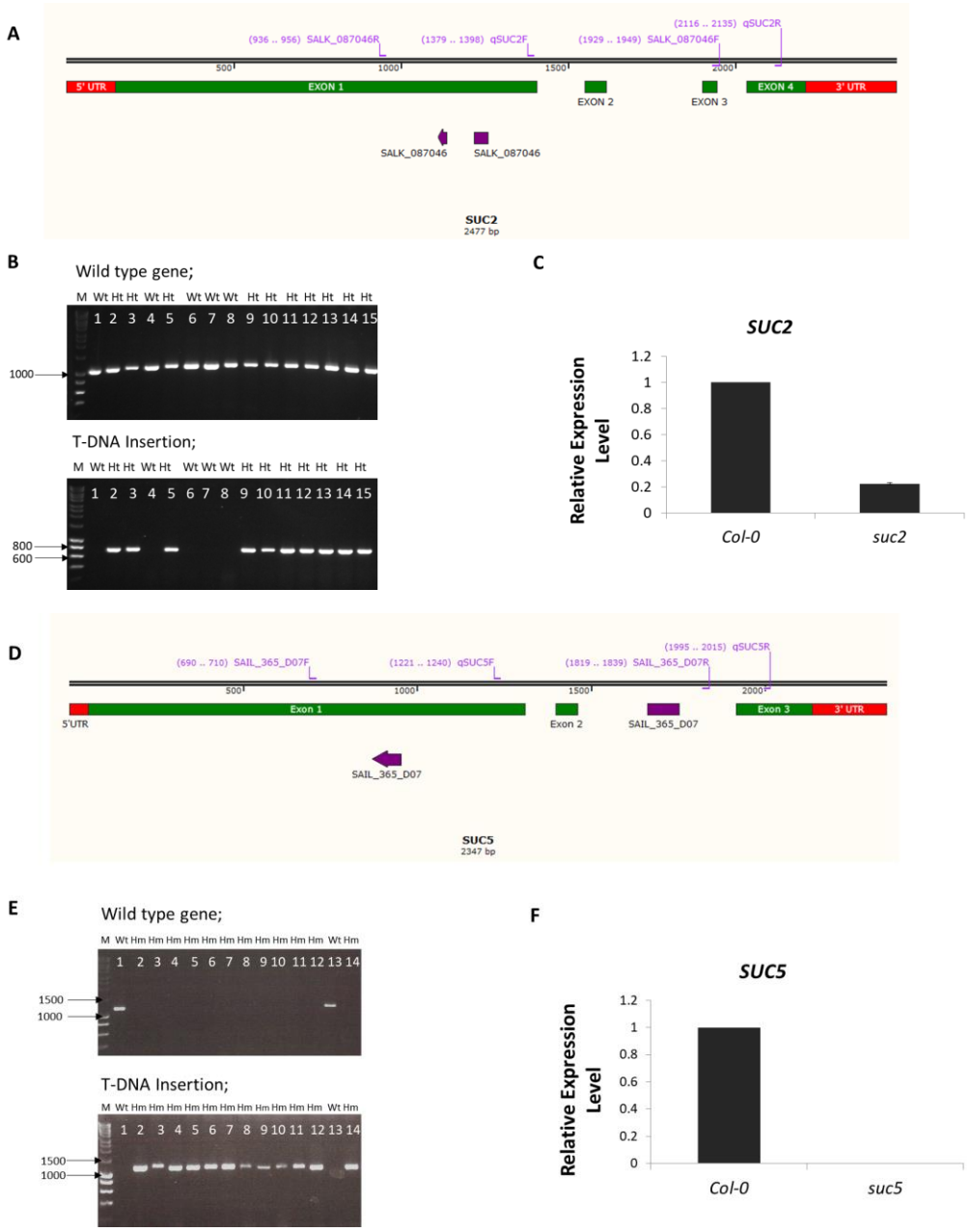

Figure A5: Analysis of T-DNA insertion mutants SALK_087046 and SAIL_365_D07

A: Map of gene *SUC2* (AT1G22710) showing the position and direction of the T-DNA insert for line SALK_087046 (purple arrow). The position of primers used for genotyping and qRT-PCR are shown.
B: Genotyping example of the *suc2* T-DNA insertion mutant SALK_087046. M, hyperladder™ 1kb, Wt, wild type, Ht, heterozygous. PCR was performed using primer pairs SALK_087046F/SALK_087046R (top gel) and Lb1b.3F/ SALK_087046R (bottom gel).
C: Expression of gene *SUC2* in het SALK_087046 and wild type (Col-0) flowers (whole inflorescence). Reference gene *PP2A-3* (AT2G42500). Error bars, standard error.

D: Map of gene *SUC5* (AT1G71890) showing the position and direction of the T-DNA insert for line SAIL_365_D07 (purple arrow). The position of primers used for genotyping and qRT-PCR are shown.
E: Genotyping example of the *suc5* T-DNA insertion mutant SAIL_365_D07. M, hyperladder™ 1kb, Wt, wild type, Hm, homozygous. PCR was performed using primer pairs SAIL_365_D07F/ SAIL_365_D07R (top gel) and Lb1b.3F/ SAIL_365_D07R (bottom gel).
F: Expression of gene *SUC5* in hm SAIL_365_D07 and wild type (Col-0) flowers (whole inflorescence). Reference gene *PP2A-3* (AT2G42500). Error bars, standard error.

Primers used for qRT-PCR Analysis

Table A3: List of primer pairs used for qRT-PCR analysis. All primer pairs were used with an annealing temperature of 60°C. The size of the cDNA amplicon is given in base pairs. Primers designed using Primer 3 (Koressaar and Remm, 2007; Untergasser et al., 2012).

AGI Code	Primer Name	Primer Sequence 5'-3'	Size of cDNA Amplicon	Primer Efficiency
AT3G61430	qPIP1;1F	CTGGCCTTGTCCTTAGTTGCTTC	125	1.99
	qPIP1;1R	TCTCCTTTGGAACTTCTTCCTTG		
AT2G45960	qPIP1;2F	TCCTCTTCTTTGCCTAATGGAGAC	132	2.0
	qPIP1;2R	AGTTGCCTGCTTGAGATAAAC		
AT1G01620	qPIP1;3F	GCTGTGGATGATCTGGTTTTATCG	174	1.98
	qPIP1;3R	GCCGAAACAATATGGATCTTACTC		
ATG00430	qPIP1;4F	CTCTGAAGTCTAAGGTGATTAGTGC	117	1.56
	qPIP1;4R	CAACCCGAGAACTTGATGTTGA		
AT4G23400	qPIP1;5F	TGTTTCCTATGTCATGTGTGATG	143	1.91
	qPIP1;5R	GTACACAATGTATTCTTCCATTGAC		
AT3G53420	qPIP2;1F	TGTGTTTTCCACTTGCTCTTTTG	118	2.0
	qPIP2;1R	CACAACGCATAAGAACCTCTTTGA		
AT2G37170	qPIP2;2F	GGCAACTTTGCTTGTAAAACTATGC	102	2.0
	qPIP2;2R	AGTACACAAACATTGGCATTGG		
AT2G37180	qPIP2;3F	GAAACATATCCTCTTTTCCACTCG	133	1.92
	qPIP2;3R	CTCAATACACCAAACTTACATACG		

AT3G54820	qPIP2;5F	GATATGCTCTTCCCTGAGTACATC	143	1.90
	qPIP2;5R	AATATCTCTCCTCACCAAAGCTAG		
AT2G39010	qPIP2;6F	TTTCGAACTAGCGAAGAGGTGAAG	133	1.97
	qPIP2;6R	AGACACAGTAAATGTCACTCACC		
AT4G35100	qPIP2;7F	TGTGTAATGAGAGAGATGGTGGA	112	2.0
	qPIP2;7R	AGAGAAACCAAAGGCAAACGA		
AT2G16850	qPIP2;8F	CAACCCAACCAATTGATGATTCA	169	2.0
	qPIP2;8R	ACATGAAAGAAAGCAACGGAC		
AT2G36830	qTIP1;1F	CTCCCAACCACAGACTACTGAA	136	2.0
	qTIP1;1R	GCACGATCATAAACCCCTTG		
AT3G26520	qTIP1;2F	GCATCGTAATGGGTTTCTGG	128	1.99
	qTIP1;2R	TACAATTGCACAAAAGCCTTCC		
AT3G16240	qTIP2;1F	CCATGTGAACCCAGCCGTCA	179	2.11
	qTIP2;1R	TCGATCCTAGTCCAGCCGCA		
AT1G71880	qSUC1F	TCCTGATAATGGGAGCCTATGA	127	2.22
	qSUC1R	GCGATGGAAGCGACGGAGAT		
AT1G22710	qSUC2F	TCGCCATCCTCGGTATCCCC	236	2.10
	qSUC2R	TACACCACTTACCGCTGCCG		
AT2G02860	qSUC3F	CGAACCAGGGCAGCTGTTGT	199	2.08
	qSUC3R	GCCATTTTCCGCTAGCACCG		

AT1G09960	qSUT4F	TGTTGCGTCTCACCTTGGCT	128	2.06
	qSUT4R	TCAACGCATATGGGACGCTGT		
AT1G71890	qSUC5F	CGGGAAATCGCCGGTCCTTT	252	1.89
	qSUC5R	GTTTCCACCGCCGAATTGAGC		
AT2G42500	PP2A-3F	TCCGTGAAGCTGCAAAC	323	1.94
	PP2A-3R	CACCAAGCATGGCCGTATCA		
AT2G44810	DAD1_2F	GCCACGCTGACTCATCTCCC	274	2.09
	DAD1_2R	CGGTAACCATAGGCGCACGT		
AT3G13890	R1451	TTGGGAACATCAATGGGGTCAT	224	1.96
	RT345	GCTCATGTCTCACCATCATCACG		

Buffers and Media

½ MS Medium Agar Plates

Components are dissolved in 500ml distilled water and pH adjusted to pH5.8. Autoclaving is used to sterilise.

Table A4: Quantities of components required to make 500ml ½ MS media

Component	Quantity (g) for 500ml
Murashige and Skoog Basal medium (MS)	1.23
Agar	3.5
Sucrose	2.5

LB Medium and LB Agar Plates

Components are dissolved in 1L distilled water and pH adjusted to pH7.5. Autoclaving is used to sterilize. For LB agar plates 15g/L Bacto Agar is added before autoclaving.

Table A5: Quantities of components required to make 1L LB media

Component	Quantity (g) for 1L
Bacto Tryptone	10
Bacto-yeast extract	5
NaCl	10

Phosphate-Buffered Saline (PBS)

Components are dissolved in 400 ml distilled water and pH adjusted to pH7.2. Water is added to 500ml and autoclaving is used to sterilise.

Table A6: Quantities of components required to make 500ml PBS

Component	Quantity (g) for 500ml
NaCl	4
KCl	0.1
Na_2HPO_4	0.72
KH_2PO_4	0.12

Super Optimal broth with Catabolite repression (SOC) Medium

Components are dissolved in 900ml distilled water and pH adjusted to pH7.5. Water is added to 980ml and autoclaving is used to sterilise. After cooling the medium to less than 50°C, 20ml of filter sterilized 20% glucose solution is added.

Table A7: Quantities of components used to make 1L SOC medium

Component	Quantity for 1L (g)
Yeast Extract	5
Bacto Tryptone	20
NaCl	0.584
KCl	0.186
$MgSO_4$	2.4

Vectors

pCR™8/GW/TOPO Vector (Invitrogen™)

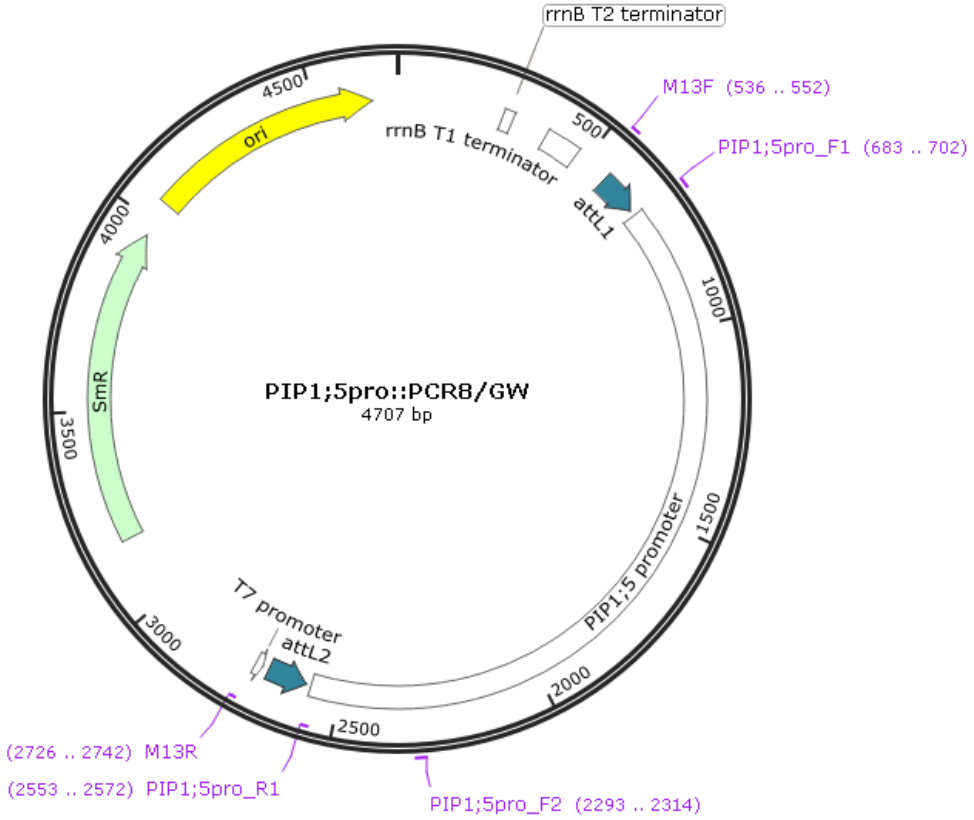

pCR™8/GW/TOPO Vector (Invitrogen™)

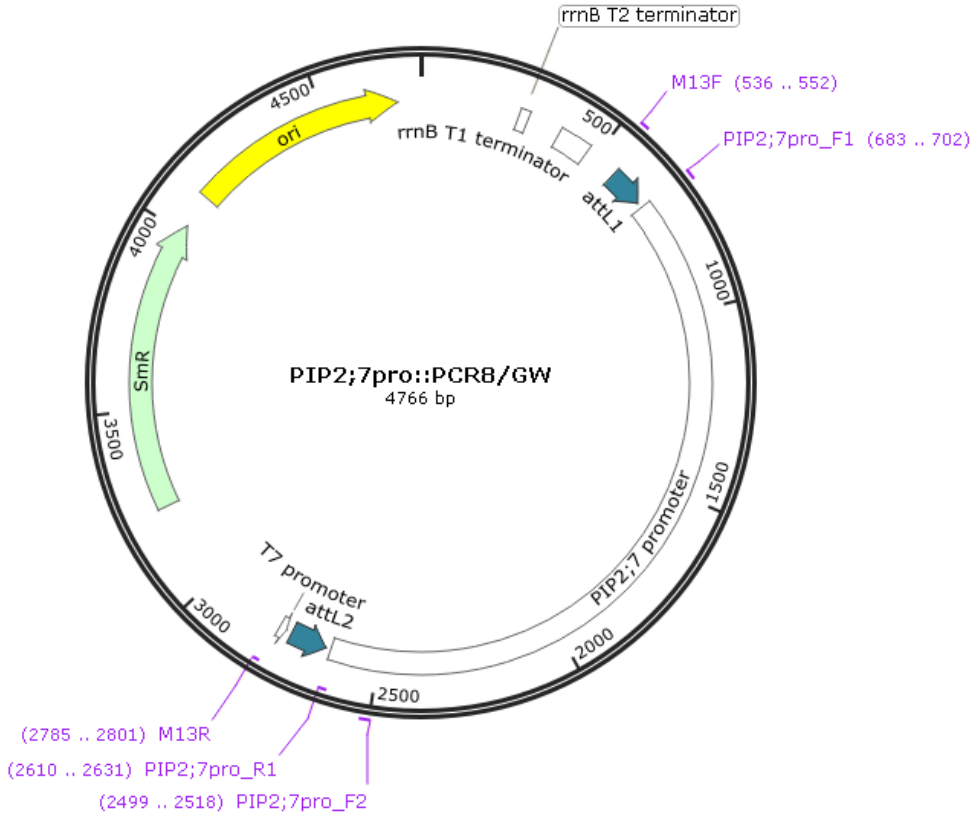

pCR™8/GW/TOPO Vector (Invitrogen™)

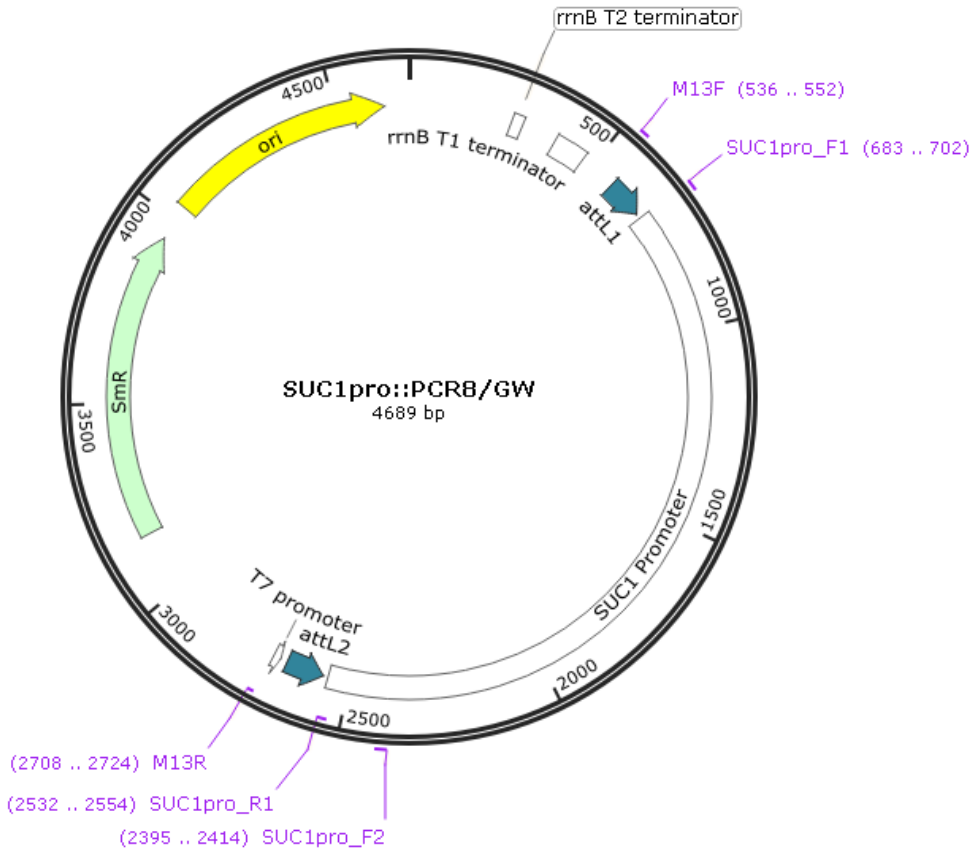

PGWB3

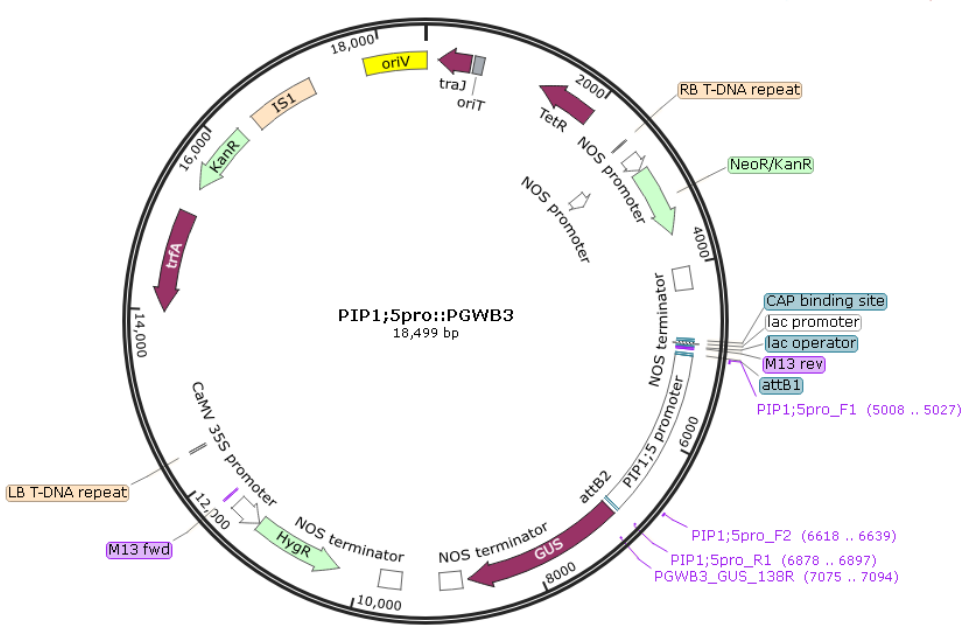
PIP1;5pro::PGWB3
18,499 bp
18,000
oriV
traJ
oriT
2000
TetR
RB T-DNA repeat
NOS promoter
NeoR/KanR
NOS promoter
4000
NOS terminator
CAP binding site
lac promoter
lac operator
M13 rev
attB1
PIP1;5pro_F1 (5008 .. 5027)
6000
PIP1;5 promoter
attB2
GUS
NOS terminator
8000
PIP1;5pro_F2 (6618 .. 6639)
PIP1;5pro_R1 (6878 .. 6897)
PGWB3_GUS_138R (7075 .. 7094)
10,000
NOS terminator
HygR
12,000
CaMV 35S promoter
LB T-DNA repeat
M13 fwd
14,000
trfA
16,000
KanR
IS1

PGWB3

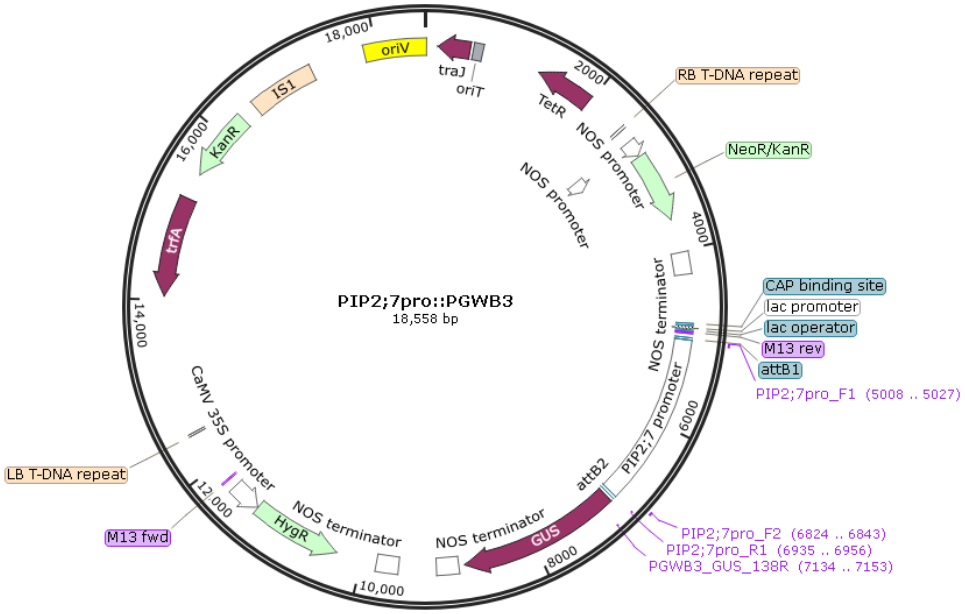
PIP2;7pro::PGWB3
18,558 bp
18,000
oriV
traJ
oriT
2000
TetR
RB T-DNA repeat
NOS promoter
NeoR/KanR
NOS promoter
4000
NOS terminator
CAP binding site
lac promoter
lac operator
M13 rev
attB1
PIP2;7pro_F1 (5008 .. 5027)
6000
PIP2;7 promoter
attB2
GUS
NOS terminator
8000
PIP2;7pro_F2 (6824 .. 6843)
PIP2;7pro_R1 (6935 .. 6956)
PGWB3_GUS_138R (7134 .. 7153)
10,000
NOS terminator
HygR
12,000
CaMV 35S promoter
M13 fwd
LB T-DNA repeat
14,000
trfA
16,000
KanR
IS1

PGWB3

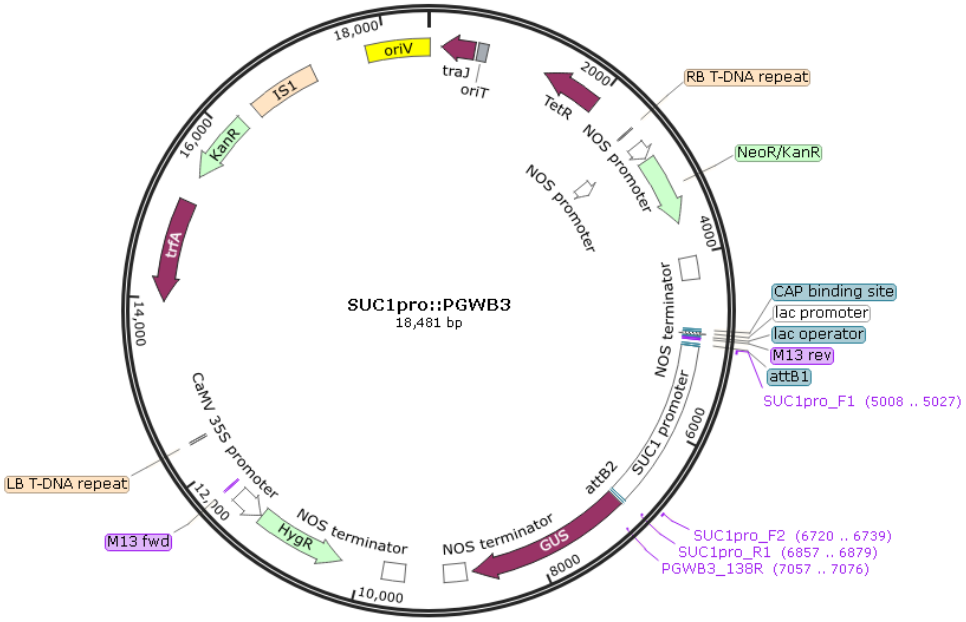
SUC1pro::PGWB3
18,481 bp
18,000
oriV
traJ
oriT
2000
TetR
RB T-DNA repeat
NOS promoter
NeoR/KanR
NOS promoter
4000
NOS terminator
CAP binding site
lac promoter
lac operator
M13 rev
attB1
SUC1pro_F1 (5008 .. 5027)
SUC1 promoter
6000
attB2
GUS
NOS terminator
8000
SUC1pro_F2 (6720 .. 6739)
SUC1pro_R1 (6857 .. 6879)
PGWB3_138R (7057 .. 7076)
NOS terminator
HygR
10,000
12,000
CaMV 35S promoter
LB T-DNA repeat
M13 fwd
14,000
trfA
16,000
KanR
IS1

EPF2 ctapi

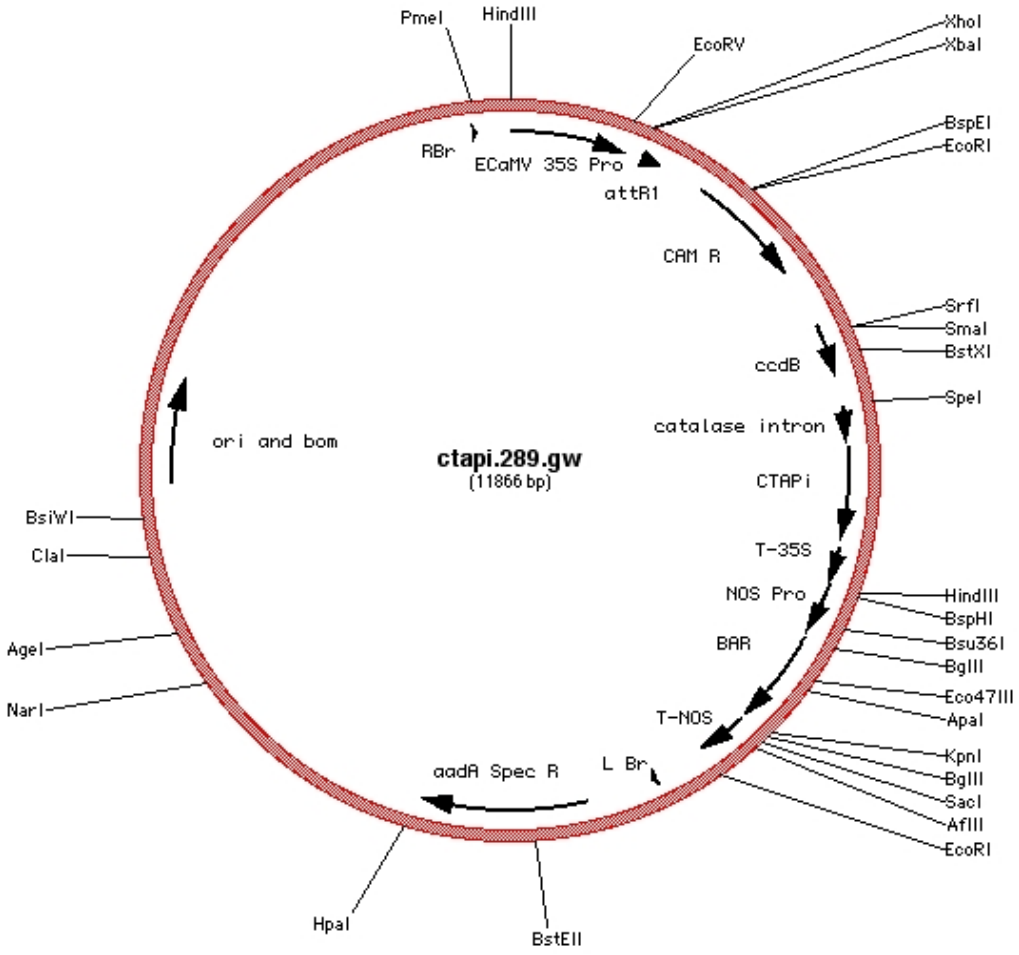
PmeI
HindIII
EcoRV
XhoI
XbaI
BspEI
EcoRI
RBr
ECaMV 35S Pro
attR1
CAM R
SrfI
SmaI
BstXI
ccdB
SpeI
catalase intron
ori and bom
ctapi.289.gw
(11866 bp)
CTAPi
BsiWI
ClaI
T-35S
NOS Pro
HindIII
BspHI
Bsu36I
BglII
AgeI
BAR
Eco47III
ApaI
NarI
T-NOS
KpnI
BglII
L Br
aadA Spec R
SacI
AflII
EcoRI
HpaI
BstEII

PROFESSIONAL INTERNSHIPS FOR PHD STUDENTS REFLECTION FORM

Name of Organisations: Shanghai Jiao Tong University (SJTU) and The University of Nottingham (UoN)

Details of Placement:

Please describe your main activities during the placement (150-200 words)

During my placement, I gained experience of the student recruitment process by working with UoN's International Recruitment Officers in Shanghai. I attended numerous student recruitment fairs, some of which required travelling to other cities in China.

Net4FS is a European funded project to enable collaboration and mobility between EU researchers and China within the area of Global Food Security. During the first half of my placement I was based with the International Mobility office at SJTU and I strengthened links between the two Universities by promoting the Net4FS and 2+2 PhD/undergraduate degree programs (2 years studying at SJTU, 2 years studying at UoN) to Chinese students.

In the second half of my internship I was based in the Life Sciences building at SJTU where I undertook some field work contributing to a project being done in collaboration between the two Universities. My main role however during this time was to organise an international conference (the 2nd Net4FS dissemination event) which was held at SJTU.

Placement Achievements:

Please detail all outcomes from the placement, including any publications, presentations given and reports written etc. (150-200 words)

While working with the International Mobility office at SJTU, I helped to develop the welcome pack for foreign students coming to SJTU which involved researching and writing material. I also discussed and helped develop the content of the orientation week for new students, as well as proof reading and amending various documents. In order to promote the 2+2 PhD and Undergraduate programs, I worked closely with the UoN's international officer to understand the requirements of the programs and I also contacted students who were already participating. I then gave a presentation to a large group of prospective students.

In the second half of my placement, as well as doing field work, I worked closely with colleagues at SJTU to organise the conference week, including the social aspects such as evening dinners and a sightseeing trip. I helped to arrange the agenda for the conference, organised the printing of programs and badges and advertised the conference to students via social media. I booked and organised accommodation, airport pickups and restaurants and helped to obtain reservation certificates required for guests' visas. During the conference week, I acted as a host for the social events and I also presented my own academic work during the conference.

Skill development:

Has this Placement helped you developed any new skills or enhanced your previous skill set? (100-150 words)

During the internship, I had numerous opportunities to develop my research and presentation skills. I presented to students and parents as well as to an academic audience during the conference. While I was organising the conference, I gained a wide range of skills including experience of handling a budget, time management and organisational skills, and experience of hosting international guests at an event. As the conference was being jointly organised between SJTU and UoN, I had to liaise on a daily basis with the organisers in Nottingham (via email and skype) to ensure that everything ran

smoothly. I also developed some management skills as I worked with many Chinese colleagues and students in the run up to the conference and I had to delegate and manage various tasks.

Future Work:

Has this Placement influenced your future career aspirations? If so, in what way? (150-200 words)

I have always been interested in events management, particularly within the field of science communication. The opportunity to organise an international conference gave me a real insight into what this involves. Not only did I gain some very valuable experience, but I also learnt how work within a different cultural framework. I found that a lot of my previous work experience was relevant to this internship (having lived and worked as a teacher in both China and the UK, previously), and it was very rewarding to be able to use this. I am interested in working with scientific organisations to promote their work to the general public, and in particular I am interested in working with young people. This internship has also inspired me to seek to use my knowledge of China and Chinese language and culture in my future career.